Design & Synthesis of Photo-reactive Receptors for the Recognition of Analytes having Biological Significance

Thesis Submitted to AcSIR for the Award of the Degree of

DOCTOR OF PHILOSOPHY

In Chemical Science

(Academy of Scientific and Innovative Research)

By

Firoj Ali

(Reg.No. 10CC13J26048)

Under the guidance of

Dr. Amitava Das

CSIR-National Chemical Laboratory
Pune, Maharashtra, India– 411008

June 2017

CANDIDATE'S STATEMENT

I hereby declare that the work incorporated in the present thesis is original and has not been submitted to any University/Institution for the award of a Diploma or a Degree. Research material obtained from other sources has been duly acknowledged in the thesis. Any text, illustration, table etc., used in the thesis from other sources, have been duly cited and acknowledged." further declare that the results presented in the thesis and the considerations made therein, contribute in general to the advancement of knowledge in chemistry and in particular to **"Design & Synthesis of Photo-reactive Receptors for the Recognition of Analytes having Biological Significance"**.

Firoj Ali

Firoj Ali

Certificate

This is to certify that the work incorporated in this Ph.D. entitled "**Design & Synthesis of Photo-reactive Receptors for the Recognition of Analytes having Biological Significance**" submitted by **Mr. Firoj Ali**, to Academy of Scientific and Innovative Research (AcSIR) in fulfillment of the requirements for the award of the Degree of Doctor of Philosophy, embodies original research work under my supervision. I further certify that this work has not been submitted to any other University or Institution in part or full for the award of any degree or diploma. Research material obtained from other sources has been duly acknowledged in the thesis. Any text, illustration, table, etc., used in the thesis from other sources, have been duly cited and acknowledged.

Firoj Ali
(Student)

Amitava Das
(Supervisor)

Acknowledgements

I whole heartedly express my deep sense of gratitude to **Dr. Amitava Das** – My Guide. I am extremely grateful to him for his continuous encouragement, timely advise, scholarly monitoring and invaluable suggestions. I am really thankful for the freedom that he gave to my research life. I grew as a research student watching him working till late night every day, which has been the source of inspiration to me.

I wish to convey my gratefulness to ***Dr. Biswajit Ganguly, Dr. Samit Chattopadhyay, Prof. Jim A Thomas and Prof. Carl G Smythe*** for fruitful discussions on research problems, appreciative comments, and continuous guidance whenever I approached which helped me to explore various aspects of the chemistry.

I wish to express my sincere thanks to my Doctoral advisor committee ***Dr. Manjusha Vilas Shelke, Dr. Santhosh Babu Sukumaran*** and ***M Muthu Krishnan*** for their continued encouragement and valuable suggestions.

I wish to express my word of thanks to ***Dr. P. K. Ghosh*** (Former Director, CSMCRI, Bhavnagar), ***Dr. Sourav Paul*** (Former Director, NCL-Pune), ***Dr. Ashwini K. Nangia*** **(**Director, NCL), ***Dr. Parimal Paul*** (Discipline Coordinator, CSMCRI) ***Dr. Pradeep Kumar***, Head, Division of Organic Chemistry for providing me opportunity and all necessary facilities to carry out my research work.

My sincere thanks to ***Prof. Bibhutosh Adhikary*** for his encouragement and guidance.

My sincere thanks to ***Dr. Avinash S. Kumbhar***, ***Dr. Sakya Singha Sen***, ***Dr. R. A. Joshi, Dr. P. S. Subramaniayan, Dr. S. P. Mukherjee, Dr. R. I. Kureshi and Dr. Adimurthy*** and all other scientists of NCL and CSMCRI for their motivation, constant encouragement and support.

I would like to express my special thanks to my seniors ***Dr. Moorthy Suresh, Dr. Prasenjit Mahato, Dr. Amal Kumar Mandal, Dr. Priyadip Das, Dr. Sukdeb Saha, Dr. Tanmay Banerjee***, ***Dr. Gandra Upendar Reddy***, ***Dr. Vadde Ramu*** and ***Dr. Hridesh Agarwalla***. They all taught me in my initial days of my research carrier and took me along with them.

I feel fortunate enough to have wonderful group of colleagues ***Monalisa, Arunava, Anila, Sunil, Ananta, Dr. Praveen L., Dr. Sovan Roy, Dr. Shilpi Kushwaha, Dr. Ketan Patel, Dr. Suman Pal, Dr. Ajoy Pal, Koushik and Sanjukta*** with whom I worked all these five year. Each one of them equally contributed in different way to take up my

course so fruitfully throughout these five years. I thank all of them individually from the bottom of my heart.

My Sincere thanks to my friends and collaborators ***Nandaraj Taye, Sreejesh Sreedharan*** and ***Mrinal Kanti Si*** who are an important part of my journey.

My sincere thanks to all my friends for their support and to my make my journey joyful and a memorable one. I thank all of you ***Suman, Mohsina, Apoorva, Aftab, Debraj Mogare, Debdeep da, Raju Da, Sikandar Ali, Sakir, Jisan, Raja Da, Santi, Pravat da, Partha da, Kanak da, Achintya da, Susanta da, Arpan da, Pati da, Saikat da, Shyam da, Krishanu da, Siba, Manzoor, Saibal, Subrata, Avijit, Sandeepan, Mohitosh, Somsuvra, Indrwadeep, Sutanu, Manik, Santanu, Tapas, Tamal, Debu, Subhrasis, Pranab, Atanu, Indranil, Monotosh, Sagar and Swamy.***

I wish to thank **CSIR** for financial assistance and **AcSIR** for allowing me to submit my work in the form of thesis.

At this moment, I invariably feel short of words to express my sincere thanks to My Grand Parent Late ***Baker Ali*** *and Late* ***Morjina Bibi***, my father ***Nazir Ali*** and my beloved mother ***Halima Bibi****,* my sister ***Reshma*** **and my uncle** ***Pear Ali*** for their love, prayers and support which inspired me and strengthen throughout my life. I thank all my well-wishers whose continuous encouragement and support in completion of this tough task.

I, sincerely thankful to ***Sneha*** for her love and support which inspired me and strengthen throughout my life.

I am also thankful to *Almighty God* for all your blessings to me and for the strength you give me each day.

CD_2Cl_2	Deuterated dichloromethane
$CDCl_3$	Deuterated chloroform
CD_3OD	Deuterated Methanol
DMSO-d_6	Deuterated Dimethyl sulfoxide
CD_3CN	Deuterated acetonitrile
DMF	N,N'-dimethylformamide
DMSO	Dimethyl sulfoxide
THF	Tetrahydrofuran
ACN	Acetonitrile
ESI	Electrospray Ionization
ET	Energy Transfer
HOMO	Highest Occupied Molecular Orbital
LUMO	Lowest Unoccupied Molecular Orbital
MLCT	Metal to Ligand Charge Transfer
ICT	Intranolecular Charge Transfer
TICT	Twisted Intramolecular Charge Transfer
PET	Photo-induced Electron Transfer
ESIPT	Excited State Intramolecular Proton Transfer
ESICT	Excited State Intramolecular Charge Transfer
TBET	Through Bond Energy Transfer
NIR	Near Infrared
HEPES	4-(2-hydroxyethyl)-1-piperazineethanesulfonic acid
NMR	Nuclear Magnetic Resonance

FTIR	Fourier Transform Infrared
MTT	3-(4,5-dimethylthiazol-2-yl)-2,5-diphenyltetrazolium bromide
CLSM	Confocal Laser Scanning Microscope
DFT	Density Functional Theory
SIM	Structured Illumination Microscopy
SRM	Super resolution Microscopy
PBS	Phosphate Buffer Saline
NEM	N-ethylmaleimide
NAC	N-acetylcystiene

Contents

Contents

Contents

CHAPTER 1

INTRODUCTION

1. Photo-reactive receptors for recognition of biologically important analytes

Certain ions and molecules play an important role in different biological processes. However, presence of such analytes beyond a limiting value may have some adverse consequences on human physiology. Owing to multifarious role played by different analytes in chemical and biological events, specific recognition of ions has indeed become an important topic in contemporary research. Thus, specific detection and quantitative estimation of such analytes is crucial for a variety of applications ranging from diagnostic, clinical biology, environmental sample analysis, probing some biochemical transformations and developing imaging reagent for important biomarkers. Accordingly, serious efforts have been made to develop molecules for qualitative and quantitative recognition of these analytes such as cations, anions and neutral molecules in aqueous medium as well as in biological objects. Most commonly used analytical techniques like voltammetric, potentiometric, methodology using ion sensitive electrodes, titrimetric and high performance liquid chromatography (HPLC) are used for the detection and quantitative estimation of such analytes. Apart from these, use of x-ray fluorescence analyzer or atomic absorption spectrometer is also common for quantitative and qualitative analysis of metal ions. However, many of the above mentioned techniques are either expensive or need multistep sample preparation. Such techniques also involve use of sophisticated instrumentation, long detection time. Few methods also require pre-treatment for sample preparation, which is neither well-suited for quick *in-field* detection nor for *in vivo* studies.

In this context, optical probes that high sensitivity, fast response time, possesses high selectivity towards a specific analyte have special relevance. Impotently, chromogenic sensors offer us the option for real time imaging or visualization of a dynamic process even in biological systems or cells. Such a detection process is often ideally suited for *in-field* visual detection methods for semi quantitative naked eye detection of targeted analytes without resorting to any spectroscopic instrumentation. Among such chromogenic reagents, fluorescence based molecular probes have an obvious edge for higher sensitivity as well as for the possibility of using such reagents for imaging application for living cells with higher resolution. Designing of an efficient

chemosensor involves an appropriate choice of receptor unit that is attached to another suitably chosen signaling unit through a conduit for effective signal transduction upon receptor-analyte binding. Choice of the receptor fragment depends on the nature of the target analyte, while that for the signaling unit, it depends on the nature of the optical responses that one desires.

1A. Artificial receptors for Cysteine Recognition

1A.1 Introduction

Among the sulphur containing bio thiols, Cysteine (Cys) is a unique example that has several distinctive features. Higher reactivity and flexibility in participating in various reactions through its sulfhydryl functionality have made it unique in the biological milieu. Cys is frequently found in metal binding sites of proteins where it serves catalytic and regulatory functions. Cys thiols are capable of forming intra and inter chain disulfide bonds between the protein chains.[1] Further, Cys thiols are also known to play a role in redox regulation through the formation of sulfinic acid intermediates as well as mixed disulfides with glutathione (GSH).[2] Cys is one of the three main precursors required for the synthesis of Glutathione (GSH), which is ultimately responsible for maintaining redox immunity in human physiology. Deficiency of Cys has adverse influences on child growth, depigmentation of hair, edema, liver damage, skin lesions and weakness. While its elevated level is responsible for neurotoxicity, cardiovascular and Alzheimer's diseases.[3] Also, some recent studies suggest that in humans, Cys mutations lead to genetic diseases.[1] Thus, understanding the role of Cys in various biochemical transformations or processes and its detection as well as quantification have deeper biological significance. In this regard, significant attention is paid to develop some methods for the specific detection/quantification of Cys either under physiological conditions or in different biofluids. Such methods include high-performance liquid chromatography (HPLC), optical (fluorescence and electronic) spectroscopy and electrochemistry.[4] Among these methods, HPLC is believed to be very sensitive and accurate but it requires post-column derivatisation of sample, as Cys doesn't absorb in the visible region of the spectrum. HPLC is time consuming as well as expensive and requires experienced man power. Moreover HPLC, electrochemical and colorimetric techniques are only limited for *in vitro* studies.[2] Hence,

fluorescence/luminescence techniques or fluorescence-based molecular probes are particularly attractive because of their high sensitivity, obvious ease in the detection process, spatio temporal as well as real time in vivo as well as in vitro analysis of Cys is biofluids, physiological conditions and exogenous or intracellular Cys. Because of the structural similarity between Cys, Homocysteine (Hcy) and GSH (Figure 1A.1), the development of fluorescence-based molecular probe that is specific for protein residues having pendant Cys functionality has special significance in chemistry, biology and clinical diagnostic.

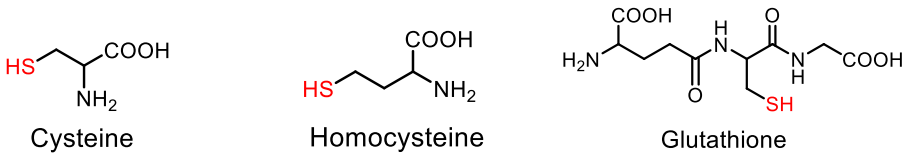

Figure 1A.1. Molecular structures of biothiols.

Considerable efforts have been devoted in last decades for developing Cys-specific reagents. To overcome the problem posed by high solvation enthalpy zwitterionic Cys species in aqueous medium as well as the weak ion-dipole interaction between Cys species and the receptor molecule at neutral pH, researchers have adopted an alternate methodology by using appropriate chemodosimetric reagents. Several approaches were proposed based on chemodosimetric methods. In this Chapter, probes that are reported for detection and quantification of Cys are summarized. We shall specifically focus on the design aspects of synthetic small-molecular probes, new sensing mechanisms, and their interesting biological applications.

1A.2 Various receptors for Cysteine

1A.2.1 Acrylate based Receptors

Since 1966, when the reaction between Cys with acrylates first reported, Michael addition and subsequent cyclization are being used for synthesise of substituted 7-membered cyclic 1,4-thiazepines.[5] It involves nucleophilic 1,4 addition of free sulfhydryl group (-SH) of Cys to acrylate to yield a thioether (Figure 1A.2), which further undergoes cyclization to produce 1,4-thiazepines derivatives. This synthetic strategy was first successfully exploited by Strongin and his co-workers for developing a new chemodosimetric reagent for Cys

detection.[6] Acrylate moiety provided option for reaction site and also it quenched fluorophore's emission due to its effective photo induced electron transfer (PET) mechanism.[7]

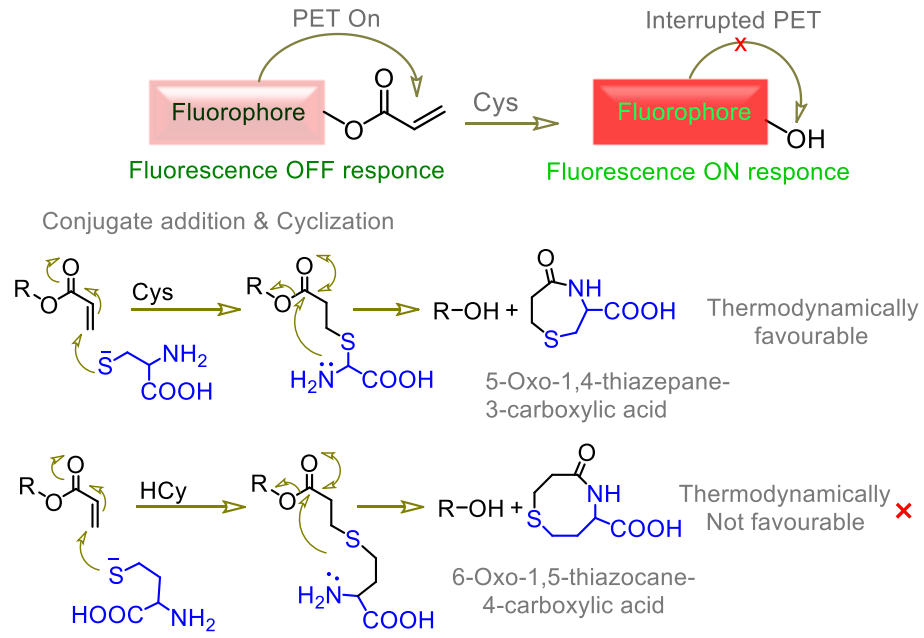

Figure 1A.2. Schematic representation of the generalized acrylate based chemodosimetric reaction for recognition of Cys and following general mechanism of conjugate addition and cyclization reactions.

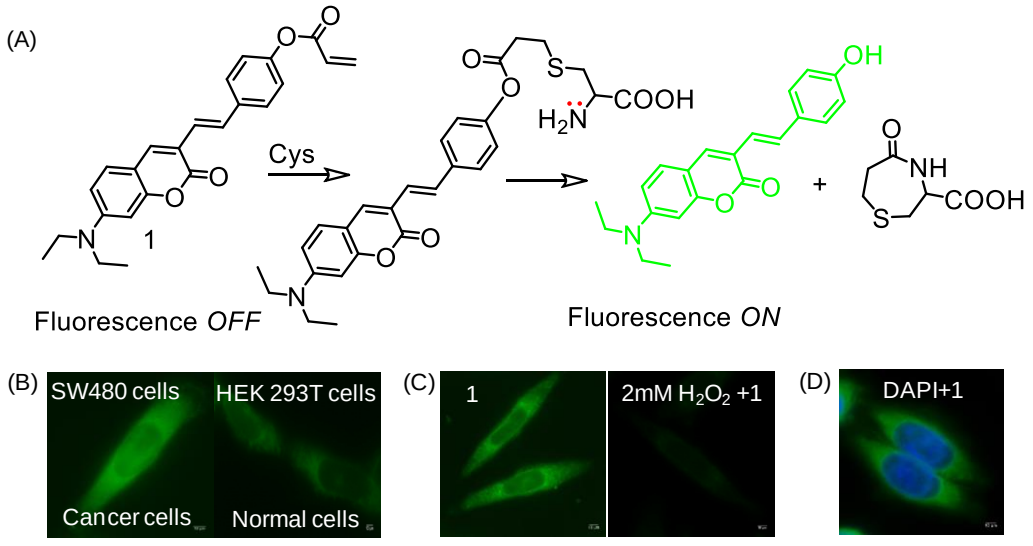

Figure 1A.3. (A) Mechanism for Cys sensing using an acrylate-based derivative; (B) Intracellular detection of Cys and comparison of Cys level in Cancereous and normal cells; (C) Confocal laser scanning microscopic images of SW480 cells incubated with **1** (10 μM) for 30 min in absence and presence of 2 mM H_2O_2; (D) Co-staining studies of **1** with DAPI. (Reprinted with permission form ref. 8. Copyright American Chemical Society).

Specificity towards Cys over structurally higher analogue Hcy typically depends on the rate of intramolecular cyclization of the Cys adducts compared to the Hcy as well as GSH. The higher thermodynamic stability of the seven membered cyclic intermediate for Cys attributes to the higher reaction rate or activity towards acrylate-based functionality. Das *et al*. reported an extended coumarin based derivative (**1**), appended with an acrylate group for this purpose.[8]

Nucleophilic addition reaction involving free sulfhydryl group (-SH) of Cys, resulted α,β-unsaturated ester, which participated in an intramolecular cyclization reaction to regenerate phenolate derivative with fluorescence *ON* response (Figure 1A.3). This probe was further used for the quantification of an important mammalian enzyme like aminoacylase-I in human blood serum as well as for monitoring H_2O_2 induced oxidative stress in live cells. Moreover, probe **1** could be used to detect in situ generated Cys, produced through biochemical transformations induced by aminoacylase-I of a commercial drug N-acetyl Cysteine (NAC).

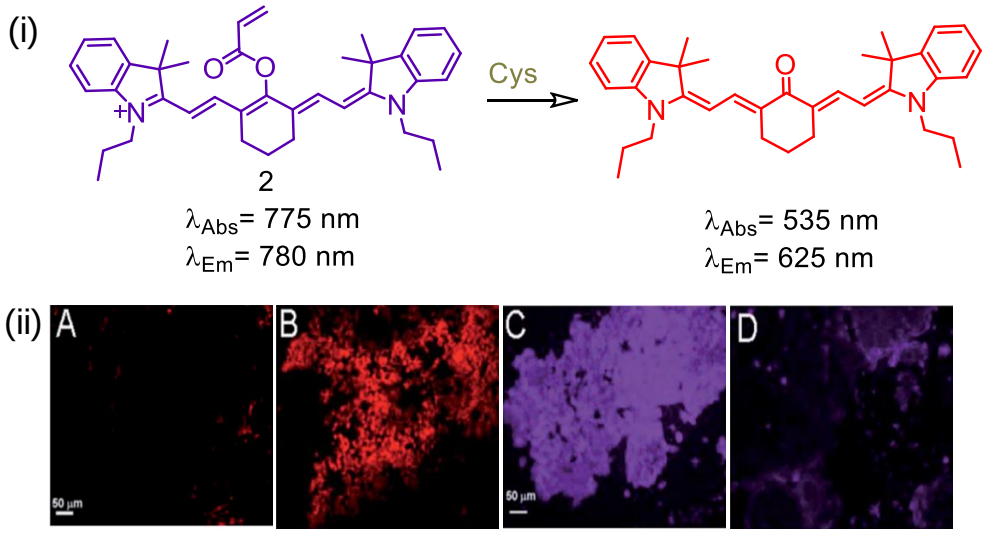

Figure 1A.4. (i) Molecular structures for the receptor (**2**) and product on reaction with Cys; (ii) confocal laser scanning microscopic (CLSM) images of MCF-7 cells grown in McCoy media (A), (C) on incubation with glucose-free DMEM, (B), (D); such cells on further incubation with **2** (5 μM) for 30 min in an EtOH:aq. HEPES buffer (1 : 9, 0.01 M, pH 7.4) medium. (A) and (B) the excitation wavelength is 510 – 560 nm and the fluorescence images were collected at 590 nm; (C) and (D) the excitation wavelength is 660 - 750 nm and the fluorescence images were collected at 760–855 nm. (Reprinted with permission form ref. 9. Copyright the Royal Society of Chemistry).

Yoon *et al*. developed a Cyanine based Near Infrared (NIR) active chemodosimeter (**2**) to detect Cys in a ratiometric fashion in EtOH-aq. HEPES

buffer (1:9, v/v, pH 7.4) medium.[9] Reaction of Cys with the acrylate functionality caused a decrease in absorption band in NIR region (775 nm, ε = 1.6 x 10^5 M^{-1} cm^{-1}) and a new band appeared at 515 nm (ε = 4 x 10^4 M^{-1} cm^{-1}) with a isosbestic point at 605 nm. This attributed to a visual colour change from light blue to red. This probe **2** was successfully utilised to detect intracellular Cys in live breast cancer cells (MCF-7 Cells).

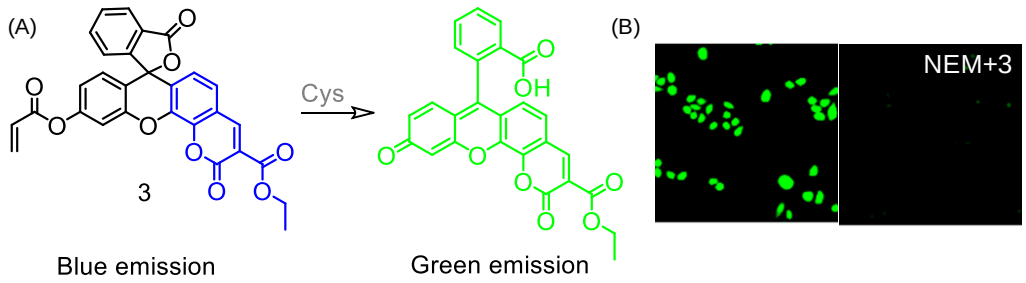

Figure 1A.5. (A) Molecular structure of **3**; (B) Intracellular detection of Cys using **3**. (Reprinted with permission form ref. 10. Copyright American Chemical Society).

Peng and co-worker recently developed a dual mode fluorescent probe (**3**) having fluorescein and coumarin as luminophores for rapid and specific detection of Cys in ratiomatric manner in DMSO-aq. PBS buffer (3:7, v/v; pH 7.4) medium.[10]

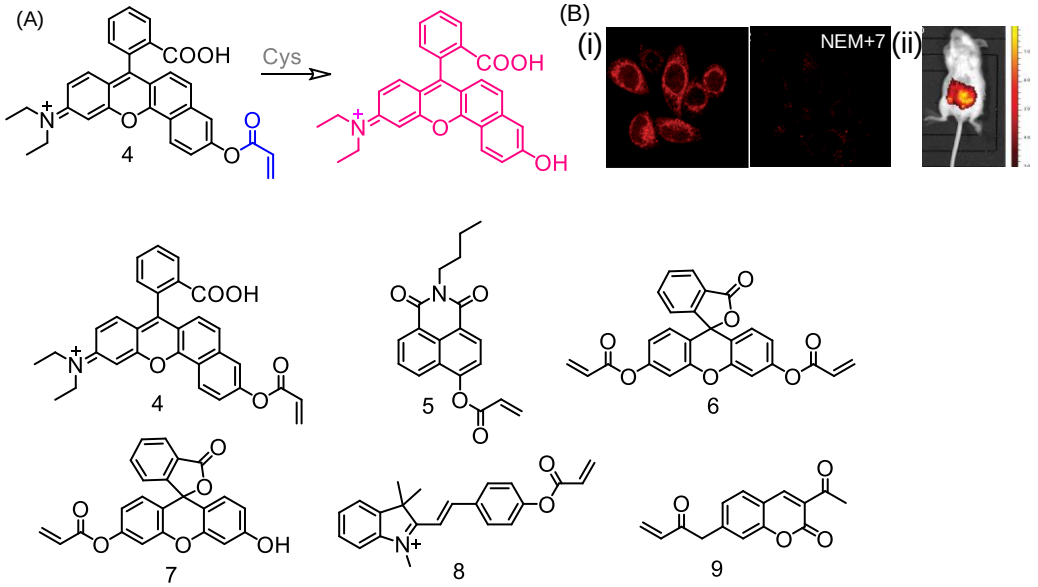

Figure 1A.6. Molecular structures of receptors **4** - **9**. (Reprinted with permission form ref. 11. Copyright the Royal Society of Chemistry).

Upon excitation at 332 nm, a strong emission signal at ~ 472 nm was observed, which was attributed to a coumarin-based emission. With subsequent increase in Cys concentration a new emission band having a maximum at 540 nm appeared with concomitant decrease in the previous band having maximum at 472 nm. This new emission band was attributed to the ring-opening structure of fluorescein. Lower detection limit was evaluated for Cys as 0.084 μM, a value much lower than the intracellular Cys concentration and was used to detect intracellular Cys in liver cancer cells (HepG2 Cells). Proposed mechanistic pathway was further rationalized by DFT studies.

Lin *et al*. presented a rhodamine based probe (4) for the detection of Cys (Figure.1.6), with a turn *ON* emission response (λ_{Max} = 638 nm) using λ_{Ext} of 580 nm in aq. PBS buffer (20 mM, 5% CH_3OH, pH: 7.4) in living cells and Mice.[11]

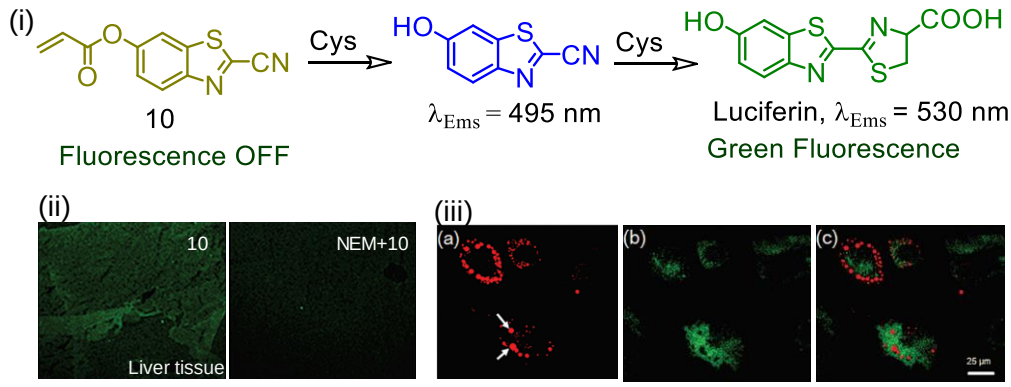

Figure 1A.7. (i) Scheme showing the reactions of Cys with the receptor molecule **10**; (ii) CLSM images in mouse liver tissues using reagent **10** (10 μM) following reaction with intracellular Cys (incubation time: 30 min in absence and presence of NEM); (iii): (a - c) CLSM images of adipogenic hMSCs after staining with **10** and Oil Red O. The cells were incubated with **10** (20 mm) at 37°C for 30 min, and the medium was then replaced with 0.3% Oil Red O solution and incubated for 20 min at room temperature. Images for Oil Red O (a) and **10** (b) were acquired using excitation wavelengths of 543 and 405 nm, and band-path emission filters at 550–650 nm and 475–575 nm, respectively. (Reprinted with permission form ref. 11. Copyright Wiley).

This ideology was further exploited for designing few other reagents for specific detection of Cys (Figure 1A.6).[11-15]

Zhang *et al*. demonstrated a new luciferine based probe for the detection of endogenous Cys with a fluorescent *ON* response.[16] This probe also was also useful for the *in-vivo* detection of Cys in tissues of mouse liver (Figure 1A.7). Moreover, this reagent could be used to evaluate Cys levels in human mesenchymal stem cells during adipogenic differentiation. Importantly, reagent

was successfully utilised for detection of Cys level in live cells under oxidative stress induced by H_2O_2 (Figure 1A.7).

With slight structural modification, Kim and co-worker had developed a new reagent based on crotonoyl ester-functionalized oxazolidinoindole (**11**) for the detection of Cys in aq-HEPES buffer medium at physiological pH.[17] As shown in Figure 1A.8, nucleophilic addition reaction of Cys is followed by cyclization to yield hydroxyethylindolium with a fluorescence *ON* response (λ_{Ext} = 405 nm, λ_{Ems} = 556 nm). A remarkable bathochromic shift (>130 nm) in the UV – vis was observed along with a distinct visual change in solution colour (Figure 1A.8). The reaction pathway was confirmed by ^{1}HNMR studies. Imaging experiment suggested that the probe (**11**) was preferentially localised in mitochondrial part of the HeLa cells and was useful for mapping the distribution of mitochondrial Cys. This was further supported by the observed decrease in the intracellular Cys level when cells pretreated with lipopolysaccharide (LPS) were used. Cells treated with LPS, showed ~20% decrease in emission intensity compared to untreated LPS cells, as part of the intracellular Cys was utilized for scavenging free radical that was generated by LPS.

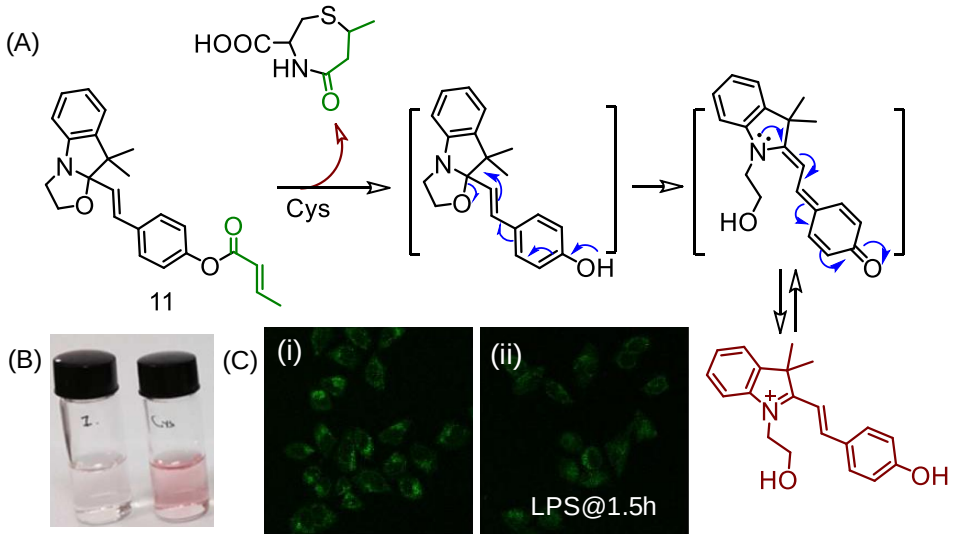

Figure 1A.8. (A) Scheme showing the reaction of **11** with Cys; (B) photographs showing the visual change in solution colour of **11** in absence and presence of Cys; (C) CLSM images of HeLa cells treated with **11** in the presence and absence of LPS. (Reprinted with permission form ref. 17. Copyright American Chemical Society).

Excited state proton transfer (ESIPT) based fluorescent probes have received significant attention due to their unique photophysical properties like fast reaction rates, large Stokes' shift (>150 nm), which minimizes the possibility for

self-absorption and reduce the interference from auto-fluorescence for *in-vivo* application.

Strongin and co-workers introduced a novel ESIPT based probe using 2-(2'-hydroxyphenyl)benzothiazole (HBT) appended with acrylate (**12**), for the detection of Cys with an associated fluorescence *ON* response (Figure 1A.9).[18]

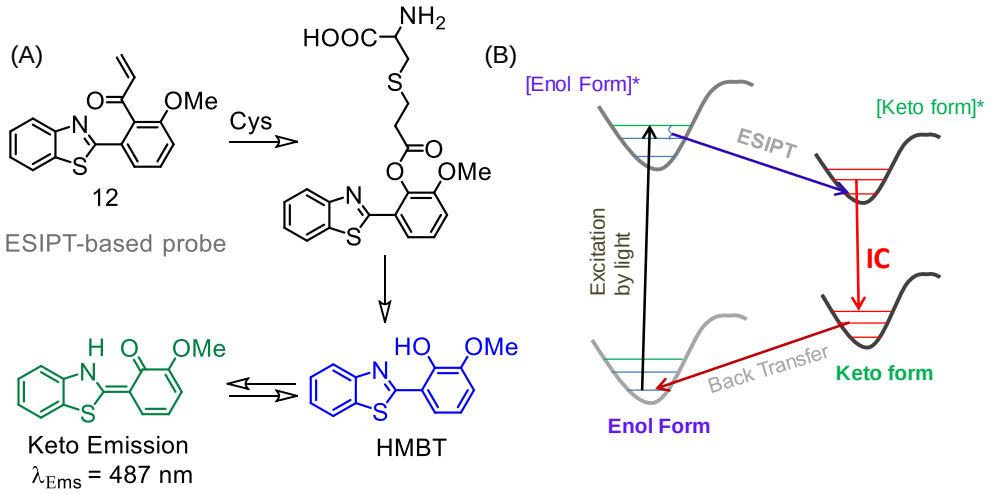

Figure 1A.9. (A) Scheme depicting the conjugate addition and cyclization strategy for Cys recognition; (B) Schematic representation of ESIPT mechanism.

As discussed earlier, this cyclization process was much slower for Hcy and based on the difference in the relative rates of intramolecular cyclization quantitative estimation for Cys and Hcy was achieved.

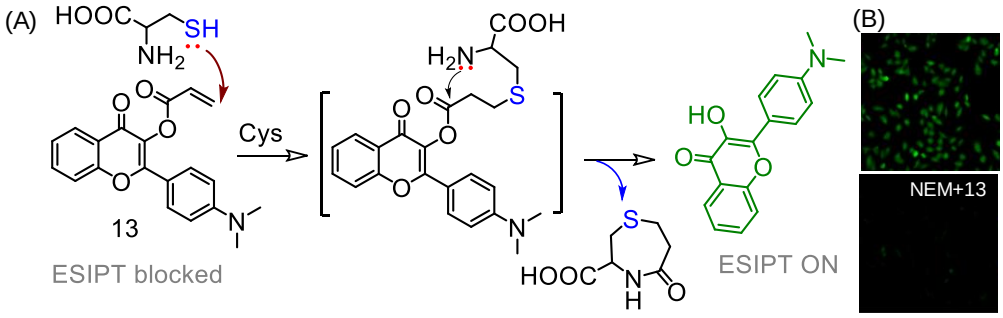

Figure 1A.10. (A) Reaction of **13** with Cys and (B) CLSM images of hMSCs cells showing mapping of intracellular Cys. (Reprinted with permission form ref. 19. Copyright American Chemical Society).

In 2014, Pang and co-workers reported a flavone based receptor (**13**) that participated in an ESIPT-based process for selective detection of Cys (Figure 1A.10).[19] Design process involved protecting the flavone hydroxyl group with

acrylate moiety that blocked the ESIPT process. Receptor **13** showed weak blue fluorescent at 380 nm when excited at 350 nm.

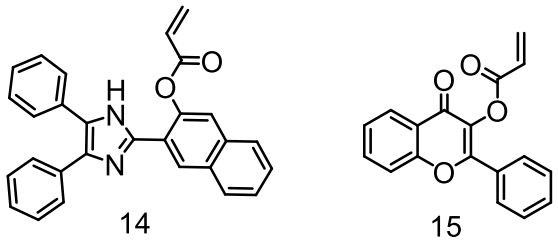

Figure 1A.11. Molecular structures of receptor molecules **14** & **15**.

On reaction with Cys, deprotection reaction was induced by conjugate addition and subsequent cyclization for the release of the free hydroxyl fluorophore, which was found to participate in tautomerism and an ESIPT process for inducing a green emission having maximum at 510 nm.

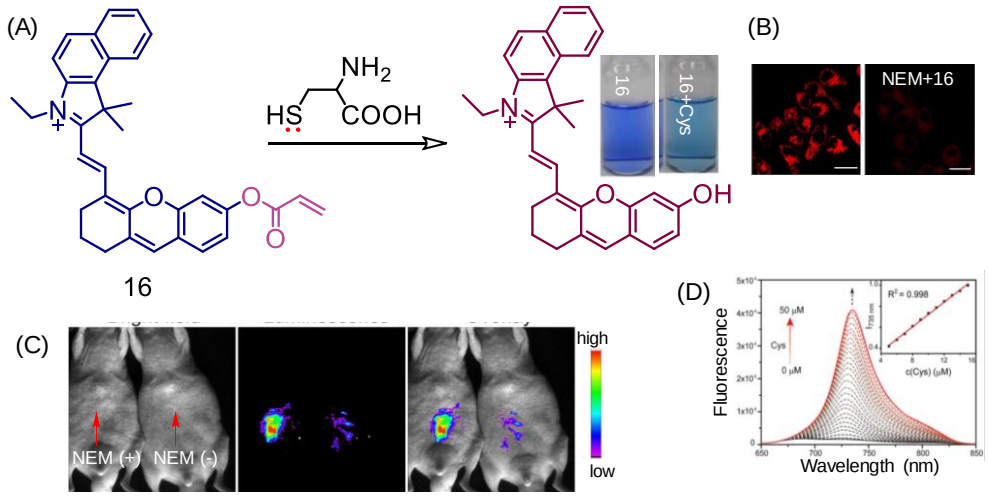

Figure 1A.12. (A) Proposed Mechanism for the Off−On Sensing of **16** for Cys; inset: visual colour changes of Probe **16** in absence and presence of Cys; (B) change in emission spectra of **16** (10 μM) upon the addition of Cys (from 0 to 50 μM) in ethanol/HEPES buffer (1:1 v/v, pH 7.4) at 37 °C for 10 min; (C) CLSM Images of **16** in absence and presence of NEM; (D) in vivo NIR images of living mice. The left mice were injected with probe **16** (10 μM, 0.2 mL) only for 10 min. The right mice were pre injected with NEM (1 mM, 0.2 mL) for 30 min and then injected with **16** (10 μM, 0.2 mL) for 10 min. (Reprinted with permission form ref. 22. Copyright American Chemical Society).

The LOD of probe **13** for Cys was estimated as 1 μM. Probe was successfully utilized for imaging intracellular Cys in human mesenchymal stem cells (hMSCs). This ideology was further exploited for designing few other ESIPT-based reagents **14** & **15** for the detection of Cys (Figure 1A.11).[20,21]

Li *et al*. introduced a Near Infrared (NIR) probe **16** for monitoring endogenous Cys with fluorescence *OFF-ON* manner.[22]

With addition of Cys, NIR emission intensity at 735 nm (λ_{Ext} = 630 nm) was found to be enhanced and this confirmed the formation of the corresponding phenolic derivative.

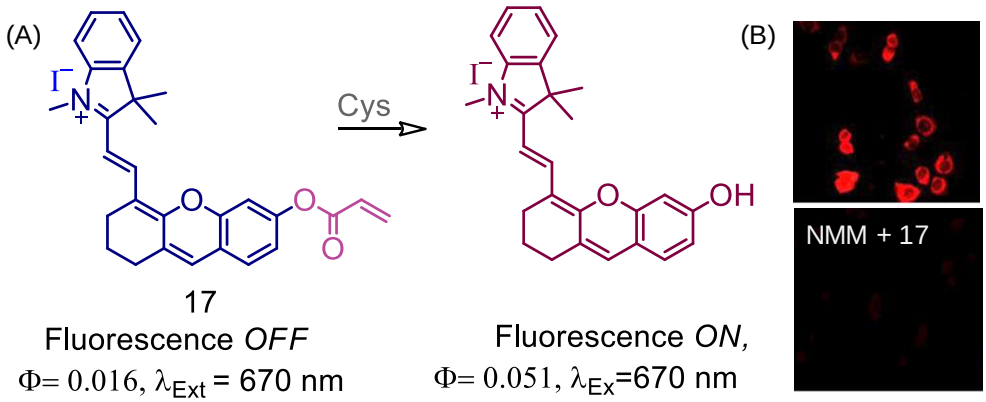

Figure 1A.13. (A) Sensing mechanism of **17** with Cys; (B) imaging in cells with **17** in absence and presence of NMM. (Reprinted with permission form ref. 23. Copyright American Chemical Society).

Reagent **16** was found to be sensitivity and selectivity for the rapid detection of Cys over other analogous and competing thiols with an ultralow detection limit of 14.5 nM.

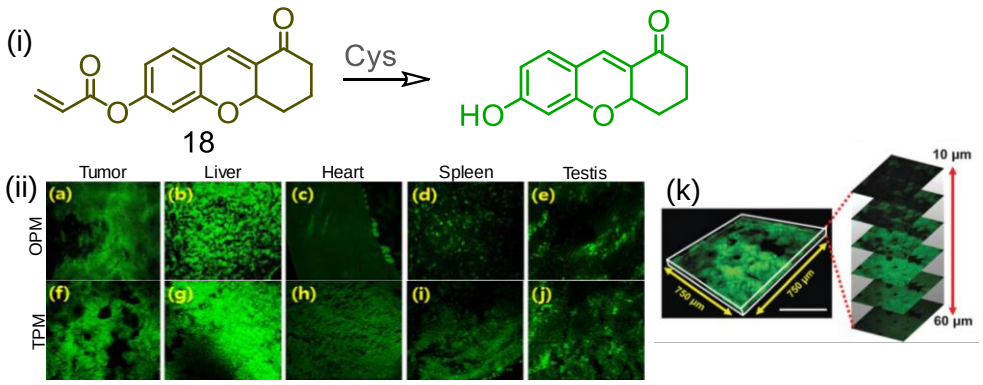

Figure 1A.14. (i) Scheme showing the reaction of **18** with Cys; (ii) (a - e) OPM and (f - j) TPM images of cryo-sectioned xenograft mouse tumors and organs (liver, heart, spleen, and testis) were stained with 10 μM probe **18** for 2 h. (Magnification: 100x), (k) (left) 3D TPM image of tumor labeled with probe **18** (10 μM) at a depth of 10 - 60 μm with magnification at 20x, (right) Serial Z-sections of TPM images of tumor tissue at different depths. (Reprinted with permission form ref. 24. Copyright the Royal Society of Chemistry).

CLSM images revealed that this reagent was localised in mitochondria of the live HeLa cells and thus, it could be used to detect mitochondrial Cys. This reagent was used for *in-vivo* studies using mouse model (Figure 1A.12).

Zhang group reported an analogous NIR derivative **17** (Figure 1A.13).[23] This probe (**17**) was successfully utilized for determination of Cys in diluted blood serum and for bio-imaging of Cys in living cells using CLSM. This reagent showed low cell toxicity.

Two photon probes recently received more attention due to its high penetration depth, low auto fluorescence levels, less photo toxicity, the possibility of three-dimensional imaging of living tissues, and prolonged observation times. Moreover, two photon imaging technique provides enhanced imaging resolution compares to conventional single photon system. Above all, this allows excitation at longer wavelength—a situation ideal for handling biological samples. Kim et al. introduced a two photon probe (**18**), using chromene as the fluorophore for specific detection of Cys.[24] This probe was further used to image intracellular Cys in cancerous cells and various mouse tissues (Figure. 1A.14).

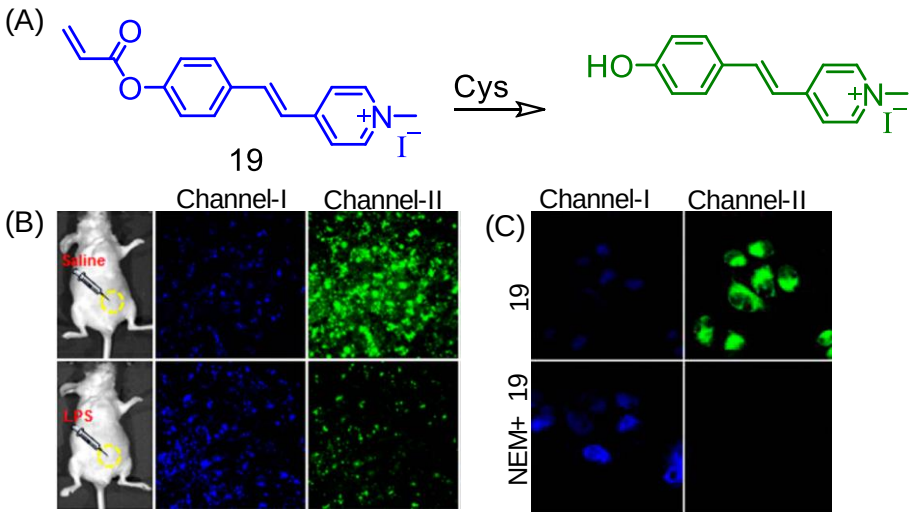

Figure 1A.15. (A) Molecular structure for **19** and proposed reaction between **19** and Cys; (B) two-photon CLSM images in tissue slices injected with **19** (50 μM) after pretreatment with saline (200 μL) and LPS (200 μL, 1.0 mg·mL^{-1}), respectively; (C) two photon confocal microscopy fluorescence images in absence and presence of NEM in living HeLa cells. Channel 1: λ_{Ems} = 430 - 470 nm, Channel 2: λ_{Ems} = 490-530 nm. (Reprinted with permission form ref. 25. Copyright American Chemical Society).

Using similar chemodosimetric approach, Wong *et al*. also reported a two photon ratiometric fluorescent probe **19** for the specific detection of mitochondrial cysteine (Cys) in live Hela cells (Figure 1A.15).[25]

With addition of Cys, a gradual decrease in the absorption band at λ_{Max} = 335 nm (ε_{Max}= 2.09 × 10^4 M^{-1} cm^{-1}) with concomitant increase in absorption intensity having maximum at ~372 nm (ε_{Max} = 2.59 × 10^4 M^{-1} cm^{-1}) were observed. A well-defined isosbestic point at 350 nm was also observed. In addition, fluorescence emission intensity at 452 nm was found to decrease with concomitant increase in intensity at 518 nm. This probe was used to estimate the intracellular Cys in ratiometric manner in live cells and tissue (Figure 1A.15).

Dong and his co-workers reported a two photon NIR probe (**20**) for monitoring the intracellular Cys. This probe exhibit a turn *ON* fluorescence response (λ_{Max} = 702 nm, λ_{Ext} = 850 nm) on specific reaction with Cys. An appreciably large Stokes shift (~150 nm) was also reported.[26] Probe **20** could be used to detect Cys in live cells (Figure 1A.16).

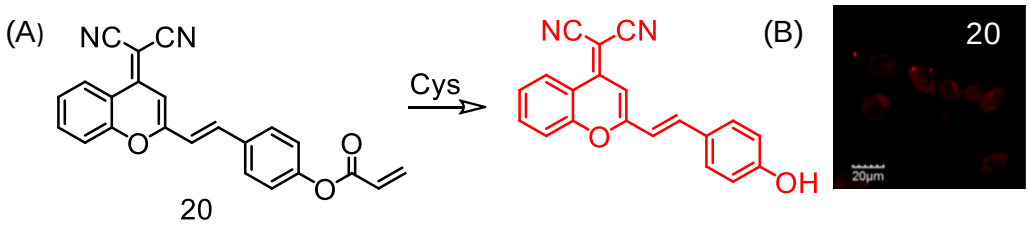

Figure 1A.16. (A) molecular structure for receptor **20** and (B) observed CLSM images for mapping intracellular Cys. (Reprinted with permission form ref. 26. Copyright American Chemical Society).

1A.2.2. Aldehyde based Receptors

Since 1937, it is known that terminal Cys residues react readily with aldehydes to form thiazolidines via cyclised intermediate. This synthetic approach was utilised by the Strongin group to introduce a fluorescent probe for the detection of Cys.[27] However, this probe showed analogous response for Hcy under identical experimental condition. Peng group developed a rhodamine based fluorescent probe that showed good selectivity towards Cys over Hcy (Figure 1A.17).[28] In an ethanol-aq. PBS buffer (3:7 v/v, pH 7.0) solution, this probe was found to be colourless and weakly emissive. On reaction with Cys, an intense

absorbance band appeared at 531 nm, and a strong the fluorescence band having maximum at 552 nm (λ_{Ext} = 500 nm) were developed.

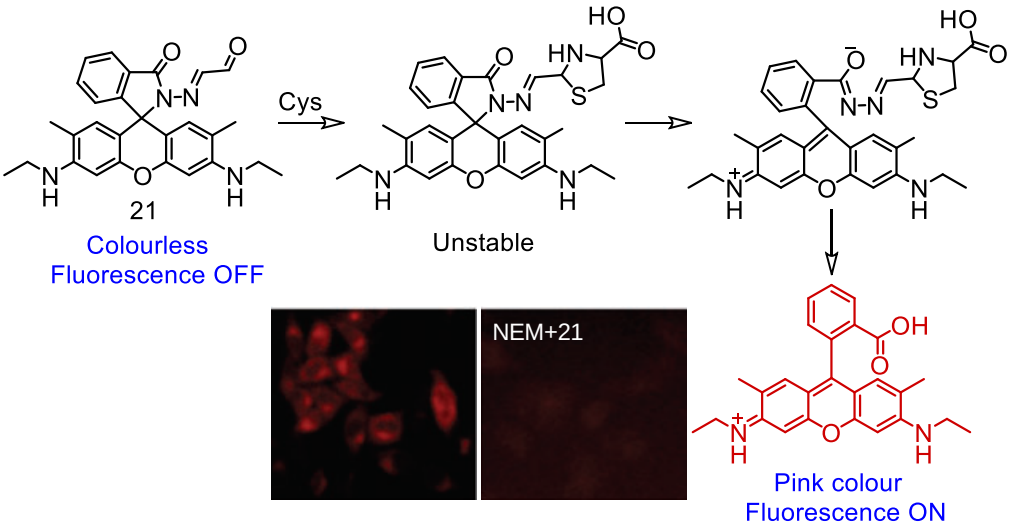

Figure 1A.17. Molecular structure for **21** and possible reaction of **21** prompted by Cys and associated CLSM images of the cells. (Reprinted with permission form ref. 28. Copyright the Royal Society of Chemistry).

Probe having an aldehyde moiety, reacted with Cys to form a cyclic thiazolidine intermediate, which further underwent spirolactam ring-opening and hydrolysis of the intermediate and subsequently resulted an acyclic xanthene derivative.

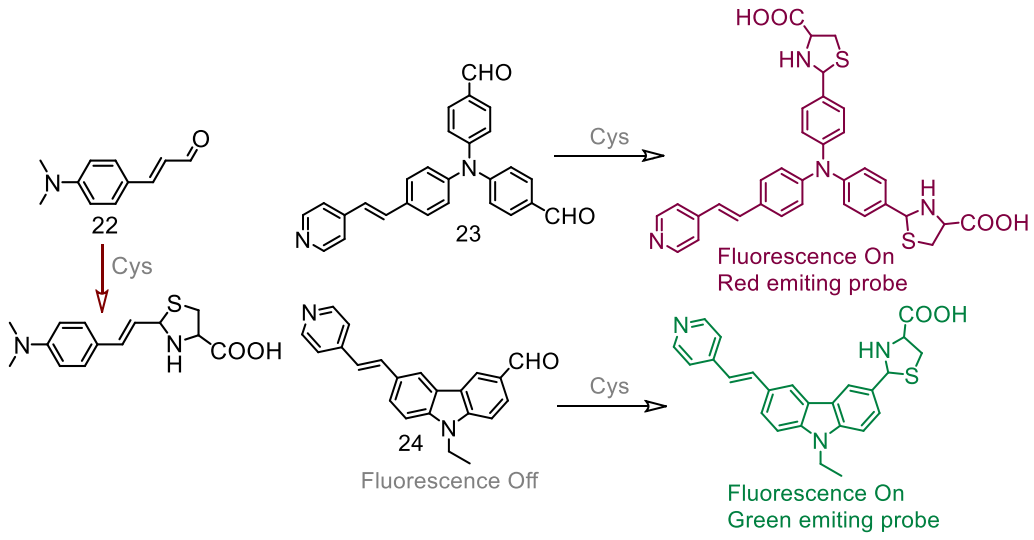

Figure 1A.18. Molecular structures of aldehyde based receptors **22**-**24** for Cys detection

The probe was further used to image Cys in cells as well as for quantification of Cys in human urine sample. Commercially available cinnamaldehyde derivative (**22**) was able to detect Cys specifically in aq. buffer solution.[29] Wong *et al*.

introduced two fluorescent probes for specific detection of Cys with different two photon spectral response (Figure 1A.18).

Probe **23** was found to be weakly emissive in methanol–aq. Tris/HCl buffer solution. Upon reaction with Cys, a fluorescence enhancement was observed with a red-shift of 84 nm (λ_{Ex} = 365 nm). Probe **23** & **24** were also utilized for imaging Cys in live Hela cells.[30]

Lin *et al*. developed a coumarin based ratiometric fluorescent probe **25** for Cys detection.[31] In absence of Cys, probe showed an emission band having maximum at 557 nm (Φ= 0.12) in aq. PBS-CH_3CN (9:1, v/v) under physiological pH medium.

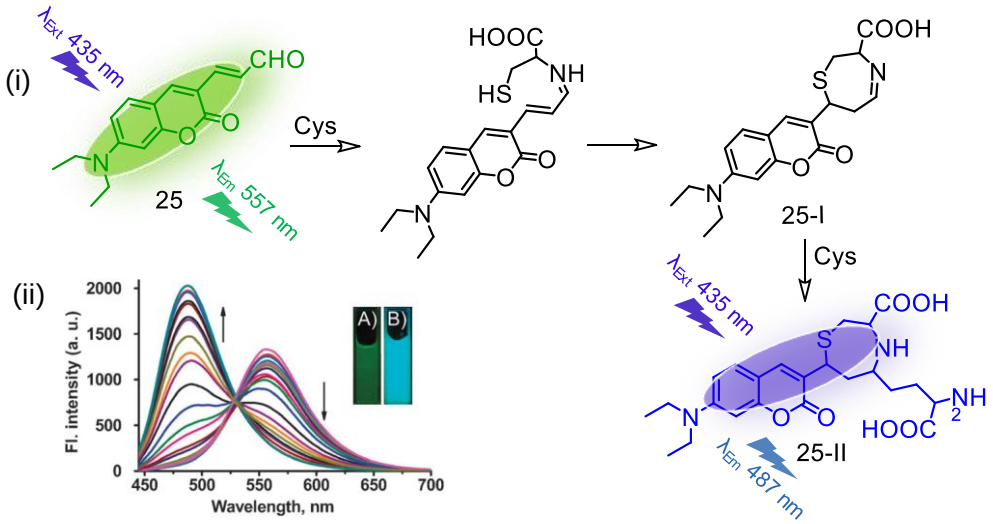

Figure 1A.19. (i) Molecular Structure of the probe **25** and its sensing mechanism with Cys; (ii) change in emission spectra of **25** in presence of Cys: inset: emission colour change of **25** in absence (A) and presence (B) of Cys. (Reprinted with permission form ref. 31. Copyright the Royal Society of Chemistry).

On addition of Cys, intensity of the emission band at 557 nm was found to decrease and subsequently a new band appeared at 487 nm (Φ= 0.25) upon excitation at 435 nm. Furthermore, the emission ratios (I_{487}/I_{557}) are linearly proportional to the amount of Cys (2 - 900 μM). Initially, free amino group ($-NH_2$) of Cys reacted with aldehyde moiety to form an imine intermediate (**25-I**), which further underwent cyclization to form another cyclic intermediate (**25-II**). Eventually this intermediate reacted with another Cys to form stable **25-III** adduct (Figure 1A.19). This probe utilised for ratiometric imaging of variations of Cys levels in the living cells.

Probe **26** could detect Cys selectively, based on of aggregation induced emission (AIE) phenomenon.[32]

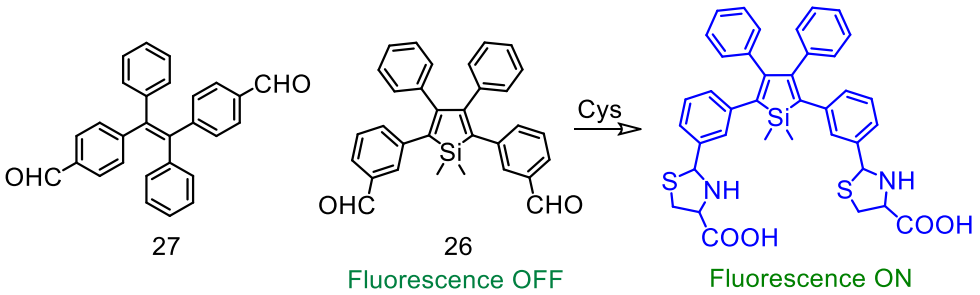

Figure 1A.20. Molecular structure of the probes **26** & **27.**

Probe **26** showed a weak emission band (λ_{Ems}) at 479 nm following excitation at 377 nm in DMSO- aq. HEPES buffer medium. With addition of Cys, an increased fluorescence response was observed for **26**, due AIE mechanism (Figure 1A.20).

1A.2.3. Michael addition based Receptors

1,4-addition of a nucleophile to an α,β-unsaturated carbonyl moiety is generally known as Michael addition. Owing to strong nucleophilicity of thiols, this reaction is being widely used as a basis for designing fluorescent probes for biothiols. Although biothiols are structurally similar, large difference in pK_a among Cys, Hcy and GSH (8.23, 10.0 and 9.2 respectively) as well as the associated steric factor play a crucial role in getting the selectivity. As, Cys having lower pK_a value at neutral pH, thiolate/thiol ratio is relatively higher for Cys compare to Hcy and GSH, which results in a better reactivity of Cys towards nucleophilic addition reaction.

Using this strategy, Kim and co-workers introduced a series of coumarin flurophores with extended conjugation having quinolone (**28**, **29** and **30**) fragment as the reaction site for selective detection of Cys (Figure 1A.21).[33] Initially these compounds were non-fluorescent in aqueous solution (10 mM PBS buffer, pH 7.4, 10% DMSO) due to an intramolecular charge transfer (ICT) process that was operational between coumarin moiety and conjugated ketone. Upon addition of Cys, conjugation was disrupted and this interrupted the ICT process, which resulted in the fluorescence *ON* response. Probe **30** could

detect Cys at the 10^{-7} M level in physiologically relevant aqueous environments. The probe was also applied for imaging intracellular Cys in HepG2 cells.

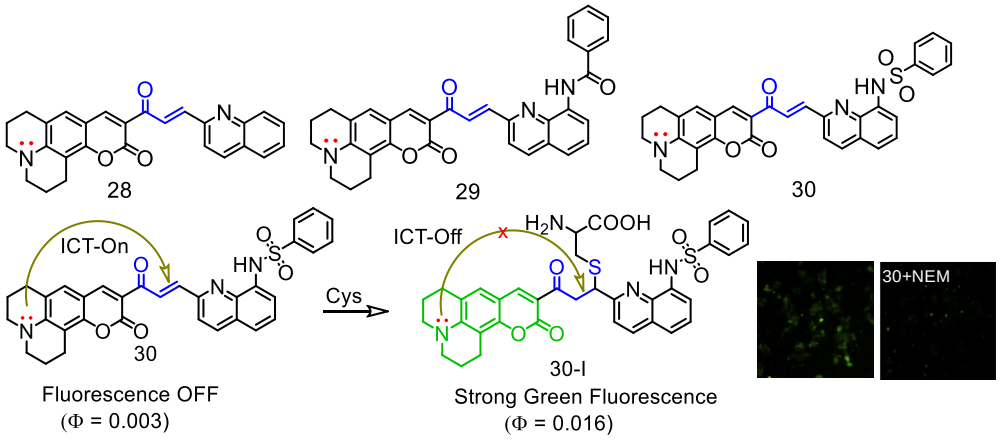

Figure 1A.21. Molecular structure of the probes **28**-**30** and sensing mechanism of **30.** (Reprinted with permission form ref. 33. Copyright Elsevier).

Wu *et al.* reported a fluorescent probe **31** for fast and selective detection of Cys based on Michael addition and response-assisted electrostatic attraction (Figure 1A.22).[34] The probe reagent underwent a Michael addition reaction with the free sulfhydryl group of Cys and this resulted modified colorimetric as well as fluorescent responses.

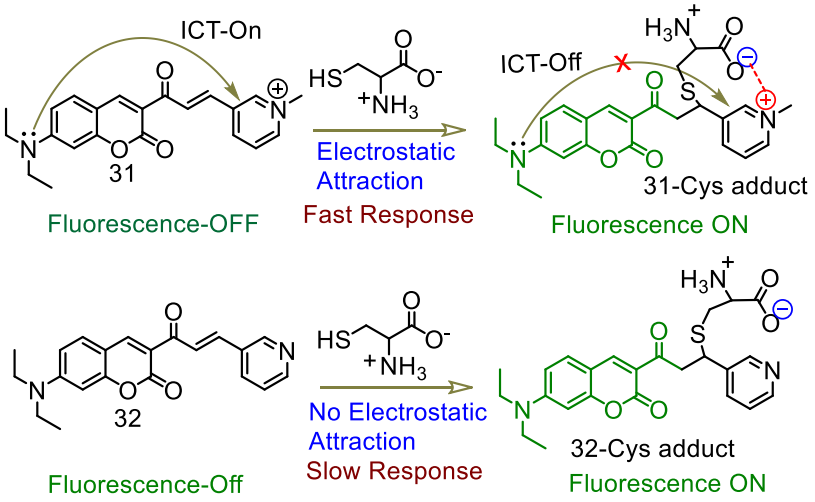

Figure 1A.22. The design concept for molecular probes **31** and **32** for Cys detection.

Free reagent **31** was found to be non-fluorescent in PBS buffer solution (Φ= 0.001, λ_{Ext} = 450 nm) due to an efficient ICT process was operational involving diethylamino group as donor and electron-deficient pyridinium moiety as acceptor. Among the tested amino acids, only those with free thiol functionality

(Cys, Hcy and GSH) showed turn *ON* fluorescence response and a blue shifted absorbance spectrum. Receptor **31** showed preference for Cys among these three biothiols and the reactivity followed the order Cys > Hcy > GSH. Upon treatment of Cys, **31**-Cys adduct was formed and accounted for the new emission band at 500 nm with significant increase (140 fold) in its intensity. Adduct formation disfavoured the ICT process, which results in the observed optical spectral changes. The LOD for Cys was evaluated as low as 25 nM.

Das and his co-workers had developed a nitro olefin derivative of coumarin as colorimetric and fluorescent probe for selective detection of Cysteine.[35] Probe showed absorption band maxima at 468 nm in aq. buffer medium and was found to be non-fluorescent because an ICT process was operational between donor diethylamino group and nitro olefin acceptor. In addition, nitro olefin itself acts as a fluorescent quencher through PET process (Figure 1A.23).

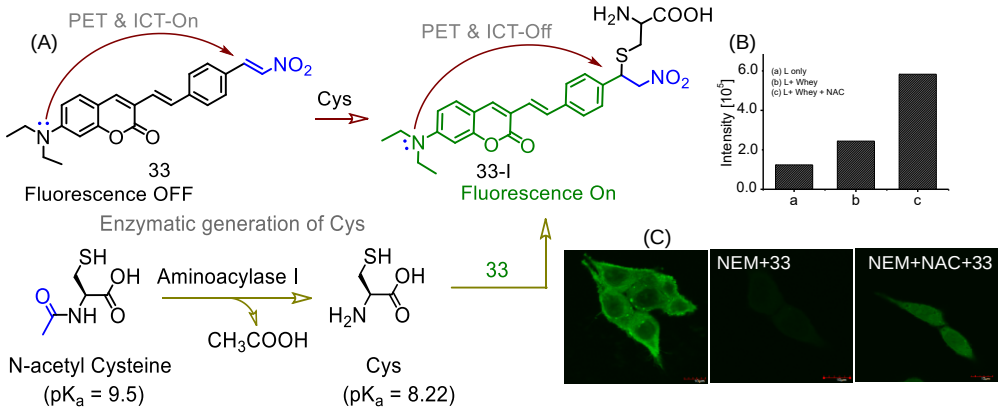

Figure 1A.23. (A) Hydrolysis of NAC by aminoacylase-1 and subsequent reaction of in situ generated Cys with **33**; (B) fluorescence response of **33 (10 μM)** with whey protein (500 μl) before and after treatment with NAC (500 μL). Spectra were recorded after incubating the samples at 37°C for 45 minutes; (C) CLSM images of **33** in presence of NEM and NAC. (Reprinted with permission form ref. 35. Copyright the Royal Society of Chemistry).

Michael addition of Cys to nitro olefin disrupt the ICT and PET processes, which resulted in colour change from red to pale green with a bright green fluorescence at 520 nm. The probe was successfully applied for imaging intracellular Cys present in Hct116 cell lines. Importantly, this reagent was used for detection of Cys generated from the enzymatic activity of aminoacylase-1 on a commercially available pro-drug N-acetyl cysteine. Enzymatic released Cys detection was also performed in living HepG2 cell lines as well. Further, probe

was applied to detect free as well as protein bound Cys present in whey protein isolated from fresh cow milk.

1A.3. References

1. S. M. Marino and V. N. Gladyshev, *J. Biol. Chem.*, 2012, **287**, 4419.
2. S. García-Santamarina, S. Boronat and E. Hidalgo, *Biochemistry*, 2014, **53**, 2560.
3. X. Yuan, Y. Tay, X. Dou, Z. Luo, D. T. Leong and J. Xi, *Anal. Chem*., 2013, 85, 1913; (b) M. Zhang,M. Yu, F. Li, M. Zhu, M. Li, Y. Gao, L. Li, Z. Liu, J. Zhang, D. Zhang, T. Yi and C. Huang, *J. Am. Chem. Soc*., 2007,**129**, 10322.
4. L.-Y. Niu, Y.-Z. Chen, H.-R. Zheng, L.-Z. Wu, C.-H. Tung and Q.-Z. Yang, *Chem. Soc. Rev.*, 2015, **44**, 6143.
5. (a) P. Blondeau, R. Gauthier, C. Berse and D. Gravel, *Can. J. Chem*.,1971, **49**, 3866–3876; (b) N. J. Leonard and R. Y. Ning, *J. Org. Chem*., 1966, **31**, 3928.
6. X. Yang, Y. Guo and R. M. Strongin, *Angew. Chem., Int. Ed.*, 2011, **50**, 10690.
7. H. S. Jung, X. Chen, J. S. Kim and J. Yoon, *Chem. Soc. Rev*., 2013, **42**, 6019.
8. H. A. Anila, F. Ali**,** S. Kushwaha, N. Taye, S. Chattopadhyay and A. Das, *Anal. Chem***.,** 2016, **88**, 12161.
9. Z. Guo, S. Nam, S. Park and J. Yoon, *Chem. Sci.*, 2012, **3**, 2760.
10. Z.-H. Fu, X. Han, Y. Shao, J. Fang, Z.-H. Zhang, Y.-W. Wang and Y. Peng, *Anal. Chem*., 2017, **89**, 1937.
11. X. Song, B. Dong, X. Kong, C. Wang, N. Zhang and W. Lin, *Anal. Methods*, 2017, **9**, 1891.
12. B. Zhu, B. Guo, Y. Zhao, B. Zhang, B.Du, *Biosensors and Bioelectronics*, 2014, **55**, 72.
13. H. Wang, G. Zhou, H. Gaib and X. Chen, *Chem. Commun*., 2012, **48**, 8341.
14. Q. Han, Z. Shi, X. Tang, L. Yang, Z. Mou, J. Li, J. Shi, C. Chen, W. Liu, H. Yang and W. Liu, *Org. Biomol. Chem*., 2014, **12**, 5023.
15. X. Dai, Q.-H. Wu, P.-C. Wang, J. Tian, Y. Xua, S.-Q. Wang, J.-Y. Miao, B.-X. Zhao, *Biosensors and Bioelectronics*, 2014, **59**, 35.
16. M. Zheng, H. Huang, M. Zhou, Y. Wang, Y. Zhang, D. Ye and H.- Y. Chen, *Chem. Eur. J*., 2015, **21**, 10506.
17. C. Y. Kim, H. J. Kang, S. J. Chung, H.-K. Kim, S.-Y. Na and H.-J. Kim, *Anal. Chem*., 2016, **88**, 7178.
18. X. Yang, Y. Guo and R. M. Strongin, *Angew. Chem. Int. Ed*., 2011, **50**, 10690.
19. Y. Liu, D. Yu, S. Ding, Q. Xiao, J. Guo and G. Feng, *ACS Appl. Mater. Interfaces*, 2014, **6**, 17543.

20. Y. Zhang, J.-H. Wang, W. Zheng, T. Chen, Q.-X. Tong and D. Li, *J. Mater. Chem. B*, 2014, **2**, 4159.

21. B. Liu, J. Wang, G. Zhang, R. Bai and Y. Pang, *ACS Appl. Mater. Interfaces*, 2014, **6**, 4402.

22. C. Han, H. Yang, M. Chen, Q. Su, W. Feng and F. Li, *ACS Appl. Mater. Interfaces*, 2015, **7**, 27968.

23. J. Zhang, J. Wang, J. Liu, L. Ning, X. Zhu, B. Yu, X. Liu, X. Yao and H. Zhang, *Anal. Chem*., 2015, **87**, 4856.

24. Y. H. Lee, W. X. Ren, J. Han, K. Sunwoo, J.-Y. Lim, J.-H. Kim and J. S. Kim, *Chem. Commun*., 2015, **51**, 14401.

25. W. Niu, L. Guo, Y. Li, S. Shuang, C. Dong and M. S. Wong, *Anal. Chem*., 2016, **88**, 1908.

26. J. Wang, B. Li, W. Zhao, X. Zhang, X. Luo, M. E. Corkins, S. L. Cole, C. Wang, Y. Xiao, X. Bi, Y. Pang, C. A. McElroy, A. J. Bird and Y. Dong, *ACS Sens*., 2016, **1**, 882.

27. O. Rusin, N. N. St Luce, R. A. Agbaria, J. O. Escobedo, S. Jiang, I. M. Warner, F. B. Dawan, K. Lian and R. M. Strongin, *J. Am. Chem. Soc*., 2004, **126**, 438.

28. H. Li, J. Fan, J. Wang, M. Tian, J. Du, S. Sun, P. Sunb and X. Peng, *Chem. Commun*., 2009, 5904.

29. W. Wang, O. Rusin, X. Xu, K. K. Kim, J. O. Escobedo, S. O. Fakayode, K. A. Fletcher, M. Lowry, C. M. Schowalter, C. M. Lawrence, F. R. Fronczek, I. M. Warner and R. M. Strongin, *J. Am. Chem. Soc*., 2005, **127**, 15949.

30. Z. Yang, N. Zhao, Y. Sun, F. Miao, Y. Liu, X. Liu, Y. Zhang, W. Ai, G. Song, X. Shen, X. Yu, J. Sun and W.-Y. Wong, *Chem. Commun*., 2012, **48**, 3442.

31. L. Yuan, W. Lin and Y. Yang, *Chem. Commun*., 2011, **47**, 6275.

32. J. Mei, Y. Wang, J.Tong, J. Wang, A. Qin, J. Z. Sun and B. Z. Tang, *Chem. Eur. J*., 2013, **19**, 613.

33. H. S. Jung, J. H. Han, T. Pradhan, S. Kim, S. W. Lee, J. L. Sessler, T. W. Kim, C. Kang, J. S. Kim, *Biomaterials*, 2012, **33**, 945.

34. X. Zhou, X. Jin, G. Sun, D. Li and X. Wu, *Chem. Commun*., 2012, **48**, 8793.

35. H. A. Anila, U. G. Reddy, F. Ali, N. Taye, S. Chattopadhyay and A. Das, *Chem. Commun*., 2015, **51**, 15592.

1B. Artificial receptors for Chromium Recognition

1B.1 Introduction

The sensitive and selective screening of trivalent chromium (Cr^{3+}) levels both *in-vivo* and *in-vitro* are crucial, considering their indispensable role in various biological processes.[1] Chromium is a widespread element of earth's crust and sea water.[2] It can exist in various oxidation states principally as metallic (Cr^{0}), trivalent (Cr^{3+}) and hexavalent (Cr^{+6}) forms. Among these, Cr^{3+} is found in most food and nutrient supplements. Arguably, Cr^{3+} is an essential nutrient with very low toxicity for human physiology.[3] Trivalent Chromium, Cr^{3+} is an important analyte for biological processes like metabolism of nucleic acid, proteins carbohydrate and fats.[4] Cr^{3+} is found to be involved in activation of certain enzymes and stabilization of certain proteins and nucleic acids.[5] Deficiency of Chromium adversely influences human physiology and causes many chronic diseases such as diabetes, cardiovascular diseases nervous system disorders.[6] Though Cr(III) is known to be non-toxic, but its presence beyond the threshold value has detrimental influences and causes destruction cellular structure.[7] It is also proposed that Cr^{3+} present in cytoplasm, bind non-specifically to DNA and other cellular components that inhibits transcription and DNA replication.[8] Most importantly, Cr(III) is an important co-factor of Insulin and it increases the glucose metabolism.[9] Its deficiency also causes symptom of diabetes mellitus or adversely influence the glucose tolerance, hypercholesteremia. Studies suggest that the long term chromium supplementation could also induces adverse influence and may enhance the possibility for DNA damage.[10] Considering its significance in human physiology, its detection and specific recognition are important. This has influenced many researchers to develop Cr^{3+} specific receptor and such few such important receptors are briefly described in the following section. However, such examples are scarce in contemporary literature.

1B.2.1 Rhodamine based reversible receptors for the recognition of Cr^{3+} ions

Due to its paramagnetic behaviour it is challenging for a chemists to develop a fluorogenic receptors that shows fluorescence ON response on specific binding to Cr^{3+}, as it is well known to quench the luminescence of the fluorophore.

Liu *et al*. introduced a rhodamine-6G based chemo sensor (**1**) for the recognition of Cr^{3+} in pure aqueous medium under physiological pH 7.2.[11] It showed a typical 1:1 binding stoichiometry with an associated new absorption band having maximum at 530 nm as well as an emission band at 560 nm. These spectral bands were attributed to the opening of rhodamine spirolactam ring with subsequent formation of the xanthenes form upon binding to Cr^{3+} (Figure 1B.1).

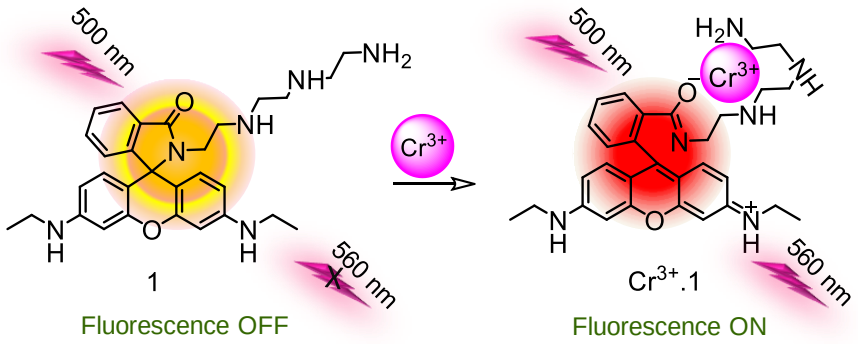

Figure 1B.1. Proposed binding mode of **1** upon addition with Cr^{3+}.

Li *et al*. had reported a rhodamine B based chemo sensor (**2**) having a pendent ferrocenyl moiety for the detection of Cr^{3+} in ethanol-water (1:1, v/v) solutions.[12]

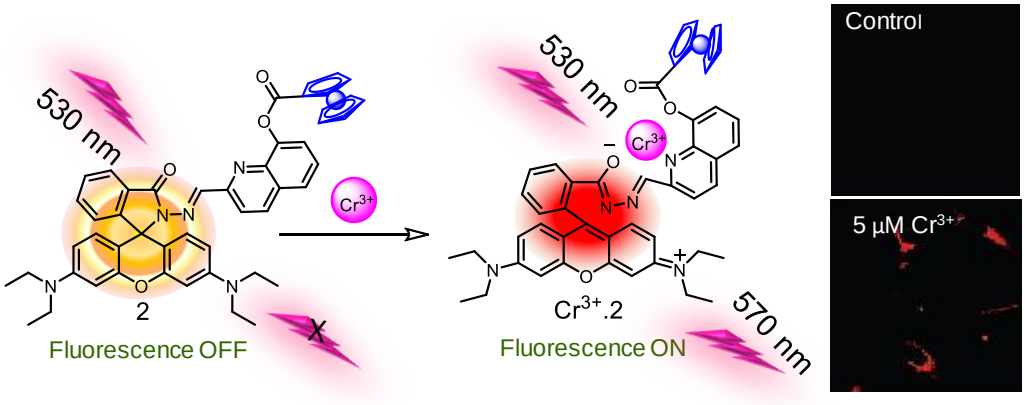

Figure 1B.2. Proposed binding mode of receptor **2** with Cr^{3+} and CLSM images for HeLa cells pretreated with Cr^{3+} and subsequently with receptor **2**. (Reprinted with permission from ref. 12. Copyright American Chemical Society)

Binding to Cr^{3+} induces ring opening of the spirolactam (Figure 1B.2) form that leads to fluorescence enhancement over a wide range of pH (5 - 10) along with visual change in solution colour to pink. The presence of ferrocene unit in the receptor **2** enabled them to utilize the receptor **2** as an electrochemical sensor

for Cr^{3+} by monitoring the binding induced changes in the potential for the Fc/Fc^{+} redox couple. A cathodic shift of ~ 140 mV in ethanol medium in presence of 1.6 equivalent of Cr^{3+} was observed. Receptor **2** was further utilised for the detection of Cr^{3+} in live HeLa cells as low as 5 μM using confocal laser scanning microscopy.

Li *et al* had reported a FRET based fluorescence probe (**3**) having naphthalimide moiety as donor and rhodamine as acceptor for monitoring Cr^{3+} in living cells for achieving the ratiometric response in ethanol-water (2:1,v/v) solvent mixture.[13] Additional of Cr^{3+} to a solution of **3** induced ring opening process (Figure 1B.3). The receptor **3** has an absorption band at 380 nm and emission band at 544 nm, which was attributed to an internal charge transfer (ICT) process for 1, 8-naphthalimide chromospheres. Upon addition of Cr^{3+} to **3** solutions shows an enhancement of the absorption band at 568 nm.

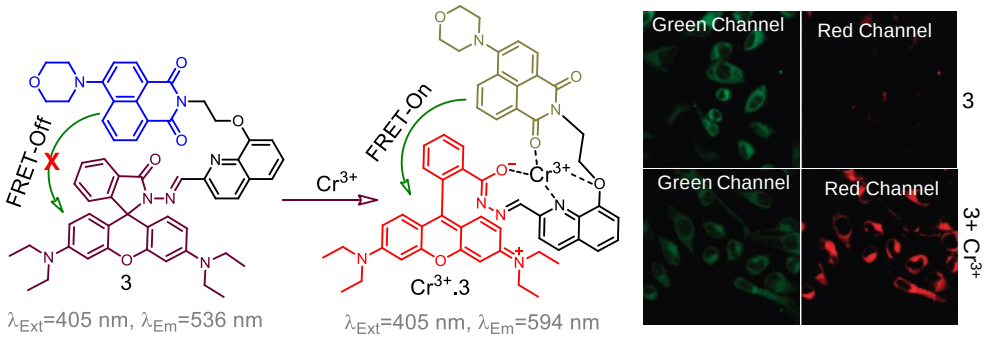

Figure 1B.3. Proposed complexation mode of **3** with Cr^{3+} and CLSM images for Hela cells pretreated with Cr^{3+} and subsequently with receptor **3**. (Reprinted with permission from ref. 13. Copyright the Royal Society of Chemistry)

1B.2.2. Non-Rhodamine based receptors of Cr^{3+}

Zhou and his co-worker developed three dansyl-based fluorescent sensors, **4**, **5** and **6** for selective recognition of Cr(III).[14] Chemosensor **4** formed a 2:1 stoichiometric complex with Cr^{3+} and exhibited selectivity towards Cr^{3+} over alkali and alkaline earth metals and most first-row transition metals in aqueous media. **4** displayed high emission quantum yield (Φ = 0.86) and fluorescence enhancement following Cr^{3+} coordination over a wide pH range. **5** contained an 8-hydroxyquinoline-carboxhydrazone tetradentate metal-binding moiety and it formed a 1:1 complex with Cr^{3+}. **5** also exhibited significant fluorescence enhancement. However, it showed much lower quantum yield following Cr^{3+} binding in aqueous solution. In contrast, their congener **6**, having a salicyl-

carboxhydrazone tridentate binding site, did not exhibit any significant fluorescence variation on binding to Cr^{3+}. These results demonstrated that the hydroxyl group played an important factor in influencing the fluorescence response to Cr^{3+} in DMF/water (9:1; v/v) media.

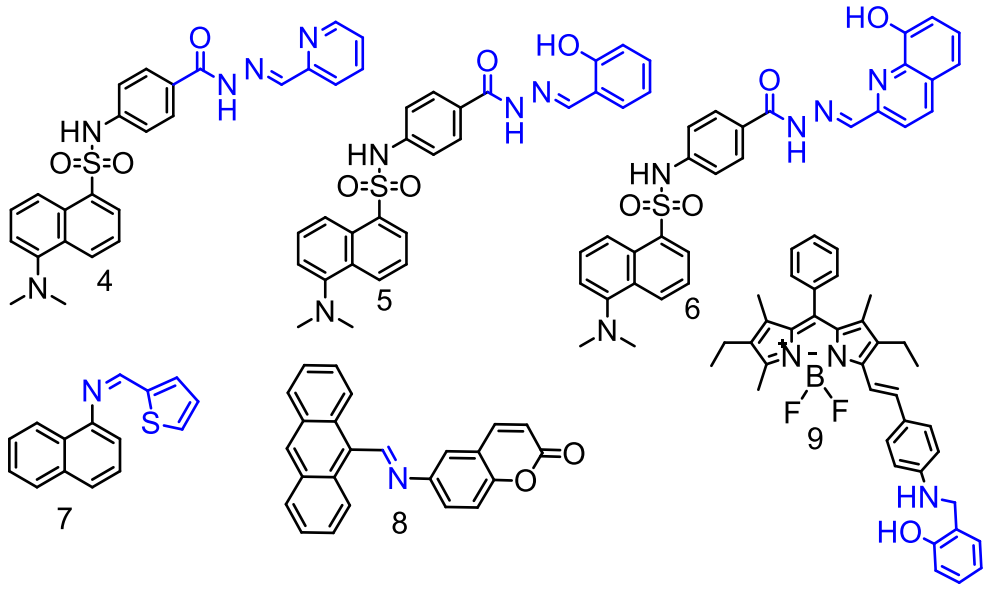

Figure 1B.4. Molecular structure of probes **4**-**9**.

Recent report also reveal that a naphthalene-based thiophene derivative **7** could act as a Cr^{3+} selective turn-*ON* fluorescence probe in aqueous methanol (water: methanol; 1:9 (v/v)) with a lower detection limit of 1.5×10^{-7} M.[15] It exhibited good cell permeability and could detect intracellular Cr^{3+} in contaminated living cells. Similar approaches were adopted for the development of Cr^{3+} specific probes (**8**-**9**) by various groups.[16-17]

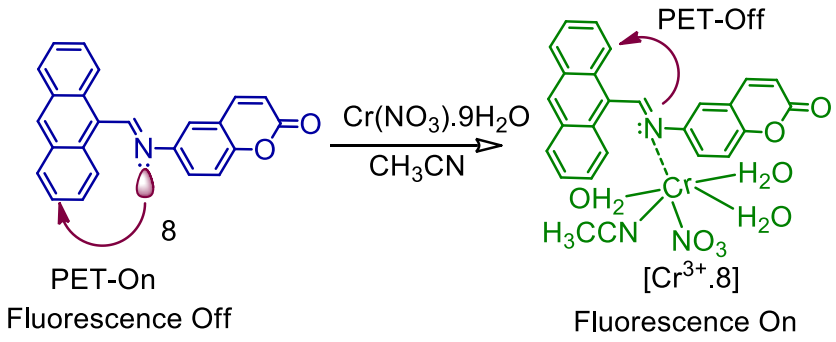

Figure 1B.5. Proposed complexation mode of **8** with Cr^{3+}.

A novel fluorescent probe, 6-(anthracen-9-yl) methylene amino)-2H-chromen-2-one (**8**) was also developed by Das and co-workers for recognition of Cr^{3+} in

CH_3CN - water (9:1; v/v) medium and using that as a fluorescence imaging probe.[16] The receptor **8** showed 1:1 binding stoichiometry with Cr^{3+} with binding constants values in CH_3CN-water (9:1; v/v) and methanol-water (9:1; v/v) solutions have been estimated to be 1.1×10^5 and 3.1×10^5, receptively, using the Benesi-Hildebrand equation. The detection limit for Cr^{3+} was reported to be 0.5×10^{-6} M (Figure 1B.5).

1B.3. References

1. V. V. Snitynskyĭ, L. I. Solohub, H. L. Antoniak, D. M. Kopachuk, M. H. Herasymiv, *Ukr Biokhim. Zh*, 1999, **71**, 5.
2. P. B. Tchounwou , C. G Yedjou, A. K Patlolla and D. J Sutton, *EXS*., 2012, **101**, 133.
3. A. Pechova and L. Pavlata, *Veterinarni Medicina,* 2007, **52**, 1.
4. W. Mertz and K. Schwarz, *Arch. Biochem. Biophys*., 1955, **58**, 504.
5. H. Arakawa, R. Ahmad, M. Naoui, H. Ali and T. Riahi, *J. Biol. Chem*., 2000, **275**, 10150.
6. J. B. Vincet, *Nutr. Rev*., 2000, **58**, 67.
7. A. K. Singh, V. K. Gupta and B. Gupta, *Anal. Chim. Acta,* 2007, **585**, 171.
8. G. Pagano, P. Manini and D. Bagchi, *Environ. Health Perspect,* 2003, **111**, 1699.
9. W. T. Cefalu, F. B. Hu, *Diabetes Care,* 2004, **27**, 2741.
10. H. A. Schroeder, *The Am. J. Clinical Nutrition*, 1968, **21**, 230.
11. J. Mao, L. Wang, W. Dou, X. Tang, Y. Yan and W. Liu, *Org. Lett*. 2007, **9**, 4567
12. K. Huang, H. Yang, Z. Zhou, M. Yu, F. Li, X. Gao, T. Yi and C. Huang, *Org. Lett*., 2008, **10**, 2557.
13. Z. Zhou, M. Yu, H. Yang, K. Huang, F. Li, T. Yi and C. Huang, *Chem. Commun*., 2008, 3387.
14. H. Wu, P. Zhou, J. Wang, L. Zhao and C. Duan, *New J. Chem*., 2009, **33**, 653.
15. S. Das, A. Sahana, A. Banerjee, S. Lohar, S. Guha, J. S. Matalobos and D. Das, *Anal. Methods,* 2012, **4**, 2254.
16. S. Guha, S. Lohar, A. Banerjee, A. Sahana, S. Mukhopadhyay, J. S. Matalobos and D. Das, D. *Anal. Methods,* 2012, **4**, 3163.
17. D. Wang, Y. Shiraishi and T. Hirai, *Tetrahedron Lett*., 2010, **51**, 2545.

1C. Artificial receptors for Hydrazine Recognition

1C.1 Introduction

Hydrazine (N_2H_4), a highly reactive species and reducing agent. It is being widely used in many chemical and agricultural industries as catalysts, corrosion inhibitors, textile dyes and pharmaceutical intermediates.[1] Further it also used as a high-energy fuel for rocket-propulsion systems and missile systems due to its detonable characteristics.[2] However, hydrazine is known to be toxic for human physiology and it can potentially lead to serious environmental contamination during its manufacture, use, transport and disposal. Most importantly, it is classified as a probable human carcinogen by the U.S. Environmental Protection Agency (EPA) and with threshold limit value (TLV) of 10 ppb.[3] Hydrazine is also a neurotoxin and has severe mutagenic effects causing severe damage to the liver, lungs, kidneys and human central nervous system.[4] Although there is no endogenous hydrazine in live cells, it is readily absorbed by oral, dermal or inhalation routes of exposure thus causing harm to live cells. Therefore, the selective and sensitive detection of trace hydrazine has gained increasing attention. During the last decade, numbers of fluorescence probes were reported for the specific detection of hydrazine. In this chapter few such important receptors are briefly described.

1C.2 Various receptors for Hydrazine

1C.2.1 Phathalimide based receptors

Gabriel synthesis is a well-known synthetic methodology named after the German scientist Siegmund Gabriel.[5] Conventionally, this methodology allows transformation of primary alkyl halides into primary amines using potassium phthalimide, and subsequently the corresponding amine derivative is produced from this phthalimide moiety upon hydrazinolysis or acidic hydrolysis reaction.[6]

Typically, the faster reaction rate of this chemodosimetric method provides an opportunity for designing fast responsive and specific probe for hydrazine under a moderate reaction conditions. This reaction has been utilized by many to design appropriate fluorescent probes for hydrazine. Xu *et al*. reported a napthalimide derivative **1** for the specific detection of hydrazine in aqueous as

well as gas phases.[7] Moreover, it applied for the imaging of hydrazine in living HeLa cells.

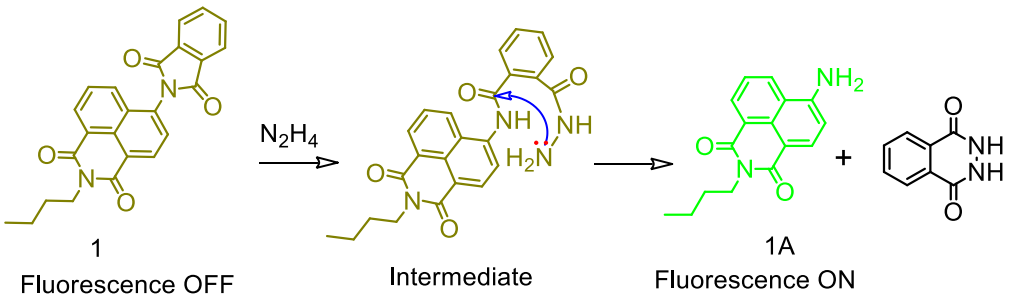

Figure 1C.1. Schematic representation of mechanistic pathway that is being utilized for the detection of hydrazine by the chemodosimetric reagent **1**.

Analogously, Gabriel-type reaction was further utilised by Xu and his co-workers.[8] They developed a tri-output optical signal based probe **2** (colorimetric, ratiometric, and chemiluminometric) for ultrasensitive detection of hydrazine. Probe **2** was selective to hydrazine over other possible/competing interfering reagents/ amines. Probe **2** was also successfully utilized for the detection hydrazine vapour over other possible interfering volatile analytes. Furthermore, hydrazinolysis product (**2-II**) showed chemiluminescence, which was induced by H_2O_2 with a maximum emission signal at 450 nm. The detection limit of hydrazine was found to be 3.2 ppb. Probe **2** could also be used for the detection of hydrazine in HeLa cells.

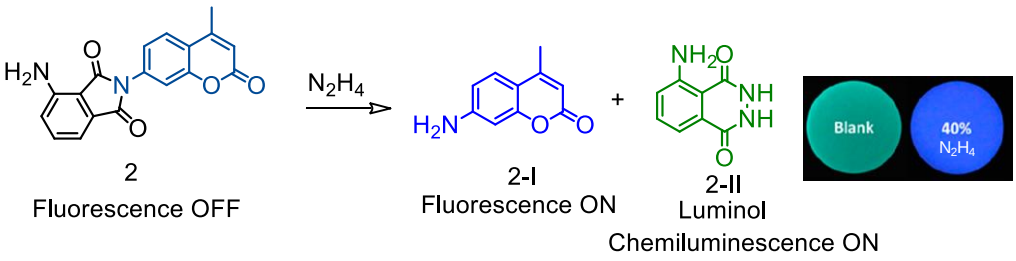

Figure 1C.2. Proposed hydrazinolysis mechanism for reaction of probe **2** with N_2H_4. (Reprinted with permission from ref. 8. Copyright American Chemical Society)

1C.2.2 O-Acetyl based receptors

Zhang *et al*. introduced a cyanine based NIR probe **3** having an acetyl group as the receptor moiety, which was also found to quench fluorescence of the cyanine moiety due to an effective PET process for specific detection of hydrazine.[9] Receptor **3** exhibited a major absorption maximum at 585 nm (ε =

2.80 × 10^4 M^{-1} cm^{-1}) and weak fluorescent (Φ = 0.018) in aq. HEPES buffer (10 mM, pH 7.4) containing 20% DMSO. With gradual addition of N_2H_4 (30.0 equiv) to the solution of **3**, the absorbance at 582 nm was found to decrease significantly, whereas a new absorption band cantered at 690 nm appeared. Probe **3** offered a rapid as well as optical (colorimetric and fluorescence based) sensing option for N_2H_4 in both aqueous solution and diluted human serum. Probe **3** was found to be less toxic and was utilized to visualize N_2H_4 in live tissues of liver, lung, kidney, heart, and spleen of mouse.

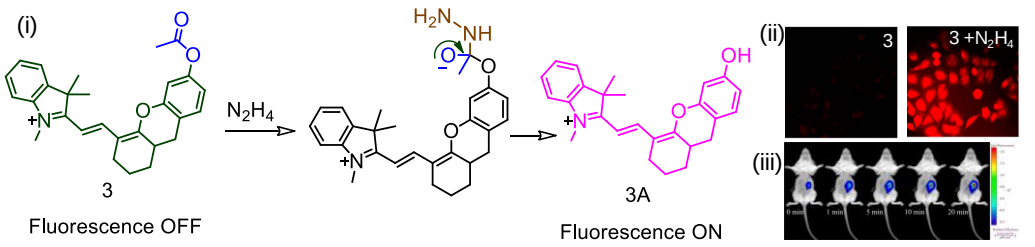

Figure 1C.3. (i) Proposed mechanism for detection of N_2H_4 by receptor **3**; (ii) CLSM images of HeLa cells incubated with **3** (10 μM) in absence and presence of N_2H_4; (iii) representative fluorescence images (psudocolor) of a Kunming mouse given a skin-pop injection of **3** (25 μL, 50 μM in a mixture of HEPES buffer (pH 7.4, 10 mM) and DMSO (4/1, v/v)) and a subsequent skin-pop injection of N_2H_4 (25 μL, 500 μM in a mixture of HEPES buffer (pH 7.4, 10 mM) and DMSO (4/1, v/v)). Images were taken after incubation for 0, 1, 5, 10, and 20 min, respectively. (Reprinted with permission from ref. 9. Copyright American Chemical Society)

1C.2.3 ESIPT based receptors

Goswami *et al*. synthesised a probe **4** based on benzothiazole for the ratiometric detection of hydrazine utilising excited state intramolecular proton transfer (ESIPT) phenomenon. Studies revealed observed Stokes shift of 90 nm.[10] Probe **4** showed an emission band at 368 nm (blue emission) upon excitation at 300 nm, which corresponds to an emission process of the "enol-form" of HBT. On reaction with hydrazine, a prominent new emission band at 458 nm (greenish emission, corresponds to "keto-form") developed, and upon progressive addition of hydrazine, the peak at 458 nm was found to increase with a ratomertic spectral response having a well-defined isoemissive point at 417 nm. Nucleophilic substitution to the bromo group and then subsequent intramolecular cyclization resulted the phenolic **4-I** derivative, which rapidly transformed to the keto form upon excitation (ESIPT), and this was responsible for the green emission at a longer wavelength (λ_{Em} = 458 nm). A linear relationship was observed between the ratio of fluorescence intensities (I_{458}/I_{368})

and concentration of hydrazine from 1-9.5 μM. The probe **4** was successfully used for the detection of hydrazine in live cells also.

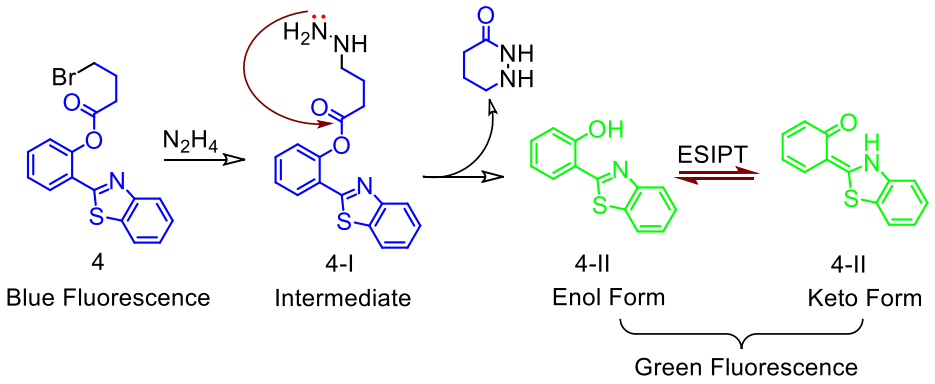

Figure 1C.4. Proposed ESIPT mechanism for detection of N_2H_4 by receptor **4**.

Qian *et al*. also introduced **5** for the specific detection of hydrazine using similar ESIPT mechanism and a substitution-cyclization-elimination cascade.[11] With the addition of hydrazine, an approximately 50-fold enhancement in fluorescence intensity of **5** at 465 nm was observed and the subsequent decrease at 375 nm was observed in 10 min. A detection limit of 0.147 μM was evaluated. Probe 5 could also utilised for the detection of hydrazine in HeLa cells.

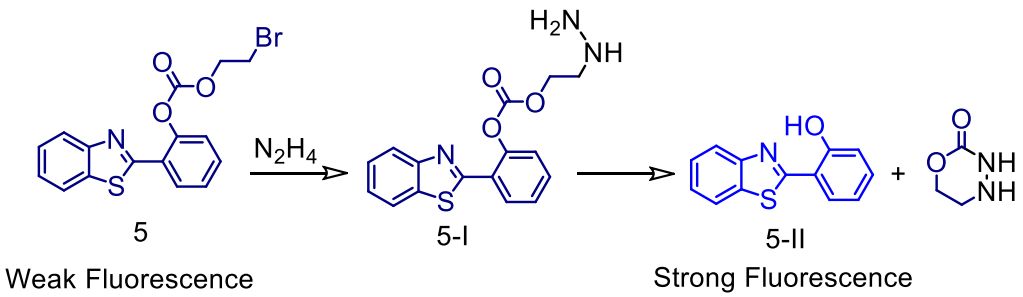

Figure 1C.5. Reaction mechanism of **5** with N_2H_4.

1C.2.4 ICT based receptors

Peng and co-worker reported an ICT based ratiometric sensor **6** having a methylene malononitrile group as electron acceptor and N, N'-diethyl group as electron donor to from the donor-acceptor system for achieving a CT process upon excitation. This specific emission response was also utilized for *in-vitro* detection of hydrazine.[12] Probe **6** showed a strong emission band at 639 nm in aq. acetate (10 mM) buffer-DMSO (1/9, v/v; pH 3.7). Upon addition of hydrazine, emission band at 639 nm was found to decrease gradually and a

new emission band appeared at 564 nm with λ_{Ext} = 510 nm due to formation of **6-II**, where ICT was effectively blocked.

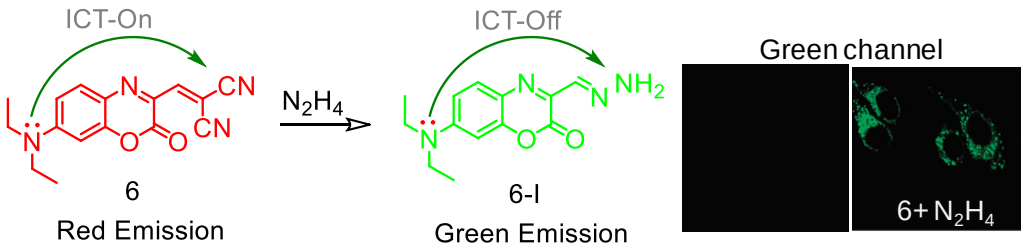

Figure 1C.6. Proposed recognition mechanism of **6** toward Hydrazine. (Reprinted with permission from ref. 12. Copyright the Royal Society of Chemistry)

Fluorescence intensity I_{564}/I_{639} was also found to be linearly related to the hydrazine concentration within 0.5-3.5 μM with a detection limit at 0.43 μM. Live cell experiments were further performed to demonstrate its applicability of detecting hydrazine in biological objects.

1C.3. References

1. I. C. Vieira, K. O. Lupetti and O. Fatibello-Filho, *Anal. Lett*., 2002, **35**, 2221–2231.
2. H. W. Schiessl, Kirk-Othmer Encyclopedia of Chemical Technology, John Wiley & Sons, Incorporation, NJ, USA, 2000, pp. 562.
3. U.S. Environmental Protection Agency (EPA), Integrated Risk Information System (IRIS) on Hydrazine/Hydrazine Sulfate, National Center for Environmental Assessment, Office of Research and Development, Washington, DC, 1999.
4. C. A. Reilly, *Chem. Res. Toxicol*., 1997, **10**, 328.
5. Gabriel, S. *Ber. Dtsch. Chem. Ges.,* 1887, **20**, 2224.
6. M. S. Gibson and R. W. Bradshaw, *Angew. Chem., Int. Ed. Engl*., 1968, **7**, 919.
7. L. Cui, Z.Peng, C. Ji, J. Huang, D. Huang, J. Ma, S. Zhang, X. Qian and Y. Xu, *Chem. Commun.,* 2014, **50**, 1485.
8. L. Cui, C. Ji, Z. Peng, L. Zhong, C. Zhou, L. Yan, S. Qu, S. Zhang, C. Huang, X. Qian and Y. Xu, *Anal. Chem.*, 2014, **86**, 4611.
9. J. Zhang, L. Ning, J. Liu, J. Wang, B. Yu, X. Liu, X. Yao, Z. Zhang and H. Zhang, *Anal. Chem.*, 2015, **87**, 9101.
10. S. Goswami, S. Das, K. Aich, B. Pakhira, S. Panja, S. K. Mukherjee and S. Sarkar, *Org. Lett.*, 2013, **15**, 5412.
11. J. Zhou, R. Shi, J. Liu, R. Wang, Y. Xu and X. Qian, *Org. Biomol. Chem*., 2015, **13**, 5344.
12. J. Fan, W. Sun, M. Hu, J.Cao, G. Cheng, H. Dong, K. Song, Y. Liu, S. Sun and X. Peng, *Chem. Commun.,* 2012, **48**, 8117.

1D. Artificial receptors for Reactive Species Recognition

1D.1 Introduction

Reactive Oxygen and Nitrogen Species (ROS and NOS, respectively) are hemlock for the living organism. ROS/RNS are conserved regulator of various cellular functions and overproduction of ROS/RNS interferes with different physiological processes. Hypochlorous acid (HOCl) and Nitroxyl (HNO) are well-known ROS and RNS respectively. These play a role as an oxidant in biological processes.[1] The biochemistry of HOCl promotes the ability of activated phagocytes to kill a wide range of pathogens. It is generated during an oxidation reaction between chloride ions and H_2O_2 that is catalyzed by myeloperoxidase (MPO) secreted by activated phagocytes in the inflammatory state.[2] Although it plays a protective role in human health, excess HOCl can cause tissue damage and diseases such as hepatic ischemiareperfusion injury, atherosclerosis, lung injury, rheumatoid and cardiovascular diseases, neuron degeneration, arthritis, and cancer.[3]

Chemistry of HNO (nitroxyl, also known as nitrosyl hydride, nitroso hydrogen or azanone) and its conjugated base NO^- is rather less explored as compared to HOCl. HNO is a product of one electron reduction of nitric oxide ($NO^\bullet$), isoelectronic with molecular oxygen (O_2). Unlike HOCl, role of HNO in human physiology is rather less explored. The linear HNO structure is less stable than the bent form by ca. 67 kcal/mol. Results of the theoretical studies predicted the probable existence of a triplet "^{3}A" state having energy 18.0 to 19.0 kcal above the ground state. However, till date experimental evidence for ^{3}HNO is missing. Importantly, for $^3NO^-$ the triplet state is more stable than the singlet one by ca. 16 kcal/mol. Thus, generation of corresponding deprotonated species, $^3NO^-$ is spin forbidden (adiabatic singlet-triplet transition energy is 18.45 kcal/mol)[4] and a slow process and this attributes to HNO as the predominant species (pK_a^{HNO} = 11.4) [5] at physiological pH.

Angeli's salt is the most widely used reagent for the in situ generation of HNO and commercial availability of this salt has helped in developing the mechanistic insights of reactions involving HNO with a particular emphasis on elucidation of biochemical/physiological role. Angeli's salt is a spontaneous donor of HNO with a half-life of ~ 3 min under physiological conditions.[6]

Studies have revealed that HNO may induce critical functions in various physiological processes. It is argued that HNO can enhance the contractility of heart cells, elicit vasorelaxation in muscle cells, deregulate platelet aggregation and facilitate the relaxation of resistant-like arteries by triggering the voltage-dependent K^+ channel. Further, oxidation of HNO produces strong oxidizing species, which can cause damage in DNA and result in the depletion of cellular thiols, some of which are crucial for maintaining the redox immunity of the human physiology. HNO is also known to act as a therapeutic agent and is used for the treatment of heart failure.[7]

Therefore, early detection and sensing of these species are desired and this has attracted much attention not only among chemists, but also biologists and environmentalist. In recent years, number of reports describes specific detection of metal ions for various applications among them fluorogenic receptors are the most important ones. In this chapter, few such important receptors were briefly described.

1D.2 Various receptors for HOCl

Yang and co-workers designed and synthesized a simple, water-soluble p-methoxyphenol derivative **1** that showed colorimetric as well as fluorimetric responses on specific reaction with HOCl in aqueous PBS buffer (0.01 M, pH 7.4) medium (Figure 1D.1).[8] In the presence of ClO^-, a change in solution colour was registered due to the shift in the original absorbance maximum of **1** from 314 nm to 393 nm. Fluorescence emission maximum at 388 nm was found to decrease dramatically with subsequent increase in ClO^- concentration. The observed behaviour was attributed to p-methoxyphenol oxidation. The addition of other reactive oxygen and nitrogen species (H_2O_2, $^1O_2$, $^{\bullet}NO$, $O_2^{\bullet-}$, $^{\bullet}OH$, $ONOO^-$ and $ROO^{\bullet}$) did not induce any such changes.

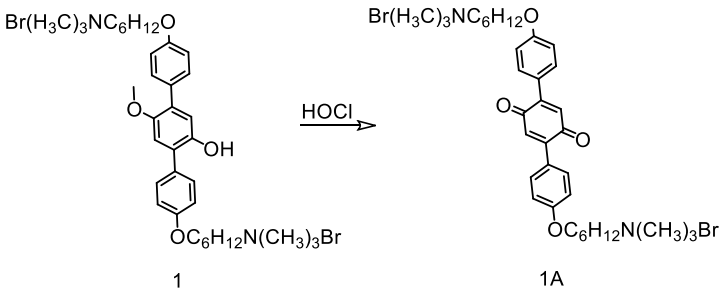

1 1A

Figure 1D.1. Molecular structures for receptor **1** and product on reaction with HOCl.

Chen *et al*. reported a Ir(III)-complex (**2**) with an oximated 2,2′-bipyridine for detection of ClO^-.[9] Complex **2** is non-fluorescent due to -C=N-OH isomerization as a predominant non-radiative decay process in the excited state (Figure 1D.2). In presence of ClO^-, a selective oxidation of the oxime to an aldehyde or carboxylic acid was achieved and this caused a strong enhancement in fluorescence emission at 578 nm when excited at 346 nm in DMF: aq. HEPES (50 mM, 4:1 (v/v); pH 7.2).

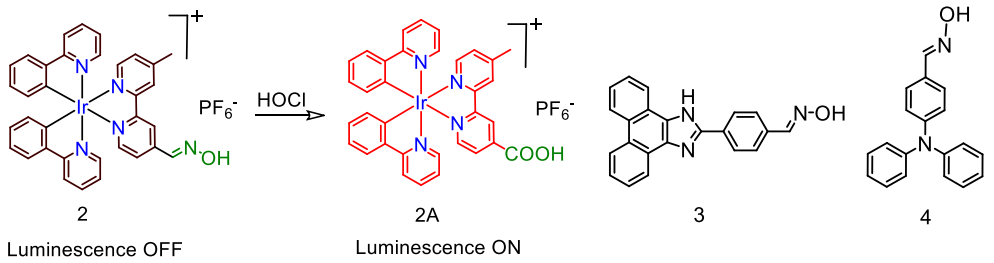

Figure 1D.2. Molecular structures of chemosensors **2** - **4**.

DFT studies revealed that the bright orange-yellow luminescence of $[Ir(bpy)_2(L_2)](PF_6)$ originated from [5d(Ir) → π*(bpy)]-based ^{3}MLCT transition and [π(ppy) → π*(bpy)]-based ^{3}LLCT excited states. The selectivity of probe **2** towards ClO^- was shown to remain unaffected in presence of H_2O_2, $^{\bullet}NO$, $O_2^{\bullet-}$, $^{\bullet}OH$, $ROO^{\bullet}$ and various metal ions. In addition, the use of test strips developed using the receptor **2** showed high sensitivity towards ClO^-. Similar oxime based probes **3** and **4** were also reported for specific detection of ClO^-.[10,11]

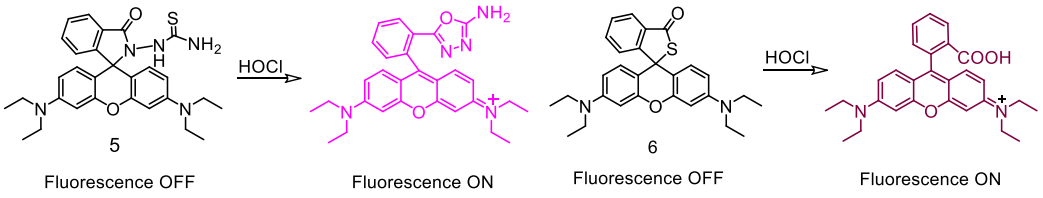

Figure 1D.4. Molecular structures for receptor **5** and **6** product on reaction with HOCl.

Loo, Zhang and co-workers reported a novel water-soluble organic-nano up-conversion luminescent (UCL) detection system for HOCl using a rhodamine-modified thiosemicarbazide **5** derivative as a chemodosimetric reagent (Figure 1D. 3).[12] Upon reaction of **5** with HOCl, the green UCL emission intensity was found to decrease gradually, while NIR emission did not show any change—a desirable property for ratiometric UCL detection. These nanoparticles were successfully used for ratiometric UCL visualization of HOCl that was released

by MPO-mediated peroxidation of chloride ions in living cells. Similar probe **6** was further reported by Xu *et al*. for specific detection of HOCl.[13]

1D.3. Various receptors for HNO

A close look at the contemporary literature reveals that few Cu(II)-based molecules have been utilized as a HNO probe. Interestingly, this also reveal that there is a general trend in developing probe molecule (**7**-**11**) that show luminescence ON response in the far-red region of the spectrum.

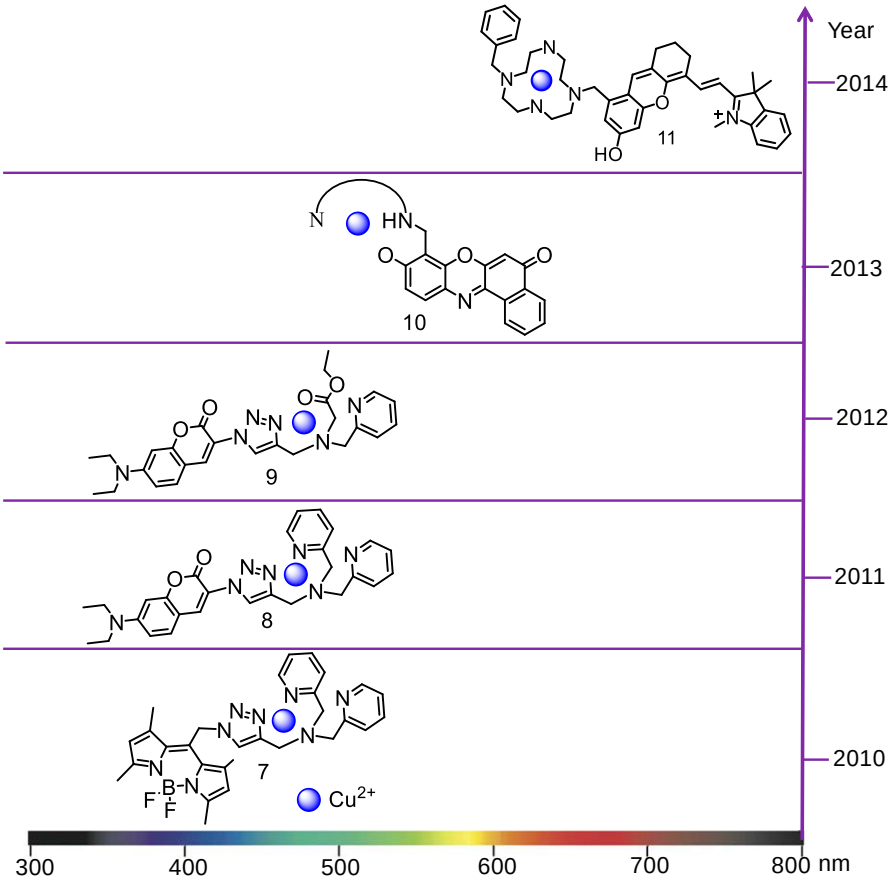

Figure 1D.5. Molecular structures and emission wavelengths of the Cu(II)-based HNO probes that showed luminescence ON response on conversion of Cu(II) to Cu(I) by HNO. (Reprinted with permission from The Chemistry and Biology of Nitroxyl (HNO) Edited by Fabio Doctorovich, Patrick J. Farmer, Marcelo A. Marti, Elsiveior, Chapter 11)

Lippard group reported a series of Cu complexes (**12**-**14**) for detection of HNO. Copper complexes, **12**-**14**, showed emission enhancement in response to HNO due to the effective reduction from Cu(II) to Cu(I). The three sensors differ in the nature of the metal-binding site. These probes were successfully imaged HNO in HeLa cells and RAW 264.7 macrophages (Figure 1D.6).[14]

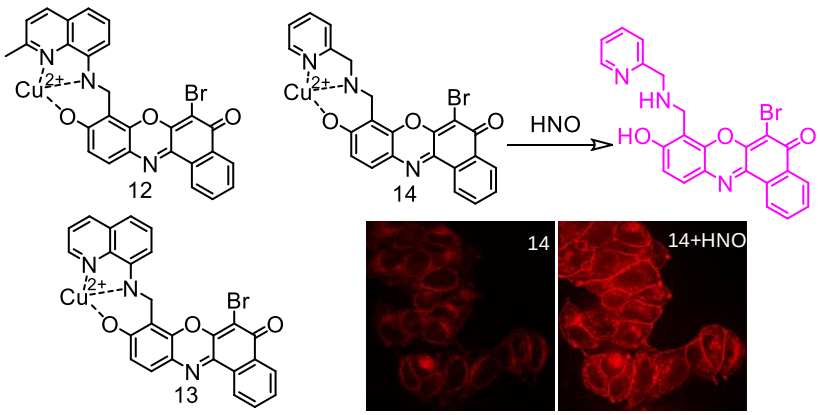

Figure 1D.6. Molecular structures of probe **12**-**14**. (Reprinted with permission from ref. 14. Copyright American Chemical Society)

HNO-induced deprotection of 2-(diphenylphosphino)benzoate-moiety is being utilized for designing chemodosimetric probe molecules (**15**-**23**) for the development of the HNO specific probes with luminescence ON response for biological imaging applications (Figure 1D.7).

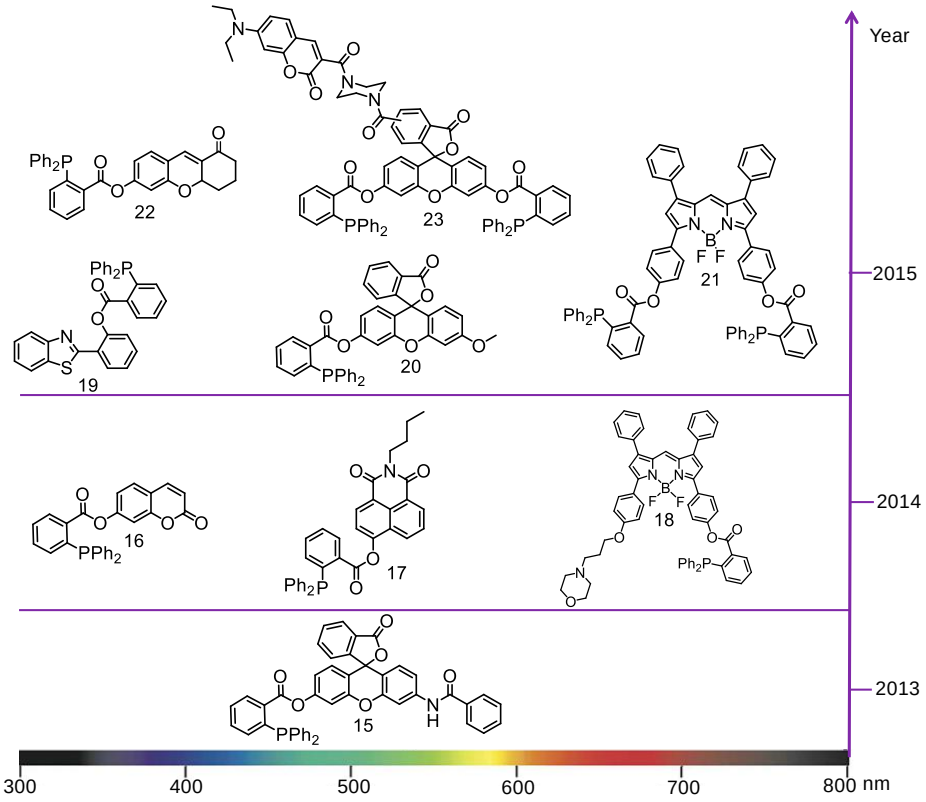

Figure 1D.7 Molecular structures and emission wavelengths of the phosphine-based HNO probes that showed luminescence ON response. (Redraw from The Chemistry and Biology of Nitroxyl (HNO) book edited by Fabio Doctorovich, Patrick J. Farmer, Marcelo A. Marti, Elsevier, Chapter 11)

Nakagawa et al. introduced a Rhodol-based HNO specific probe **15** having a triphenylphosphine functionality as the receptor unit. HNO reacted with probe by Intramolecular attack of the aza-ylide on the ester carbonyl group releases a fluorescent rhodol derivative with fluorescence ON response (Figure 1D.8). **15** could detect not only HNO enzymatically generated in the enzymatic conversion induced by horseradish peroxidase on hydroxylamine system *in vitro* but also intracellular HNO release from Angeliûs salt in living cells.[15]

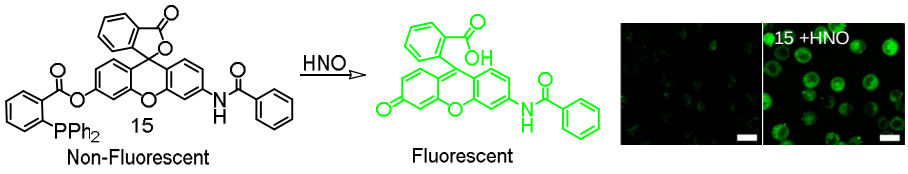

Figure 1D.8. Molecular structure of probe 15 and its reaction product with HNO. (Reprinted with permission from ref. 15. Copyright American Chemical Society)

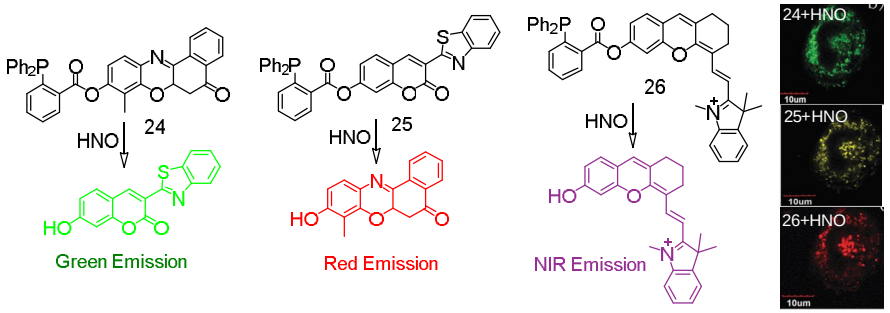

Figure 1D.9. Molecular structures of probes **24**-**26**. (Reprinted with permission from ref. 16. Copyright Royal Society of Chemistry)

Similarly, Lin *et al*. reported three novel turn-on molecular probes (**24**-**26**), as sensitive turn-ON fluorescence probes for detecting HNO. Design aspect involved use of triphenylphosphine as a receptor site.[16] The probes could exhibit different emission colours from green to near-infrared (NIR) in response to HNO in aqueous solution and cells (Figure 1D.9). The probes exhibited high sensitivity, excellent selectivity, desirable performance at physiological pH and low cytotoxicity. These probes allowed the multicolour imaging of HNO with emission colours in the range of green to near-infrared (NIR) in living systems for the first time. Furthermore, **26** responded to HNO with a significant turn-on NIR fluorescence signal upon excitation in the NIR region, and it was successfully applied for sensing HNO in living mice.

1D.4. References

1. P. R.-Fuentes and S. J. Lippard, *Acc. Chem. Res*. 2015, **48**, 2927.
2. Z. Q. Ye, R. Zhang, B. Song, Z. C. Dai, D. Y. Jin, E. M. Goldys and J. L. Yuan, *Dalton Trans*., 2014, **43**, 8414.
3. F. J. Huo, J. J. Zhang, Y. T. Yang, J. B. Chao, C. X. Yin, Y. B. Zhang and T. G. Chen, *Sens. Actuators B*, 2012, **166**-**167**, 44.
4. M. D. Bartberger, J. M. Fukuto, and K. N. Houk , *Proc. Natl. Acad. Sci*., 2001, **98**, 2194.
5. V. Shafirovich and S. V. Lymar, *Proc. Natl. Acad. Sci., USA*., 2002, **99**, 7340.
6. (a) MN. Hughes and PE. Wimbledon, *J Chem Soc Dalton Trans*., 1976, 703; (b) CM. Maragos, D. Morley, DA. Wink, TM. Dunams, JE. Saavedra, A. Hoffman, A. A. Bove, L. Isaac, J. A. Hrabie, L. K. Keefer, *J. Med. Chem*., 1991, **34**, 3242.
7. (a) F. Doctorovich, D. Bikiel, J. Pellegrion, S. A. Sua´rze, A. Larsen and M. A. Martı´, *Coord. Chem. Rev*., 2011, **255**, 2764; (b) H. Nakagawa, *Nitric Oxide*, 2011, **25**, 195; (c) G. M. Johnson, T. J. Chozinski, E. S. Gallagher, C. A. Aspinwall and K. M. Miranda, *Free Radical Biol. Med*., 2014, **76**, 299; (d) K.M.Miranda, *Coord. Chem. Rev*., 2005, **249**, 433; (e) R. Foresti, S. Bains, F. Sulc, PJ. Farmer, CJ. Green and R. Motterlini, *J. Pharmacol. Exp. Ther*., 2006, **317**, 1125; (f) K. M. Miranda, R. W. Nims, D. D. Thomas, M. G. Espey, D. Citrin, M. D. Bartberger, et al., *J. Inorg. Biochem*., 2003, **93**, 52; (g) V. Shafirovich and S. V. Lymar, *Proc. Natl. Acad. Sci*., 2002, **99**, 7340; (h) K. M. Miranda, N. Paolocci, T. Katori, D. D. Thomas, E. Ford, M. D. Bartberger, et al. *Proc. Natl. Acad. Sci. USA*, 2003, **100**, 9196; (i) S. V. Lymar, V. Shafirovich and G. A. Poskrebyshev, *Inorg. Chem*., 2005, **44**, 5212; (j) D. A. Bazylinski and T. C. Hollocher, *J. Am. Chem. Soc*.,1985, **107**, 7982.
8. W. J. Zhang, C. Guo, L. B. Liu, J. G. Qin and C. L. Yang, *Org. Biomol. Chem*., 2011, **9**, 5560.
9. N. Zhao, Y. H. Wu, R. M. Wang, L. X. Shi and Z. N. Chen, *Analyst*, 2011, **136**, 2277.
10. W. Y. Lin, L. L. Long, B. B. Chen and W. Tan, *Chem. – Eur. J*., 2009, **15**, 2305.
11. J. Shi, Q. Q. Li, X. Zhang, M. Peng, J. G. Qin and Z. Li, *Sens. Actuators, B*, 2010, 1**45**, 583.
12. Y. Zhou, W. B. Pei, C. Y. Wang, J. X. Zhu, J. S. Wu, Q. Y. Yan, L. Huang, W. Huang, C. Yao, J. S. C. Loo and Q. C. Zhang, *Small*, 2014, **10**, 3560.
13. X. Q. Zhan, J. H. Yan, J. H. Su, Y. C. Wang, J. He, S. Y. Wang, H. Zheng and J. G. Xu, *Sens. Actuators, B*, 2010, **150**, 774.
14. U.-P. Apfel, D. Buccella, J. J. Wilson and S. J. Lippard, *Inorg. Chem*., 2013, **52**, 3285.

15. K. Kawai, N. Ieda, K. Aizawa, T. Suzuki, N. Miyata and H. Nakagawa, *J. Am. Chem. Soc*., 2013, **135**, 12690.

16. B. Dong, K. Zheng, Y. Tanga and W. Lin, J*. Mater. Chem. B*, 2016, **4**, 1263.

CHAPTER 2

FLUORESCENT PROBE FOR SPECIFIC DETECTION OF CYSTEINE IN LIPID DENSE REGION OF CELLS

Publication:
Chem. Commun., 2015, **51**, 16932-16935

2.1. Introduction

For eukaryotic cells, Endoplasmic Reticulum (ER)—a lipid dense region, plays a central role in biosynthesis of lipids and proteins.[1] Oxidized glutathione (GSH) and Cys are believed to participate in disulfide interchange reactions for ER-resident as well as newly made proteins.[2] It has been argued that the homeostasis of the redox state in the ER depends on the flux of small disulfides, secreted together with their reduced counterparts, primarily GSH and Cys, which are being released during the process of protein disulfide bond formation.[2] Cys is the important precursor for synthesis of GSH, which plays crucial roles in maintaining cellular antioxidant immune system.[3] Apart from these, Cys is also involved in various biological activities like cellular detoxification and metabolism.[4,5] A nuance in Cys concentration in cells or in HBP affect crucial biological processes. For example diseases like haematopoiesis, leucocyte loss, hair depigmentation caused by decreased Cys level,[5,6] while its elevated level is responsible for neurotoxicity, cardiovascular and Alzheimer's diseases.[7] Thus, any reagent that allows specific detection and quantification of Cys in biological fluids as well as that allows imaging of endogenous Cys in live cells is of immense importance, as this has a direct relevance for diagnostic application. Such a reagent is even more significant if it is capable of detecting subtle changes in Cys distribution in ER, as this would help in probing protein modification in the ER through a conversion of Cys to formylglycine.[8] Among various analytical techniques, high-performance liquid chromatography (HPLC) with post column derivatisation and a spectrophotometric assay using 5,5'-dithiobis(2-nitrobenzoic acid) (DTNB; Ellman's Reagent) are most common for estimation of Cys in bio-fluids or in protein residues.[9] Use of HPLC technique involves skilled manpower, expensive instrumentation and time consuming analysis process, while Ellman's reagent is sensitive to O_2/OH^- and produces strongly absorbing 4-nitrothiophenolate on reaction with various amino acids (AAs) and protein residues having sulfhydryl group. Thus, this reagent fails to delineate between Cys from Hcy/GSH or Cys/Hcy/GSH residue with free –SH functionality present in a protein. Also, none of these two procedures are appropriate for imaging application. Some recent reports on Cys-specific α,β-unsaturated receptors reveal that such receptors fail to distinguish between Cys and Cys residue present in certain protein molecules with free sulfhydryl (-SH) group.[10] Additionally, receptors that work on the cleavage of -S–S- or –alkoxy

bond cleavage, induced by –SH group, fail to distinguish between Cys and Hcy/GSH.[11] Considering these limitations, a receptor that is specific for Cys and capable of showing instant fluorescence *ON* response is highly desirable. However such example remained elusive until recently, when Peng *et al.* reported a fluorescent probe for specific detection of Cys.[12] Also Strongin *et al.* and Yoon *et al.* developed an acrylate based reagent for Cys detection.[13] Herein, we have described a new molecular probe **ER-F** that is specific for Cys and capable of detection Cys localized in lipid dense region in live Hct116 cells as well as in bio-fluids like HBP samples. Moreover, this reagent could be used for imaging the release of Cys during metabolism of N-acetyl cysteine drug in live HepG2 cells and for developing a test strip based technique for quantitative estimation of Cys in HBP.

2.2. Experimental Section

2.2.1. Materials

Benzoyl Chloride, 2,4-Dimethylpyrrole, 4-Hydroxybenzaldehyde, Acryloyl chloride, Boron trifluoride diethyl etherate, Triethylamine, Piperidine, Glacial acetic acid were obtained from Sigma Aldrich and were used as received. Cysteine, N-acetyl Cysteine, Histidine, Glutathione, Arginine, iso-Leucine, Proline, Methionine, Glycine, Alanine, Serine, Threonine, Tryptophan, Tyrosine, Valine, Leucine were purchased from SD Fine Chemicals in India. Solvents used for synthesis of various intermediates and final compounds were of AR grade (S.D. Fine Chemicals) and were used as received without further purification. HPLC grade (S.D. Fine Chemicals) solvents were used for various spectroscopic studies.

2.2.2. Analytical Methods

^{1}H NMR spectra were recorded on a Bruker 500 MHz FT NMR (Model: Avance-DPX 500) using $CDCl_3$ as the solvent and tetra methyl silane (TMS) as an internal standard. IR spectra were recorded on Bruker Alpha FT IR spectrometer. UV-Vis spectra were recorded using Shimadzu UV-1800 spectrometer. All the Fluorescence measurements were carried out on *PTI* Quanta Master™ Steady State Spectrofluorometer. High-resolution mass spectra were recorded on JEOL JM AX 505 HA mass spectrometer. Confocal images were acquired in Olympus Fluoview microscope.

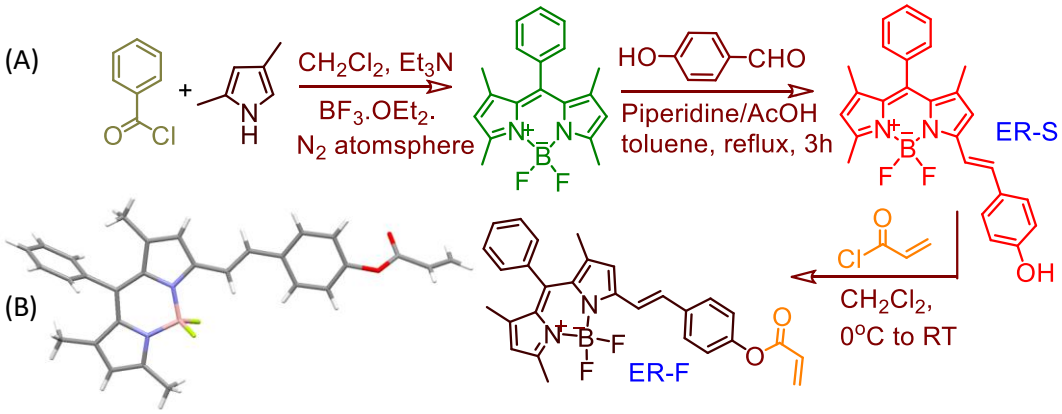

Scheme 2.1. Methodologies that were adopted for synthesis of **ER-F**. (B) Single-crystal X-ray structure of probe **ER-F** [Hydrogen atoms are omitted for clarity]

Summary of crystallographic data is given in Table 2.1. Single crystal of suitable dimension was chosen under an optical microscope and mounted on a glass fiber for data collection on a Bruker SMART APEX diffractometer equipped with CCD area detector at 150K. Intensity data for crystal was collected using graphite-mono chromated MoK$_\alpha$ (λ=0.71073 Å) radiation. The data integration and reduction were performed with SAINT software.[14] Data were subjected to empirical absorption correction using SADABS.[15] The structure was solved by direct methods using SHELXTL[16] and was refined by full matrix least square procedures based on F^2 using the program SHELXL-97.[17] All non-hydrogen atoms were refined anisotropically till convergence was reached. Hydrogen atoms, attached to the organic moieties, were either located from the difference of Fourier map or stereochemically fixed in the compound. Details of crystallographic data for compound **ER-F** are provided table 2.1.

Table 2.1: Crystallographic data for probe **ER-F**

Identification code	ER-F	
CCDC	1420800	
Empirical formula	C_{29} H_{25} B F_2 N_2 O_2	
Formula weight	482.32	
Temperature	296(2) K	
Wavelength	0.71073 Å	
Crystal system	Triclinic	
Space group	P-1	
Unit cell dimensions	a = 10.4699(7) Å	α= 108.143(3)°
	b = 10.9521(7) Å	β= 95.509(4)°
	c = 12.2593(7) Å	γ = 106.047(4)°
Volume	1258.03(14) Å^3	

Z	2
Density (calculated)	1.273 Mg/m^3
Absorption coefficient	0.089 mm^{-1}
F(000)	504
Crystal size	0.45 x 0.38 x 0.32 mm^3
Theta range for data collection	1.78 to 27.22°.
Index ranges	-13<=h<=13, -14<=k<=14, -15<=l<=15
Reflections collected	24454
Independent reflections	5573 [R (int) = 0.0532]
Completeness to theta = 27.22°	99.00%
Absorption correction	multi-scan
Max. and min. transmission	0.9719 and 0.9608
Refinement method	Full-matrix least-squares on F^2
Data / restraints / parameters	5573 / 0 / 329
Goodness-of-fit on F2	1.031
Final R indices [I>2sigma(I)]	R1 = 0.0516, wR2 = 0.1417
R indices (all data)	R1 = 0.0758, wR2 = 0.1606
Extinction coefficient	0.014(3)
Largest diff. peak and hole	0.521 and -0.325 $e.Å^{-3}$

2.2.3. General experimental procedure for UV-Vis and Fluorescence studies

Stock solution of probe **ER-F** (1 $\times 10^{-4}$ M) was prepared in HPLC grade acetonitrile. All the analytes stock solution (1×10^{-2} M) was prepared in aqueous HEPES buffer (10 mM) medium at pH 7.2. 500 µl of this stock solution of probe **ER-F** was added to 4.5 ml of HEPES (10 mM) aqueous buffer medium having solution pH 7.2 to make the effective **ER-F** concentration of (1×10^{-5}) M. This solution was used for all the photophysical studies. All the photophysical studies were performed in aq. HEPES: CH_3CN medium (9: 1, v/v) at pH 7.2. All emission studies in solution were done using λ_{Ext} = 530 nm with an emission slit width of 2/2 nm, unless and otherwise mentioned. The relative fluorescence quantum yields (Φ_f) were estimated (using an equation that is discussed in the previous chapter) using rhodamine B (Φ_f = 0.31) as reference compound in aq. medium.

4.2.4. Preparation of TLC test strips and solid state fluorescence studies

TLC test strips were prepared by drop-casting of 20 µL of probe **ER- F** (0.1 mM) solution of CH_3CN on silica TLC plates. Then it was dried and different concentration of Cys solution in 10 mM aq. HEPES buffer (pH 7.2) was added on it by the same process. Again it was dried properly and after that the fluorescence colour changes

were recorded. The same was repeated for Hcy, GSH and other analytes as well. Images were captured using Canon 630D camera. The silica coated TLC plates treated with different concentration of Cys were used for solid state fluorescence measurements using λ_{Ext} = 530 nm with an emission slit width of 1/1 nm.

2.2.5. Cell culture and Confocal imaging

For confocal studies, Hct116 cells (3×10^5) were seeded on cover slips placed in 6 well plates. After 24 hours, Hct116 cells were treated with **ER-F** (1 μM) for 30 minutes at 37˚C in a 5% CO_2 air environment. Cells were then washed thrice with Phosphate Buffer (1X PBS) and fixed with 4% PFA for 20 minutes and washed again with 1X PBS. Nail paint was used to seal the cover slips mounted on the glass slides for each well plates. For control experiment Hct116 cells were pre-treated with 1 mM of N-ethylmaleimide (NEM) for 30 minutes. Then cells were washed thrice with media and followed by incubation with **ER-F** (1 μM) for another 30 minutes under same conditions. Cells were again washed with 1XPBS buffer and fixed with 4% PFA for 20 minutes and washed again with 1X PBS. Confocal laser scanning microscopic (CLSM) images were acquired in Olympus Fluoview Microscope with $\lambda_{Ext}/\lambda_{Mon}$ = 530/573 nm.

For confocal studies with N-acetyl cysteine (NAC) drug we have used HepG2 liver cancer cells. HepG2 cells (3×10^5) were seeded on cover slips placed in 6 well plates. After 24 hours, cells were treated with 1 mM NEM for 30 minutes. Cells were then washed with media and treated with 25 μM of NAC and incubated for 1 hour. Further, cells were incubated with **ER-F** (1 μM) for 20 minutes. Cells were then washed thrice with Phosphate Buffer Saline (1X PBS) and fixed with 4% PFA for 20 minutes and again washed with 1X PBS. CLSM images were acquired in Olympus Fluoview Microscope with $\lambda_{Ext}/\lambda_{Mon}$ = 530/573 nm.

The *in-vitro* cytotoxicity of **ER-F** on Hct116 cells (Colon cancer cells) were determined by conventional MTT (3-(4,5-Dimethylthiazol-2-yl)-2,5-diphenyltetrazolium bromide, a yellow tetrazole) assay. Hct116 colon cancer cells (7×10^3) were seeded in each well of a 96 well plate and cultured in a 37°C incubator supplied with 5% CO_2. Cells were maintained in DMEM medium, supplemented with 10% Fetal Bovine Serum and 100 Units of Penicillin Streptomycin antibiotics. After 24 hours the cells were treated with different concentrations of the **ER-F** in triplicates for 12 hours. After treatment cells were added with 0.5 μg/mL of MTT reagent. The plate was then incubated for 4 hours at 37°C and then later added to each well with 100 μL of Isopropyl Alcohol. The optical density was measured at 570 nm using Multiskan Go (Thermo Scientific) to find the

concentration of the cell inhibition. IC_{50} value has been calculated to be 14 μM. Formula used for the calculation of the MTT assay for evaluation of the cell viability is as follows: Cell viability (%) = (means of Absorbance value of treated group/ means of Absorbance value of untreated control) X 100.

2.2.6. Determination of detection limit

The detection limit was calculated based on the fluorescence titration. To determine the S/N ratio, the emission intensity of **ER-F** without Cys was measured by 10 times and the standard deviation of blank measurements was determined. The detection limit (DL) of **ER-F** for Cys was determined from the following equation:

$DL = K * Sb_1/S$

Where, K = 2 or 3 (we take 3 in this case); Sb_1 is the standard deviation of the blank solution; S is the slope of the calibration curve. From the graph we get slope = 4.49 $x10^8$, and Sb_1 value is 2.49. Thus using the formula we get the Detection Limit = 15 $x10^{-9}$ M.

2.2.7. Methodology for the estimation of Cys in Human blood plasma (HBP) sample

Fresh and human blood samples (5 mL) with added lithium anticoagulant were centrifuged in a vacutainer tube at 3000 rpm for 15 min. The supernatant solution (plasma), which contains proteins and amino acids, was collected. 2 mL of collected plasma was vigorously mixed with appropriate amount of $NaBH_4$ and incubated for 5 minutes at room temperature in order to hydrolyse the disulphide bond. Various protein residues present in the sample after reduction were precipitated by the addition of methanol, followed by centrifugation of the sample for 10 minutes. The supernatant liquid, which contained Cys in blood plasma, was used for the spectroscopic studies.

2.3. Synthesis and Characterisation

2.3.1. Synthesis of ER-S

A mixture of BODIPY (400 mg, 1.23 mmol), 4-hydroxybenzaldehyde (165 mg, 1.35 mmol), 0.9 mL piperidine and 0.6 mL glacial acetic acid was refluxed in 30 mL toluene in a Dean- Stark apparatus for 3h. Then water was added into it and crude was extracted with dichloromethane. The organic layer was collected and dried over anhydrous sodium sulphate and solvent was removed under reduced pressure. It was then subjected to column chromatography using silica gel (100-200 mesh) as stationary phase and 10% EtOAc in hexane as mobile phase to get compound **ER-S**

as red solid. Yield: 56%; ^{1}H NMR (500 MHz, $CDCl_3$, *J* in Hz, δ ppm): 7.52 (1H, d, *J* = 16.5), 7.47 (5H, m), 7.30 (2H, d, *J* = 8.0), 7.18 (1H, d, *J* = 16.0), 6.83 (2H, d, *J* = 8.5), 6.58 (1H, s), 5.99 (1H, s), 5.40 (1H, s), 2.59 (3H, s), 1.42 (3H, s), 1.38 (3H,s); ^{13}C NMR (125 MHz, $CDCl_3$, δ ppm): 156.80, 154.68, 153.47, 142.74, 142.40, 140.08, 136.24, 135.13, 132.84, 131.68, 129.38, 129.22, 129.09, 128.93, 128.25, 121.14, 117.55, 116.90, 115.82, 14.69, 14.59, 14.32. HRMS (ESI): m/z calcd for $C_{26}H_{23}BF_2N_2O$ [M+ H]: 429.1872, found 429.1943.

2.3.2. Synthesis of ER-F

In a 100 mL two neck R.B flask, **ER-S** (30 mg, 0.07 mmol) was dissolved in 10 ml of anhydrous dichloromethane. Then 100 µL of Et_3N was added to the reaction mixture and allowed to stir for 10 minutes at room temperature under N_2 atmosphere. Then 20 µL of acryloyl chloride was added to this and resulting mixture was stirred at room temperature until all the starting material was consumed, monitored by TLC. Then water was added to it and organic layer was extracted using dichloromethane. The organic layer was collected and dried over anhydrous sodium sulphate and solvent was removed under reduced pressure. It was then subjected to column chromatography using silica gel (100-200 mesh) as stationary phase and 5% EtOAc in hexane as mobile phase to get probe **ER-F** as solid. Yield: 70%. ^{1}H NMR (500 MHz, $CDCl_3$, *J* in Hz, δ ppm) : 7.55 (1H, d, *J*= 15.5), 7.53 (3H, d, *J* = 8.2), 7.41 (3H, d, *J* = 5.8), 7.25 – 7.21 (2H, m), 7.13 (1H, d, *J* = 16.3), 7.07 (2H, d, *J* = 8.4), 6.56 (1H, s), 6.52 (1H, s), 6.25 (1H, dd, *J* = 17.3, 10.5), 5.95 (2H, d, *J* = 11.1), 2.52 (3H, s), 1.35 (3H, s), 1.31 (3H, s); ^{13}C NMR (125 MHz, $CDCl_3$, δ ppm): 164.35, 155.92, 152.21, 150.90, 143.27, 142.34, 140.65, 135.03, 134.69, 134.39, 132.78, 132.05, 129.15, 129.01, 128.44, 128.14, 127.86, 121.88, 121.55, 119.41, 117.48, 14.79, 14.57, 14.42. HRMS (ESI): m/z calcd for $C_{29}H_{26}BF_2N_2O_2$ [M + H]: 483.1977, found 483.2057.

2.4. Results and Discussions

Methodology for synthesis of this new chemodosimetric reagent **ER-F** is shown in Scheme 2.1. Analytical as well as spectroscopic data confirmed the proposed molecular structure and desired purity of **ER-F**. Single crystal X-ray structure for **ER-F** also confirmed its proposed molecular structure. All studies were performed in aqueous HEPES-CH_3CN (9:1, v/v) medium at physiological pH 7.2, unless mentioned otherwise.

Electronic spectrum recorded for **ER-F** showed three distinct band maxima at ~335, ~535 and ~575 nm in aq. buffer medium. Band at ~575 nm and 535 nm

were attributed to the 0-0 and 0-1 vibrational band, respectively, of a strong S_0-S_1 transition.[18] Relatively weak and shorter wavelength bands (< 400 nm) were assigned for the S_0-S_2 and S_0-S_3 transitions. Modest detectable shifts to longer wavelength were observed for bands at ~535 and ~575 nm on increase in solvent polarity. This confirmed some ICT nature of these transitions with alkoxy/phenoxy moiety for **ER-F**/**ER-S** as donor and BODIPY core as acceptor. Two weak emission bands at 565 and 610 nm were observed ($\Phi_{\lambda Ext}^{530nm}$ = 0.004, Φ: integrated quantum yield) on excitation at 530 nm. While, a weak emission band was observed at 610 nm ($\Phi_{\lambda Ext}^{575nm}$ = 0.001) on excitation at 575 nm. Shifts of these emission bands to longer wavelength were relatively more prominent than that was observed for electronic spectra, which suggested that ICT states became more prominent in their excited state.[19]

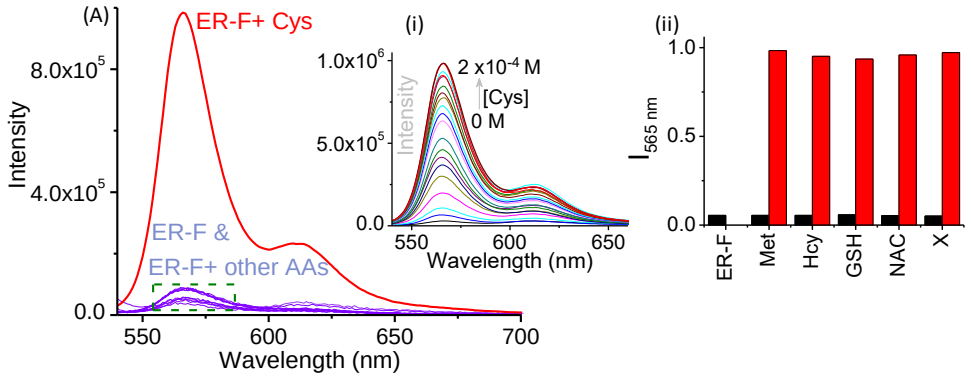

Figure 2.1. (A) Change in emission spectrum of **ER-F** (10 μM) in absence and presence of different AAs (0.2 mM; AA: Cys, Met, Hcy, GSH, NAC and X (X = His, Leu, Phe, Try, Tyr, Val , Ala, Arg, Gly, Glu, Pro, Ser, Asp, Glu, Thr, Iso & Lys)); Insets: (i) emission titration profile for **ER-F** (10 μM) with varying [Cys] (0-200 μM) and (ii) changes in emission intensity of **ER-F** (10 μM) induced by Cys (50 μM) in presence of large excess (0.2 mM) of other AAs like Met, Hcy, GSH, NAC and X. Red bar and black bar represent emission response in presence and absence of Cys, respectively. Studies were performed in aq. HEPES buffer-CH_3CN (9:1, v/v; pH 7.2) medium; $\lambda_{Ext}/\lambda_{Em}$: 530/565 nm.

In order to explore the potential bio analytical application of the probe **ER-F**, we checked emission responses of **ER-F** (10 μM) in presence of 20 mole equivalence of various AAs and certain anionic analytes (e.g. CN^-, SCN^-, etc.) in an essentially aq. buffer medium (Figure 2.1). No detectable change in emission spectrum for **ER-F** was observed for all these analytes that we had used for this study, except Cys. An apparent switch *ON* emission response was observed for Cys with maxima at 565 ($\Phi_{\lambda Ext}^{530nm}$ =0.102) nm. Literature reports reveal that for unsubstituted BODIPY,[20] band around 610 nm is absent and this further confirms the ICT nature of this transition.

Interference studies were performed by recording emission spectra of **ER-F** (10 μM) with Cys (50 μM) in presence of large excess (200 μM) of other AAs and anions under identical condition (Figure 2.1). Results of such studies confirmed insignificant interference from these analytes mentioned. A close look at the ESI-Ms data tends to suggest that reagent **ER-F** reacts with Cys to produce **ER-S**. To confirm this, we further isolated and purified the product of the reaction between **ER-F** and Cys. ^{1}H NMR and ESI-Ms spectral data of the isolated product clearly confirmed the formation of **ER-S**. Importantly, electronic and emission spectra for this pure isolated product was found to be identical with **ER-S** in aq. buffer medium and this further corroborated our proposition.

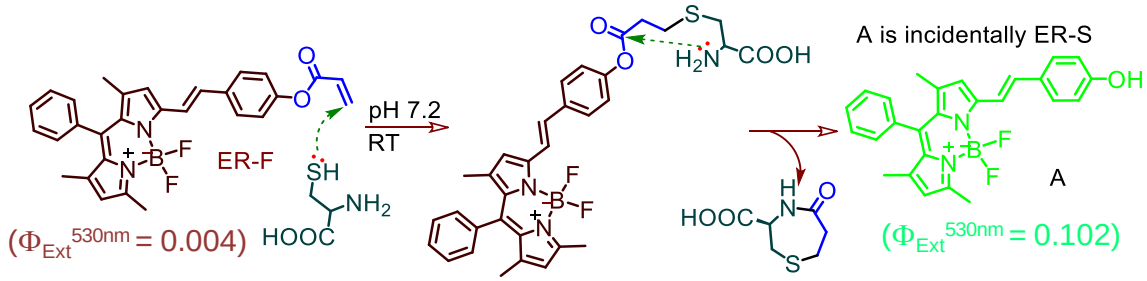

Scheme 2.2. Proposed mechanistic pathway for the reaction between the reagent **ER-F** and Cys (Φ values are reported at 565 nm).

Nucleophilic conjugate addition reaction involving free sulfhydryl group of Cys moiety was anticipated with α,β-unsaturated ester functionality of **ER-F** to yield an intermediate, which underwent an intramolecular cyclization reaction to eliminate (R)-5-oxo-1,4-thiazepane-3-carboxylic acid and regenerate **ER-S** and accounted for the luminescence *ON* response (Scheme 2.2).

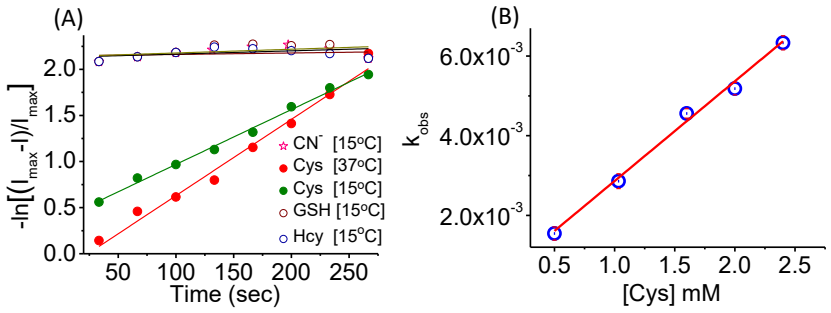

Figure 2.2. (A) Representative ($-\ln(I_{Max}-I) / I_{Max}$] vs. time) plots for evaluation of k_{obs} for **ER-F** (10 μM) & Cys/Hcy/GSH/CN^- (2 mM) at specified temperature and these plots clearly revealed no change in solution luminescence for Hcy/GSH/CN^- was observed; (B) plot of k_{obs} vs. [Cys] for evaluating the overall rate constant for the reaction between **ER-F** and Cys. All kinetic studies were performed in aq HEPES-CH_3CN (9:1, v/v; pH 7.2) medium & $\lambda_{Ext}/\lambda_{Em}$: 530/565 nm.

A linear dependency of the pseudo first order rate (k_{obs}) constants ($k_{obs} = k_c$ [Cys] + c, where k_c: rate constant for the overall reaction) and c is insignificant intercept; Figure 2.2A) on [Cys] was observed by monitoring luminescence changes at 565 nm (λ_{Ext}: 530 nm) (Figure 2.2A). This clearly suggested that the rate determining step for this reaction involved Cys.

Negligible intercept also suggested absence of any detectable side reaction that could contribute to this observed luminescence changes. This helped us in evaluating k_c as 2.51×10^{-3} s^{-1} at 15°C. These results confirmed that the luminescence enhancement at 565 nm, involved Cys in the slow step of the reaction and led to the generation of **ER-S** with much improved Φ value.

Hcy, GSH and NAC are most common analytes which interfere with Cys recognition that involve free -SH functionality. For the present study, Hcy, GSH and N-acetyl cysteine (NAC) failed to participate in such reaction presumably due to their unfavourable pK_a values.[10g,21]

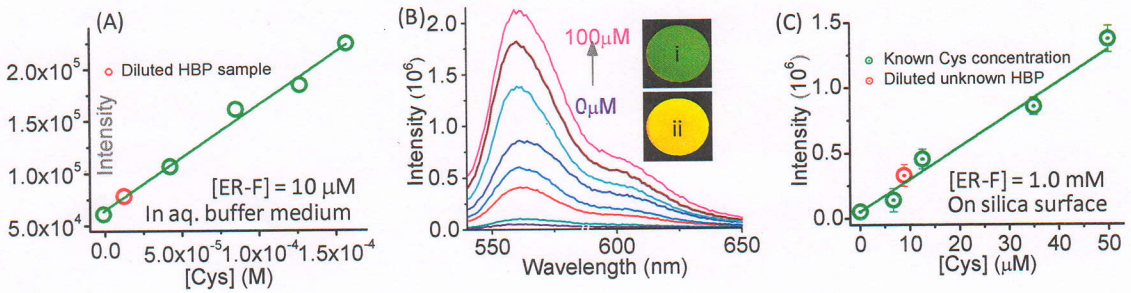

Figure 2.3. (A) and (C) Calibration plots for emission intensity vs. [Cys] for **ER-F** (λ_{Mon} = 565 nm & λ_{Ext} = 530 nm) in presence of known (O) [Cys] and (O) unknown [Cys] in HBP sample; (B) solid state emission spectra for silica surface modified with **ER-F** (0.1 mM) and exposed to varying [Cys], Insets: snap shot of visually detectable change in fluorescence of the silica surface modified with **ER-F** on irradiation with 365 nm light in (i) absence and presence all other AAs (except Cys) & NAC and in (ii) presence of on Cys; Aq. HEPES buffer-CH_3CN (9:1, v/v; pH 7.2) solution was used for studies in (A) and Cys solution in pure aq. HEPES buffer medium was used for studies described in (B) and (C).

Interestingly, no change in fluorescence for **ER-F** was observed upon addition of Bovine serum albumin (BSA, a protein molecule that has free sulfhydryl$_{Cys}$ group). However, Cys residue in BSA lacks the free $-NH_2$ functionality, unable to participate in the intramolecular cyclization reaction to regenerate **ER-S**. Thus, above discussions confirmed that the fluorescence *ON* response at ~ 565 and ~ 610 nms could only be achieved for reaction between **ER-F** and Cys having–SH

and $–NH_2$ moieties (Scheme 2.2). Feasibility of such a mechanistic pathway is also discussed in earlier reports.[13,22] Apart from unfavourable pK_a, this could have also contributed to the inactivity of NAC towards the reagent **ER-F**. Good linear fit of the B-H plot, obtained from the data available from the emission titration profile, confirmed a 1:1 reaction stoichiometry for the reaction between **ER-F** and Cys.

Further, pH studies confirmed that the probe **ER-F** was stable for the pH range 4.5–9 and this supported the basis for performing all our studies in physiologically relevant pH (7.2). Lowest detection limit was evaluated as 15 nM. The concentration level of Cys in HBP sample of a healthy person is typically in the range of 240–360 μM.[7b,23] Considering this, reagent **ER-F** is sensitive enough for analysis of Cys in real HBP sample and this led us to explore such a possibility. Diluted HBP (200 μl) was added to the reagent **ER-F** (10 μM) solution (aq. HEPES-CH_3CN medium (9:1, v/v; pH 7.2) at RT and emission measurements were performed after the solution mixture was allowed to equilibrate for 2 min. Emission intensity of such solution was measured and $[Cys]_{Free}^{HBP[dilute]}$ was evaluated by comparing observed intensity with the standard calibration curve (Figure 2.3A & 2.3C). This on multiplication with the appropriate dilution factor, revealed the exact $[Cys]_{Free}^{HBP}$ ((310 ± 4) μM) in HBP sample and this value was within the allowed limit for a healthy human being.[7b]

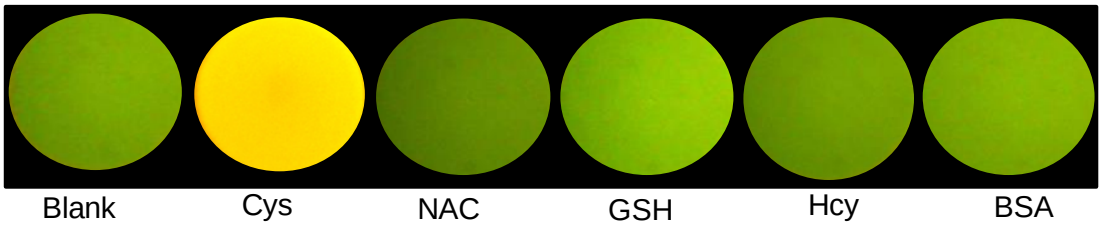

Figure 2.4. Snap shot of the visually detectable changes in fluorescence of silica surface, modified with the probe **ER-F** in absence and presence of (100 μM) different analytes (Cys, NAC, GSH, Hcy, BSA (Bovine serum albumin) and diluted HBP sample). Fluorescence colour changes were observed using 365 nm UV lamp; [**ER-F**] used for the study was 0.1 mM.

Possibility of developing test strip for detection of Cys was also explored. Acetonitrile solution of **ER-F** was drop casted on silica TLC strips and was dried at 35°C. These plates were exposed to different AAs (100 μM) solution (aq. HEPES buffer, pH 7.2). Results clearly revealed (Figure. 2.4 & 2.3B: inset) that the plate exposed to Cys showed visually detectable yellow luminescence, while

no such change was observed for all other AAs and NAC. Interestingly, luminescence spectra recorded for such strips dipped in pure aq. buffer solutions (pH 7.2) of varying [Cys] helped us in developing a calibration plot (Figure 2.3A & 2.3C), which could be utilized for quantitative estimation of Cys in an HBP sample. Thus, this result confirmed that this reagent could be utilized for developing test strip for qualitative and quantitative estimation of Cys in HBP samples. MTT assay studies confirmed insignificant toxicity of the reagent **ER-F** towards Hct116 cells (Figure 2.5(ii)). This encouraged us to explore the option of using this reagent for mapping endogenous Cys in Hct116 cells.

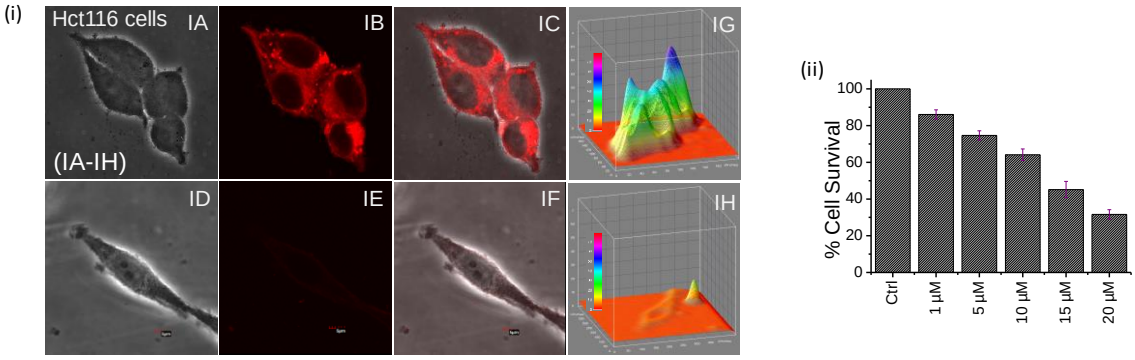

Figure 2.5. (i) CLSM images of Hct116 cells (IA-IH), cells incubated with 1 μM of **ER-F**, (IA): bright field images, (IB): dark field image and (IC): overlay images of (IA) & (IB); Cells pre-treated with 1 mM of NEM then incubated with 1 μM of **ER-F**, (ID): bright field image, (IE): dark field image, (IF): overlay of (ID) & (IE). (IG) and (IH) 3D intensity plot of (IB) & (IE) respectively; (ii) MTT assay to determine the cell viability percentage in presence of **ER-F** in Hct116 colon cancer cells.

It is evident from Figure 2.5(IB) & 2.5(IG) that the bright-red fluorescence images were observed for Hct116 cells that were treated only with **ER-F** (1 μM), which confirmed that the intracellular Cys reacted with probe **ER-F** and accounted for the formation of **ER-S**. To confirm this, further experiments were performed. Hct116 cells were washed thoroughly after pre-treated with excess NEM (1 mM), an effective thiol blocker, and then these cells were exposed to the reagent **ER-F**. Quenched intracellular red fluorescence (Figure 2.5(IE) & 2.5(IH)) clearly established that intracellular red fluorescence was solely due to the chemodosimetric reaction of endogenous Cys with **ER-F.**

To explore the suitability of the reagent **ER-F** for probing any intracellular enzymatic transformations, HepG2 cells with higher abundance of aminoacylase-I were exposed to N-acetyl cysteine (NAC), a well known drug for Cys supplement. HepG2 cells were first pre-treated with NEM and after thorough

washing; cells were further exposed to NAC. Red fluorescence (Figure 2.6 (IIA & IIC)) of these HepG2 cells exposed to NAC and the complete absence of any intracellular red fluorescence in control experiment (Figure 2.6) clearly confirmed the generation of Cys from NAC by enzymatic action of aminoacylase-I.

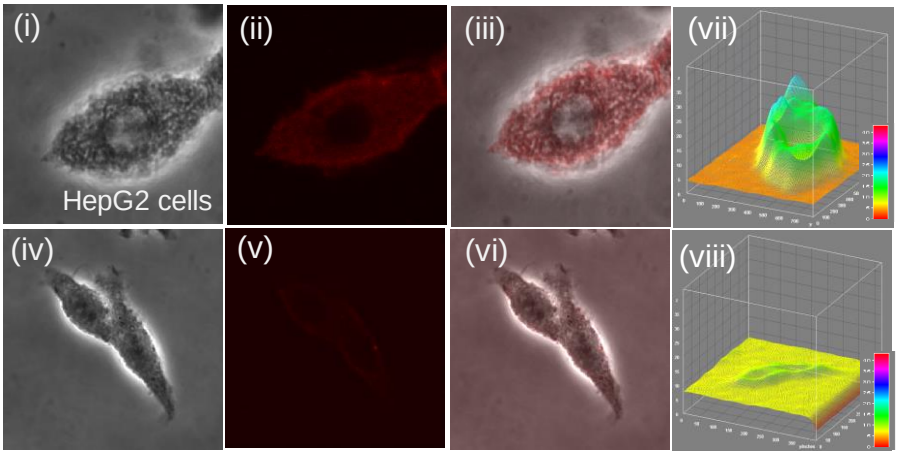

Figure 4.6. CLSM images of live HepG2 cells: (i) - (iii): bright field, dark field and overlay images of cells treated first with 1 mM NEM and then treated with 25 µM NAC for 1h, followed by incubation of 1 µM of **ER-F** for 20 min, respectively and (vii): 3D intensity profile plot of image (ii); (iv)**–**(vi): cells treated with 1 mM NEM, and followed by incubation of 1 µM of **ER-F** for 20 min and (viii): 3D intensity profile plot of image (v).

CLSM images shown in Figure 2.7 reveal that this reagent **ER-F** as well as the product (**ER-S**) is preferentially localized in the lipid dense region,

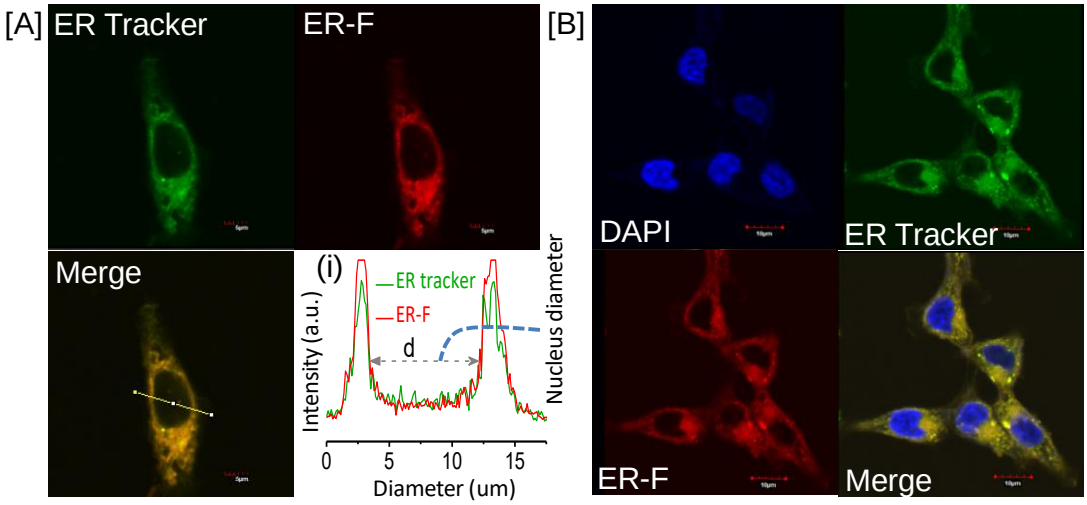

Figure 2.7. (A) Hct116 cells stained with 1 µM of **ER-F** in presence of ER tracker green; (i) Intensity profile of ROIs across cells: red line represent intensity of **ER-F** and green line indicate intensity for ER Tracker green; (B) co-localization experiment: Cells were co-stained with **ER-F**, ER tracker green and DAPI; $\lambda_{Ext}/\lambda_{Em}$: 530/573 nm.

Endoplasmic Reticulum (ER) of Hct116 cells. Results of the co-localization studies with ER-tracker green (ER-specific reagent) and DAPI (nuclei specific reagent, with little or no cytoplasmic labelling) as well as the high Pearson's co-localization coefficient of 0.9682 for this co-localization study confirmed this (Figure 2.7).

2.5. Conclusion

Thus, this reagent offered us an option of mapping endogenous Cys in the ER region of Hct116 cells. To the best of our knowledge such reports are scarce. Thus, this chapter reveals a new chemodosimetric imaging probe **ER-F** for detection of spatial and temporal distribution of Cys as well as its *in-situ* generation during the enzymatic action of aminiacylase-I in NAC in ER region of live HepG2 cells. Interference studies confirmed specificity of this reagent towards Cys among all other AAs, including Hcy, GSH and NAC. Notably this reagent could even be used for developing a modified silica strip for qualitative and quantitative estimation of Cys present in human bio-fluid like HBP without any interference from other derivatives of cysteine (like NAC, BSA). Example of such a versatile Cys-specific regent is rare in contemporary literature.

2.6. References

1. (a) J. C. Bardwell, K. McGovem and J. Beckwith, *Cell*, 1991, **67**, 581; (b) M.-J. Gething and J. Sambrook, *Nature*, 1992, **355**, 33-35; (c) M. LaMantia and W. Lennarz, *Cell* , 1993, **74**, 899.

2. (a) C. Hwang, A. J. Sinskey and H. F. Lodish, *Science*, 1992, **257**, 1496; (b) S. Carelli, A. Ceriotti, A. Cabibbo, G. Fassina, M. Ruvo and R. Sitia, *Science*, 1997, **277** ,1681.

3. (a) R. O. Ball, G. Courtney-Martin, and P. B. Pencharz, *J. Nutr*., 2006, **136**, 1682S-1693S; (b) V. I. Lushchak, *J. Amino Acids*, 2012, doi:10.1155/2012/736837.

4. C. E. Paulsen and K. S. Carroll., *Chem. Rev*., 2013, **113**, 4633.

5. K. G. Reddie and K. S. Carroll, *Curr. Opin. Chem. Biol*., 2008, **12**, 746.

6. (a) E. Weerapana, C. Wang, G. M. Simon, F. Richter, S. Khare, D. M. B. D.illon, D. A. Bachovchin, K. Mowen, D. Baker and B. F. Cravatt, *Nature*, 2010, **468**, 790. (b) D. M. Townsend, K. D. Tew and H. Tapiero, *Biomed. Pharmacother*., 2003, **57**, 145. (c) S. Shahrokhian, *Anal. Chem*., 2001, **73**, 5972.

7. (a) X. F. Wang and M. S. Cynader, *J. Neurosci*., 2001, **21**, 3322; (b) U. G. Reddy, H. Agarwalla, N. Taye, S. Ghorai, S. Chattopadhyay and A. Das, *Chem. Commun.,* 2014, **50**, 9899.

8. T. Dierks, B. Schmidt and K. V. Figura, *Proc. Natl. Acad. Sci*., 1997, **94**, 11963.

9. (a) P.W. Riddles, R.L. Blakeley and B. Zerner, *Methods Enzymol.*, 1983, **91**, 49; (b) N. Ercal, P. Yang and N. Aykin, *J. Chromatogr. Biomed. Appl.,* 2001, **753**, 287; (c) S. D. Fei, J. H. Chen, S. Z. Yao, G. H. Deng, D. L. He and Y. F. Kuang, *Anal. Biochem*., 2005, **339**, 29; (d) T. Inoue and J. R. Kirchhoff, *Anal. Chem*., 2002, **74**, 1349; (e) P. Ryant, E. Dolezelova, I. Fabrik, J. Baloun, V. Adam, P. Babula and R. Kizek, *Sensors*, 2008, **8**, 3165; (f) Y. Sato, T. Iwata, S. Tokutomi and H. Kandori, *J. Am. Chem. Soc*., 2005, **127**, 1088. (g) X. Guan, B. Hoffman, C. Dwivedi and D. P Matthees, *J. Pharm. Biomed. Anal*., 2003, **31**, 251.

10. (a) L. Yi, H. Li, L. Sun, L. Liu, C. Zhang and Z. Xi, *Angew. Chem. Int. Ed*., 2009, **48**, 4034; (b) X. Chen, S.-K. Ko, M. J. Kim, I. Shin and J. Yoon, *Chem. Commun*., 2010, **46**, 2751, (c) X. Zhou, X. Jin, G.Sun, and X. Wu, *Chem. Eur. J*., 2013, **19**, 7817; (d) H. S. Jung, K. C. Ko, G.-H. Kim, A.-R. Lee, Y.-C. Na, C. Kang, J.Y. Lee and J. S. Kim, *Org. Lett*., 2011, **13**,1498; (e) V. Hong, A. A. Kislukhin and M. G. Finn, *J. Am. Chem. Soc*., 2009, **131**, 9986; (f) L. E. Santos-Figueroa, M. E. Moragues, E. Climent, A. Agostini, R. Martı´nez-Ma´n˜ez and F. Sanceno´n, *Chem. Soc. Rev*., 2013, **42**, 3489; (g) H. A. Anila, U. G. Reddy, F. Ali, N. Taye, S. Chattopadhyay and A. Das, *Chem. Commun*., 2015, **51**, 15592.

11. (a) S. R. Malwal, A. Labade, A. S. Andhalkar, K. Sengupta and H. Chakrapani, *Chem. Commun*., 2014, **50**, 11533; (b) B. Zhu, X. Zhang, Y. Li, P. Wang, H. Zhangb and X. Zhuang, *Chem. Commun*., 2010, **46**, 5710; (c) R. R. Nawimanage, B. Prasai, S. U. Hettiarachchi, and R. L. McCarley, *Anal. Chem*., 2014, **86**, 12266.

12. H. Li, J. Fan, J. Wang, M. Tian, J. Du, S. Sun, P. Sun and X. Peng, *Chem. Commun*., 2009, 5904.

13. (a) X. Yang, Y. Guo and R. M. Strongin, *Angew. Chem. Int. Ed*., 2011, **50**, 10690; (b) Z. Guo, S. W. Nam, S. Park and J. Yoon, *Chem. Sci*., 2012, **3**, 2760.

14. G. M. Sheldrick, SAINT 5.1 ed., Siemens Industrial Automation Inc., Madison, WI, 1995.

15. SADABS, Empirical Absorption Correction Program, University of Göttingen, Göttingen, Germany, 1997.

16. G. M. Sheldrick, SHELXTL Reference Manual: Version 5.1, Bruker AXS, Madison, WI, 1997.

17. G. M. Sheldrick, SHELXL-97: Program for Crystal Structure Refinement, University of Göttingen, Göttingen, Germany, 1997.

18. R. Hu, E. Lager, A. Aguilar-Aguilar, J. Liu, J. W. Y. Lam, H. H. Y. Sung, I. D. Williams, Y. Zhong, K. S. Wong, E. Pen˜a-Cabrera and B. Z. Tang, *J. Phys. Chem. C***,** 2009**, 113**, 15845.

19. M. Baruah, W. Qin, C. Flors, J. Hofkens, R. A. L. Valle´e, D. Beljonne, M. V. d. Auweraer, W. M. De Borggraeve and N. Boens, *J. Phys. Chem. A,* 2006**, 110***,* 5998.

20. (a) M. Emrullahog˘lu, M. Üçüncü and E. Karak, *Chem. Commun.,* 2013, **49**, 7836.

21. C. A. S. Regino and D. E. Richardson, *Inorg. Chim. Acta*, 2007, **360**, 3971.

22. (a) Q. Zhang, D. Yu, S. Ding and G. Feng, *Chem. Commun*., 2014, **50**, 14002; (b) B. Liu, J. Wang, G. Zhang, R. Bai, and Y. Pang, *ACS Appl. Mater. Interfaces*, 2014, **6**, 4402.

23. (a) P. Das, A. K. Mondal, N. B. Chandar, M. Baidya, H. B. Bhatt, B. Ganguly, S. K. Ghosh and A. Das, *Chem. Eur. J*., 2012, **18**, 15382; (b) S. Sreejith, K. P. Divya and A. Ajayaghosh, *Angew. Chem. Int. Ed*., 2008, **47**, 7883.

CHAPTER 3

SPECIFIC REAGENT FOR Cr(III): IMAGING CELLULAR UPTAKE OF Cr(III) IN HCT116 CELLS AND THEORETICAL RATIONALIZATION

Publication:

J. Phys. Chem. B, 2015, **119**, 3018 − 13026

3.1. Introduction

Apart from its natural source, Chromium is also added to the soil through anthropogenic and various industrial activities.[1-2] The most common form of Chromium that exist in soil, is Cr(III). Cr(III) is an important analyte for biological processes at cellular level.[3] Cr(IV) is known to be reduced by intracellular reducing agents to the Cr(III), which binds DNA through guanine N_7 and the adjacent phosphate backbone.[4] Studies also reveal that Cr(IV) to Cr(III) reduction takes place in certain wetland plants.[5] It is argued that this Cr(VI) to Cr(III) reduction initially happens in the fine lateral roots, while the Cr(III) subsequently translocates to leaf tissues and gets localized there presumably in the form of oxalate salt. Cr(III) is believed to be less toxic than Cr(IV) for mammalians and for certain biological processes Cr(III) is used as a nutrient. Cr(III) containing glucose tolerance factor is believed to be an important co-factor of insulin and catalyses the glucose metabolism to enhance the peripheral actions of insulin. Cr(III) is also available in many common food stuff, vegetable and animal fats.[6-7] Deficiency of Cr(III) may cause several chronic diseases such as diabetes, cardiovascular and nervous system disorders.[8] Though Cr(III) is known to be non-toxic, but high doses may have adverse influences on human physiology.[9] Several researchers have expressed their reservations about the usefulness of Cr(III) as a long-term nutritional supplement for its possible genotoxic effects and the general notion is that all forms of chromium, including Cr(III), are to be considered as human carcinogens.[10-12] This is especially true as the risk to benefit ratio for usages of Cr(III) has not yet been adequately characterized.[6-7] Solubility of Cr(III) compounds is generally less in aqueous medium and this accounts for its lower mobility and bioaccumulation.[13] Thus, there is a pressing need to develop an efficient and non-cytotoxic molecular receptor that allows specific recognition and binding to Cr(III) with an associated optical responses.

There exist only few receptors that discuss some specificity towards Cr(III) either in organic or in mixed aqueous-organic medium that are predominantly organic in nature.[14-22] Few literature reports discuss about selective binding to Cr(III) with interference either from Fe(III) or Hg(II) in mixed solvent medium that is predominantly aqueous.[18,23-26] These reports further suggest that masking of Hg^{2+} (as HgI_4^{2-}) could be achieved in the presence of an excess of I^- and it allows the specific detection of Cr(III). There are only three previous reports that describe the use of reagents for the detection of Cr(III) in pure aqueous solution;[23,27,28] one of them describes the

interference by Fe^{3+}. The most recent report reveals that a rhodamine derivative within a polymeric matrix could be utilized for specific detection of Cr(III) in pure aqueous medium and the hydrophobic micro-environment generated around the binding core of the receptor induces a favorable influence for the detection of Cr(III).[28] However, such a reagent is not appropriate for use as an imaging reagent.

More recently, use of various molecular aggregates like micelles and vesicles have gained significance as drug carriers and cellular markers or imaging reagents, which provides such drug/markers a direct access to the cytoplasm; while subsequent steps are then needed for their release into the cytoplasm.[29] Earlier studies have also established that TX100 is actually biologically benign and is being widely use for improving the cell membrane permeability of various drugs and molecular probes.[30-39] We have adopted this methodology to allow the new receptor **L_1** to be self-assembled inside the micellar structure of Triton X-100 (TX100) and this self-assembled molecular aggregate is found to be specific towards Cr(III) in an ensemble of all common alkali/alkaline earth/transition/lanthanide metal ions in pure aqueous buffer medium having pH 7.2. Interestingly, the specific binding of the reagent **L_1** to Cr(III) inside the micellar structure resulted a sharp luminescence ON response. For unambiguous assignment and understanding of the nature of the binding mode of **L_1** with Cr(III), studies with a model reagent **L_2** under identical experimental condition were also performed. Cr(III)-η^2-olefin π-interactions involving two olefin bonds in **L_1** are proposed based on the results of various spectroscopic as well as computational studies.

3.2. Experimental Section

3.2.1. Materials

Rhodamine B, Ethylenediamine, 3-bromoprop-1-ene, 1-bromopropane, all metal perchlorate salts (e.g $LiClO_4$, $NaClO_4$, $KClO_4$, $CsClO_4$, $Mg(ClO_4)_2$, $Ca(ClO_4)_2$, $Ba(ClO_4)_2$, $Sr(ClO_4)_2$, $Cu(ClO_4)_2$, $Zn(ClO_4)_2$, $Co(ClO_4)_2$, $Ni(ClO_4)_2$, $Cr(ClO_4)_3$, $Fe(ClO_4)_2$, $Cd(ClO_4)_2$, $Hg(ClO_4)_2$, and $Pb(ClO_4)_2$) and lanthanide ions as nitrate salts were obtained from Sigma-Aldrich and were used as received. Dulbecco's Modified Eagle's Medium (DMEM) (Invitrogen), Fetal Bovine Serum (FBS) (Invitrogen), Penicillin Streptomycin antibiotics (Invitrogen), Hct116 cell line (National Centre For Cell Science), trypsin-EDTA, MTT (3-(4,5-dimethylthiazol-2-yl)-2,5-diphenyltetrazolium bromide) (Sigma), Iso-propanol (Fischer Scientific), Triton X 100 (USB Corporation), and Paraformaldehyde (Sigma) were used as received. Et_3N, Tris Buffer, NaCl was

procured from S.D. fine chemicals, India and was used as received. Solvents such as acetonitrile, chloroform were also purchased from S.D. Fine Chemicals, India and were used without further purification unless mentioned otherwise. Silica gel 100-200 mesh was used for column chromatography. Analytical thin layer chromatography was performed using silica Gel GF 254. HPLC grade water (Merck, India) was used for experiments and all spectral studies. Aminoethylene rhodamine B (**L**) was synthesized following a standard procedure.[40-46]

3.2.2. Analytical Methods

ESI-MS measurements were performed using a Micromass QTof- Micro instrument. FT-IR spectra were recorded as KBr pellets using a Perkin Elmer Spectra GX 2000 spectrometer. NMR spectra were recorded on Bruker 500 MHz FT NMR (model: Avance-DPX 500). Electronic spectra were recorded with a Varian Cary 500 Scan UV-Vis-NIR Spectrophotometer, Isothermal Titration Calorimetry studies (ITC) were performed in Microcal iTC200, while emission spectra were recorded using either Edinburgh Instrument Xe-900 Spectrofluorometer or PTI.

Summary of crystallographic data for $\mathbf{L_1}$ is given in Table 3.1. Single crystal of suitable dimension was chosen under an optical microscope and mounted on a glass fibre for data collection on a Bruker SMART APEX diffractometer equipped with CCD area detector at 150K. Intensity data for the crystal was collected using graphite-monochromated MoK_α (λ=0.71073 Å) radiation. The data integration and reduction was performed with SAINT software.[47] Data was subjected to empirical absorption correction using SADABS.[48] The structure was solved by direct methods using SHELXTL[49] and was refined by full matrix least square procedures based on F^2 using the program SHELXL-97.[50] All non-hydrogen atoms were refined anisotropically till convergence was reached. Hydrogen atoms, attached to the organic moieties, were either located from the difference of Fourier map or stereochemically fixed in the complex.

3.2.3. General Methodology Adopted for Spectroscopic Studies

A solution of the perchlorate salts of the respective ion (Li^+, Na^+, K^+, Cs^+, Ca^{2+}, Mg^{2+}, Ba^{2+}, Sr^{2+}, Fe^{2+}, Ni^{2+}, Co^{2+}, Cu^{2+}, Mn^{2+}, Cd^{2+}, Pb^{2+}, Ba^{2+}, Zn^{2+}, Sr^{2+}, Hg^{2+} and Cr^{3+}) and nitrate salts of lanthanides ions (Tb^{3+}, Ho^{3+}, Ce^{3+}, Sm^{3+}, Rb^+, Pr^{3+}, Eu^{3+}, Gd^{3+}, Nd^{3+}, Dy^{3+}, Tm^{3+}, Er^{3+}, Yb^{3+}) in pure aqueous buffer medium having pH 7.2 were used for all studies. The effective final concentrations of all metal salts were maintained at 1.62 x

10^{-4} M. A stock solution of the receptor **L_1** (6.9 x 10^{-4} M) was prepared in acetonitrile medium and 57 µL of this stock solution was added to 2.5 ml of 0.4 mM TX100 in Tris-HCl aqueous buffer medium having solution pH 7.2 to make the effective ligand concentration of 1.59 x 10^{-5} M. The solution was used for all the photophysical studies.

Table 3.1: Crystallographic data for probe **L_1**

Identification code	Compound 1
Chemical formula	$C_{36}H_{44}N_4O_2$
Formula weight	564.75
Crystal Colour	Light Yellow
Crystal Size (mm)	0.28 x 0.14 x 0.08
Temperature (K)	150(2)
Crystal System	Monoclinic
Space Group	$P2_1$
a(Å)	11.8685(12)
b(Å)	11.7864(12)
c(Å)	12.3181(13)
α(°)	90.0
β(°)	115.4960(10)
γ (°)	90.0
Z	2
V(Å3)	1555.3(3)
Density (Mg/m^3)	1.206
Absorption Coefficient(mm^{-1})	0.075
F(000)	608
Reflections Collected	9020
Independent Reflections	5874
$R_{(int)}$	0.0179
Number of parameters	383
S(Goodness of Fit) on F2	1.039
Final R1 , wR2 (I>2σ(I))	0.0527/ 0.1438
Weighted R1,wR2(all data)	0.0570/ 0.1493
CCDC number	961378

Cr^{3+} stock solution (4.75 x 10^{-3} M) was prepared in pure aqueous medium and was used for all studies. Emission titrations were also performed as a function of [TX100] (0.1 mM, 0.23 mM, 0.32 mM, 0.4 mM, 0.6 mM) in Tris-HCl buffer medium of pH 7.2 by monitoring the increase in emission intensity (using λ_{Ext} = 530 nm, λ_{Mon} = 583 nm and slit width 2/2 nm) on binding of **L_1** to Cr^{3+} for optimizing the maximum enhancement of the emission intensity. The relative fluorescence quantum yields (Φ_f) were estimated using equation 1 for different concentration of TX100 (0.1 mM, 0.23 mM, 0.32 mM, 0.4 mM, 0.6 mM) in Tris-HCl buffer medium (having solution pH of 7.2) and by using the Rhodamine B (Φ_f' = 0.3 in aqueous medium at 37 °C) as a reference.

$$\Phi_f = \Phi_f' \ (I_{sample}/I_{std})(A_{std}/A_{sample})(\ \eta^2_{sample}/\eta^2_{std}) \qquad \text{Eq. 1}$$

where, Φ_f' was the absolute quantum yield for the rhodamine B and was used as reference; I_{sample} and I_{std} are the integrated emission intensities; A_{sample} and A_{std} are the

absorbances at the excitation wavelength, and η_{sample} and η_{std} are the respective refractive indices.

3.2.4. Details of Computational Methodology

The interaction of olefinic π-bonds in the model compound with the chromium ion was examined with DFT M06-2X functional level of theory in water using polarizable continuum (PCM) solvent model.[51,52] The Cr^{3+} ion was treated with LANL2DZ[53,54] basis set and the rest of the atoms were treated with 6-31G* basis set.[55] All structures were optimized in Gaussian 09 version.[56] This interaction was modeled with the core unit around the Cr^{3+} ion. The optimized geometry shows that the Cr^{3+} ion is coordinated with two nitrogen atoms, one oxygen atom, two olefinic π-bonds and a water molecule (Figure 3.4C(i)). The "atoms in molecules" AIM analysis performed with the optimized geometry showed significant interaction of Cr^{3+} ion with these ligand units.[57] The AIM calculations were performed by using multiwfn software.[57,58-60]

3.2.5. Details of the Biological Study

Hct116 cells were seeded on cover slips placed in 6 well plates using DMEM medium and supplemented with 10% FBS and Penicillin Streptomycin antibiotics. After 24 hours of incubation at 37ºC, cells were treated with **L_1** (15.9 μM) for 30 minutes. Cells were then washed thrice with Phosphate Buffer Saline (1X PBS). The **L_1**-stained colon cancer cells Hct116 incubated with Cr^{3+} (10 μM) for 30 min. Then these cultures were washed thoroughly and fixed with 4% PFA for 20 minutes. After washing, cover slips were mounted onto glass slides using Fluoroshield with DAPI (Sigma) mounting medium. Nail paint was used to seal the cover slips mounted on the glass slides. Images were acquired in Olympus Fluoview Microscope ($\lambda_{Ext}/\lambda_{Em}$ = 530/573 nm). 0.4 mM TX100 in aqueous Tris buffer solution (25 mM; pH 7.2) were used for confocal imaging studies and this allowed reagent **L_1** to be trapped inside the micellar structure of TX100 and this allowed us to perform all recognition and binding studies in pure aqueous medium having a physiologically relevant pH of 7.2.

The in vitro cytotoxicity of **L_1** on Hct116 cells Colon cancer cell were determined by MTT (3-(4, 5-Dimethylthiazol-2-yl)-2, 5-diphenyltetrazolium bromide, a yellow tetrazole) assay. Hct116 colon cancer cells (7×10^3) were seeded in each well of a 96 well plate and cultured in a 37°C incubator supplied with 5% CO_2. Cells were maintained in DMEM medium, supplemented with 10% Fetal Bovine Serum and 100 Units of Penicillin Streptomycin antibiotics. After 24 hours the cells were treated with

different concentrations of the **L_1** in triplicates for 12 hours. After treatment cells were added with 0.5 µg/mL of MTT reagent. The plate was then incubated for 4 hours at 37°C and then later added to each well with 100 µL of Isopropyl Alcohol. The optical density was measured at 570 nm using Multiskan Go (Thermo Scientific) to find the concentration of the cell inhibition. The formula used for the calculation of the MTT assay for evaluation of the cell viability is as follows:

Cell viability (%) = (means of Absorbance value of treated group/ means of Absorbance value of untreated control) x 100.

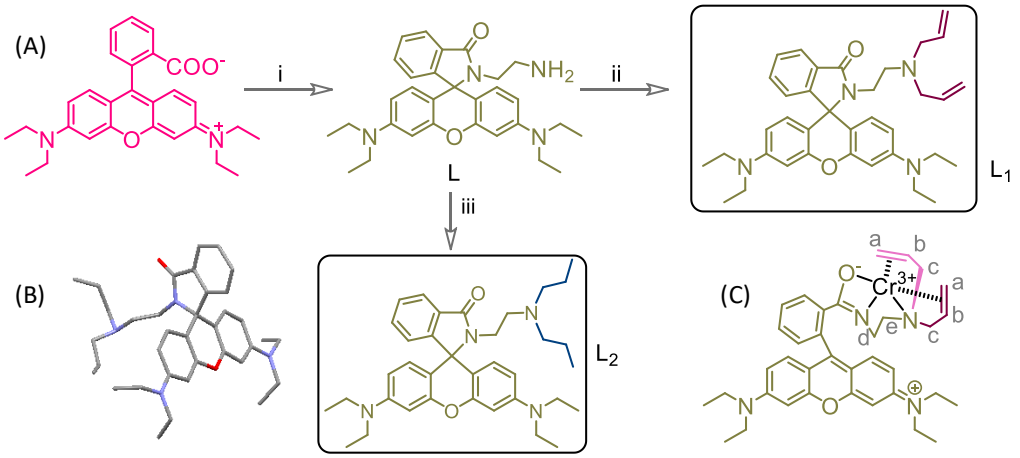

i: $H_2NCH_2CH_2NH_2$, MeOH, Reflux; ii: Dry $CHCl_3$, $H_2C{=}CHCH_2Br$, Et_3N, Inert atmosphere; iii. Dry $CHCl_3$, $H_3CCH_2CH_2Br$, Et_3N, Inert atmosphere

Scheme 3.1. (A) Methodology followed for synthesis of **L_1** and **L_2**. (B) single-crystal X-ray structure of **L_1** [Hydrogen atoms are omitted for clarity]; (C) proposed molecular structure for Cr^{3+}.**L_1**.

3.3. Synthesis and Characterization

3.3.1. Synthesis of L_1

Amino ethyl rhodamine B (400 mg, 0.83 mmol) was dissolved in 20 mL dry chloroform. To this Et_3N (3 mL) was added and the resulting solution was stirred under N_2 atmosphere for 20 minutes. Then, 3-bromoprop-1-ene (530 µL, 5.91 mmol) was added and reaction mixture was refluxed for 12h with constant stirring. Progress of the reaction was monitored by TLC and was continued till all reactants were consumed. The reaction mixture was allowed to attain the room temperature and 10 mL of water was added. Then organic layer was collected and dried over anhydrous Na_2SO_4. Crude product was obtained when solvent was removed under vacuum. It was finally purified by column chromatography using silica gel column and ethyl acetate-hexane (1:9, v/v) as eluent. This enabled us to isolate **L_1** in pure form with 50% yield. ^{1}H NMR

(500 MHz, $CDCl_3$, $SiMe_4$, *J* (Hz), δ ppm): 7.8 (1H, d, *J* = 4.6, H_{18}), 7.32 (2H, m, H_{16}, H_{17}), 6.99 (1H, d, *J* = 4.4, H_{15}), 6.35 (4H, t, *J* = 10, H_4, H_5, H_9, H_{10}), 6.16 (2H, d, *J* = 8.8, H_2, H_{12}), 5.56 (2H, td, *J* = 16.5, 6.5, H_{27}, H_{24}), 4.92 (4H, d, *J* = 18.5, H_{25}, H_{28}), 3.24 (8H, q, J = 6.8, H_{29}, H_{31}, H_{33}, H_{35}), 3.18 (2H, t, *J* = 6.8, H_{22}), 2.85 (4H, d, *J* = 6.2, H_{23}, H_{26}), 2.1 (2H, t, *J* = 6.8, H_{21}), 1.07 (12H, t, *J* = 6.8, H_{30}, H_{32}, H_{36}, H_{34}). ^{13}C NMR (125 MHz, $CDCl_3$, $SiMe_4$, δ ppm): 167.70, 153.38, 148.70, 135.13, 132.22, 131.54, 128.98, 127.97, 123.78, 122.63, 117.53, 108.03, 105.58, 97.73, 64.85, 56.60, 50.46, 44.37, 37.75, 29.69, 12.60. IR (KBr): v_{max}/cm^{-1} = 1684, 1617. ESI-MS (+ve mode, m/z): 565.93 ($M + H^+$), Calc. for $C_{36}H_{44}N_4O_2$ is 564.76.

3.3.2. Synthesis of L_2

Amino ethyl rhodamine B (200 mg, 0.41 mmol) was dissolved in 15 mL dry chloroform. To this Et_3N (500 µL) was added and the resulting solution was stirred for 20 minutes under N_2 atmosphere. Then 1-bromopropane (120 µL, 1.35 mmol) was added and the resulting reaction mixture was refluxed for 24h until all the starting materials were consumed and this was monitored by TLC. After this reaction mixture was allowed to attain the room temperature, 10 mL of water was added. The organic layer, after drying over anhydrous Na_2SO_4, was collected and followed by the removal of chloroform under vacuum to yield the crude product. Column chromatography was performed using silica gel as stationary phase and 10% ethyl acetate in hexane as mobile phase for isolating **L_2** in pure form with 40% yield. ^1H NMR (500 MHz, $CDCl_3$, $SiMe_4$, *J* (Hz), δ ppm): δ 7.81 (dd, 1H, *J* = 5.9, 2.6 , H_{18}), 7.37 (dd, 2H, *J* = 5.6, 3.0, H_{16}, H_{17}), 7.05 – 7.00 (m, 1H, H_{15}), 6.35 (s, 1H, H_{12}), 6.33 (s, 1H, H_2), 6.31 (d, 2H, *J* = 2.5, H_5, H_9), 6.19 (dd, 2H, *J* = 8.9, 2.6, H_4, H_{10}), 3.26 (q, 8H, *J* = 7.0, H_{29}, H_{31}, H_{33}, H_{35}), 3.09 (d, 2H, *J* = 5.8, H_{21}), 2.15 (s, 6H, H_{22}, H_{23}, H_{26}), 1.18 (d, 4H, *J* = 6.7, H_{24}, H_{27}), 1.09 (t, 12H, *J* = 7.0, H_{30}, H_{32}, H_{36}, H_{34}), 0.68 (t, 6H, *J* =6.8, H_{25}, H_{28}).^{13}C NMR (125 MHz, $CDCl_3$, $SiMe_4$, δ ppm): 167.75, 153.77, 148.72, 148.25, 132.25, 129.18, 127.78, 123.93, 122.59, 108.48, 105.63, 97.94, 64.95, 56.78, 50.96, 44.34, 37.79, 37.47, 20.27, 12.54, 11.82. IR (KBr): v_{max}/cm^{-1} = 1680. ESI-MS (+ve mode, m/z): 569.29 ($M + H^+$), Calc. for $C_{36}H_{44}N_4O_2$ is 568.79. Elemental Analysis: Calculated C 76.02, H 8.51, N 9.85; experimentally obtained C 76.20, H 8.50, N 9.88.

3.4. Results and Discussions

Reported literature procedure was adopted for synthesis of the intermediate compound **L**.[40-46] Methodologies used for synthesis of the receptor **L_1** and the model compound **L_2**

are described in scheme 3.1. Desired compound **L_1** and **L_2** were isolated in pure form after necessary workup and were characterized by using various analytical/spectroscopic techniques. Analytical and spectroscopic data confirmed the desired purity and these compounds were utilized for further studies. Molecular structure for the receptor **L_1** was also confirmed by X-ray single crystal structural analysis (Scheme 3.1B). Receptor **L_1** and **L_2**, being present in cyclic spirolactam form, did not show any absorption band beyond 380 nm in acetonitrile medium.[40-46,61-62]

Limited solubility of **L_1** in water restricted us from studying the preferential binding of this reagent towards different metal ions in water. Further, the deleterious and high solvation enthalpy of the target cation could also impose an effective energetic barrier to inhibit binding in aqueous medium. More recently, it has been demonstrated that the micelles obtained from appropriate surfactant not only provide the suitable hydrophobic environment for solubilizing such lypophobic reagents in water, but also provides a favourable local hydrophobic environment for an efficient receptor-cation binding.[63-67] TX100 (CMC = 0.23 mM) was used as a neutral surfactant for solubilizing the receptor **L_1** in aq. medium.

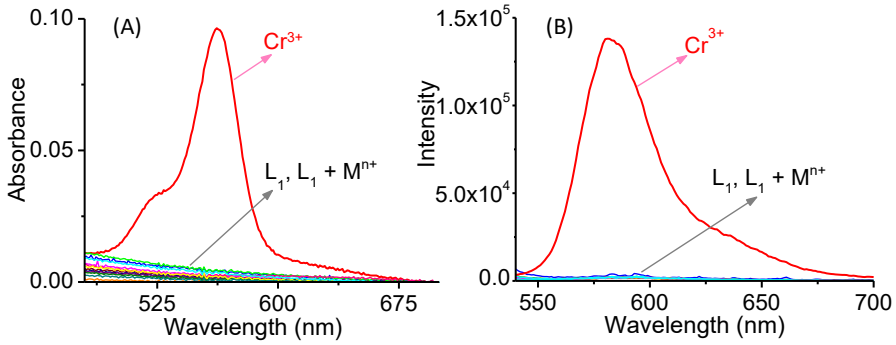

Figure 3.1. Changes in (A) absorption and (B) emission spectra (λ_{Ext} of 530 nm**)** of the receptor **L_1** (1.59 x10^{-5} M) in absence and presence of different metal ions (M^{n+}: 1.62 x 10^{-4}M: Li^+, Na^+, K^+, Cs^+, Ca^{2+}, Mg^{2+}, Sr^{2+}, Ba^{2+}, Cr^{3+}, Fe^{2+}, Co^{3+}, Ni^{2+}, Cu^{2+}, Zn^{2+}, Hg^{2+}, Cd^{2+} and Pb^{2+}); All studies were performed in aq. solution of 0.4 mM TX100 and Tris buffer (5 mM, 25 mM NaCl; pH 7.2).

Reagent **L_1** was found to form water soluble self-assembled micellar structure with TX100 having average diameter of 8.2 nm. It is also reported that the micellar structure is expected to improve the cell membrane permeability of such lypophobic reagent.[67, 68] Typically, aqueous solution of Tris buffer (5 mM, 25 mM NaCl; pH 7.2) was used as solvent for the studies that contained 0.26 gL^{-1} of TX100 (0.4 mmol dm^{-3}). This

concentration for TX100 was optimized based on the results of the fluorescence studies and is discussed latter.

Electronic and steady state luminescence spectra for **L_1** were recorded in the absence and presence of various metal ions in aq. buffer medium of pH 7.2 (Figure 3.1). This clearly revealed that spectra recorded for **L_1** and **L_1** + M^{n+} (when M^{n+} was all other metal ions, except for Cr(III)) did not show any change in absorption or emission spectra of **L_1** (Φ_{L1} = 0.003 with λ_{Ext} = 530 nm). The complete absence of any absorption or emission band in the visible region of the spectrum accounted for the colourless nature of its aqueous solution under the specific experimental conditions.

This also confirmed that **L_1** remained exclusively in the spirolactam form at pH 7.2. However, sharp changes in the electronic and emission spectra were observed when respective spectrum was recorded in presence of Cr(III). Figure 3.1 clearly reveals that among all these cations new absorption and emission spectral bands at 562 nm and 583 nm ($\Phi_{Cr3+.L1}$ = 0.022 with λ_{Ext} = 530 nm), respectively, are evident only in the presence of Cr(III).

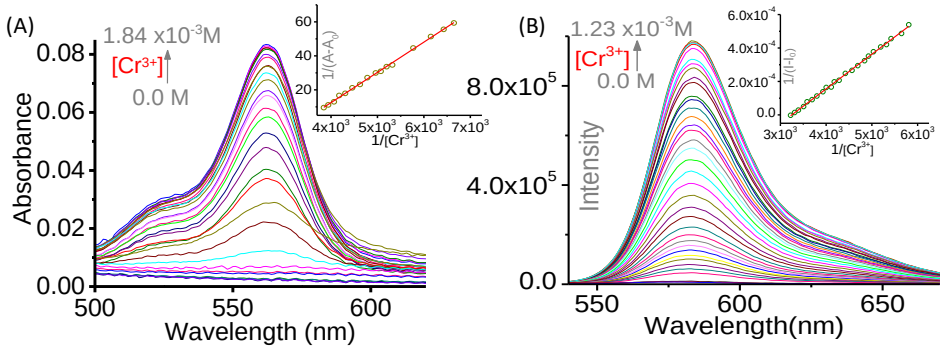

Figure 3.2. Change in (A) Uv-Vis and (B) emission (λ_{Ext} of 530 nm) spectral pattern for **L_1** (1.59 x 10^{-5} M) in presence of varying [Cr^{3+}] (0 - 1.84 x10^{-3} M for Uv-Vis spectral titration and 0 - 1.23x10^{-3} M for emission spectral titration studies). Inset: Benesi-Hildebrand (B-H) plots of spectral titration. All studies were performed in aq. solution of 0.4 mM TX100 and Tris buffer (5 mM, 25 mM NaCl; pH 7.2).

This spirolactam structure for **L_1** was also confirmed by characteristic signal at 64.85 ppm for the tertiary C-atom in the ^{13}C NMR spectrum recorded in $CDCl_3$ medium.[40-46,61,62] Emission spectra recorded for the receptor **L_1** in aq. medium at various pH revealed that the spirolactam form was stable within the pH range 5-12. Thus, the observed absorption and emission spectral responses in presence of Cr(III) were solely due to a specific binding of Cr(III) to **L_1**, which accounted for the conversion of the spirolactam form to an acyclic xanthene form of the rhodamine derivative.[40-46,61,62]

Further, interference studies in presence of 10 mole excess of all other metal ions ensured that the reagent **L_1** was specific towards Cr(III) even in an ensemble of all other common competing cationic analytes. Apart from the specific affinity of the reagent **L_1** towards Cr(III), higher solvation enthalpy of the other probable competing cations could have also imposed an unfavourable energy barrier for inhibiting the binding process. These influences eventually had contributed to the observed specificity towards Cr(III). Results of the Job plot as well as the B-H plot confirmed a 1:1 binding stoichiometry (Figure 3.3C). Formation of Cr^{3+}.**L_1** was also confirmed from the result of maldi MS study. Affinity of **L_1** towards Cr(III) and the associated binding constant for the formation of Cr^{3+}.**L_1** in aq. buffer medium (pH = 7.2) was evaluated from the data obtained from B-H plots of the systematic absorption (K_a^{Abs} = (3.2 ± 0.2).10^3 M^{-1}) and emission (K_a^{Ems} = (3.3 ± 0.2).10^3 M^{-1}) spectral titrations (Figure 3.2).

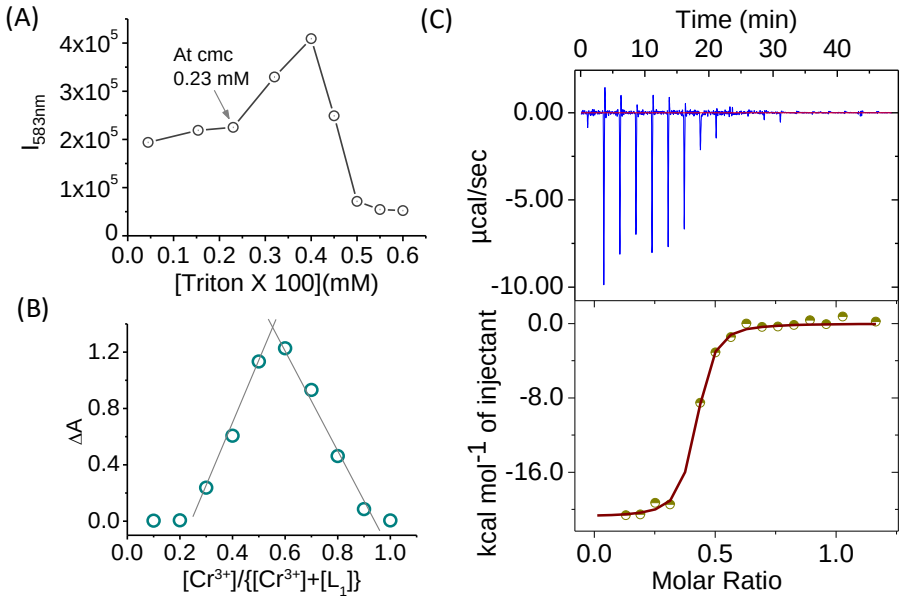

Figure 3.3. (A) Changes in emission intensity of receptor **L_1** (1.59 x 10-5 M) with 5 mole equiv. of [Cr^{3+}] and varying [TX100] in aq. buffer medium; (B) Job's plot of **L_1** with Cr^{3+} showing 1:1 complex formation in aq. Buffer medium; (C) Isothermal Titration Calorimetry (ITC) titration profile for the binding of Cr^{3+} to receptor **L_1** at 25°C in acetonitrile; Top plot: raw data for the sequential 2 µL injection of Cr^{3+} (1.2 x 10^{-3} M) into solution of **L_1** (2.0 x 10^{-4} M) and bottom plot of the heat evolved (kcal mol^{-1}) of Cr^{3+} added.

Analogous absorbance and emission titrations performed with $Cr(ClO_4)_3$ and **L_1** ([Cr(III)] = (0 - 1.93) x 10^{-4} M; [**L_1**] = 1.59 x 10^{-5} M; without using TX 100) in acetonitrile medium helped us in evaluating formation constant for Cr^{3+}.**L_1** in acetonitrile: K_a^{Abs} = (1.1 ± 0.03).10^6 M^{-1}, K_a^{Ems} = (1.0 ± 0.02).10^6 M^{-1} (using λ_{Ext}: 530 nm and λ_{Mon}: 583 nm for emission titration). The binding affinity of **L_1** towards Cr^{3+} was also evaluated as

K_a^{ITC} = (1.6 ± 0.02).10^6 M^{-1} in acetonitrile medium at 25°C using ITC experiments (Figure 3.3C). Comparison of the binding constants evaluated in pure aq. buffer medium and in acetonitrile clearly revealed the unfavourable energy barrier imposed by the deleterious solvation of Cr^{3+} in aqueous medium. Thermodynamic parameters were obtained from ITC studies (ΔG = -(8.48 ± 0.02) kcal mol^{-1}, ΔH = -(20.8 ± 0.4) kcal mol^{-1} and ΔS = -(41.4 ± 0.05) cal mol^{-1}; all symbols are used following standard terminology).

The observed plot of the data from ITC experiment (Figure 3.3C) also supported the 1:1 binding stoichiometry.[69,70] The higher -ΔH value revealed that binding was exclusively driven by enthalpy change; while small but negative entropy of binding supported the formation of the adduct Cr^{3+}.**L_1**. Reversible binding of Cr(III) to receptor **L_1** was also established with the restoration of the original absorption or emission spectra for **L_1** on treating the solution of Cr^{3+}.**L_1** with excess Na_2EDTA. $EDTA^{2-}$ is known to have a much higher affinity (pK_a = 23.6 in aq. medium) towards Cr(III) than **L_1** and thus leads to generation of free **L_1**, which eventually underwent the cyclization reaction restoring the original receptor **L_1** in its spirolactam form. This was evident from the restoration of the spectra of **L_1** in aq. solution of 0.4 mM TX100 and Tris buffer (5 mM, 25 mM NaCl; pH 7.2) in the absence of any Cr(III).

Further, to examine the role of structural variation in **L_1** and **L_2** on the binding affinity towards Cr(III), emission spectra for **L_2** were also recorded in absence and presence of various metal ions that were used for scanning responses of the reagent **L_1** (Figure 3.4).

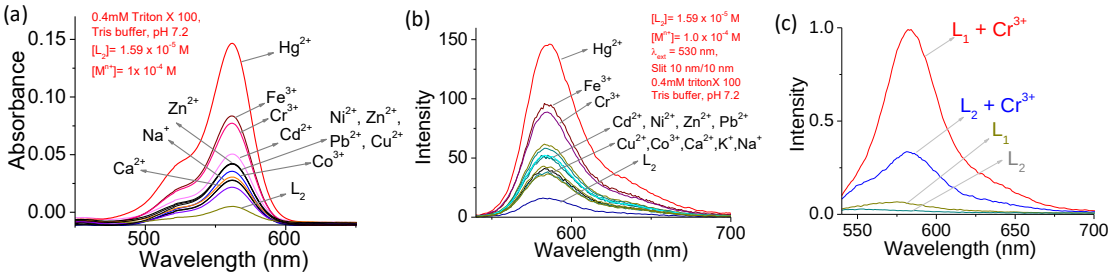

Figure 3.4. (a) Emission spectra and (b) absorption spectra of **L_2** (1.59 x 10^{-5} M) in 0.4 mM Triton X-100 in Tris buffer medium having pH 7.2 in presence of excess of aqueous metal ions (1 x 10^{-4} M); (c) emission spectrum of **L_1** (1.59 x 10^{-5} M) and **L_2** (1.59 x 10^{-5} M) in 0.4 mM Triton X 100 in Tris buffer medium having pH 7.2 in presence and absence of 10 equivalent excess of Cr^{3+}. λ_{Ext} = 530 nm, slit width = 2/2 nm.

Spectroscopic studies under identical experimental condition (solvent medium having 0.4 mM Triton X-100 in Tris buffer, pH 7.2; Figure 3.4) with the model reagent (**L_2**; Scheme 3.1) and different cations, like Hg^{2+}, Fe^{3+}, Cr^{3+}, Pb^{2+}, Cd^{2+}, Ni^{2+}, Zn^{2+}, Cu^{2+},

Ca^{2+}, Na^{+}, and K^{+} were carried out. Results of such studies revealed that on substituting olefin group (of **L_1**) with $–C_2H_5$ group (in **L_2**) (Scheme 3.1), the observed specificity towards Cr(III) was lost when **L_2** was used for studies (Figure 3.4). **L_2** was found to bind all metal ions like Hg(II), Fe(III), Cr(III), Pb(II) with associated increase in absorbance and emission band intensity at 561 nm and 585 nm, respectively in 0.4 mM TX100 and Tris buffer medium (pH 7.2). Results of such studies revealed that the extent of absorption and emission changes as well as the binding efficiency for **L_2** towards Cr(III) was found to be much lower than that compared to **L_1.** Respective binding constants for these ions were evaluated: $K_a^{Hg2+.L2}$ = 1.08 x 10^3 M^{-1}; $K_a^{Fe3+.L2}$ = 5.80 x 10^2 M^{-1}; $K_a^{Cr3+.L2}$ = 5.20 x 10^2 M^{-1}; $K_a^{Pb2+.L2}$ = 2.10 x 10^2 M^{-1}. A comparison of these results with those for reagent **L_1**, tends to suggest that the appended olefin functionality/ies in the rhodamine derivative (**L_1**) has a distinct role in achieving the desired specificity for Cr(III). Our results clearly revealed that in absence of appended olefin groups, seemingly analogous reagent **L_2** showed much lower binding affinity towards Cr(III). Despite efforts, we failed to get suitable single crystal of Cr^{3+}.**L_1** for structural analysis.

FTIR spectra recorded for **L_1** and Cr^{3+}.**L_1**, revealed a distinct shift from 1617 cm^{-1} to 1587 cm^{-1} ($\Delta\tilde{\nu}$ = 30 cm^{-1}) for C=C stretching frequency (Figure 3.5).

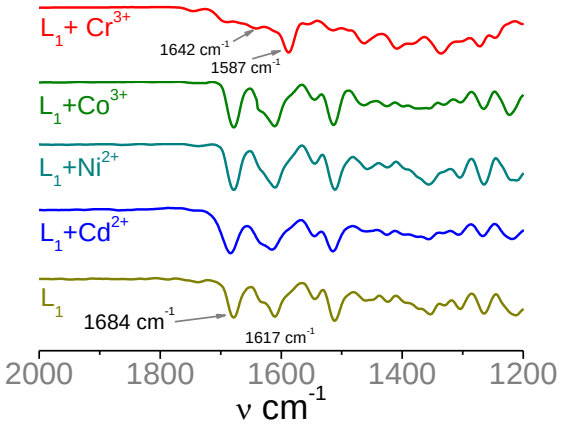

Figure 3.5. FTIR spectra of **L_1** recorded in absence and presence of 5 mole equivalent excess of Cr^{3+}, Cd^{3+}, Ni^{2+}, Co^{3+}. Spectra for **L_1** remained almost unchanged for Cd^{3+}, Ni^{2+} and Co^{3+}; while substantial changes were observed when recorded in presence of Cr^{3+}.

Blue shift in absorption of vinyl group in the FTIR spectrum on coordination to metal ion is reported earlier.[71,72] This supported the involvement of olefin functionality(ies) in coordination to Cr(III)-centre. A recent report reveals that Cr(III) could form a high yield air stable isolable coordination complex with soft donor ligand bis(2-picolyl)phenyl

phosphine.[73] This also support the possibility of Cr(III)-olefin interaction in Cr^{3+}.$\mathbf{L_1}$ complex for achieving the observed specificity of the reagent $\mathbf{L_1}$ towards Cr(III).

To examine the feasibility of the proposed complex formation between Cr(III) and $\mathbf{L_1}$ (Scheme 3.IC), DFT calculations and "atoms in molecules" AIM analyses with a model compound ($\mathbf{L_M}$) (Figure 3.6B(i) and 3.6C(i)) was performed. These model compounds were used to reduce the computational time, however, the active site of the reagent $\mathbf{L_1}$ for binding to Cr(III) was retained. Results of these studies revealed that the proposed Cr(III) interactions with olefinic π-bonds could exist in such systems in aqueous medium.

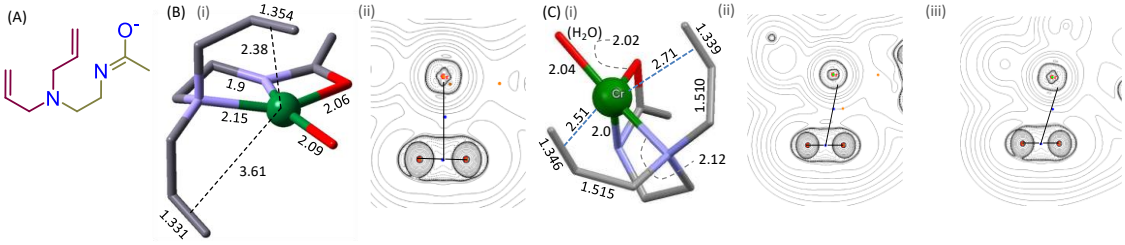

Figure 3.6. (A) Molecular structure of the model compound ($\mathbf{L_M}$) that was used for computational studies; B(i) optimized structure with the possible binding sites of the model reagent to Cr(III) where one olefinic double bond is interacted; B(ii) contour plots of the Laplacian distributions $\nabla^2\rho(r)$ in the plane containing the atom Cr and two carbon atoms in olefinic double bonds in model compound B(i); solid and dotted lines designate regions of local charge concentration and depletion, respectively; the bond paths are indicated by solid black lines, bond critical points are marked with a blue sphere; C(i) optimized structure with the possible binding sites of the model reagent to Cr(III) where two olefinic double bond is interacted; C(ii) and (iii) contour plots of the Laplacian distributions $\nabla^2\rho(r)$ in the plane containing the atom Cr and two carbon atoms in olefinic double bonds showing bond critical path and bond critical point. C(ii) and C(iii) represents the interaction of two different π-bonds with Cr^{3+} ion in model compound C(i) [H-atoms are omitted for clarity; Green: Cr(III), Gray: C; Blue: N; Red: O; distances are shown in Å).

We have optimized two model geometries as shown in Figure 3.6B(i) and 3.6C(i), which represent the interaction of Cr(III) with one (Figure 3.6B(i)) and two (Figure 3.6C(i)) olefin bond(s), respectively. The optimized geometry of Figure 3.6B(i) suggests that the Cr^{3+} ion is coordinated with two nitrogen atoms, one oxygen atom, one olefinic π-bond of the ligand and a water molecule. The optimized geometry of Figure 3.6C(i) showed the participation of the two olefinic π-bonds. The "atoms in molecules" AIM analysis performed with the optimized geometry showed significant interaction of Cr^{3+} ion with probable coordinating sites in both cases.[58]

The NBO charge calculated for the Cr(III) centre in the Cr(III) complex with the **L_M** (Figure 3.6B(i)) is (+1.295), which was much smaller than the bare Cr(III) ion.

Table 3.2: Topological parameters calculated of B(ii), C(ii) and C(iii) (in au): electron density at C=C bond…Cr(III) bond critical point (BCP) and Laplacian, $\nabla^2\rho(r)$ are given.

Interacted bond	ρ(r)	$\nabla^2\rho(r)$
B(ii)	0.03758	0.12930
C(ii)	0.03213	0.11784
C(iii)	0.02119	0.08227

The polar functional groups of the model ligand **L_M** upon coordination with Cr(III) is expected to reduce the formal charge on the metal ion, which is further exhibited with 1.110 on the metal center of the complex shown in Figure 3.6C(i).

The Laplacian is obtained using this equation of ¼[$\nabla^2\rho(r)$] = 2G(r)+V(r).[59] The interaction between C=C π-bond and Cr(III) ion is a closed shell interaction as the Laplacian calculated to be positive in these cases. Laplacian value of B(ii) is relatively larger than C(ii) and C(iii), however, the cumulative effect in the later case override the stability than the former case.

The calculated results with DFT M06-2X functional level of theory using basis set 6-31G* (C, N, H, O) and LANL2DZ (Cr) in aqueous phase suggest that the structure shown in 3.6C(i) is energetically more stable than 3.6B(i) by 4.9 kcal mol^{-1}. The experimental results corroborate the calculated results. The AIM calculations were performed by using Multiwfn software, a multifunctional program for wave function analysis.[58-60] The AIM analysis indicates the T-shaped paths of maximum electron density, the so called bond paths, which connect the Cr(III)-ion with the bond critical point of C=C bonds. The contour plots of the Laplacian distributions $\nabla^2\rho(r)$ also reveals the interaction of olefinic π-bonds with Cr(III) ion (Table 3.2).[60]

3.5. Cell Imaging Study

After ensuring the fact that reagent **L_1** binds specifically to Cr(III) in an ensemble of several other interfering metal ions under physiological condition, possibility of using this molecule as an imaging reagent for detection of cellular uptake of Cr(III) by human colon cancer cells (Hct116) was examined. However, prior to such an experiment,

toxicity of this reagent towards live Hct116 cells was tested using MTT assay technique. MTT assay confirmed insignificant toxicity of the reagent **L_1** towards Hct116 cells (Figure 3.7(ii)). This reagent **L_1** was further used for the detection of Cr^{3+} in Hct116 cells by confocal laser scanning microscopic (CLSM) studies using laser excitation source of 530 nm. Hct116 cells were incubated with **L_1** (15.9 μM) for 30 min at 37 ˚C.

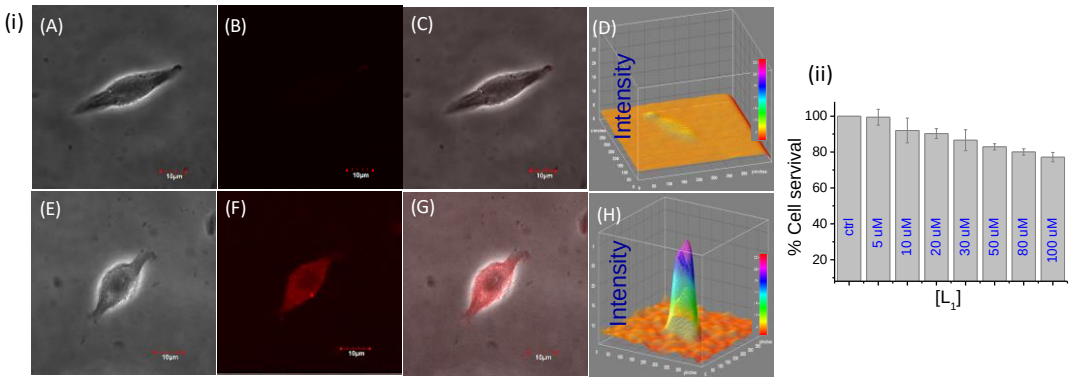

Figure 3.7. (i) CLSM image of Hct116 cells treated with probe **L_1** (15.9 μM) for 30 min at 37 °C: (A) the bright field image, (B) red channel image, (c) overlay of (A) and (B); CLSM Images of the cells upon treatment with probe **L_1** (15.9 μM) and then Cr^{3+} (10 μM) for 30 min at 37 °C: (E) bright field image, (F) red channel image, (G) overlay images of (E) and (F); (D) 3D representation of CLSM images of **L_1** (15.9 μM), (H) 3D representation of CLSM images of **L_1**+10 μM of Cr^{3+}, ($\lambda_{Ext}/\lambda_{Em}$ = 530/573 nm); (ii) MTT assay to determine the cell viability percentage of **L_1** in Hct116 cells.

After necessary washing, no intracellular fluorescence was observed in the confocal images of these cells and these were used as control.

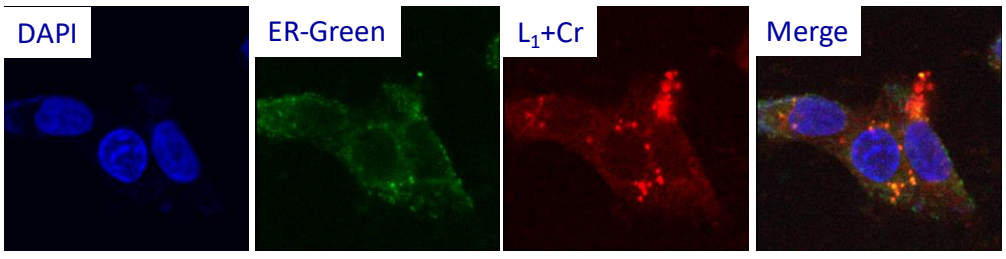

Figure 3.8. Colocalization studies of **L_1** in presence of 10 μM of $Cr^{3+}$with DAPI, ER-Green.

Further, pre-treated Hct116 cells (with 15.9 μM reagent **L_1**) were washed thoroughly and subjected to a follow-up treatment with Cr^{3+} (10 μM) showed strong intracellular fluorescence when viewed through the red channel of the confocal microscope (Figure 3.7). Images shown in Figure 3.7(i) also reveal that intracellular fluorescence is preferentially localized in the lipid dense region of the cells.

This was further confirmed from CLSM images recorded after colocalization studies with ER-tracker green (ER-specific reagent) and DAPI (It stains nuclei specifically, with little or no cytoplasmic labeling) (Figure 3.8), which confirmed that the reagent **L_1** was preferentially localized in the lipid dense region of Hct116 cells. This was further substantiated by the high value for the overlap coefficient (0.931) of **L_1** (15.9 μM) in presence of 10 μM of Cr^{3+} and ER-tracker green. Thus, our studies confirmed that the biologically benign reagent **L_1** could permeate through the cell membrane and was preferentially localized in the lipid dense region of the cells. Further, this reagent could detect the cellular uptake of Cr^{3+} in Hct116 cells.

3.6. Conclusion

Thus, studies presented in this chapter, reveal that a new molecular probe **L_1**, which was found to be self-assembled inside the micellar structure of TX100 in aqueous medium. This self-assembled molecular aggregate could be used as a reagent for specific detection of Cr(III) in pure aqueous buffer medium (pH 7.2) with an associated fluorescence *turn-on* response even in presence of several other competing cations. Interestingly, this reagent can be easily up-taken by cells via permeation across cell membrane of human colon cancer cells (Hct116). Further, results of the MTT assay studies confirmed that the reagent **L_1** showed insignificant toxicity towards human colon cancer cells (Hct116). This reagent could detect the Cr(III) ion uptake in Hct116 cells from aqueous environment and showed a luminescence *ON* response on binding to Cr(III) ions. Use of the rhodamine based reagent with conversion from non-luminescent spirolactam form to the strongly luminescent acyclic form on binding to Cr(III) had helped us in achieving the luminescence *ON* response. Most importantly the reagent **L_1** could be utilized as an imaging reagent for the detection of Cr^{3+} in Hct116 colon cancer cells. To the best of our knowledge, this is a rare example of a chemosensor that is completely specific towards Cr(III) and works is pure aqueous medium with an associated fluorescence *turn on* response. Example of the luminescence *ON* based receptor for Cr(III) is not common due to the paramagnetic nature of Cr(III), which is known to efficiently quench the luminescence of the organic fluorophore to which it is bound.

3.7. References

1. A. K. Shanker, C. Cervantes, H. Loza-Tavera and S.Avudainayagam, *Environ. Int.,* 2005, **31**, 739.
2. J. O. Nriagu and E. Nieboer, *Chromium in the Natural and Human Environments*; Wiley, New York, 1988.
3. S. Latva, J. Jokiniemi, S. Peraniemi and M. Ahlgren, *J. Anal. At. Spectrom*., 2003, **18**, 84.
4. H. Arakawa, R. Ahmad, M. Naoui, H. Ali and T. Riahi, *J. Biol. Chem*., 2000, **275**, 10150.
5. C. M. Lytle, F. W. Lytle, N. Yang, J.-H. Qian, D. Hansen, A. Zayed and N. Terry, *Environ. Sci. Technol*., 1998, **32**, 3087.
6. S. Sundaram and P. S. Raghavan, *Chromium-VI Reagents: Synthetic Applications*; Springer: Berlin, 2011.
7. H. J. Sawyer, *Chromium and its compounds, c.f. Occupational medicine, eds: Zenz C., Dickerson O.B., Horvath E.P*.: 487-495. Mosby-Year Book Inc., St Louis, 1994.
8. J. B. Vincent, *Nutr. Rev*., 2000, **58**, 67.
9. A. K. Singh, V. K. Gupta and B. Gupta, *Anal. Clim. Acta*., 2007, **585**, 171.
10. D.A. Eastmond, J.T. Macgregor and R.S. Slesinski, *Crit Rev Toxicol*., 2008, **38**, 173.
11. *Concise International Chemical Safety Documents 76: Inorganic Cr(III) Compounds*, WHO, 2009.
12. S. DM, B. JJ, W. KE, *FASEB J*., 1995, **9**, 1650.
13. *Agency for Toxic Substances and Disease Registry, Toxicological Profile for Chromium*, Health Administration Press, Atlanta, Ga, USA, 2000.
14. X. Chen, T. Pradhan, F. Wang, J. S. Kim and J. Yoon, *Chem Rev*., 2012, **112**, 1910.
15. H. Wu, P. Zhou, J. Wang, L. Zhao and C. Duan, *New J. Chem*., 2009, **33**, 653.
16. K. Huang, H. Yang, Z. Zhou, M. Yu, F. Li, X. Gao, T. Yi and C. Huang, *Org. Lett*., 2008, **10**, 2557.
17. Z. Zhou, M. Yu, H. Yang, K. Huang, F. Li, T. Yi and C. Huang, *Chem. Commun*., 2008, 3387.
18. P. Das, A. Ghosh, H. Bhatt and A. Das, *RSC Advances,* 2012, **2**, 3714.
19. S. Guha, S. Lohar, A. Banerjee, A. Sahana, S. K. J. Mukhopadhyay, S. Matalobos, D. Das, *Anal. Methods,* 2012, **4**, 3163.

20. J. Zhang, L. Zhang, Y. Wei, J. Chao, S. Wang, S. Shuang, Z. Caia and C. Dong, *Anal. Methods,* 2013, **5**, 5549.

21. D. Wang, Y. Shiraishi and T. Hirai, *Tetrahedron Lett.,* 2010, **51**, 2545.

22. V. K. Gupta, N. Mergu and A. K. Singh, *Sensors and Actuators B*, 2015, **220**, 420.

23. J. Mao, L. Wang, W. Dou, X. Tang, Y. Yan and W. Liu, *Org. Lett*., 2007, **9**, 4567.

24. S. Saha, M.U. Chhatbar, P. Mahato, L. Praveen, A. K. Siddhanta and A. Das, *Chem. Commun*., 2012, **48**, 1659.

25. S. Saha, P. Mahato, G, U. Reddy, E. Suresh, A. Chakrabarty, M. Baidya, S. K. Ghosh and A. Das, *Inorg. Chem*., 2012, **51**, 336.

26. P. Mahato, S. Saha, E. Suresh, R. Di Liddo, P. P. Parnigotto, M.T. Conconi, M. K. Kesharwani, B. Ganguly and A. Das, *Inorg. Chem*., 2012, **51**, 1769.

27. J. Mao, Q. He and W. Liu, *Anal. Bioanal. Chem*., 2010, **396**, 1197.

28. X. Wan, H. Liu, S. Yao, T. Liu and Y. Yao, *Macromol. Rapid Commun*., 2014, **35**, 323.

29. M.R. Neutra and P A. Kozlowsk, *Nat. Rev. Immunol*., 2006, **6**, 148.

30. D. Koley and A. J. Bard, *Proc. Nat. Acad. Sci*., 2010, **107**, 16783.

31. P. Pallavicini, Y. A. Diaz-Fernandez and L. Pasotti, *Coord. Chem. Rev*., 2009, **253**, 2226.

32. F. Denat, Y. A. Diaz-Fernandez, L. Pasotti, N. Sok and P. Pallavicini, *Chem. Eur. J*., 2010, **16**, 1289.

33. J. Voskuhl and B. J. Ravoo, *Chem. Soc. Rev*., 2009, **38**, 495.

34. B. Gruber and B. Kçnig, *Chem. Eur. J*., 2013, **19**, 438.

35. D. Wang, T. Liu, J. Yin and S. Liu, *Macromolecules,* 2011, **44**, 2282–2290.

36. B. Gruber, E. Kataev, J. Aschenbrenner, S. Stadlbauer and B. König, *J. Am. Chem. Soc*., 2011, **133**, 20704.

37. A. Mallick, M. C. Mandal, B. Haldar, A. Chakrabarty, P. Das and N. Chattopadhyay, *J. Am. Chem. Soc*., 2006, **128**, 3126.

38. P. Grandini, F. Mancin, P. Tecilla, P. Scrimin and U. *Angew. Chem. Int. Ed*., 1999, **38**, 3061.

39. B. Kim, E. Lee, Y. Kim, S. Park, G. Khang and D. Lee, *Adv. Funct. Mater.,* 2013, **23**, 5091.

40. J-H. Soh, K. M. K. Swamy, S. K. Kim, S. Kim, S.-H. Lee and J. Yoon, *Tetrahedron Lett*., 2007, **48**, 5966.

41. M. Suresh, A. Shrivastav, S. Mishra, E. Suresh and A. Das, *Org. Lett*., 2008, **10**, 3013.

42. L. Praveen, S. Saha, S. K. Jewrajka and A. Das, *J. Mater. Chem. B,* 2013, **1**, 1150.

43. P. Mahato, S. Saha, P. Das, H. Agarwalla and A. Das, *RSC Adv.,* 2014, **4**, 36140.

44. U. G. Reddy, F. Ali, N. Taye, S. Chattopadhyay and A. Das, *Chem. Commun.,* 2015, **51**, 3649.

45. U. G. Reddy, V. Ramu, S. Roy, N. Taye, S. Chattopadhyay and A. Das, *Chem. Commun*., 2014, **50**, 14421.

46. M. Kumar, N. Kumar, V. Bhalla, P. R. Sharma and T. Kaur, *Org. Lett*., 2012, **14**, 406.

47. G. M. Sheldrick, *SAINT 5.1 ed., Siemens Industrial Automation Inc*., Madison, WI, 1995.

48. SADABS, *Empirical Absorption Correction Program*, University of Göttingen, Göttingen, Germany, 1997.

49. G. M. Sheldrick, *SHELXTL Reference Manual*: *Version 5.1*, Bruker AXS, Madison, WI, 1997.

50. G. M. Sheldrick, *SHELXL-97: Program for Crystal Structure Refinement*, University of Göttingen, Göttingen, Germany, 1997.

51. Y. Zhao and D.G. Truhlar, *Theor. Chem. Acc*., 2008, **120**, 215.

52. S. Miertuš, E. Scrocco and J. Tomasi, *Chem. Phys*., 1981, **55**, 117.

53. P. J. Hay and W. R. *J. Chem. Phys*., 1985, **82**, 270.

54. P. J. Hay and W. R. Wadt, *J. Chem. Phys*., 1985, **82**, 299.

55. W. J. Hehre, L. Radom, P. V. R. Schleyer and J. A. Pople, *Ab initio Molecular Orbital Theory*; Wiley, New York, 1988.

56. M. J. Frisch, G. W. Trucks, H. B. Schlegel, G. E. Scuseria, M. A. Robb, J. R. Cheeseman, G. Scalmani, V. Barone, B. Mennucci, G. A. Petersson, *et al*. *Gaussian 09, Revision B01, Gaussian*, Inc, Wallingford CT 2010.

57. R. W. F. Bader, *Atom in Molecules –A Quantum Theory*; Oxford University Press, Oxford, 1990.

58. T. Lu and F. Chen, *J. Comput. Chem*., 2012, **12**, 580.

59. N. J. M. Amezaga, S. C. Pamies, N. M. Peruchena and G. L. Sosa, *J. Phys. Chem. A,* 2010, **114**, 552.

60. T. Muller, C. Bauch, M. Bolte and N. Auner, *Chem. Eur. J*., 2003, **9**, 1746.

61. S. Saha, P. Mahato, M. Baidya, S. K. Ghosh and A. Das, *Chem. Commun*., 2012, **48**, 9293.

62. B. N. Ahamed and P. Ghosh, *Inorg. Chim. Acta,* 2011, **372**, 100.

63. Y. Zhao and Z. Zhong, *Org. Lett***.,** 2006, **8**, 4715.

64. R. R. Avirah, K. Jyothish and D. Ramaiah, *Org. Lett***.,** 2007, **9**, 121.

65. Y. Nakahara, T. Kida, Y. Nakatsuji and M. Akashi, *Org. Biomol. Chem***.,** 2005, **3**, 1787.

66. T. Abalos, S. Royo, R. Martı´nez-Ma´nez, F. Sancenon, J. Soto, A. M. Costero, S. Gilad, M. Parra, *New J. Chem***.,** 2009, **33**, 1641.

67. A. L. Van de Van, K. A. Storthz, R. R. Kortum, *J. Biomed. Opt*., 2009, DOI:10.1117/1.3065544.

68. A. Hellebust, R. R. Kortu, *Nanomedicine,* 2012, **7**, 429.

69. F. Schmidtchen, *Isothermal titration calorimetry in supramolecular chemistry, in Analytical Methods in Supramolecular Chemistry*; *ed. C. A. Schalley*, Wiley-VCH, Weinheim, 2006.

70. M. Suresh, A. K. Mandal, E. Suresh and A. Das, *Chem. Sci*., 2013, **4**, 2380.

71. A. Wooten, P. J. Carroll, A. G. Maestri, P. J. Walsh, *J. Am. Chem. Soc*., 2006, **128**, 4624.

72. K. Nakamoto, *Infrared and Raman Spectra of Inorganic and Coordination Compounds: Part. A: Theory and Applications in Inorganic Chemistry*; Wiley, 6th Edtn. 2009.

73. S. Liu, R. Peloso, R. Pattacini, P. Braunstein, *Dalton Trans*., 2010, **39**, 7881.

CHAPTER 4

SPECIFIC RECEPTOR FOR HYDRAZINE: MAPPING THE IN-SITU RELEASE OF HYDRAZINE IN LIVE CELLS AND *IN VITRO* ENZYMATIC ASSAY

Publication:
Chem. Commun., 2016, **52**, 6166-6169

4.1. Introduction

Despite being branded as a potent carcinogen, Hydrazine is widely used as an intermediate in industry.[1] Further reports confirmed that hydrazine induces hepatotoxicity, neurotoxicity and mutagenicity.[2] It is also known to cause lipid peroxidation, ROS formation to elevate oxidative stress and eventually leads to nonspecific damages of proteins and DNA.[3,4] Owing to such adverse influences on human physiology and environments, United States Environmental Protection Agency (EPA) classified hydrazine as a human carcinogen with low threshold limit value of 10 ppb.[5] Typically, in clinical diagnosis hydrazine estimation is performed using capillary gas chromatography using electron capture detector.[5b] Hydrazine has been also found to be a metabolite of an important drug, isoniazid, which has featured in World Health Organization's (WHO) list of essential medicines that constitute the bare minimum for a basic health system and is used as a first-line agent in the prevention and treatment of both latent and active tuberculosis.[5c] Hydrazine produced *in-situ* adds to high hepatotoxicity in human physiology and adds to the severe health concern.[6,7] Accordingly, a number of hydrazine specific molecular probes have been synthesized and utilized for intracellular detection of hydrazine in aqueous medium and biological samples.[8] However, example of a reagent that could be used for detection of intracellular release of hydrazine through a biochemical or enzymatic transformations as well as capable of its effective and rapid scavenging has eluded us till date. Such a reagent would have a direct relevance for developing an efficient imaging reagent for hydrazine and reducing the cytotoxicity induced by isoniazid, which would have serious implication in clinical diagnostic and developing a more effective drug formulation. Considering the scope for such a reagent, we report herein a *turn on* luminescent molecular probe (**L_2**) for the detection of hydrazine in aqueous buffer medium under physiological pH. This reagent is specific towards N_2H_4 in presence of all other possible interfering analytes, including other amines and hydrazine derivatives. We have discussed the possibility of using this reagent for detection of the intracellular release of hydrazine by isoniazid through an enzymatic process affected by intracellular enzymes in live HepG2 cells. Importantly, MTT assay reveal that the rapid and near quantitative reaction of N_2H_4 with this chemodosimetric probe is effective in lowering the cytotoxic influence on the live HepG2 cells. To the best of our knowledge, such an example is not available in the contemporary literature.

4.2. Experimental Section

4.2.1. Materials

9,10-Phenanthrenequinone, 4-nitrobenzaldehyde, phthalic anhydride, isoniazid, aminoacylase-1 enzyme and glacial acetic acid were obtained from Sigma Aldrich and were used as received. Hydrazine hydrate ($NH_2NH_2.H_2O$) (99%) AR Grade was procured from S. D. fine chem. Limited, India. N-acetyl hydrazine, cysteine, glutathione, arginine, ethylenediamine, triethylamine, n-butyl amine, ammonia, diisopropylamine, urea, thiourea, hydroxyl amine and leucine were purchased from SD Fine Chemicals in India. TLC plates, Silica gel on aluminum, with layer thickness 0.2 mm were used for solid state studies. Solvents used for synthesis of various intermediates and final compounds were of AR grade (S.D. Fine Chemicals) and were used as received without further purification. HPLC grade (S.D. Fine Chemicals) solvents were used for various spectroscopic studies.

4.2.2. Analytical Methods

^{1}H NMR spectra were recorded on a Bruker 500 MHz FT NMR (Model: Avance-DPX 500) using DMSO-d_6 as the solvent and tetra methyl silane (TMS) as an internal standard. IR spectra were recorded on Bruker Alpha FT IR spectrometer. UV-Vis spectra were recorded using Shimadzu UV-1800 spectrometer. All the Fluorescence measurements were carried out on *PTI* Quanta Master™ Steady State Spectrofluorometer. MALDI Ms spectrum was recorded using Dithranol (1,8-dihydroxy-9,10-dihydroanthracen-9-one) as the inert matrix using instrument AB SCIEX MALDI TOF/TOF^{TM} 5800.

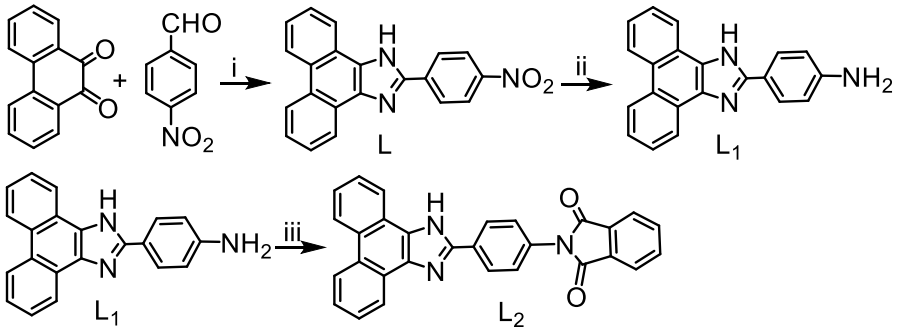

i : CH_3COONH_4 / CH_3COOH / Δ, 2h; ii : Fe/ HCl/ THF-Water mixture, 6 h;
iii : Phthalic anhydride / CH_3COOH / Δ, 24h.

Scheme 4.1. Synthetic route of **L_1** and **L_2**.

High-resolution mass spectra were recorded on JEOL JM AX 505 HA mass spectrometer. Confocal images were acquired in Olympus Fluoview microscope.

4.2.3. General experimental procedure for UV-Vis and Fluorescence studies

Stock solution of probe **L_2** (5×10^{-3} M) was prepared in DMSO and the same solution was used for all the studies after appropriate dilution to 3 ml of 0.4 mM TX100 in HEPES aqueous buffer medium having solution pH 7.2 to make the effective **L_2** concentration of 7.8 μM. Unless and otherwise mentioned, 10 mM and pH 7.2 solution of aq. HEPES buffer was used for all spectroscopic studies. All amines solutions of 1×10^{-3} M were prepared in aq-HEPES buffer (pH 7.2). All luminescence measurements were done using λ_{Ext} = 360 nm with an emission slit width of 1 nm. The fluorescence quantum yield was determined according to literature method using perylene (in cyclohexane) as reference.

4.2.4. Preparation of TLC test strips and solid state fluorescence studies

TLC test strips were prepared by drop-casting 1.5 mM of probe (**L_2**) solution in DMSO on silica TLC plates. Then it was dried properly and this silica coated TLC plates were used for solid state experiments. These TLC plates were expose to the vapour as well as solution of hydrazine and other amines for 20 min, dried and change of emission colour were recorded using lamp with excitation of 365 nm. Furthermore, silica coated TLC plates treated with different concentration of hydrazine were used for solid state fluorescence measurements using λ_{Ext} = 360 nm with an emission slit width of 1/1 nm. Images were captured using Canon 630D camera.

4.2.5. General procedure for enzymatic study

N-Acetyl-hydrazine was purchased from commercially available sources. 1×10^{-1} M Acetyl-hydrazine solution was prepared in 10 mM aq-HEPES buffer solution (pH 7.2). Aminoacylase-1 enzyme solution was prepared according to the requirement by dissolving 1 mg/ml in 10 mM aq-HEPES buffer solution (pH 7.2). A fixed concentration of Acetyl-hydrazine (200 equiv.) was added to the 7.8 μM of **L_2** in 0.4 mM Triton X 100 solution. Since 1 mg of solid enzyme contains 3301 units of protein and 1 unit can hydrolyse 1 μM of substrate, accordingly enzyme concentration was varied with respect to the substrate concentration.

4.2.6. Cell culture and Confocal imaging

Hct116 cells were seeded on cover slips placed in 6 well plates. After 24 hours cells were treated with **L_2** (7.8 μM) for 40 minutes. Cells were then washed thrice with Phosphate Buffer Saline (1X PBS) and fixed with 4% PFA for 10 minutes and washed again with Phosphate Buffer Saline (1X PBS). Permeabilization of the cells was done using 0.2% Triton X 100 for 5 minutes. The **L_2**-stained colon cancer cells Hct116 incubated with hydrazine (20 μM) for 40 min. Again three washes were given and then cover slips mounted using mounting medium. Nail paints was used to seal the coverslips mounted on the glass slides. Images were acquired in Olympus Fluoview Microscope.

For enzymatic studies in Hct116 cells, cells were incubated with **L_2** (7.8 μM) for 40 mins, then cells were washed thoroughly with buffer and acetyl hydrazine (1 mM) was incubated for 40 min. After that different concentration of Aminoacylase-1 (0, 0.4, 0.7, 1.0 mU) were added to cellular medium for 1h and after the above mentioned treatment, CLMS images were captured.

For drug metabolism studies, we have used HepG2 liver cancer cells. HepG2 cells (3×10^5) were seeded on cover slips placed in 6 well plates. After 24 hours, Hct116 cells were treated with 1 mM of Isoniazid (a well known drug for Tuberculosis) for 3h at 37˚C in a 5% CO_2 air environment. Cells were then washed thrice with Phosphate Buffer (1X PBS). Then **L_2** (7.8 μM) was incubated for 1h and fixed with 4% PFA for 20 minutes and washed again with 1X PBS. Nail paint was used to seal the cover slips mounted on the glass slides for each well plates. For control experiment Hct116 cells were pre-treated with 1 mM of Isoniazid for 3h. Then cells were washed thrice with media and followed under same conditions. Confocal laser scanning microscopic (CLSM) images were acquired in Olympus Fluoview Microscope with $\lambda_{Ext}/\lambda_{Mon}$ = 352/455 nm.

4.2.7. Cytotoxicity Assay

The in vitro cytotoxicity of **L_2** on Hct116 cells (Colon cancer cell) were determined by conventional MTT (3-(4, 5-Dimethylthiazol-2-yl)-2, 5-diphenyltetrazolium bromide) assay. Hct116 colon cancer cells (7×10^3) were seeded in each well of a 96 well plate and cultured in a 37°C incubator supplied with 5% CO_2. Cells were maintained in DMEM medium, supplemented with 10% Foetal Bovine Serum and 100 Units of Penicillin Streptomycin antibiotics. After 24 hours the cells were treated with different concentrations of the **L_2** in triplicates for 12 hours. After the treatment, cells were added

with 0.5 µg/ml of MTT reagent. The plate was then incubated for 4 hours at 37°C. 100 µl of Isopropyl Alcohol was added to each well. Optical density was measured at 570 nm using Multiskan Go (Thermo Scientific) to find the concentration of the cell inhibition. IC_{50} value has been calculated to be 70 µM.

The formula used for the calculation of the MTT assay for evaluation of the cell viability was as follows:
Cell viability (%) = (means of Absorbance value of treated group/ means of Absorbance value of untreated control) X 100.

4.2.8. Determination of detection limit

The detection limit was calculated based on the fluorescence titration. To determine the S/N ratio, the emission intensity of **L_2** without hydrazine was measured 6 times and the standard deviation of blank measurements was determined. The detection limit (DL) of **L_2** for hydrazine was determined from the following equation:

DL = K * Sb1/S

Where K = 2 or 3 (we took 3 in this case);

Sb1 is the standard deviation of the blank solution;

S is the slope of the calibration curve.

From the graph we get slope = 1.1798×10^7, and Sb1 value is 0.123

Thus using the formula we get the Detection Limit = 1.58 ppb.

4.2.9. Methodology for the Kinetic studies

Time dependent studies of (7.8 µM) **L_2** with different concentration of (0.5, 1.5, 3.0, 6.0 mM) hydrazine were carried out by mixing the reactants and monitored by fluorescence measurements in 0.4 mM TX100 medium of pH 7.2 at 37^0C. λ_{Ext} = 360 nm. λ_{Mon} = 430 nm. Data were collected under pseudo-first-order conditions. The pseudo-first order rate constant for the reaction was determined by fitting the fluorescence intensity changes of the samples to the pseudo first-order equation:

$\ln[(I_{max}-I)/I_{max}] = -k_{obs}\, t$

Where, I and I_{max} represent the fluorescence intensities at times t and the maximum value obtained after the reaction was complete. k_{obs} is the observed rate constant of the reaction. From the slope we get k_{obs} value for each reaction.

4.3. Synthesis and Characterisation

4.3.1. Synthesis of L

Synthetic procedure that was adopted for synthesis of **1** from our previous report.[9]

4.3.2. Synthesis of L_1

Compound **L** (100 mg, 0.27 mmol) was dissolved in 5 mL of methanol. H_2O (3 mL) and Fe (200 mg, 3.58 mmol) were added and the reaction mixture was heated to reflux. Hydrochloric acid in a methanol solution (2 ml, 0.6 mol L^{-1}) was added drop wise. The solution was refluxed for 2 h until TLC monitoring indicated complete consumption of the starting material. After cooling to room temperature, it was filtered and concentrate at reduced pressure, the crude product was purified by silica-gel column chromatography. Yield: 68%, HRMS (ESI) (m/z) calculated for [$C_{21}H_{15}N_3$+H]: 310.1266 ,observed: 310.1333 [M + H^+], ^{1}H NMR [500 MHz, DMSO-d6: δ (ppm)]: 8.82 (2H, s), 8.53 (2H, d, *J* = 7.8), 7.99 (2H, d, *J* = 8.5), 7.77 (2H, d, *J* = 14.8), 7.72 (2H, d, *J* = 14.9), 6.83 (2H, d, *J* = 8.5); ^{13}C NMR (125 MHz, DMSO-d_6, δ (ppm)) : 152.89, 149.38, 129.76, 128.44, 128.22, 127.69, 127.18, 124.56, 122.73, 122.00, 114.15, 111.45.

4.3.3. Synthesis of L_2

A mixture of $\mathbf{L_1}$ (280 mg, 0.96 mmol) and phthalic anhydride (331 mg, 2.24 mmol) in acetic acid (15 mL) then heated to reflex and stirred for 8 hours. It was filtered under hot condition and solid was collected washed with excess amount of acetic acid. Yield: 71%. MALDI-Ms (m/z) calculated for [$C_{29}H_{17}N_3O_2$+ H^+] : 440.4642, observed: 440.0731 [M + H^+], ^{1}H NMR [500 MHz, DMSO-d6: δ (ppm)]: 8.93 (2H, d, *J* = 7.8), 8.74 (2H, d, *J* = 7.3), 8.55 (2H, d, *J* = 7.7), 8.02 (2H, s), 7.95 (2H, s), 7.85 – 7.77 (4H, m), 7.75 (2H, d, *J* = 7.0). ^{13}C NMR (125 MHz, DMSO-d6, δ (ppm)): 169.15, 167.31, 148.21, 135.35, 133.99, 133.27, 132.00, 131.25, 128.79, 128.49, 128.12, 127.99, 127.80, 126.66, 124.58, 124.02, 122.75.

4.4. Results and Discussions

Probe $\mathbf{L_2}$ was synthesized following a methodology that is outlined in scheme 4.1. This and the other intermediate reagents ($\mathbf{L_1}$) were adequately characterized

using various analytical and spectroscopic techniques. Reagent **L_2** showed limited solubility in pure aqueous medium. However, in presence of 0.4 mM (micellar concentration) of Triton X 100 (TX100) in HEPES buffer (10 mM, pH 7.2), this reagent was found to be effectively trapped inside the micellar structure and completely soluble in pure aq. HEPES buffer solution having pH 7.2. This solution was used throughout our studies, unless mentioned otherwise.

Absorption spectra of **L_2** showed an absorption band maximum at 329 nm (ε =2.55 × 10^{-4} L mol^{-1} cm^{-1}), which was attributed to a π-π* transition associated with the phenanthrene moiety of the benzimidazole derivative. No significant change was observed in the absorption spectra for compounds **L_1** and **L_2**. To examine the selectivity of probe **L_2** (7.8 μM) in presence of 200 mole equivalent of various amines (hydrazine, ethylenediamine (edm), triethylamine (tem), n-butyl amine (nbm), ammonia, diisopropylamine (dipm), urea, thiourea, cysteine (cys), hydroxyl amine (NH_2OH) and leucine (leu)) luminescence spectral response were recorded and are shown in Figure 4.1.A. A turn on luminescence response was observed for probe **L_2** only in presence of hydrazine with λ_{Ems}^{Max} = 430 nm (λ_{Ext} = 360 nm). Further, no fluorescence change was either observed for different cationic (Na^+, Cr^{3+}, Fe^{2+}, Cu^{2+}, Al^{3+}, Mg^{2+}, Hg^{2+}, Ni^{2+} and Zn^{2+}) and anionic (F^-, Cl^-, Br^-, $C\bar{N}$, $SC\bar{N}$, HPO_4^{--}, CH_3COO^-, OCl^-, etc) analytes under identical experimental conditions.

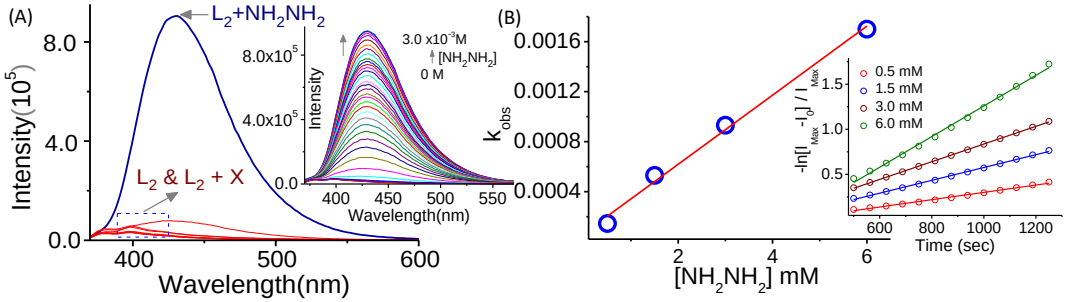

Figure 4.1. (A) Luminescence spectra for **L_2** in the absence and presence of various molecules having –NH_2 functionality (N_2H_4 and X: edm, tem, nbm, NH_3, dipm, urea, thiourea, cys, NH_2OH, leu, F^- ,Cl^-, Br^-, $C\bar{N}$, $SC\bar{N}$, HPO_4^{--}, CH_3COO^-, OCl^-, Na^+, Cr^{3+}, Fe^{2+}, Cu^{2+}, Al^{3+}, Mg^{2+}, Hg^{2+}, Ni^{2+} and Zn^{2+}); Inset: changes in emission spectral patterns for **L_2** (7.8 μM) in presence of varying [NH_2NH_2] (0.0 –3 mM); (B) plot for the k_{obs} with varying [N_2H_4] for the evaluation of rate constant (k) for the reaction between **L_2** and N_2H_4, Inset: plots of the ln[I_{Max} – I_0]/ I_{Max} as a function of time for evaluation of respective k_{obs} for certain [N_2H_4]. Changes in fluorescence intensity at 430 nm were measured for all kinetic studies. All the studies were performed in aq. solution having 0.4 mM TX100 in HEPES buffer (10 mM, pH 7.2); λ_{Ext} = 360 nm.

Interference studies also confirmed that luminescence response of **L_2** in presence of N_2H_4 remained unaltered even in presence of large excess of above mentioned molecules and ionic analytes (Figure 4.2.).

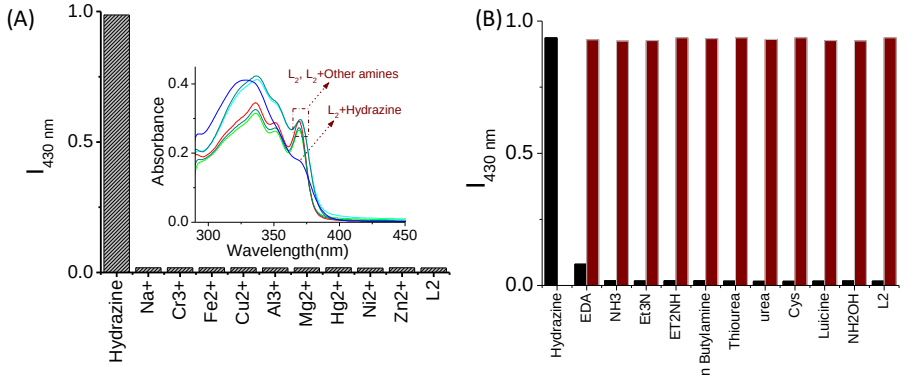

Figure 4.2. (A) Emission response of **L_2** (7.8 μM) in the absence and presence of various (A) amines; inset: Absorbance spectra of **L_2** (7.8 μM) in presence and absence of different amines (2 mM) in 0.4 mM TX100 medium at pH 7.2; (B) anionic analytes (200 mole equiv. each) in 0.4 mM TX100 at pH 7.2, λ_{Ext} = 360 nm, λ_{Mon} = 430 nm.

These results confirmed that **L_2** could be used as a turn on fluorescence probe for specific detection of hydrazine in physiological condition (aq-HEPES buffer medium having media pH of 7.2). Emission spectra of **L_2** were also recorded at different pH, which revealed that **L_2** was stable in aq. solution for the pH range 4-10. Accordingly, all studies were performed at physiologically relevant pH of 7.2. Only a weak emission spectrum (λ_{Ems}^{Max} of 430 nm with Φ = 0.008; perylene was used as reference) was observed for **L_2** under the experimental condition.

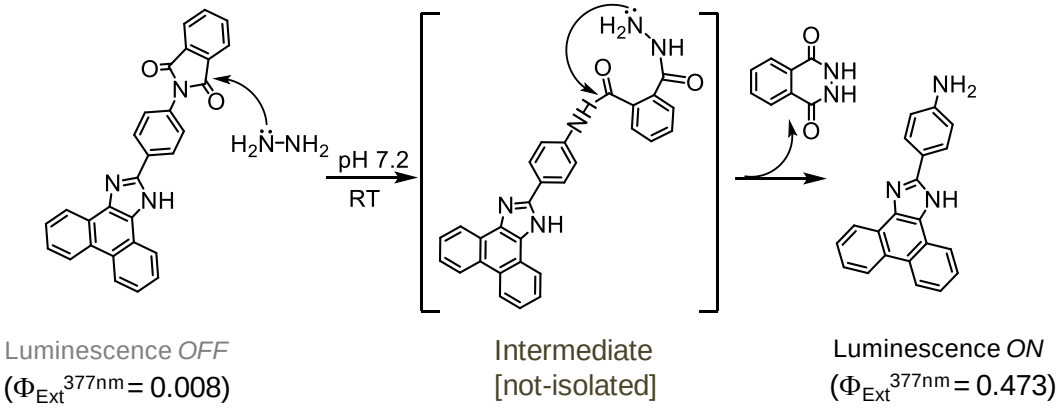

Scheme 4.2. Proposed mechanistic pathway for the reaction between **L_2** and N_2H_4.

With gradual increase in [N_2H_4], about 60-fold enhancement in luminescence intensity was observed at λ_{Ems} of 430 nm (Φ = 0.473 for λ_{Ext} = 360 nm) and these are shown as

inset in Figure 4.1.(A). Importantly, relative changes in luminescence intensity showed a linear dependency on [N_2H_4] over a concentration range of 0-30 μM. The evaluated lowest detection limit (3σ/slope) of 1.5 ppb was much lower than that of TLV (10 ppb) recommended by EPA and WHO.[5]

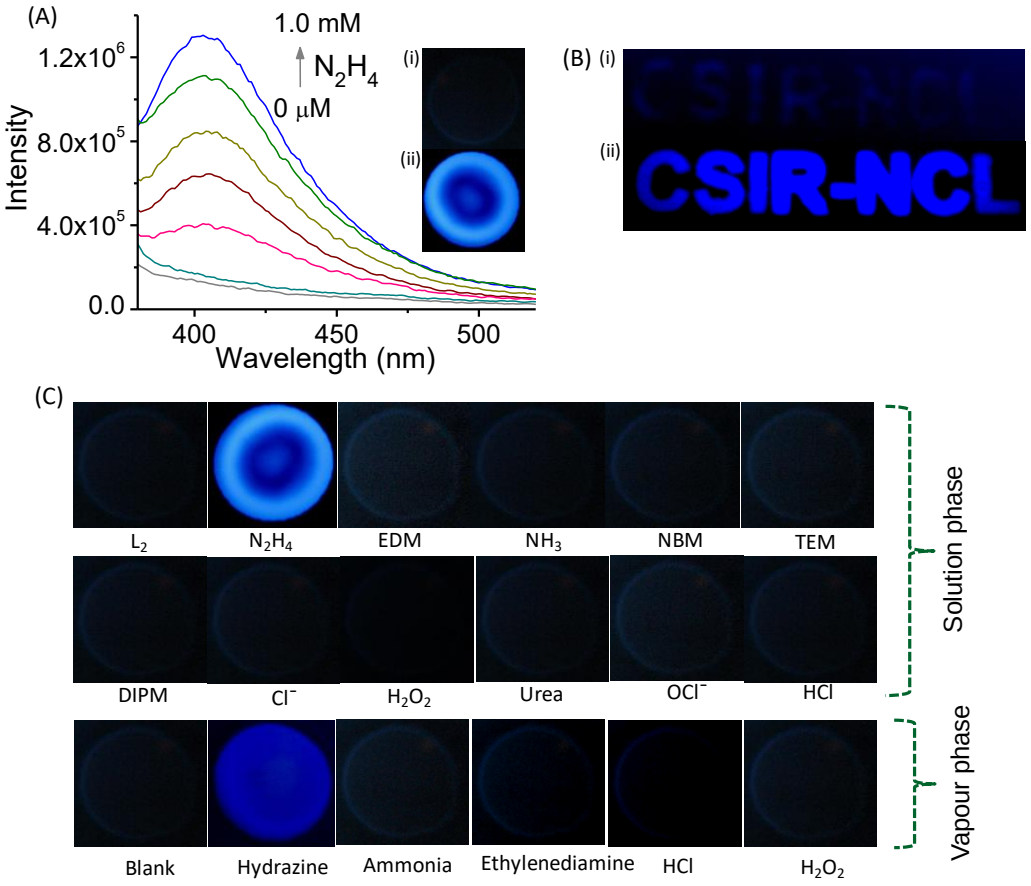

Figure 4.3. (A) Emission spectra of the silica film modified with the reagent **L_2** and subsequently exposed to aq. solution of varying [N_2H_4] (pH 7.2); Inset: snap shot of the visually detectable fluorescence of **L_2** coated silica surface in (i) absence/ presence of different amine derivatives (edm, tem, nbm, NH_3, dipm, urea, thiourea, Cys, NH_2OH) and (ii) presence of added aq. solution of N_2H_4; (B) snap shot of the silica surface marked with the script CSIR-NCL using the reagent **L_2** in (i) absence and (ii) presence of hydrazine vapour. Lamp with excitation of 365 nm was used for studies; (C) Snap shot of the visually detectable changes in fluorescence of silica surface, modified with the probe **L_2** in absence and presence of different analytes (Hydrazine, ethylenediamine, ammonia, butylamine, triethylamine, diisopropyl amine, Cl^-, H_2O_2, urea, OCl^- and HCl) in solution and vapour phase. Fluorescence colour changes were observed using 365 nm UV lamp; [**L_2**] used for the study was 1.5 mM. For all studies, aq. buffer solution (pH 7.2) was used.

All these results confirmed that the probe molecule **L_2** could potentially be used for detection, quantification of the trace amount of N_2H_4 under physiological condition as well as for imaging the generation of intracellular N_2H_4 following any bio-chemical

transformation. Prior to checking such possibilities, rate constant for the reaction between **L_2** and N_2H_4 was evaluated. Studies revealed that hydrazinolysis reaction of probe **L_2** (7.8 μM) was complete within 40 min and rate constant (k) was found to be 2.76×10^{-4} s^{-1} (Figure 4.1.B). Such a reaction is consistent with typical nucleophilic substitution reaction proposed for Gabriel synthesis,[8a-8c] which involves chemical transformation of phthalimide to amine upon reaction with hydrazine. Accordingly, a mechanistic pathway for the present reaction is shown in scheme 4.2.

Use of a strip for detection of N_2H_4 in any water sample has relevance for analysis of an in-field environmental sample. To check such a possibility, silica surface (silica layer thickness 0.2 mm on aluminium foil) was modified with the reagent **L_2**, through physisorption from a DMSO solution of 1.5 mM of **L_2**. This modified surface was dried and dipped into aq. solution having various amine based and ionic analytes discussed above. A bright blue fluorescence was observed only when such silica plate was exposed to a hydrazine solution and on further irradiation with 365 nm light source (Figure 4.3.).

Linear luminescence responses for varying [N_2H_4] for such modified silica surface (Figure 4.3.) further revealed that such solid surfaces are ideally suited for quantitative estimation of N_2H_4 (Figure 4.3.A) that could be present in a water body and for developing a strip type sensor.

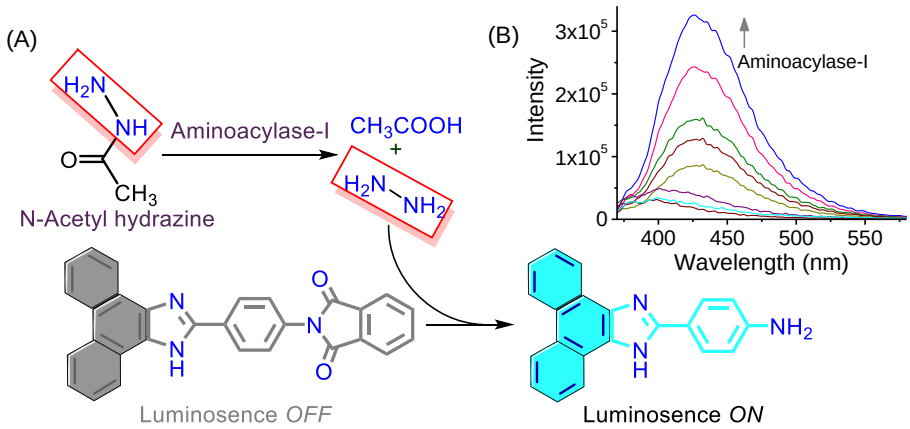

Figure 4.4. (A) Release of hydrazine from N-acetyl hydrazine by aminoacylase-1; (B) changes in fluorescence spectra of **L_2** (7.8 μM) on reaction with N_2H_4, released from N-acetyl hydrazine (10 mM) by varying [Acy-1) (λ_{Ext} = 360 nm, slit width 1/1 nm) in 0.4 mM TX-100 in HEPES buffer (10 mM, pH 7.2) medium, each spectra was recorded after 3.5h incubation of Acy-1 at 37°C.

Aminoacylase-1 (Acy-1) is an important enzyme and is found in many mammalian tissues. The enzyme hydrolyzes N-acetyl hydrazine at pH 7.2; however, the physiological role and the exact cellular localization of Acy-1 are still a matter of debate.[10] Incubation of probe **L_2** (7.8 μM) with N-acetyl hydrazine (10 mM) showed only a weak luminescence.

However, enhanced luminescence intensity was observed with increasing [Acy-1]. This signified higher [N_2H_4] that was generated *in situ* through the biochemical transformations of N-acetyl hydrazine induced by Acy-1 (Figure 4.4.B).

These results clearly demonstrated that the reagent **L_2** could actually be used for developing an assay for the Acy-1. MTT assay confirmed the non-toxic nature of probe **L_2** towards live Hct116 and HepG2 cells. This encouraged us to explore the possibility of using **L_2** as an imaging reagent for detection of N_2H_4 in Hct116 colon cancer. Cells were incubated with probe **L_2** (7.8 μM) for 1h at 37°C in 0.4 mM TX-100/PBS buffer at pH 7.2 and no intracellular florescence was observed. CLSM images for cells that were further incubated with N_2H_4 (20 μM) showed a strong intracellular fluorescence (Figure 4.5). Results shown in Figure 4.5 clearly reveal that the reagent **L_2** could be used as an imaging reagent for the detection of N_2H_4 uptake in Hct116 cells.

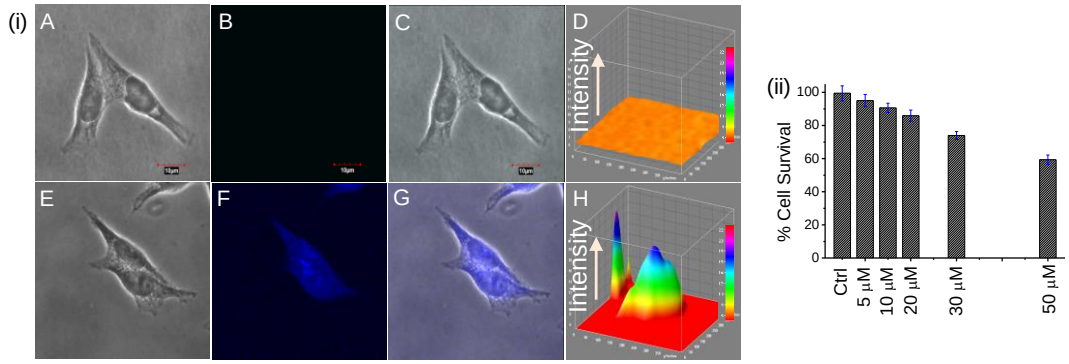

Figure 4.5. (i): (A–D) Confocal laser scanning microscopic (CLSM) images of Hct116 colon cancer cells incubated with **L_2** (7.8 μM) as control: (A) bright field, (B) dark field laser and (C) overlay images of (A) and (B); (D) 3D intensity plot of image (B); (E–H) CLSM images of Hct116 cells incubated with **L_2** (7.8 μM) for 1h and then further exposed to N_2H_4 (20 μM) for 1h at 37°C: (E) bright field, (F) dark field laser and (G) overlay images of (E) and (F), (H) 3D intensity plot of image (F). $\lambda_{Ext}/\lambda_{Em}$= 352/455 nm, Scale bar: 10 μm; (ii) MTT assay to determine the cell viability percentage in presence of **L_2** in Hct116 colon cancer cells.

We further utilized this reagent for probing the generation of N_2H_4 in Hct116 cells following an enzymatic reaction. Probe **L_2** (7.8 μM) was incubated with N-acetyl hydrazine for 1h and was treated as control.

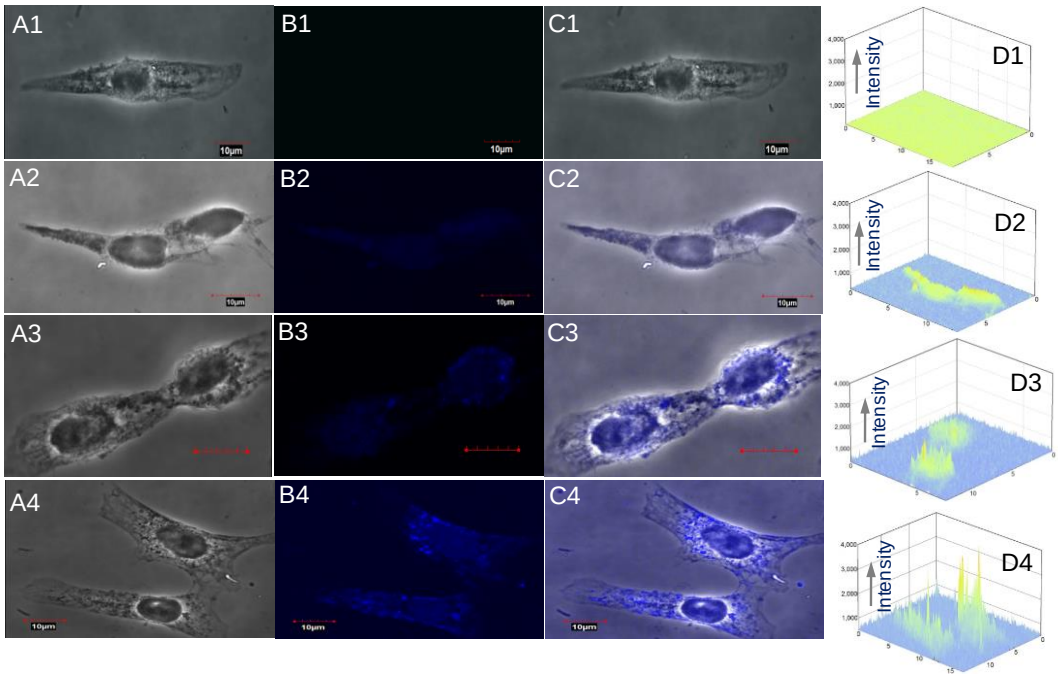

Figure 4.6. (A1–C1) CLSM images of Hct116 cells incubated with **L_2** (7.8 μM) and acetyl hydrazine (1 mM), treated as control; (A2-C4) CLSM images of Hct116 cells incubated with **L_2** (7.8 μM) and acetyl hydrazine (1 mM), then further exposed to varying [Acy-I] (0 U, A1-C1), (0.4 mU, A2-C2), (0.7 mU, A3-C3) and (1 mU, A4-C4); (A1-A4) bright field images, (B1-B4) dark field laser images and (C1-C4) overlay images of corresponding (A and B), (D1-D4): respective 3D intensity plot of images B1 to B4). $\lambda_{Ext}/\lambda_{Em}$= 352/455 nm, Scale bar: 10 μm.

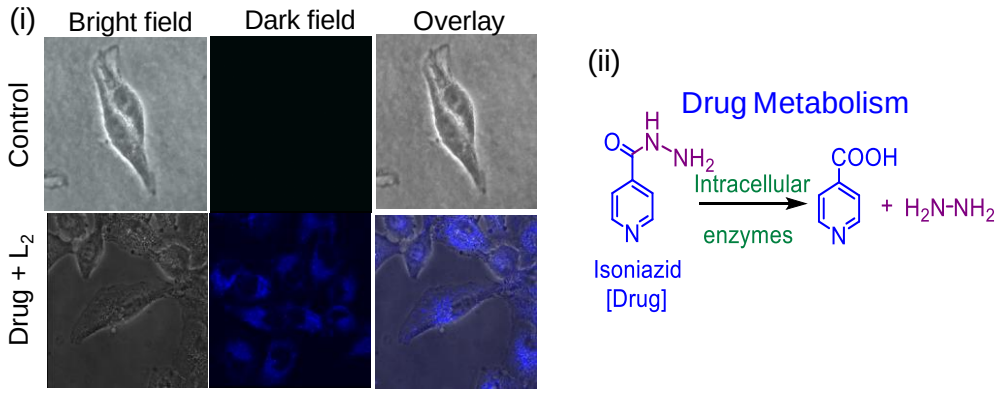

Figure 4.7. (i) Confocal micrographs of live HepG2 cells in the presence of **L_2** (7.8 μM). The images were acquired after pre incubation of drug for 3h then **L_2** was incubated for another 40 min; (ii) schematic representation of hydrazine released from drug by intracellular enzymes in live HepG2 cells.

Then these cells were further treated with varying concentration of Acy-1 for another 3h at 37°C (Figure 4.6).

Intracellular fluorescence intensities were found to increase with increasing [Acy-1], revealing of the in vitro generation of N_2H_4. Thus, this reagent could successfully be used for assaying the in-vitro enzymatic generation of N_2H_4 in Hct116 cells. Ensuring this, we looked into the possibility of imaging the release of N_2H_4 from Isoniazid by endogenous amidase in live HepG2 cell (Figure 4.7). Cells were incubated with Isoniazid (1 mM) for 3h at 37°C and then these cells were further incubated with **L_2** for another 40 min.

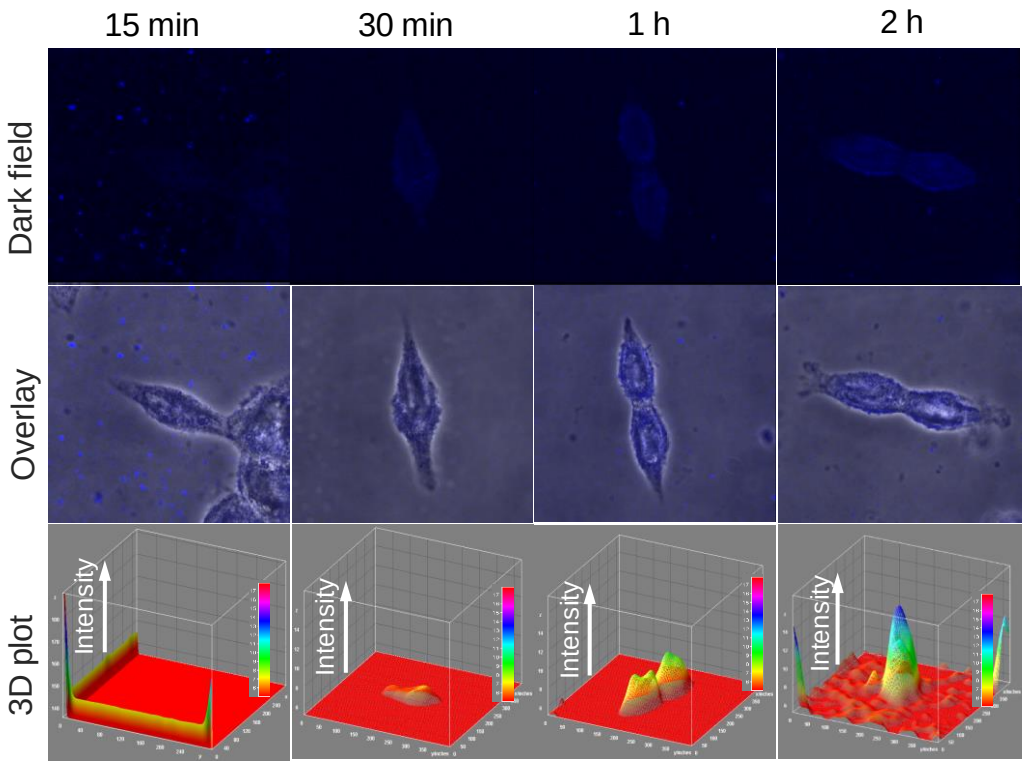

Figure 4.8. Time dependent confocal microscopic analysis of live HepG2 cells treated with isoniazid drug (1 mM) and **L_2** (7.8 μM): cells were incubated with drug at different time intervals: after 15 min, 30 min, 1h and 2h. Then **L_2** (7.8 μM) incubated for another 1h. $\lambda_{Ext}/\lambda_{Em}$= 352/455 nm.

Control experiments that were performed in absence of isoniazid after incubation solely with **L_2** did not show any intracellular emission, while cells exposed to isoniazid showed strong intracellular emission. This distinctly revealed the formation of metabolite hydrazine from isoniazid. CLSM images of HepG2 cells

incubated with isoniazid and then with **L_2** were also recorded at different time interval (Figure 4.8).

Role of endogenous amidase in live HepG2 cell was evident from the substantial increase in intracellular blue emission as a function of time (Figure 4.8). To the best of our knowledge, such an example demonstrating the role of amidase enzyme in generation of toxic hydrazine from a commonly prescribed drug like isoniazid is rather unique.

We hypothesized that effective scavenging of intracellular hydrazine, released by an enzymatic action on isoniazid, and could reduce *in vitro* cytotoxicity. To test this hypothesis, MTT assay of drug was carried out in presence and absence of **L_2** (7.8 μM) in live HepG2 cells (Figure 4.9). MTT assay confirmed that in presence of **L_2**, toxicity of the drug (isoniazid), eventually lowered. It would not be unreasonable to predict that scavenging of hydrazine by **L_2** would effectively lowed the effectual intracellular [N_2H_4] produced through the drug metabolism. Thus, our reagent offers as a distinct option for developing a combination TB drug like Isoniazid with lower cytotoxicity.

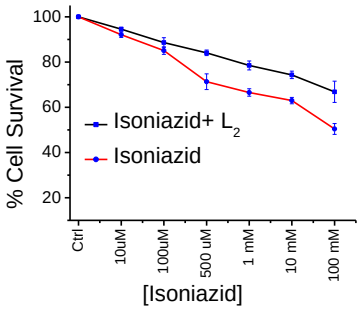

Figure 4.9. MTT assay of isoniazid (drug) in presence & absence of **L_2** (7.8 μM).

4.5. Conclusion

Thus, this chapter reveals a novel reagent and appropriate methodology for specific detection of hydrazine in pure aq-buffer medium under physiological pH. This reagent is suitable for developing a fluorescence based assay for monitoring enzymatic release of hydrazine in solution as well as Hct116 or HepG2 cells. Importantly probe **L_2** could be used as a protective reagent against toxicity induced by the tuberculosis drug Isoniazid and may possibly useful for clinical purpose to liver related diseases. This reagent is also suitable for developing a strip type sensor for hydrazine vapour as well as for quantitative estimation of hydrazine present in physiological condition.

4.6. References

1. (a) International Agency for Research on Cancer. Re-evaluation of some organic chemicals, hydrazine, and hydrogen peroxide. IARC Monographs on the Evaluation of Carcinogenic Risk of Chemicals to Humans; IARC: Lyon, 1999, **71**, 991; (b) S. D. Zelnick, D. R. Mattie and P. C. Stepaniak, *Aviat. Space Environ. Med*., 2003, **74**, 1285; (c) I. C. Vieira, K. O. Lupetti and O. Fatibello-Filho, *Anal. Lett*., 2002, **35**, 2221.

2. (a) M. D. Scales and J. A. Timbrell, *J. Toxicol. Environ. Health,* 1982, **10**, 941; (b) C. J. Waterfield, J. A. Turton, M. D. Scales and J. A. Timbrell, *Arch. Toxicol*., 1993, **67**, 244; (c) S. J. Moloney and R. A. Prough, *Biochemical Toxicology of Hydrazine*, Hodgson E, Philpot RM (eds). Elsevier Science: New York, 1983, 313; (d) K. Bando, T. Kunimatsu, J. Sakai, J. Kimura, H. Funabashi, T. Seki, T. Bamba and E. Fukusaki, *J. Appl. Toxicol*., 2011, **31**, 524.

3. (a) R. Heidari, H. Babaei and M. A. Eghbal, *Arh Hig Rada Toksikol,* 2013, **64**, 201; (b) G. Kleno T, R. Leonardsen L, O. Kjeldal H, M. Laursen S, N. Jensen O, D. Baunsgaard, *Proteomics*, 2004, **4**, 868.

4. (a) S. Virji, R. B Kaner, and B. H Weiller, *Chem. Mater.*, 2005, **17**, 1256; (b) H. Yang, B. Lu, L. Guo and B. Qi, *J. Electroanal. Chem*., 2011, **650**, 171; (c) S. J. R. Prabakar and S. J. S. Narayanan, *Electroanal. Chem*., 2008, **617**, 111; (b) G. Wang, C. Zhang, X. He, Z. Li, X. Zhang, L. Wang and B. Fang, *Electrochim. Acta*., 2010, **55**, 7204.

5. (a) G. Choudhary and H. Hansen, *Chemosphere*, 1998, **37**, 801–843; (b) A. Umar, M. M. Rahman, S. H. Kim and Y.-B. Hahn, *Chem. Commun*., 2008, 166; (c) B. Lei, C.-J. Wei and S.-C. Tu, *J. Biol. Chem.,* 2000, **275**, 2520.

6. A. Tostmann, M. J. Boeree, R. E. Aarnoutse, W. C. M. De Lange, A. J. van der Ven and R. Dekhuijzen, *J Gastroenterol Hepatol.,* 2008, **23**, 192.

7. (a) T. C. Sarich, *J. Pharmacol. Toxicol. Methods,* 1995, 34, 109; (b) *B. E. Senousy, S. I. Belal and P. V. Draganov, gastroenterology & hepatology,* 2010*,* **7,** 543; (c) W. L. Gent, H. I. Seifart, D. P. Parkin, P. R. Donald, and J. H. Lamprecht, *Eur. J. Clin. Pharmacol.,* 1992, **43**, 131.

8. (a) L. Cui, C. Ji, Z. Peng, L. Zhong, C. Zhou, L. Yan, S. Qu, S. Zhang, C. Huang, X. Qian, and Y. Xu, *Anal. Chem.*, 2014, **86**, 4611; (b) L. Cui, Z. Peng, C. Ji, J. Huang, D. Huang, J. Ma, S. Zhang, X. Qian and Y. Xu, *Chem. Commun*., 2014, **50**, 1485; (c) X.-X. Zhao, J.-F. Zhang, W. Liu, S. Zhou, Z.-Q. Zhou, Y.-H. Xiao, G. Xi, J.-Y. Miao and B.-X. Zhao, *J. Mater. Chem. B*, 2014, **2**, 7344; (d) M. H. Lee, B. Yoon, J. S. Kim and J. L. Sessler, *Chem. Sci.*, 2013, **4**, 4121; (e) D. Zhou, Y. Wang, J. Jia, W. Yu, B. Qu, X. Lia and X. Sun, *Chem Commun*., 2015, **51**, 10656; (f) C. Hu, W. Sun, J. Cao, P. Gao, J. Wang, J. Fan, F. Song, S. Sun, and X. Peng, *Org. Lett*., 2013, **15**, 4022; (g) S. Goswami, S. Das, K. Aich, B. Pakhira, S. Panja, S. K. Mukherjee, and S. Sarkar, *Org. Lett*., 2013, **15**, 5412; (h) J. Zhou, R. Shi, J. Liu, R. Wang, Y. Xu and X. Qian, *Org. Biomol. Chem.,* 2015*,* **13**, 5344; (i) Fan, W. Sun, M. Hu, J. Cao, G. Cheng, H. Dong, K. Song, Y. Liu, S. Sun and X. Peng, *Chem. Commun.,* 2012, **48**, 8117; (j) J. Zhang, L. Ning, J. Liu, J. Wang, B. Yu, X. Liu, X. Yao, Z. Zhang, and H. Zhang, *Anal. Chem*., 2015, **87**, 9101.

9. Y. Sun, W. Huang, C.-G. Lu and Y.-P. Cui, *Dyes Pigm*., 2009, **81**, 10.

10. H. Lindner, S. Höpfner, M. Täfler-Naumann, M. Miko, L. Konrad, KH. Röhm, *Biochimie*., 2000, **82**, 129.

CHAPTER 5

SUPER RESOLUTION PROBES FOR THE RECOGNITION OF REACTIVE SPECIES IN LIVE CELLS

CHAPTER 5A

SUPER RESOLUTION PROBE TO MONITOR HNO LEVELS IN THE ENDOPLASMIC RETICULUM OF CELLS

Communicated….

5A.1. Introduction

Recently, nitrosyl (HNO) has been identified as an enigmatic reactive nitrogen species and a potential pharmacological agent.[1] It is thought that HNO is generated from $NO^{\bullet}$ synthases through oxidation of N-hydroxy-L-arginine or via reduction of $NO^{\bullet}$ by mitochondrial xanthine oxidase, cytochrome c.[2] Recent advances in the understanding of the chemistry of HNO reveals that this species displays unique cardiovascular properties.[3] It is established that HNO accounts for positive lusitropic and ionotropic effects in failing hearts without a chronotropic effect, and it also causes a release of the neurotransmitters, glutamate and calcitonin-gene related peptide which modulates calcium channels such as ryanodine receptors.[4] Apart from its beneficial effects in cardiovascular disease, HNO is known to inhibit GAPDH, a key glycolytic enzyme for tumor proliferation and cancer cell apoptosis.[5] Furthermore, studies have also established that HNO interacts with thiol containing enzymes such as polymerase, aldehyde dehydrogenase, glyceraldehyde-3-phosphate dehydrogenase, and ADP-rybose to inhibit enzyme activity.[6] It also interferes with redox-based immunity mechanisms through fast depletion of glutathione,[7] and is more efficient in inhibiting platelet aggregation compared to traditional nitrovasodilators.[8]

Interestingly, biochemical transformations induced by HNO are significantly different than those induced by NO. The biochemical accumulation of HNO depends on a delicate balance between scavenging and activating/deactivating pathways.[9] HNO, is an electronic singlet, since the generation of the corresponding deprotonated species, $^{3}NO^{-}$ is spin forbidden (its adiabatic singlet-triplet transition energy is 18.45 kcal/mol)[10] HNO is the predominant species (pK_a^{HNO} = 11.4)[11] at physiological pH. Given the diversity of its biological functions and the fact that HNO rapidly converts to N_2O[12], thus fast and specific recognition/estimation of HNO is essential in understanding the biochemical role of HNO in human physiology.[13]

Several methodologies based on various analytical techniques such as colorimetric methods, EPR, HPLC, mass spectrometry, and electrochemical analysis, for the detection of HNO are available in the literature.[1] Such methodologies are either time consuming or involve destruction of cells and tissues and are thus not ideally suited to *in-vivo* tracking and detection of HNO.

In this context, reagents that show fluorescence ON response on detection of HNO have an obvious edge for use as an imaging reagent as well as for studying bio-species in living samples. Such reagent also allows high sensitivity, and spatiotemporal resolution. Among the various reagents that show such a response, phosphine-based reagents have received considerable attention.[1] King and co-workers were first to report the reaction of HNO with organic phosphines to produce the corresponding phosphine oxide and azaylide.[14] Since then, chemodosimetric probe molecules have been exploited this reaction for specific detection of HNO using flourophores like rhodamine, coumarine, napthalimide and BODIPY.[15] This reaction has also been exploited in developing FRET based receptors for HNO.[16.] Most of these receptors show a luminescence response within the visible region of the spectrum. For example, Lippard and co-workers have reported a Cu(II)-complex of a coumarin-derivative that shows specificity towards HNO with an luminescence ON response (λ_{Max} = 625 nm).[17] Unlike most other Cu(II)-based reagents, this reagent shows remarkable specificity towards HNO over L-(+)-cysteine, GSH, or methionine. In related work, Lin and co-workers have used a phosphile based derivative for two photon imaging of exogenous HNO in HeLa cells following excitation at 780 nm (λ_{Mon} = 512 nm).[18] Despite such efforts, examples of probes for the targeted detection/ scavenging of HNO in specific organelle is rather uncommon, thus there is ample scope to develop such reagents.

Despite it many attractions, one of the drawbacks of employing optical microscopy is that it has a practical resolution limit of around 250 nm.[19] More recently this drawback is being addressed through super resolution microscopy, SRM, which breaks this resolution limit. Amongst the range of SRM techniques, the particular advantages of structured illumination microscopy (SIM) is that it provides enhanced, 100 nanometers resolution while being less demanding of the property of luminophore and is ideally suited for 3-D sectioning. However, as image acquisition in SIM involves exposure of the luminophores to a high-power laser source over an extended time windows, compared to conventional optical microscopic techniques, effective SIM compatible probes must show high photo stability. In this study we describe a probe that is suitable for SIM that specifically detects HNO in the ER.

5A.2. Experimental Section

5A.2.1. Materials

All commercial reagents were procured from suppliers, were used as received without further purification. Angeli's salt was used as HNO donor. Solvents were dried as and when required by using standard procedures. **ER-S** was synthesized as described previously.[1] ^{1}H and ^{13}C NMR spectra were recorded on Bruker 400/500 MHz FT NMR (Model: Advance-DPX 400/500) using TMS as an internal standard. All the Fluorescence measurements were carried out on *PTI* Quanta Master™ Steady State Spectrofluorometer. High-resolution mass spectra were recorded on JEOL JM AX 505 HA mass spectrometer. UV Spectra were recorded using Shimadzu UV-1800 spectrometer. Confocal images were acquired in Olympus Fluoroview Microscope. All the Structured illumination Microscopy (SIM) experiments and Wide Field Fluorescence Microscopy Experiments were performed by using Delta Vision OMX-SIM (GE Health care). The Post processing SIM reconstructions were performed by using Soft Worx software. Quantum yield was recorded using standard methods and Rhodamine B as standard. Reagents used for the Tissue culture include, Dulbecco's Modified Eagle's Medium (DMEM) with L-glucose and Sodium bi carbonate (Aldrich), Phosphate Buffer Saline (PBS) (Aldrich), Fetal Bovine Serum (Aldrich), Penicillin Streptomycin (Aldrich). Reagents used for sample preparation for Structured Illumination Microscopy (SIM) and Wide Field Fluorescence Microscopy include 4% Paraformaldehyde (PFA) (Aldrich),Vectashield h-1000 (Mounting agent) (Aldrich), 50 mM Ammonium chloride (Aldrich), Angeli's Salt (Aldrich) Hoechst 33342 (Aldrich), ER Tracker Green (Aldrich). Other items required for sample preparation include 26 mm X 76 mm Microscopy glass slides, 22 mm X 22 mm (170 ± 5 µm square Cover glasses (Thor labs.)

.5A.2.2. Analytical Methods

^{1}H NMR spectra were recorded on a Bruker 500 MHz FT NMR (Model: Avance-DPX 500) using DMSO-d_6 as the solvent and tetra methyl silane (TMS) as an internal standard. IR spectra were recorded on Bruker Alpha FT IR spectrometer. UV-Vis spectra were recorded using Shimadzu UV-1800 spectrometer. All the Fluorescence measurements were carried out on *PTI* Quanta Master™ Steady State Spectrofluorometer. MALDI Ms spectrum was recorded using Dithranol (1,8-dihydroxy-9,10-dihydroanthracen-9-one) as the inert matrix using instrument AB SCIEX MALDI TOF/TOF™ 5800. High-resolution mass spectra were recorded on JEOL JM AX 505

HA mass spectrometer. Confocal images were acquired in Olympus Fluoview microscope.

5A.2.2.1. Confocal Microscopy Experiments

RAW 264.7 cells were seeded on cover slips placed in 6 well plates. After 24 hours cells washed with DMEM medium then cells were treated with **ER-HNO** (1 μM) for 25 minutes. Cells were then washed thrice with culture medium and further treated with Angeli's salt (HNO donor) of different concentration for 30 min. After that cells were washed again with Phosphate Buffer Saline (3X PBS). Then cells were fixed with 4% PFA for 10 min. Again cells were washed thrice and then cover slips mounted using mounting medium. Nail paints was used to seal the coverslips mounted on the glass slides. Images were acquired by using Olympus FluoView FV-1000 Confocal Microscope.

5A.2.2.2. Structured Illumination Microscopy Experiments

5A.2.2.2A. General description

The important aspect of using Structured Illumination Microscopy is because of its unique features compared to Traditional Optical Microscopy techniques. Multiple images are obtained by adjusting the fringe pattern and by slicing through the sample with respect to different focal planes generating a series of images of the sample and this Image volume is known as Z-stack. Each frame of the Z-stack is reconstructed so that it could provide definitive information of the details of the sample which we are Imaging thereby improving the resolution close to two fold which is not achieved by using normal Light Microscopy.

5A.2.2.2B. Sample preparation (SIM and Wide Field)

RAW 264.7 cells were seeded on Cover slips (22 mm X 22 mm, 170 ± 5 μm square Cover glasses) placed in 6 well plates in DMEM culture medium containing (10% FBS and 1% Penicillin Streptomycin) for 24 hours at 37°C, 5% CO_2. After 24 hours when 70% Confluency was achieved the cells were washed with DMEM culture medium then cells were treated with **ER-HNO** probe (1 μM) for 30 minutes. Cells were then washed thrice with culture medium and further treated with different Angeli's salt for 30 min. After that cells were washed again with Phosphate Buffer Saline (3X PBS). After carrying out the Live cell uptake of the **ER-HNO** probe and the small molecule, the cells were fixed with 4% PFA for 15 min and then washed thrice with PBS and two times and

then the cover slips were mounted using Mounting medium (Vectashield h-1000).The Coverslips were then sealed using Nail varnish and the sample were then imaged. As Structured Illumination Microscopy (SIM) relies on the cell morphology, the cells were examined with light microscope and then imaged using SIM.

5A.2.2.3. Structured Illumination Microscopy (SIM) and High Resolution Microscopy (HR)

The Delta Vision OMX system is a Microscope allows to image beyond the surface of the Coverslips by using multiple probes to retrieve exhaustive biological information from all directions. This Instrument's Structured Illumination Microscopy technology enables to image deeply the biology and resolves features which are literally close to invisible through Traditional Light Microscopy techniques. Delta Vision OMX can image from one to two microns in to Cells and Tissues. Delta Vision OMX is a very flexible Microscope and it works well with all kinds of probes including Fluorophores both conventional and engineered, Fluorescence proteins or any other synthesized probe.

SIM acquisition is dependent mainly on the Imaging parameters and Acquisition parameters and this varies depending on the sample and in particularly on the nature of the probe. The Resolution improvement is achieved based on the Reconstruction of the acquired image by using the inbuilt software namely Soft Worx. The Z stacks acquired during the Imaging are post processed by using the Reconstruction option of Soft Worx. The **ER-HNO** probe was Excited at 568 nm and the emission was collected at 586 nm (Alexa Flour 568 Channel of the Delta Vision OMX). In the case of **ER**-**HNO** probe the Structured Illumination experimental condition employed for running the Single Colour SI experiment were mainly dependent on the Thickness of the Z stack (Sections 50 to 80), Section spacing (0.125 to 0.150), thickness of the sample (8 to 12). The **ER-HNO** probe is a very bright probe the SIM acquisition. We needed to vary the %T and Exposure time. Therefore in all our Single colour experiments (ER-HNO-SIM-vid-1) the Exposure time was between 50 to 100 and the %T was in the range of 10 to 50.

The Wide field Microscopy technique involves improvement in resolution only after post processing the Z-stacks acquired. Post processing of acquired data is done by using Soft Worx software provided in the Delta Vision OMX. Off line Image processing were carried out by using Fiji software. The **ER-HNO** probe was Excited at 568 nm and the emission was collected at 586 nm (Alexa Flour 568 Channel of the Delta Vision OMX).

The Wide Field imaging conditions employed for Single Colour imaging of the RAW cells by using the **ER- HNO** probe are, Thickness of the Z stack (Sections 30 to 60), Section spacing (0.25 to 0.50), Thickness of the sample (8 to 12). As **ER-HNO** probe is a very bright probe the SIM acquisition we need to vary the %T and Exposure time and in all our Single colour experiments the Exposure time was between 50 to 100 and the %T was in the range of 10 to 50.

5A.2.2.3A. 3D SIM (Processed using Software)

The off line processing of Structured illumination Microscopy (SIM) images was carried out by using FIJI software. The option Stacks (3D project) was employed in obtaining a 3D projection of the Structured Illumination Microscopy images obtained by using the Delta Vision OMX-SIM Microscope. The 3D projections were also obtained by using the IMARIS 3D Software. The Intra cellular detection of HNO is represented using 3D-SIM illustrated by the Figure 5A.2.

5A.2.2.3B. Deconvolved Wide Field Microscopy

The Deconvolution procedure involves the processing of the raw Wide Field images obtained from the Delta vision OMX. This Image processing is carried out by using the Soft Worx software, which is used for carrying out the post processing of the SIM data. Deconvolution is a computationally intensive image processing technique, which helps in improving the contrast and Axial resolution post acquisition of the images from 400 nm to 350 nm. During the Deconvolution procedure, the raw Wide Field images are processed by removing the out of focus blur from stack of acquired images called as Z-Stack. The Deconvolution in effect improves the Quasi random disarrangement, improves the signal to noise ratio, improves the point spread function, thereby retrieves more information from the post-processed wide field image, and hence contributes in an improved resolution.

5A.2.2.3C. Comparitive SIM and Wide Field Microscopy Experiments

A Comparison between SIM and Wide Field Microscopy techniques is essential to understand the effectiveness of the **ER-HNO** probe as a Super resolution Microscopy probe. Intensity Vs Distance plots were generated by using FIJI software and this initiated a perfect comparison of the region of interest using two different techniques namely Structured Illumination Microscopy (SIM) and the Wide Field Microscopy (WF).

The extent of improvement of Resolution and Sharpness is directly proportional to the extent of retrievable biological information.

5A.2.2.3D. Colocalization SIM and Wide Field Microscopy Experiments

The Co-staining experiments with ER-Tracker Green was carried out by Incubating the **ER-HNO** (1 μM) further for 30 minutes after incubating the RAW cells with **ER-HNO** probe (1 μM) initially for 25 minutes. The Cells were washed regularly three times with DMEM culture media and PBS. The Cellular uptake of both the probes are carried out in live cells and then the Cells were fixed with 4% PFA and mounted and navigated initially for proper cell morphology by using Light Microscope and then imaged by using Structured Illumination Microscopy (SIM) and Wide Field Microscopy (WF). The **ER-HNO** probe was excited at 568 nm and the emission was collected in the Alexa Fluor Channel (570 nm to 620 nm) and the ER-Tracker was Excited at 488 nm and the Emission was collected in the FITC Channel (500 nm to 550 nm). The SIM imaging conditions maintained are, For **ER-HNO** probe: Thickness of the Z stack (Sections 40 to 80), Section spacing (0.125 to 0.150), Thickness of the sample (7 to 10), Exposure time was between 10 to 50 and the %T was in the range of 2 to 30. The SIM imaging conditions maintained are, For **ER-Tracker Green**: Thickness of the Z stack (Sections 40 to 80), Section spacing (0.125 to 0.150), Thickness of the sample (7 to 10), Exposure time was between 50 to 100 and the %T was in the range of 10 to 50. The WF imaging conditions maintained are, For **ER-HNO** probe: Thickness of the Z stack (Sections 30 to 60), Section spacing (0.250 to 0.500), Thickness of the sample (7 to 10), Exposure time was between 10 to 50 and the %T was in the range of 2 to 30. The WF imaging conditions maintained are, For **ER-Tracker Green**: Thickness of the Z stack (Sections 30 to 60), Section spacing (0.250 to 0.500), Thickness of the sample (7 to 10), Exposure time was between 50 to 100 and the %T was in the range of 10 to 50.

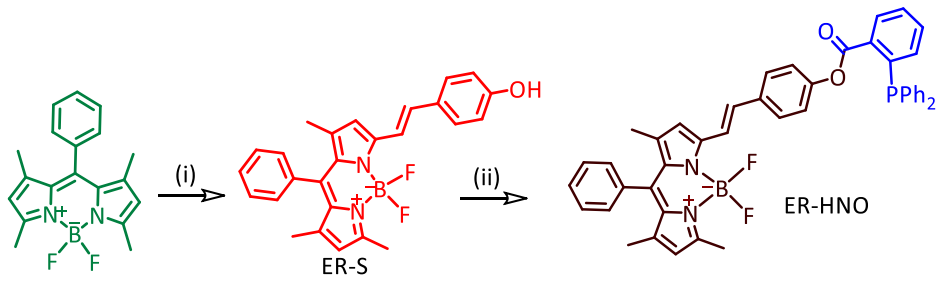

(i)= 4-Hydroxy benzaldehyde, Piperidine, acetic acid, tolune

(ii)= 2-(diphenylphosphino) benzoic acid, DCC, DMAP, Dry CH_2Cl_2

Scheme 5A.1. Synthetic route of **ER-HNO.**

5A.2.3. General experimental procedure for UV-Vis and Fluorescence studies

Stock solution of probe **ER-HNO** (5 $\times 10^{-3}$ M) was prepared in HPLC grade acetonitrile and the same solution was used for all the studies after appropriate dilution to 5 ml of PBS (pH 7.2) to make the effective ligand concentration of 10 μM. Unless and otherwise mentioned, 10 mM and pH 7.2 solution of aq. HEPES buffer was used for all spectroscopic studies. All reactive oxygen species and nitrogen species solutions of 1×10^{-3} M were prepared in PBS buffer medium having pH 7.2. All luminescence measurements were done using λ_{Ext} = 530 nm with an emission slit width of 2/2 nm.

5A.3. Synthesis and Characterisation

5A.3.1. Synthesis of ER-HNO

Under N_2 atmosphere, to a solution of 2-(diphenylphosphino) benzoic acid (100 mg, 0.32 mmol) in dry CH_2Cl_2, DCC (80 mg, 0.39 mmol) was added and stirred at 0^{o}C for 2h. To this, Compound **ER-S** (150 mg, 0.35 mmol) and DMAP (20 mg, 0.16 mmol) were added and it was stirred at room temperature for 6 h. Reaction was monitored by TLC. Then the mixture was concentrated under vacuum, and the crude product was purified by silica gel column chromatography by using 5% Ethyl acetate in PET ether medium to give the compound **ER-HNO**. Yield: 21%. (ESI) (m/z) calculated for [$C_{45}H_{36}BF_2N_2O_2P$ + K]: 755.22 , observed: 755.2 [M + K^+], ^{1}H NMR ($CDCl_3$, 400 MHz, δ ppm): 7.73 (2H, d, *J* 6.7), 7.68 (5H, dd, *J* 12.4, 7.4), 7.63 (2H, d, *J* 5.4), 7.56 (3H, d, *J* 8.5), 7.51 (5H, t, *J* 8.6), 7.47 (5H, d, *J* 5.6), 7.32 (2H, d, *J* 4.9), 7.19 (1H, d, *J* 16.3), 6.92 (1H, d, *J* 8.3), 6.60 (1H, s), 6.03 (1H, s), 2.62 (3H, s), 1.44 (3H, s), 1.41 (3H, s). ^{13}C NMR ($CDCl_3$, 125 MHz): 190.99, 164.54, 155.27, 155.06, 153.99,153.80, 142.51, 141.53, 137.30, 134.76, 134.53,134.15, 133.94, 133.68, 133.48, 133.16,132.88, 132.35, 131.94, 131.85, 131.75, 131.44, 131.11, 130.98, 128.91, 128.67, 128.60, 128.48,128.41, 122.42, 116.15, 25.98.

5A.4 Results and Discussions

This probe exploits the use of phosphine derivative for specific recognition of HNO and relies on a reductive ligation process. The phosphine functionality reacts with HNO to produce an intermediate azaylides, leading to cleavage of the 2-diphenylphosphino)benzoate moiety.[20]

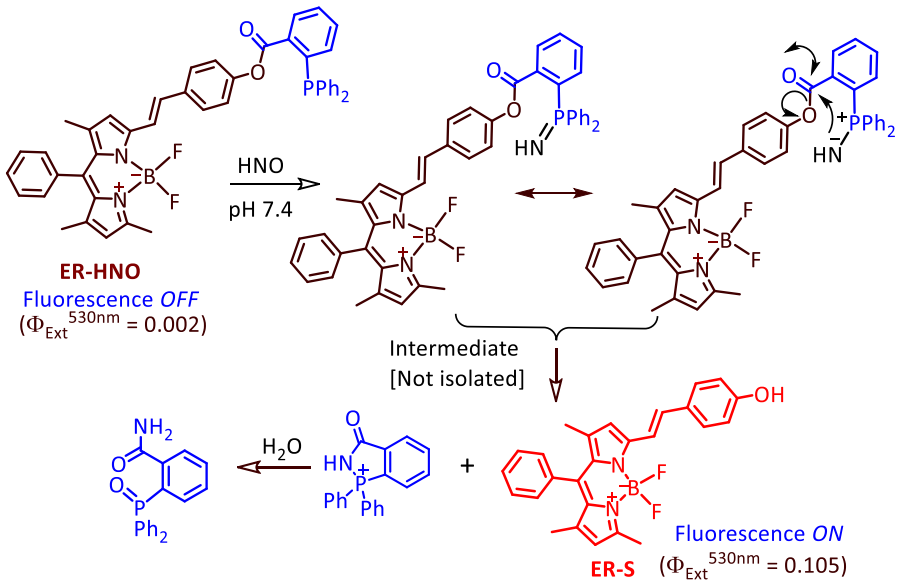

Scheme 5A.2. **ER-HNO** releases emissive BODIPY derivative ER-S when exposed to HNO.

As mentioned earlier, HNO exists solely at pH 7.2. Electronic spectrum recorded for **ER-HNO** and band maxima was observed at 562 nm in PBS-CH_3CN (9:1,v/v) buffer medium and this was attributed to a S0 →S1 transition. Following excitation at 530 nm, Reagent **ER-HNO** showed a weak emission band (Φ= 0.002, for λ_{Ext}= 530 nm) with maxima at 570 nm under identical experimental condition. Reaction of **ER-HNO** with HNO generated by Angeli's salt[21] leads to the generation of the corresponding derivative of the BODIPY moiety (**ER-S**) which has an appreciably higher emission quantum yield. This enhancement in emission response can be exploited to detect and quantify HNO in PBS-CH_3CN (9:1, v/v) buffer medium under physiological conditions (pH 7.2). Formation of **ER-S** as the reaction product of **ER-HNO** was also confirmed by ESI-MS. A systematic emission titration of **ER-HNO** with increasing concentrations of HNO revealed a gradual increase in solution emission with subsequent generation of **ER-S** (Figure 5A.1B) accompanied by the generation of a new emission band at maximum at λ_{Max}= 586 nm (Φ=0.105, for λ_{Ext}= 530 nm). A good linear relationship between emission intensity and concentration of HNO in the range of 2 - 15 µM is observed. To examine the selectivity of the probe, we performed in-vitro tests incubating **ER-HNO** (10 µM) with other RNS and ROS species (100 µM of HNO and 200 µM of HOCl, H_2O_2, OH, NO_3^-, NO_2^-, Cys, GSH and S^{2-}) in PBS-CH_3CN (9:1, v/v) buffer medium. The resultant emission spectra, recorded in PBS, are shown in Figure 5A.1.

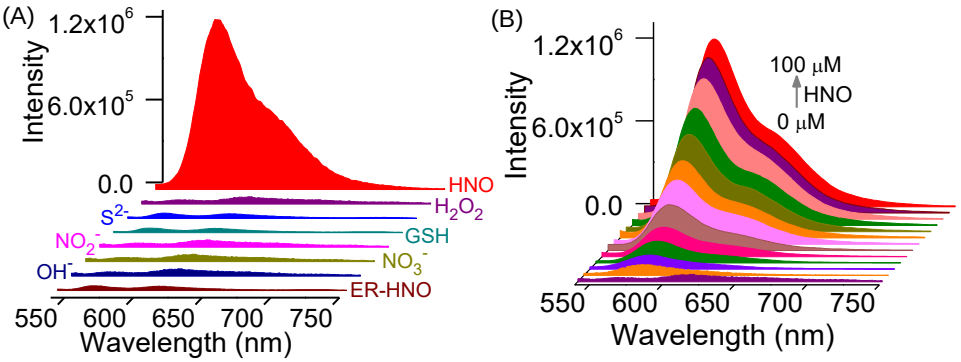

Figure 5A.1. (A) Change in emission of **ER-HNO** solution (10 μM) in the absence and presence of different analytes (0.1 mM of HNO and 0.2 mM; HOCl, H_2O_2,·OH, NO_3^-, NO_2^-, Cys, NAC, GSH and S^{2-}; (B) emission titration profile on varying [HNO] (0–100 μM).Studies were performed in aq. PBS buffer–CH_3CN (9:1, v/v; pH 7.2) medium; $\lambda_{Ext}/\lambda_{Em}$: 530/585 nm.

Except for HNO, which induces the expected turn ***ON*** emission response, no significant change in emission intensity is observed in the presence of any other RNS and ROS species. Even other potential anionic and cationic analytes, as well as biologically relevant thiols (Cys, GSH and NAC), under identical experimental condition failed to show any such change. The results of these interference studies also reveal that the emission response of **ER-HNO** in the presence of 10 mole equivalent of HNO remains unchanged in the presence of even higher concentrations of the other analytes mentioned above. These results confirm that the probe molecule **ER-HNO** is specific towards HNO. Further studies also reveal that the emission spectrum of **ER-HNO** remains unchanged over a wide range of pH 4-10. This distinctive emission response under physiological condition, as well as its specificity to HNO, led us to examine the toxicity of the probe molecule towards live human RAW 264.7 cells and cytotoxicity assays confirmed the low toxicity of the probe. This encouraged us to explore the use of the probe as an imaging reagent for the intracellular detection of HNO in these macrophage cells. Cells in DMEM culture media were incubated with **ER-HNO** (1.0 μM) for 15 minutes at 37 °C and subsequently viewed under confocal laser scanning microscope (CLSM) using a 530 nm laser as an excitation source. No intracellular fluorescence was observed until these pre-treated cells were also exposed to HNO, then a strong intracellular fluorescence was observed under CLSM (Figure 5A. 2).

High emission quantum yield, photo stability and non-toxicity are primary important factors for a reagent to be used for the super resolution microscopy (SRM) technique, SIM. Unarguably SIM is one of the most attractive SRM imaging techniques. However, image acquisition involves exposure of luminophores to a high power laser source over

an extended period of time windows, thus SIM compatible probes must show high photostability and low bleach rates. Given the photophysical properties of **ER-HNO**, its compatibility with SIM was also investigated.

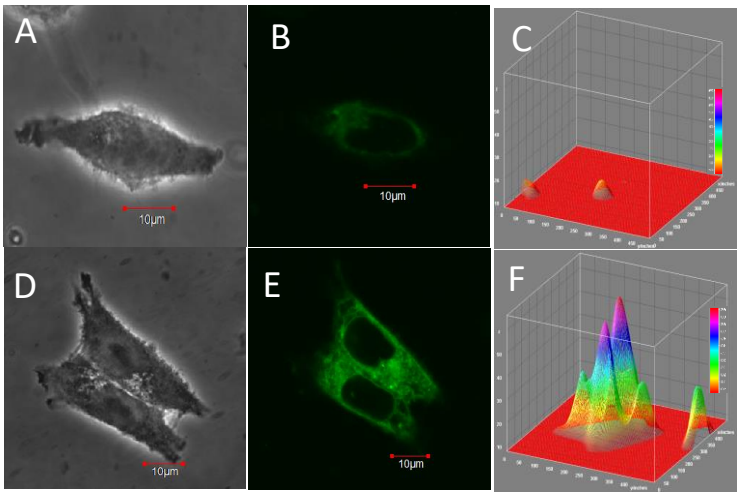

Figure 5A.2. (A–C) Confocal laser scanning microscopic (CLSM) images of RAW 264.7 cells incubated with **ER-HNO** (1 μM) as the control: (A) bright field; (B) dark field laser and (C) 3D intensity plot of image (B); (D–F) CLSM images of cells incubated with **ER-HNO** (1 μM) for 15 min and then further exposed to HNO (20 μM) for 20 min at 37 ^{0}C: (D) bright field; (E) dark field laser; (F) 3D intensity plot of image (E). $\lambda_{Ext}/\lambda_{Em}$ = 530/573 nm.

As for the CLSM experiments, RAW macrophage cells incubated with **ER-HNO** (1 μM) for 15 min at 37 ˚C in acetonitrile-PBS buffer (0.2:99.8, v/v) at pH 7.2 displayed no intracellular fluorescence. In contrast, cells incubated with **ER-HNO** (1 μM) and then treated with HNO for 30 min, showed strong intracellular fluorescence (Figure 5A.3). These results confirm that **ER-HNO** is sufficiently bright and stable to be used as an imaging reagent for the detection of HNO uptake in live RAW macrophage cells through SIM imaging. To illustrate the resultant increased resolution of SIM compared to wide-field, a comparison of respective intensity/distance plots is also provided in Figure 5A.3. A close look at the images shown in Figure 5A.3, suggest that the probe specifically localizes in the lipid dense region of RAW 264.7 cells. To explore this issue in more detail, co-localization studies were performed with the ER-specific reagent ER-Tracker Green, ER-TG. These studies revealed that emission from **ER-HNO**-treated cells in the presence of HNO showed a very high Pearson's co-localization coefficient of 0.936 with ER-TG; thus, **ER-HNO** uniquely provides a method of mapping HNO in the ER region of RAW 264.7 cells. We then examined the potential of **ER-HNO** for dual colour SIM, D-SIM imaging. Simultaneous use of different probes with complementary

optical properties is often required for probing more than one intracellular biological process in real-time.

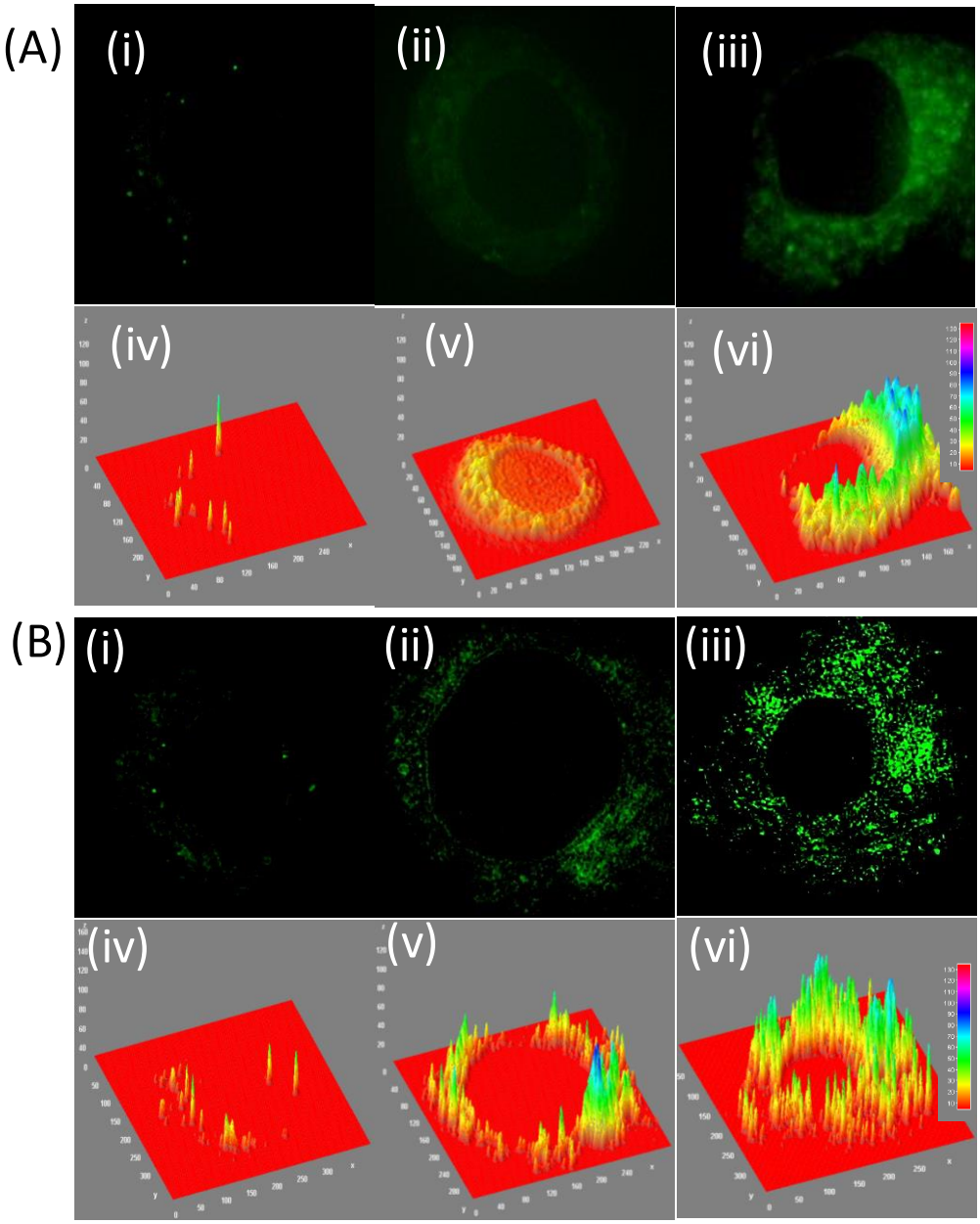

Figure 5A.3. Comparison of Wide field (A) and SIM (B) Microscopic images of RAW 264.7 cells incubated with **ER-HNO** (i); Images of cells incubated with **ER-HNO** (1 µM) for 15 min and then further exposed to (ii) 2 µM, (iii) 20 µM HNO for 30 min at 37 ^{0}C (iv - vi) 3D intensity plot of image (i - iii). $\lambda_{Ext}/\lambda_{Em}$ = 568/586 nm.

For this to be effected, the two probes used need to have complementary chemical and photophysical properties. As **ER-HNO** localizes in the ER, we looked to use a probe that is specific for a separate organelle with complementary optical properties.

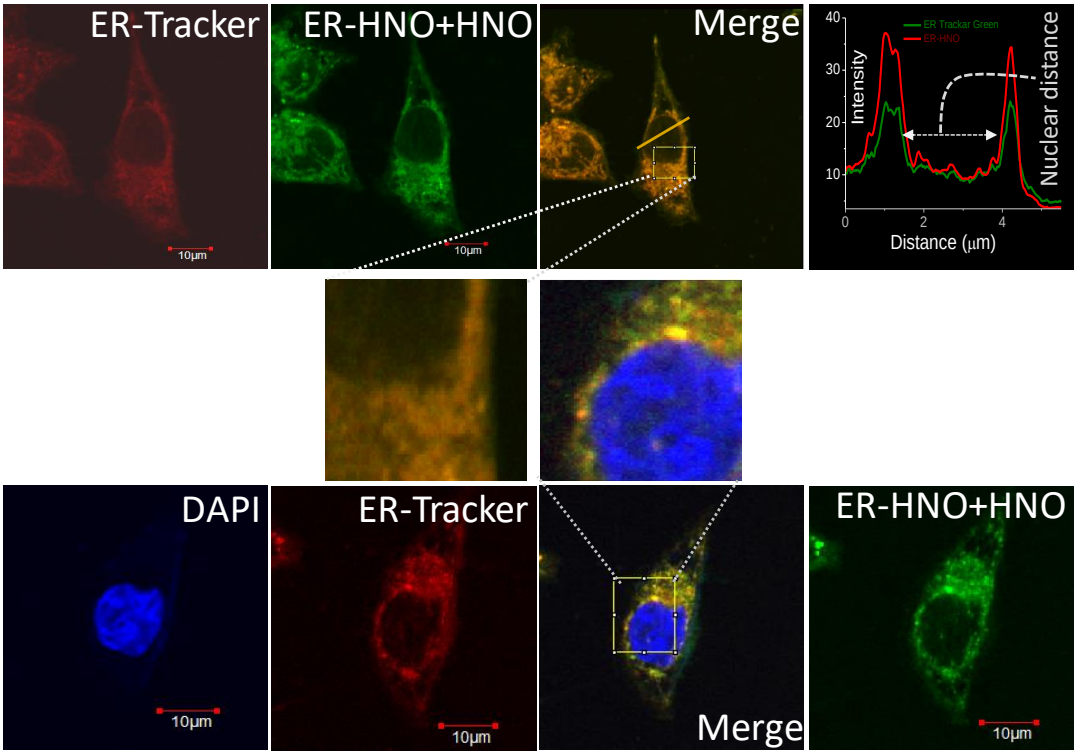

Figure 5A.4. Colocalization studies of **ER-HNO** in presence of HNO with DAPI and ER-Tracker Green in RAW 264.7 cells using CLSM imaging.

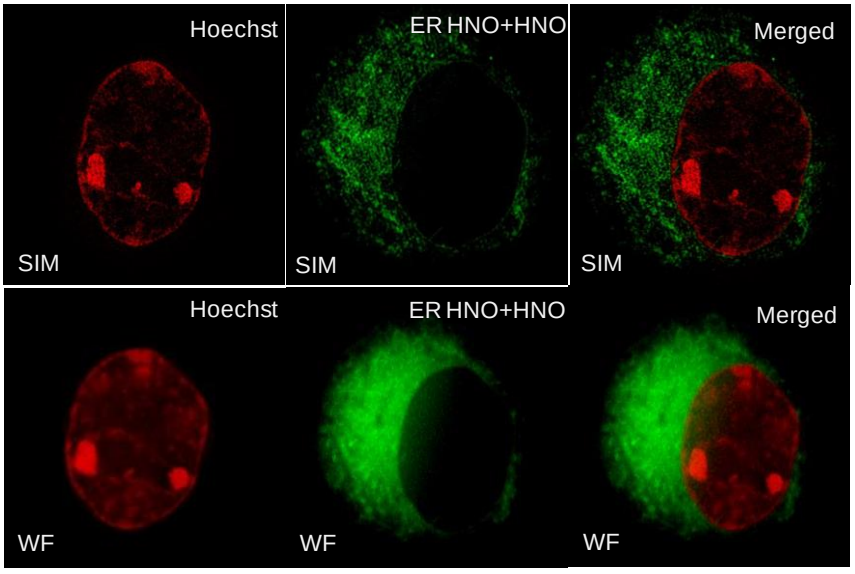

Figure 5A.5. Dual Colour (A) SIM and (B) comparative Wide Field Fluorescence Microscopic images with Hoechst as the nuclear stain (Pseudo Colouring has been employed in all the Images) and **ER-HNO** as ER specific stain.

Since it is known that ROS generation in remote cell compartments can affect processes within the nucleus, as an initial proof of concept, we chose to use the common nuclear stain Hoechst 33342 (that groove binds to and visualizes

chromatin DNA) as a complimentary probe in D-SIM imaging so as to simultaneously visualize HNO in the ER and also the nucleus. Fig 5 demonstrates that SIM images of both HNO generation in the ER and chromatin morphology can be accomplished through this combination of ER-HNO and Hoechst 33342 staining. This provides a route to future studies in which the effects of a specific ROS generation within the ER has on the structure and function of the nucleus can be simultaneously probed. Hence these results will facilitate future works aimed at investigating the effect of HNO mediated processes on whole cell morphology, which will be reported in forthcoming studies.

5A.5. Conclusion

In Summary, **ER-HNO** exhibits high selectivity, excellent sensitivity and low cytotoxicity in the detection of HNO. The probe effectively detects HNO generated in the ER of live cells and its photophysical properties are compatible with its use in SIM and two colour SIM imaging, allowing more than one organelle to be imaged at super resolution.

5A.6. References

1. (a) F. Doctorovich, P. J. Farmer and M. Marti, *The Chemistry and Biology of Nitroxyl (HNO): 2nd edn, Elsevier*, **2016**; (b) J. M. Fukuto, M. D. Bartberger, A. S. Dutton, N. Paolocci, D. A. Wink and K. N. Houk, *Chem. Res. Toxicol*., 2005, **18**, 790.

2. A. J. Hobbs, J. M. Fukuto and L. J. Ignarro, *Proc. Natl. Acad. Sci. U.S.A.*, 1994, **91**, 10992.

3. (a) J. L. Favaloro and B. K. Kemp-Harper, *Cardiovasc. Res*., 2007, **73**, 587–596; (b) N. Paolocci, M. Jackson, B. Lopez, K. Miranda, CG. Tocchetti, DA. Wink, AJ. Hobbs, JM. Fukuto, *Pharmacol. Ther*., 2007,**113**, 442.

4. (a) N. Paolocci,T. Katori, H. C. Champion, M. E. St. John, K. M. Miranda, J. M. Fukuto, D. A. Wink, and D. A. Kass, *Proc. Natl. Acad. Sci. U.S.A*, 2003, **100**, 9, 5537.

5. A. Augustyniak, J. Skolimowski and A. Błaszczyk, *Chem. Biol. Interact*., 2013, **206**, 262.

6. (a) G. Keceli and JP. Toscano, *Biochemistry*, 2014, **53**, 3689-98; (b) A. T. Wrobel, T. C. Johnstone, A. D. Liang, S. J. Lippard, and P. R.-Fuentes, *J. Am. Chem. Soc*., 2014, **136**, 4697.

7. N. Paolocci, W.F. Saavedra, K. M. Miranda, C. Martignani, T. Isoda, J. M. Hare, M. G. Espey, J. M. Fukuto, M. Feelisch, D. A. Wink and David A. Kass, *Proc. Natl. Acad. Sci*., 2001, **98**, 10463.

8. CH. Switzer, W. Flores-Santana, D. Mancardi, S. Donzelli, D. Basudhar, LA. Ridnour, et al. *BBA-Bioenergetics*, 2009, **178**7, 835.

9. K. M. Miranda, N. Paolocci, T. Katori, D. D. Thomas, E. Ford, M. D. Bartberger , M. G. Espey, D. A. Kass, M. Feelisch, J. M. Fukuto and David A. Wink, *Proc. Natl. Acad. Sci*., 2003, **100**, 9196.

10. M. D. Bartberger, J. M. Fukuto, and K. N. Houk , *Proc. Natl. Acad. Sci*., 2001, **98**, 2194.

11. V. Shafirovich and S. V. Lymar, *Proc. Natl. Acad. Sci., USA*., 2002, **99**, 7340.

12. K. M. Miranda, *Coord. Chem. Rev*., 2005, **249**, 433.

13. (a) J. Rosenthal and S. J. Lippard, *J. Am. Chem. Soc*., 2010, **132**, 5536; (b) Y. Zhou, K. Liu, J.-Y. Li, Y. Fang, T.-C. Zhao and C. Yao, *Org. Lett*., 2011, **13**, 1290; (c) S. A. Suárez, D. E. Bikiel, D. E. Wetzler, M. A. Martí, and F. Doctorovich, *Anal Chem*., 2013, **85**, 10262.

14. (a) J. A. Reisz, C. N. Zink and S. B. King, *J. Am. Chem. Soc*., 2011, **133**, 11675; (b) J. A. Reisz, E. B. Klorig, M.W. Wright and S. B. King, *Org. Lett*., 2009, **11**, 2719.

15. (a) K. Kawai, N. Ieda, K. Aizawa, T. Suzuki, N. Miyata and H. Nakagawa, *J. Am. Chem. Soc*., 2013,**135**, 12690; (b) X. Jing, F. Yu and L. Chen, *Chem. Commun*., 2014, **50**, 14253; (c) C. Liu, H. Wu, Z.Wang, C. Shao, B. Zhu and X. Zhang, *Chem Commun*. 2014, **50**, 6013; (d) G.-J. Mao, X.-B. Zhang, X.-L. Shi, H.-W. Liu, Y.-X. Wu, L.-Y. Zhou, W. Tan and R.-Q. Yu, *Chem. Commun*., 2014, **50**, 5790.

16. H. Zhang, R. Liu, Y. Tan, W. H. Xie, H. Lei, H.-Y. Cheung and H. Sun, *ACS Appl. Mater. Interfaces*, 2015, **7**, 5438.

17. J. Rosenthal and S. J. Lippard, *J. Am. Chem. Soc*., 2010, **132**, 5536.

18. K. Zheng, W. Lin, D. Cheng, H. Chen, Y. Liub and K. Liu, *Chem. Commun.*, 2015, **51**, 5754.

19. J. A. Thomas, *Chem. Soc. Rev*., 2015, **44**, 4494.

20. (a) B. Dong, K. Zheng, Y. Tanga, W. Lin, *J. Mater. Chem. B*, 2016, **4**, 1263—1269; (e) K. Sunwoo, K. N. Bobba, J.-Y. Lim, T. Park, A. Podder, J. S. Heo, S. G. Lee, S. Bhuniya and J. S. Kim, *Chem. Commun*., 2017, **53**, 1723; (f) P. Rivera-Fuentes, S. J. Lippard, *Acc. Chem. Res*., 2015, **48**, 2927.

21. KM. Miranda, HT. Nagasawa and JP Toscano, *Curr. Top. Med. Chem*., 2005, **5**, 649.

CHAPTER 5B

LUMINESCENCE PROBE FOR SUPER HIGH RESOLUTION IMAGING OF ENDOGENOUSLY GENERATED HOCl IN THE GOLGI BODY OF LIVE CELLS

To be communicated….

5B.1. Introduction

Bio-imaging technologies to probe the molecular basis of life are increasingly in demand. In this context, optical microscopy has proven its utility and versatility. Fluorescence-based methods involving luminescent probes for specific biomolecules and cellular structures are particularly attractive due to the increased contrast they provide over traditional bright-field techniques. The ideal characteristics of such cell permeable probes are that they display low toxicity, organelle specificity, and are photostable with a bright emissive excited state. These probes have been used to provide information on the structure and function of intracellular organelles.

One of the disadvantages of conventional fluorescence microscopy is its spatial resolution limit. Even for high-resolution methods, such as confocal laser scanning microscopy (CLSM) the smallest distance at which two close points within an image merge into one is roughly half the wavelength of the imaging light, restricting resolution to features above 200–250 nm. However, more recently, instrumental techniques to break these limitations have been identified to produce super-resolution microscopy, SRM, where scaling down to tens of nanometers has been accomplished.

Apart from structural features, optical microscopy has also been used to investigate specific cellular processes and responses to changes in environment. A case in point is the generation of - and cellular response to - reactive oxygen species, ROS. After the pioneering discovery that hydrogen peroxide is generated during phagocytosis, ROS have been found to play a wide range of biological roles from cell signalling and regulation, to dysfunctions that lead to many degenerative diseases and cancers. Along with H_2O_2, common endogenous ROS include species such as superoxide, singlet oxygen, ozone, hydroxyl radical, hypochlorous acids, and organic peroxides. A panoply of redox pathways involved in homeostasis and cell activation are controlled by strict regulation of the concentration, location, and chemical identity of these individual ROS. On the other hand, overproduction, or high exposure to exogenous ROS, is deleterious to cells as it leads to cellular dysfunction and ultimately cell death. The complex interrelationship of ROS signalling pathways is illustrated by the fact that they are can often be in opposition to each other; for example, ROS can both promote or prevent cell death, inflammation, and ageing.

For all these reasons, dissecting the role of individual ROS signaling and oxidative stress pathways in specific cell compartments and in real-time is a highly demanding task. However, given the convenience of optical microscopy it is not surprising that over the last few years the number of luminescent probes designed to detect ROS within live cells has burgeoned. Although general probes for these species have been identified, recent studies have focused on probes for specific ROS. One target for probe development is the highly potent oxidant hypochlorous acid (HOCl), which is naturally produced by the myeloperoxidase-H_2O_2-Cl^- system and catabolised through oxidation by glutathione and cellular thiols.[1]

HOCl plays an essential role in the immune response to pathogens,[2] as it is generated during phagocytosis.[3] Activated phagocytic cells also generate HOCl[4] as part of the inflammation response, and its overproduction is associated with cardiovascular disease, neurodegenerative disorder and inflammatory-related diseases.[5] These effects may be due to quite specific cellular mechanisms; for example, it is suggested that - along with other ROS - HOCl plays a part in the Golgi stress response, a phenomenon that is linked to a number of neurodegenerative diseases.[6] To fully understand the details of signalling processes like these dedicated HOCl probes that also display localisation in specific cellular compartments are required.

Herein we report the synthesis of a small molecule-based brightly fluorescent probe which specifically detects HOCl in the Golgi body of live cells. Furthermore we find the chemical and photophysical properties of the probe make it ideally suited to be employed as a fluorophore for the SRM technique of structured illumination microscopy, SIM. Although a number of fluorescent probes that can detect HOCl inside living cells have been reported recently[7], this probe is the first to show high specificity for this organelle and also SRM imaging capabilities.

5B.2. Experimental Section

5B.2.1. Materials

All commercial reagents were procured from suppliers, were used as received without further purification. Quantum yield was recorded using standard methods and Rhodamine B as standard. Reagents used for the Tissue culture include, Dulbecco's Modified Eagle's Medium (DMEM) with L-glucose and Sodium bi carbonate (Aldrich),

Phosphate Buffer Saline (PBS) (Aldrich), Fetal Bovine Serum (Aldrich), Penicillin Streptomycin (Aldrich). Reagents used for sample preparation for Structured Illumination Microscopy (SIM) and Wide Field Fluorescence Microscopy include 4% Paraformaldehyde (PFA) (Aldrich),Vectashield h-1000 (Mounting agent) (Aldrich), 50 mM Ammonium chloride (Aldrich), Hoechst 33342 (Aldrich), ER Tracker Green (Aldrich). Other items required for sample preparation include 26 mm X 76 mm Microscopy glass slides, 22 mm X 22 mm (170 ± 5 µm square Cover glasses (Thor labs.)

5B.2.2. Analytical Methods

^{1}H NMR spectra were recorded on a Bruker 500 MHz FT NMR (Model: Avance-DPX 500) using DMSO-d_6 as the solvent and tetra methyl silane (TMS) as an internal standard. IR spectra were recorded on Bruker Alpha FT IR spectrometer. Confocal images were acquired in Olympus Fluoroview Microscope. All the Structured Illlumination Microscopy (SIM) experiments and Wide Field Fluorescence Microscopy Experiments were performed by using Delta Vision OMX-SIM (GE Health care). The Post processing SIM reconstructions were performed by using Soft Worx software. UV-Vis spectra were recorded using Shimadzu UV-1800 spectrometer. All the Fluorescence measurements were carried out on *PTI* Quanta Master™ Steady State Spectrofluorometer. MALDI Ms spectrum was recorded using Dithranol (1,8-dihydroxy-9,10-dihydroanthracen-9-one) as the inert matrix using instrument AB SCIEX MALDI TOF/TOF™ 5800. High-resolution mass spectra were recorded on JEOL JM AX 505 HA mass spectrometer.

5B.2.2.1. Structured Illumination Microscopy Experiments

5B.2.2.1A. General description

The important aspect of using Structured Illumination Microscopy is because of its unique features compared to Traditional Optical Microscopy techniques. Multiple images are obtained by adjusting the fringe pattern and by slicing through the sample with respect to different focal planes generating a series of images of the sample and this Image volume is known as Z-stack. Each frame of the Z-stack is reconstructed so that it could provide definitive information of the details of the sample which we are Imaging thereby improving the resolution close to two fold which is not achieved by using normal Light Microscopy.

5B.2.2.1B. Sample preparation (SIM and Wide Field)

RAW 264.7 cells were seeded on Cover slips (22 mm X 22 mm, 170 ± 5 µm square Cover glasses) placed in six well plates in DMEM culture medium containing (10% FBS and 1% Penicillin Streptomycin) for 24 hours at 37°C, 4% CO_2. After 24 hours when 70% Confluency was achieved the cells were washed with DMEM culture medium then cells were treated with **SF-1** (10 µM) for 30 minutes. Cells were washed thrice with culture medium and further treated with different NaOCl for 30 minutes. Then cells were washed again with Phosphate Buffer Saline (2X PBS). After carrying out the Live cell uptake of the **SF-1** probe and the small molecule, the cells were fixed with 4% PFA for 15 minutes and then washed thrice with PBS and two times and then the cover slips were mounted using Mounting medium (Vectashield h-1000).The Coverslips were then sealed using Nail varnish and the sample were then imaged. As Structured Illumination Microscopy (SIM) relies on the cell morphology, the cells were examined with Light microscope and then imaged using SIM.

5A.2.2.1C. Colocalization SIM and Wide Field Microscopy Experiments

The Co-staining experiments with ER Tracker Green was carried out by Incubating the ER Tracker Green (1 uM) further for 30 minutes after incubating the RAW cells with **SF-1** probe (10 uM) initially for 25 minutes. The Cells were washed regularly three times with DMEM culture media and PBS. The Cellular uptake of both the probes are carried out in live cells and then the Cells were fixed with 4% PFA and mounted and navigated initially for proper cell morphology by using Light Microscope and then imaged by using Structured Illumination Microscopy (SIM) and Wide Field Microscopy (WF) (SF-1-SIM-video-3). The **SF-1** probe was excited at 568 nm and the emission was collected in the Alexa Fluor Channel (570 nm to 620 nm) and the ER-Tracker Green was Excited at 488 nm and the Emission was collected in the **FITC** Channel (500 nm to 550 nm). The SIM imaging conditions maintained are, For **SF-1** probe: Thickness of the Z stack (Sections 50 to 100), Section spacing (0.125 to 0.150), Thickness of the sample (8 to 11), Exposure time was between 3 to 30 and the %T was in the range of 10 to 50. The SIM imaging conditions maintained are, For **ER Tracker Green**: Thickness of the Z stack (Sections 50 to100), Section spacing (0.125 to 0.150), Thickness of the sample (8 to 11), Exposure time was between 10 to 50 and the %T was in the range of 10 to 50. The WF imaging conditions maintained are, For **SF-1** probe: Thickness of the Z stack (Sections 40 to 80), Section spacing (0.250 to 0.500), Thickness of the sample (8 to 11), Exposure time was between 1 to 30 and the %T was

in the range of 2 to 30. The WF imaging conditions maintained are, For **ER Traker Green**: Thickness of the Z stack (Sections 40 to 80), Section spacing (0.250 to 0.500), Thickness of the sample (8 to 11), Exposure time was between 10 to 50 and the %T was in the range of 2 to 30.

The Co-staining experiments with Cytopainter Golgi Tracker Green was carried out by Incubating the Cytopainter Golgi Tracker Green (1 uM) further for 30 minutes after incubating the RAW cells with **SF-1** probe (10 uM) initially for 25 minutes. The Cells were washed regularly three times with DMEM culture media and PBS. The Cellular uptake of both the probes are carried out in live cells and then the Cells were fixed with 4% PFA and mounted and navigated initially for proper cell morphology by using Light Microscope and then imaged by using Structured Illumination Microscopy (SIM) and Wide Field Microscopy (WF) (SF-1-SIM-video-4 and SF-1-WF-video-4a). The **SF-1** probe was excited at 568 nm and the emission was collected in the **Alexa Fluor** Channel (570 nm to 620 nm) and the Cytopainter Golgi Tracker Green was Excited at 488 nm and the Emission was collected in the **FITC** Channel (500 nm to 550 nm). The SIM imaging conditions maintained are, For **SF-1** probe: Thickness of the Z stack (Sections 50 to 100), Section spacing (0.125 to 0.150), Thickness of the sample (8 to 11), Exposure time was between 10 to 50 and the %T was in the range of 2 to 30. The SIM imaging conditions maintained are, For Golgi Tracker Green: Thickness of the Z stack (Sections 50 to 100), Section spacing (0.125 to 0.150), Thickness of the sample (8 to 11), Exposure time was between 10 to 50 and the %T was in the range of 2 to30. The WF imaging conditions maintained are, For **SF-1** probe: Thickness of the Z stack (Sections 30 to 60), Section spacing (0.250 to 0.500), Thickness of the sample (8 to 11), Exposure time was between 2 to 30 and the %T was in the range of 2 to 30. The WF imaging conditions maintained are,

For Golgi Tracker Green**:** Thickness of the Z stack (Sections 80 to 100), Section spacing (0.250 to 0.500), Thickness of the sample (8 to 11), Exposure time was between 2 to 30 and the %T was in the range of 2 to 30.

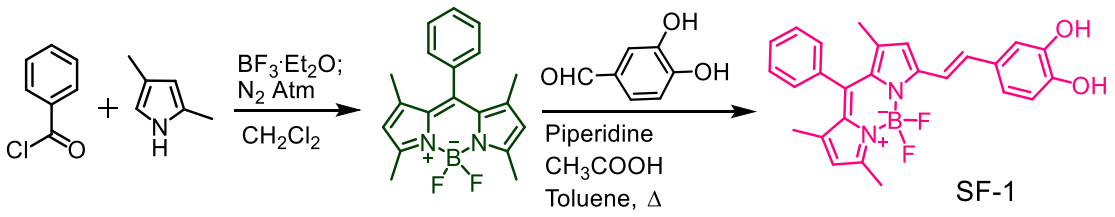

Scheme 5A.1. Synthetic route of **SF-1.**

5B.2.3. General experimental procedure for UV-Vis and Fluorescence studies

Stock solution of probe **SF-1** (1 ×10^{-4} M) was prepared in HPLC grade Acetonitrile and the same solution was used for all the studies after appropriate dilution to 5 ml of PBS (pH 7.2) to make the effective ligand concentration of 10 μM. Unless and otherwise mentioned, 10 mM and pH 7.2 solution of aq. PBS buffer was used for all spectroscopic studies. All reactive oxygen species and nitrogen species solutions of 1×10^{-2} M were prepared in PBS having pH 7.2 and used with appropriate dilution. All luminescence measurements were done using λ_{Ext} = 550 nm with an emission slit width of 2/2 nm.

5B.3. Synthesis and Characterisation

5B.3.1. Synthesis of SF-1

Mixture of BODIPY core (280 mg, 0.864 mmol), 3,4-Dihydroxy benzaldehyde (119.3 mg, 0.864 mmol), Glacial acetic acid (0.53ml) and Piperidine (0.65 ml) were refluxed in 10 ml toluene in a dean-stark apparatus for 3h. Crude compound was then evaporated under vacuum and then it was purified by silica gel column chromatography using 5% Ethylacetate in Dichloromethane to get pink colour **SF-1** (yield= 18%). ^{1}H NMR (400MHz, CD_3OD, δ ppm, *J* in Hz): 7.50 (3H, m, Ar-H), 7.46 (1H, *J*=15.89 Hz (CH=C)), 7.27-7.25 (2H, m) , 7.23 (1H, d, *J*=16.38 Hz (CH=CH)), 7.14 (1H, d, *J*=1.96 Hz), 6.94 (1H, dd, *J*=1.96 Hz, *J*=8.07 Hz), 6.80 (1H, d, *J*=8.07 Hz) , 6.65 (2H, s) , 6.02 (1H, s), 2.52 (3H, s), 1.39 (3H, s), 1.37 (3H, s). ^{13}C NMR (400 MHz CD_3OD): 14.56, 14.65, 14.89, 114.24, 116.61, 117.02, 118.81, 121.91, 122.23, 129.55, 130.15, 130.29, 130.32, 132.03, 134.03, 136.41, 138.56, 141.36, 143.13, 144.36, 146.5, 148.52, 155.00, 155.39, (MALDI MS (M/Z) = 444.7)

5B.4 Results and Discussion

The absorption spectrum of **SF-1** was recorded in an aqueous PBS buffer-acetonitrile (9:1, v/v) solution. An intense absorption band having maximum at ~ 550 nm (ε = 40000 L $mol^{-1}cm^{-1}$) was observed and this was assigned to S_0-S_1 electronic transition.[8] On excitation at 540 nm, a weak emission band (Φ_{590nm}^{SF-1} = 0.0034) with maximum at 590 nm was observed. The luminescence spectral response of probe **SF-1** towards a variety of ROS and reactive nitrogen species, RNS, and ionic analytes was tested using 20 mole equivalent of the respective

analytes. No observable change in luminescence signal was observed in presence of any of the species investigated (H_2O_2, $^{\bullet}OH$, HNO, Na_2S_2, NO_3^-, NO_2^-, Fe^{2+}, Fe^{3+} , Cu^{2+}, Cr^{3+}, Hg^{2+}, Zn^{2+} and K^+) except for HOCl, which produced a distinctive eight-fold "turn-on" luminescence enhancement (Fig. 1(A)) at 585 nm (Φ_{590}^{SF-2} = 0.0257; λ_{Ext} = 540 nm and Rhodamin B was used for evaluation of relative emission quantum yield values). Furthermore, even in presence of large excesses of other ROS/RNS, the emission response of **SF-1** towards HOCl remains unchanged, illustrating its specificity towards HOCl.

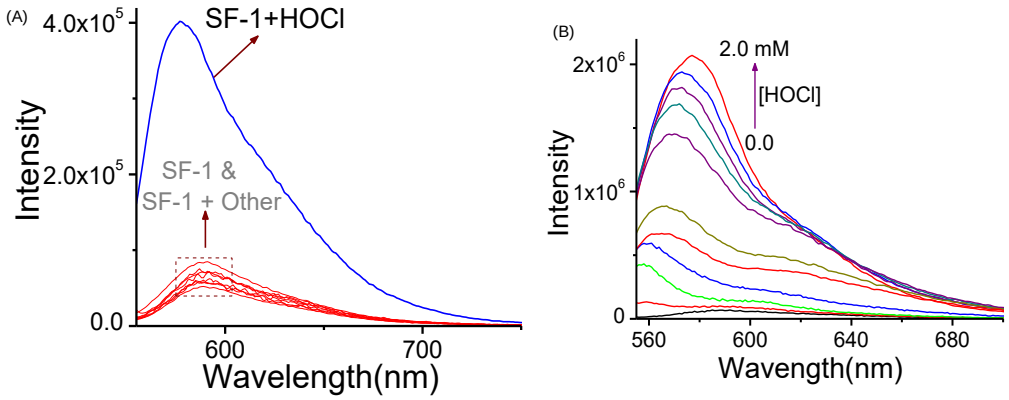

Figure 5B.1. (A) Change in emission spectra of **SF-1** in absence and presence of different ROS/NOS species (X: HOCl, H_2O_2, $^{\bullet}OH$, Na_2S_2, Cysteine, NO_3^-, NO_2^-, Fe^{2+}, Fe^{3+}, Cu^{2+}, Cr^{3+}, Hg^{2+}, Zn^{2+} and K^+); (B) emission titration profile for **SF-1** in presence of varying concentration of HOCl. All emission spectra were recorded using λ_{Ext} = 540 nm in aq. PBS buffer-acetonitrile (9:1, v/v) solution.

This isolated compound was identified as the quinone derivative (**SF-2**, Scheme 5B.2) based on the detailed analytical and spectroscopic (ESI-Ms spectral) studies. Previous report on related molecule indicates the observed output is due to the chemical mechanism shown in Scheme 5B.2.[9] Analysis of the emission titration profile revealed a lower HOCl detection limit of 2 µM in aqueous buffer medium. Further emission studies, performed at different pH confirmed that **SF-1** was stable across a wide pH range (pH = 4 – 9).

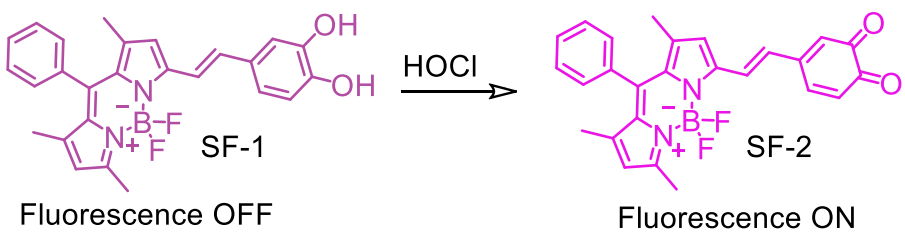

Scheme 5B.2. Proposed sensing mechanism of **SF-1** with HOCl.

Time dependent luminescence assays employing 10 µM solutions of the probe in the presence of 2 mM HOCl, reveal that the reaction shown in scheme 5B.2 is completed within 15 min.

The suitability of **SF-1** as a fluorescent probe in live cell imaging was then investigated. Prior to demonstrating its biological imaging properties, the probe's cytotoxicity towards RAW 264.7 macrophage cells was evaluated by MTT assay. MTT assay confirmed the non-toxic nature of probe **SF-1.**

High emission quantum yield, photo stability and non-toxicity are primary important factors for a reagent to be used for the super resolution microscopy (SRM) technique, SIM. Unarguably SIM is one of the most attractive SRM imaging techniques. However, image acquisition involves exposure of luminophores to a high power laser source over an extended period of time windows, thus SIM compatible probes must show high photostability and low bleach rates. Using SIM, the *in cellulo* effect of HOCl concentration on probe emission was then tested. As expected, live RAW 264.7 macrophage cells treated with only **SF-1** (10 µM) showed minimal intracellular fluorescence (Figure 5B.2). However, cells exposed to increasing concentrations of HOCl show a concomitant increase in probe emission.

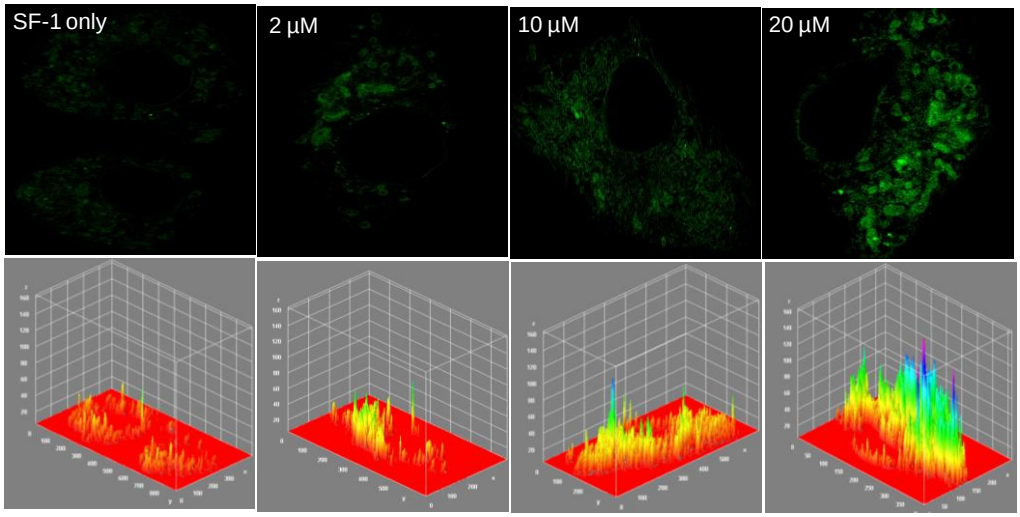

Figure 5B.2. Detection of HOCl by **SF-1**: (Externally added): SIM images and emission intensity profiles of live RAW 264.7 cells after 30 minutes exposure to increasing concentrations of HOCl.

These promising results prompted us to look at imaging endogenously generated HOCl. RAW Macrophage cells are known to generate HOCl, when they are stimulated by lipopolysaccharide (LPS).[12] Initially RAW macrophage cells were incubated with LPS (5000 ng/mL) for 24h in DMEM culture medium with 10% FBS and then further

treated with **SF-1** (10 µM) for another 30 min. After this protocol SIM images showed bright fluorescence signal from the cells (Figure 5B.3). A control experiment, where cells were treated only with **SF-1** (10 µM) was also carried out and this showed no intracellular fluorescence. We also carried out LPS dose dependent studies; again it was observed that increasing concentrations of LPS led to enhanced intracellular fluorescence from the probe in Figure 5B.3.

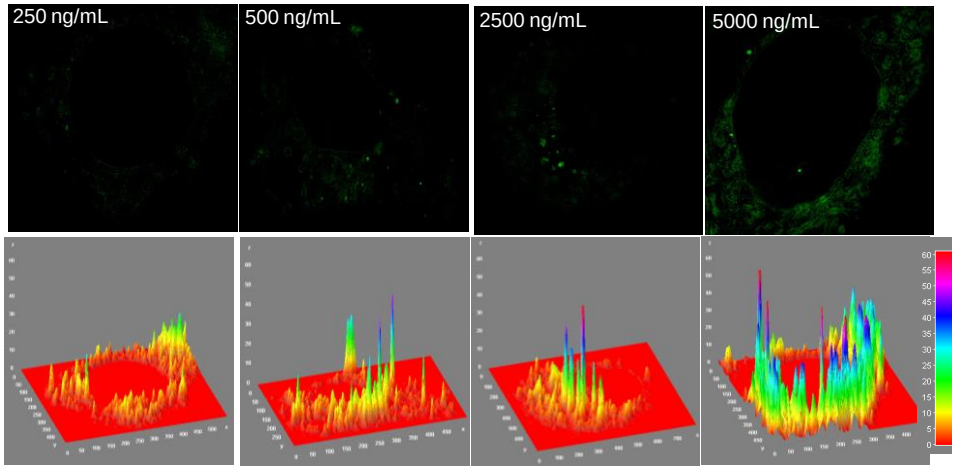

Figure 5B.3. Detection of Endogenous HOCl by **SF-1**: SIM images and emission intensity profiles of **SF-1** in presence of different concentration of LPS incubated for 24h in live RAW 264.7 cells.

It was evident from the collected wide-field and SIM images that the probe was not found to be localized in the nucleus. Rather, it appeared to be localized in specific region of the cytoplasm.

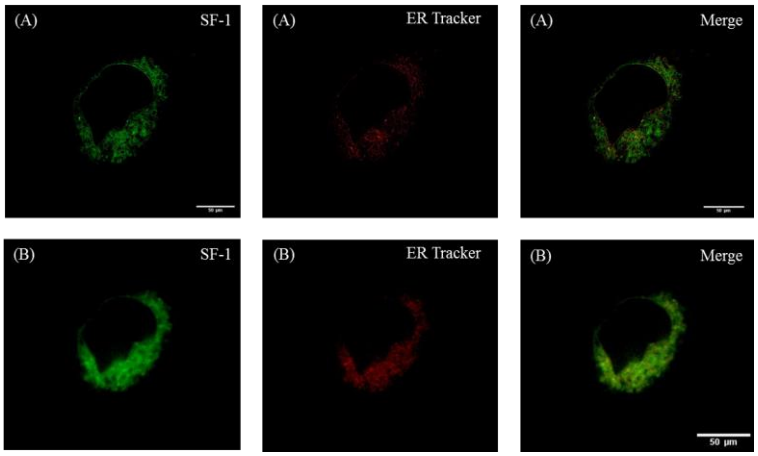

Figure 5B.4. Colocalization studies of probe **SF-1** with ER Tracker using Conventional Wide Field Fluorescence Microscopy (A) and SIM (B) using RAW 264.7 cells

Further details of its exact sub-cellular localization were explored through co-localisation with ER Tracker Green and CytoPainter Golgi Green. Initial studies involved ER Tracker as a co-stain.

SIM Images from co-staining with **SF-1 (**Figure 5B.4), show low colocalisation, with a calculated Pearson's correlation coefficient (PCC) of <0.05. Next colocalization experiments with commercially available CytoPainter Golgi Green were carried out. As the wide field images shown n Figure 5B.5. illustrate, a very close spatial correlation between probe **SF-1** and the commercial dye was observed.

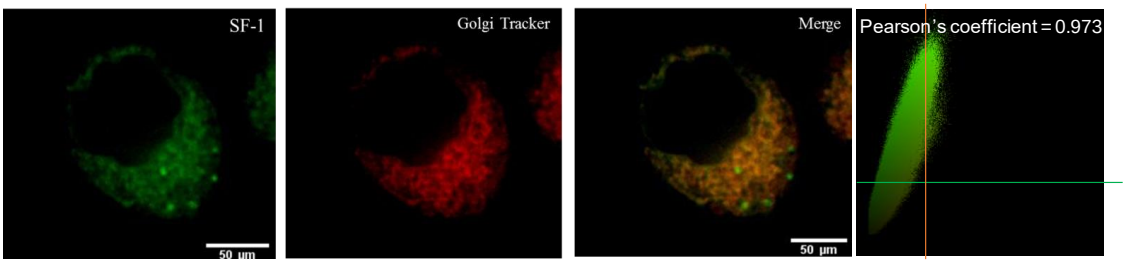

Figure 5B.5. Colocalization studies of Golgi tracker with **SF-1** in presence of HOCl in RAW 264.7 cells.

A calculated Pearson's Coefficient of 0.97 confirmed the close colocalisation of the two probes, establishing that **SF-1** is a specific probe for HOCl in the Golgi body.

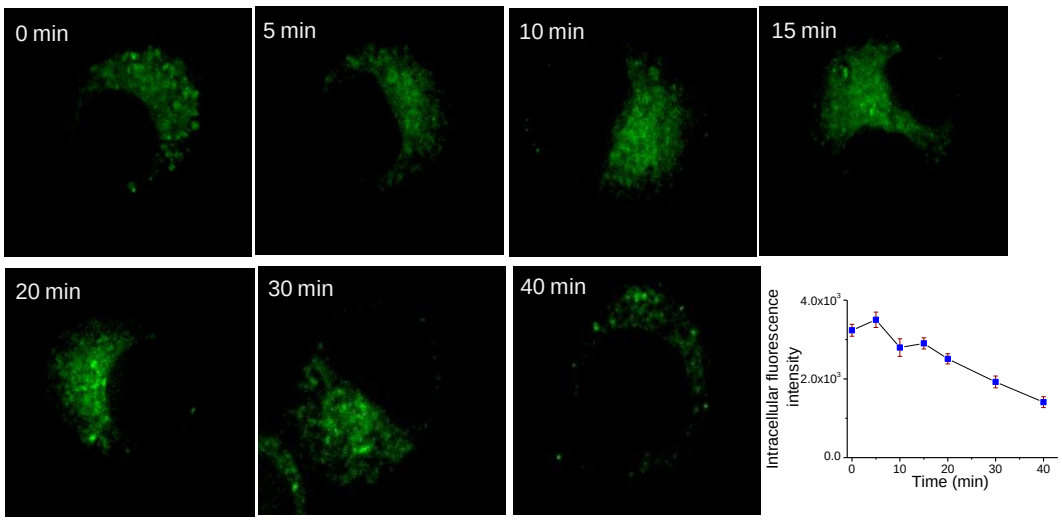

Figure 5B.6. Wide field images of RAW 264.7 cells pre-treated 40 µM HOCl, then further treated with **SF-1** (10 µM) with different time interval.

Attempts to confirm the localization of **SF-1** within the Golgi body using super resolution imaging proved to be unsuccessful as, due to photobleaching, CytoPainter Golgi Green was not suitable as a SIM probe. Clearly, in this respect, **SF-1** is superior to the commercial system.

As discussed above, HOCl is implanted to play a role as a ROS in several specific biological processes,[6] thus the stability of endogenously generated HOCl in live cells is of interest. Given the chemical and photostability of **SF-1** we investigated this question using an exogenous source of HOCl.

In this experiment, we treated cells with 40 μM of HOCl for 30 mins, then cells were treated with **SF-1** (10 μM) in different time interval like 0, 10, 20, 30, 40 min maintaining identical experimental conditions and then imaged through Wide Field Imaging – Figure 5B.6. These results confirmed internalized HOCl was detectable for up to 20 min, after that it indicated that some other biological process is happening possibly apoptosis. The Stability of HOCl for around 20 minutes indicates that the Cells can tolerate internally generated HOCl for a certain amount of time only irrespective of the concentration of the drug (in this case, **SF-1**) added. Excess accumulation of HOCl (with respect to time or concentration) is harmful for the Cells.

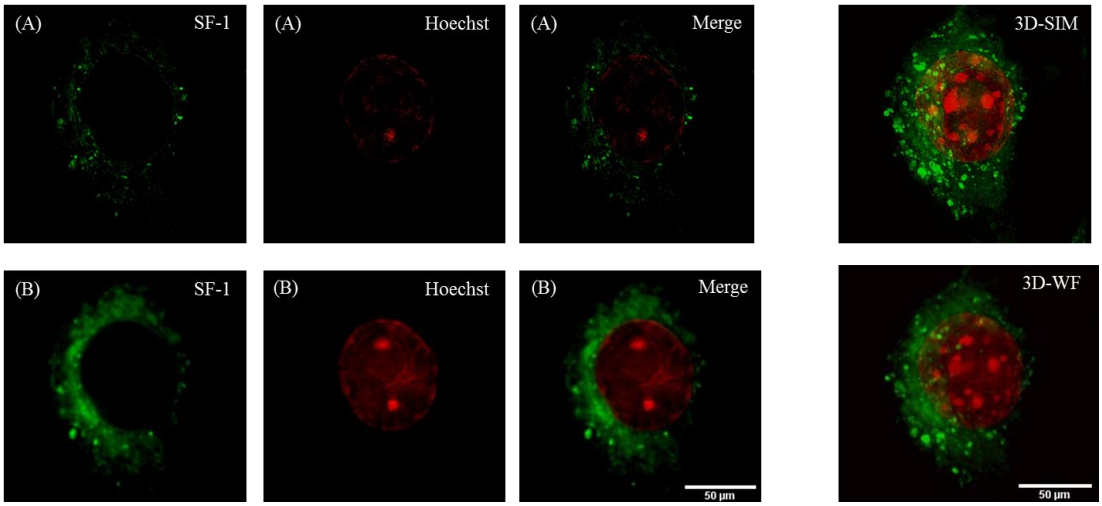

Figure 5B.7: Dual Colour Structured Illumination Microscopy images of **SF-1**

For this technique, a stain for a separate organelle with distinctly different spectral characteristics is required. In this initial study we decided to explore the use of the well known nuclear stain Hoechst 33258. Using this combination, well-defined D-SIM images could be obtained (Figure 5B.7). Indeed the brightness

and high photostability of both probes meant that they could even be used to construct 3D-SIM striking images and videos of individual cells.

5B.5. Conclusion

In Summary, **SF-1** exhibits high selectivity, excellent sensitivity and low cytotoxicity for the endogenous detection of HOCl in live cells. The probe effectively detects HOCl generated in golgi of live cells and its photophysical properties are compatible with its use in SIM and two colour SIM imaging, allowing more than one organelle to be imaged at super resolution.

5B.6. References

1. J. M. Pullar, M. C. M. Vissers and C. C. Winterbourn, *IUBMB Life,* 2000, **50**, 259.
2. S. Kenmoku, Y. Urano, H. Kojima and T. Nagano, *J. Am. Chem. Soc*., 2007, **129**, 7313.
3. C. C. Winterbourn, M. B. Hampton, J. H. Livesey and A. J. Kettle, *J. Biol. Chem*., 2006, **281**, 39860.
4. Y-ting T. Yang, M. Whiteman and Steven P. Gieseg, *Biochimica et Biophysica Acta,* 2012, **1823**, 420.
5. (a) Y. W. Yap, M. Whiteman and N. S. Cheung, *Cell Signal,* 2007, **19***,* 219; (b) Q. Xu, K.-A. Lee, S. Lee, K. M. Lee, W.-J. Lee and J. Yoon, *J. Am. Chem. Soc*., 2013*,* **135**, 9944.
6. Z. Jiang, Z. Hu, L. Zeng, W. Lu, H. Zhang, T. Li and H. Xiao, *Free Radic Biol Med*., 2011, **50**, 907.
7. (a) H. Zhu, J. Fan, J. Wang, H. Muand and X. Peng, *J. Am. Chem. Soc.,* 2014, **136**,12820; (b) L. Yuan, L. Wang, B. K. Agrawalla, S.-J. Park, H. Zhu, B. Sivaraman, J. Peng, Q.-H. Xu and Y.-T. Chang, *J. Am. Chem. Soc.,* 2015, **137**, 5930; (c) P. Panizzi, M. Nahrendorf, M. Wildgruber, P. Waterman, J.-L. Figueiredo, E. Aikawa, J. McCarthy, R. Weissleder and S. A. Hilderbrand, *J. Am. Chem. Soc*., 2009, **131**, 15739; (d) M. Ren, B. Deng, K. Zhou, X. Kong, J.-Y. Wang, G. Xu and W. Lin, *J. Mater. Chem. B,* 2016, **4**, 4739; (e) H. S. Jung, J. Han, A.-H. Lee, J. H. Lee, J.-M. Choi, H.-S. Kweon, J. H. Han, J.-H. Kim, K. M. Byun, J. H. Jung, C. Kang and J. S. Kim, *J. Am. Chem. Soc*., 2015, **137**, 3017, (f) X. Chen, K.–A. Lee, X. Ren, J.-C. Ryu, G. Kim, J.-H. Ryu, W.-J. Lee and J. Yoon, *Nature protocols,* 2016, **11**, 1219.
8. F. Ali, A. H. A., N. Taye, R. G. Gonnade, S. Chattopadhyay and A. Das, *Chem. Commun*., 2015*,* **51**, 16932.
9. J. Kim and Y. Kim, *Analyst,* 2014, **139**, 2986.
10. Handbook of Biological Confocal Microscopy, third edition, edited by James B. Pawley, *Springer Science and Business Media*, *New York* **2006**, 453.
11. M.G. Gustafsson, *J Microsc*., 2000, **198**, 82.
12. Y. Adachi, A. L. Kindzelskii, A. R. Petty, J. B. Huang, N. Maeda, S. Yotsumoto, Y. Aratani, N. Ohno and H. R. Petty, *J. Immunol*., 2006, **176**, 5033.
13. S. N. Aasen, A. Pospisilova, T. W. Eichler, J. Panek, P. Stepanek, E. Spriet, D. Jirak, K. O. Skaftnesmo, M. Hruby and F. Thorsen, *Int. J. Mol. Sci*., 2015, **16**, 21658.
14. P. A. Pellett, X. Sun, T. J. Gould, J. E. Rothman, M. Q. Xu, I. R.Jr. Correa and J. Bewersdorf, *Biomedical Optics Express,* 2011, **2**, 2364.

Conclusion of the Thesis

The thesis entitled "*Design & Synthesis of Photo-reactive Receptors for the Recognition of Analytes having Biological Significance*" describes the design and synthesis of new molecules for specific detection of analytes along with their recognition studies which have implications in various biological processes and environmental monitoring. The thesis contains overall five chapters. The first chapter is the introductory chapter, which describes significance of important analytes in biology and environment and briefly discusses about existing literature report for detection process. The aim of this thesis is to design molecules which can efficiently detect analytes having biological significances.

In chapter 2, we demonstrated a reagent that offered an option of mapping endogenous Cys in the ER region of Hct116 cells. This chapter reveals a new chemodosimetric imaging probe **ER-F** for detection of spatial and temporal distribution of Cys as well as its *in-situ* generation during the enzymatic action of aminiacylase-I in NAC in ER region of live HepG2 cells. Interference studies confirmed specificity of this reagent towards Cys among all other AAs, including Hcy, GSH and NAC. Notably this reagent could even be used for developing a modified silica strip for qualitative and quantitative estimation of Cys present in human bio-fluid like HBP without any interference from other derivatives of cysteine (like NAC, BSA).

Cr^{3+} is an important bio analyte and in chapter 3, we describe a new molecular probe $\mathbf{L_1}$, which was found to be self-assembled inside the micellar structure of TX100 in aqueous medium. This self-assembled molecular aggregate could be used as a reagent for specific detection of Cr(III) in pure aqueous buffer medium (pH 7.2) with an associated fluorescence *turn-on* response even in presence of several other competing cations. Interestingly, this reagent can be easily up-taken by cells via permeation across cell membrane of human colon cancer cells (Hct116). Further, results of the MTT assay studies confirmed that the reagent $\mathbf{L_1}$ showed insignificant toxicity towards human colon cancer cells (Hct116). Use of the rhodamine based reagent with conversion from non-luminescent spirolactam form to the strongly luminescent acyclic form on binding to Cr(III) had helped us in achieving the luminescence *ON* response. Most importantly the reagent $\mathbf{L_1}$ could be utilized as an imaging reagent for the detection of Cr^{3+} in Hct116 colon cancer cells. To the best of our knowledge, this is a rare example of a chemosensor that is completely specific towards Cr(III) and works is pure aqueous

medium with an associated fluorescence *turn on* response. Example of the luminescence *ON* based receptor for Cr(III) is not common due to the paramagnetic nature of Cr(III), which is known to efficiently quench the luminescence of the organic fluorophore to which it is bound.

In chapter 4, we discuss a novel reagent and appropriate methodology for specific detection of hydrazine in pure aq-buffer medium under physiological pH. This reagent is suitable for developing a fluorescence based assay for monitoring enzymatic release of hydrazine in solution as well as Hct116 or HepG2 cells. Importantly probe **L_2** could be used as a protective reagent against toxicity induced by the tuberculosis drug Isoniazid and may possibly useful for clinical purpose to liver related diseases. This reagent is also suitable for developing a strip type sensor for hydrazine vapour as well as for quantitative estimation of hydrazine present in physiological condition.

Reactive oxygen and nitrogen species are known to play crucial role in different biological processes. In chapter 5, we demonstrated two new super resolution probes (**ER-HNO** & **SF-1**) for the specific detection of HNO and HOCl respectively, in live cells. In chapter 5A, we have described a new reagent **ER-HNO,** which exhibits high selectivity, excellent sensitivity and low cytotoxicity in the detection of HNO. **ER-HNO** effectively detects HNO generated in the ER of live cells and its photophysical properties are compatible with its use in SIM and two colour SIM imaging, allowing more than one organelle to be imaged at super resolution. In chapter 5B, we demonstrated another super resolution probe **SF-1** that could be used for the endogenous detection of HOCl in live cells. **SF-1** effectively detects HOCl generated in golgi body of live cells and its photophysical properties are compatible with its use in SIM and two colour SIM imaging, allowing more than one organelle to be imaged at super resolution.

In a nut-shell attempt has been made to design and synthesis new molecules for specific and efficient detection of important analyte like Cysteine, Cr^{3+}, hydrazine, HNO and HOCl in aqueous medium. Changes in optical properties due to receptor analyte interaction were studied. Wherever possible, we tried to explore the application in different aspects like bio-imaging of analytes in cells and enzymatic assay, diagnostics or infield detection. We hope that reagent and strategies discussed in this thesis will certainly be useful in designing better and efficient molecules for specific detection of analytes.

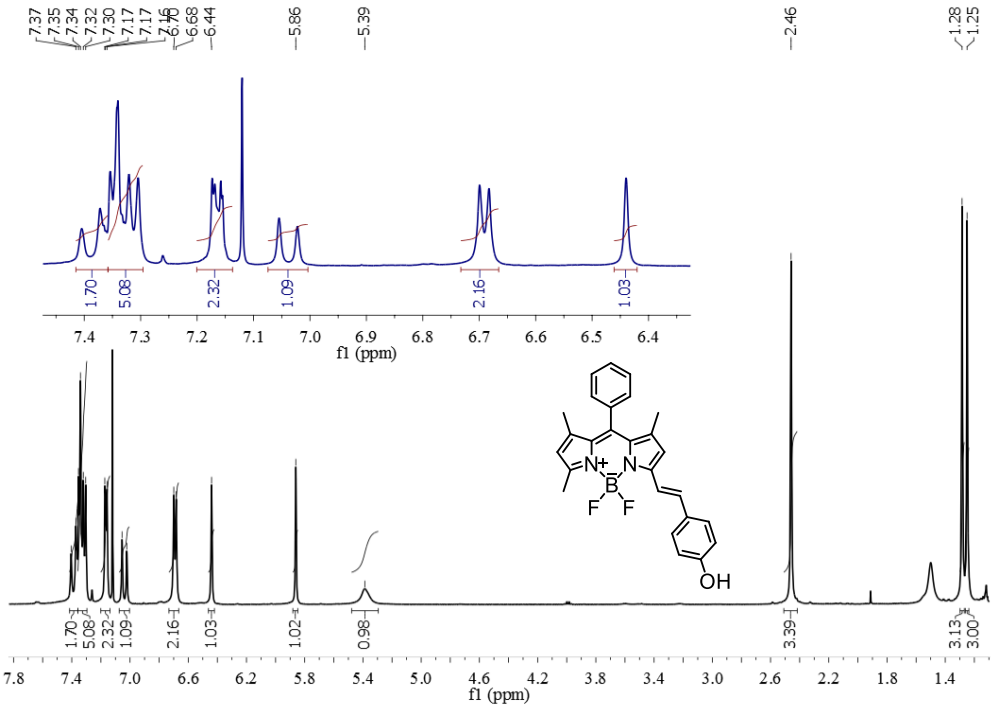

Figure 1. ^{1}H NMR spectra of ER-S recorded in $CDCl_3$.

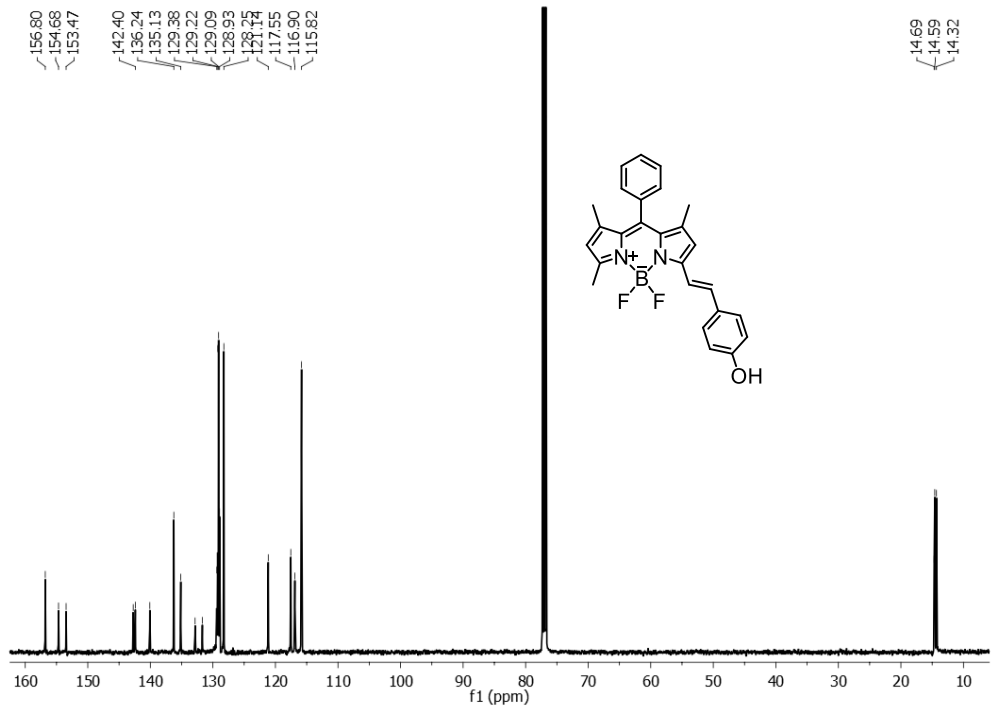

Figure 1. ^{13}C NMR spectra of ER-S recorded in CD_2Cl_2.

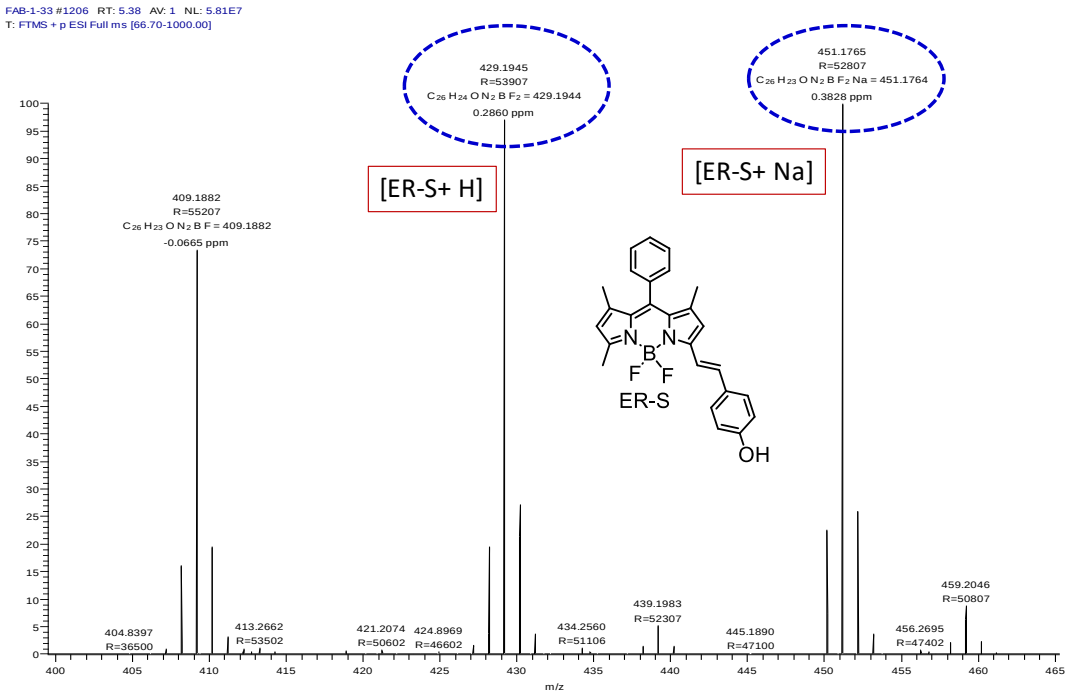

Figure 3. HR-Ms spectra of **ER-S** recorded in MeOH.

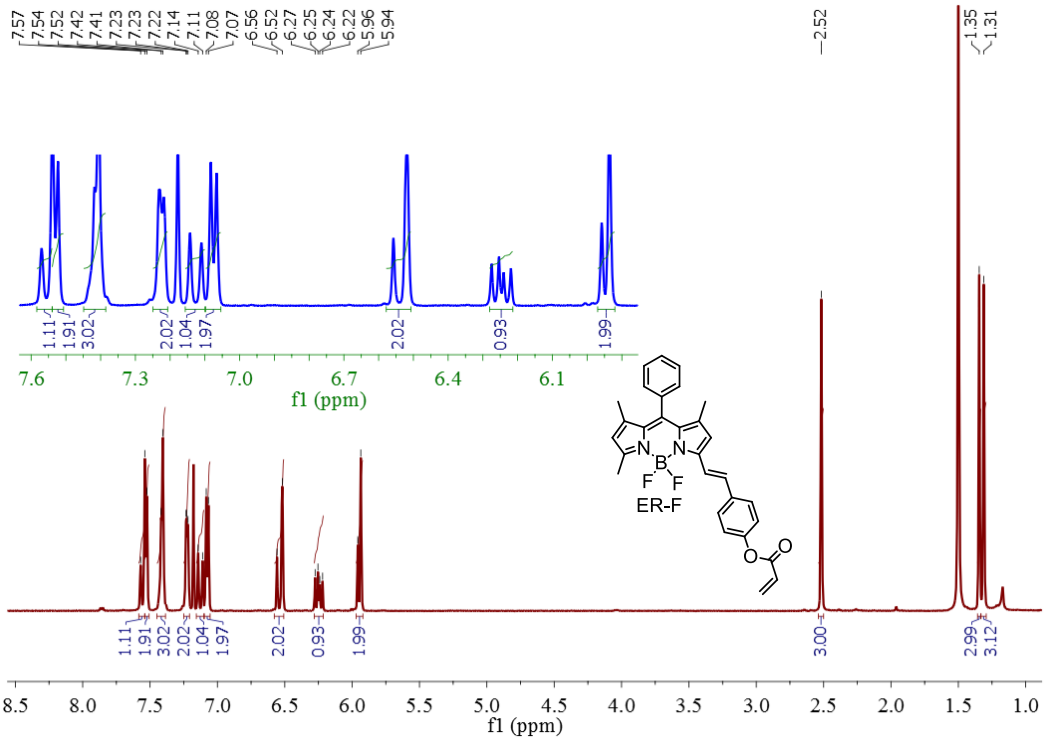

Figure 4. ^{1}H NMR spectra of **ER-F** recorded in $CDCl_3$.

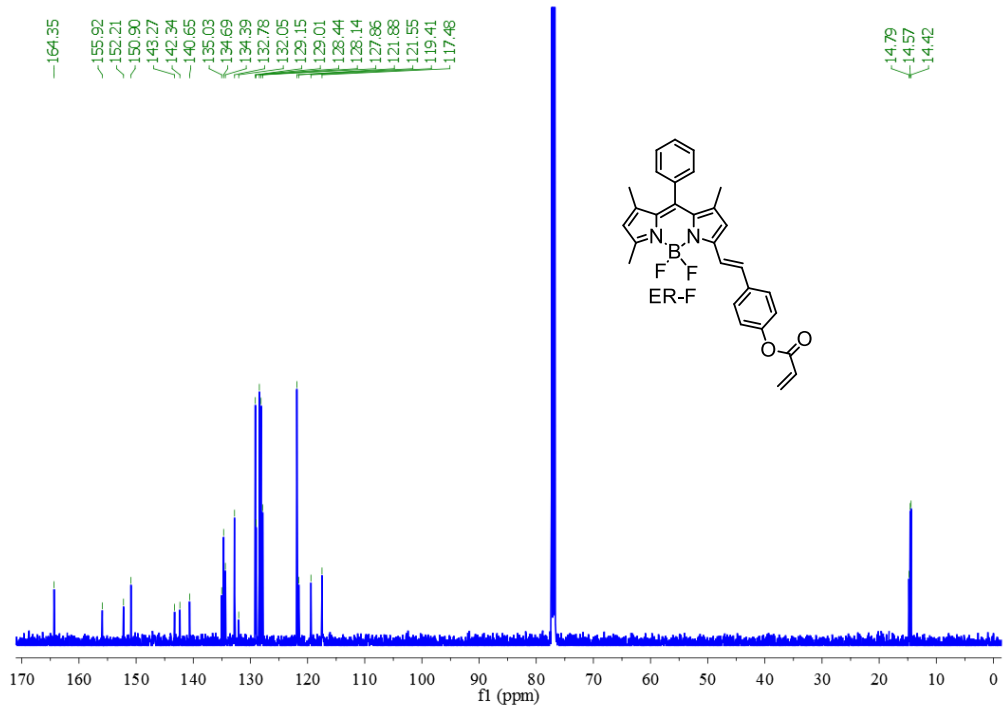

Figure 5. ^{13}C NMR spectra of **ER-F** recorded in $CDCl_3$.

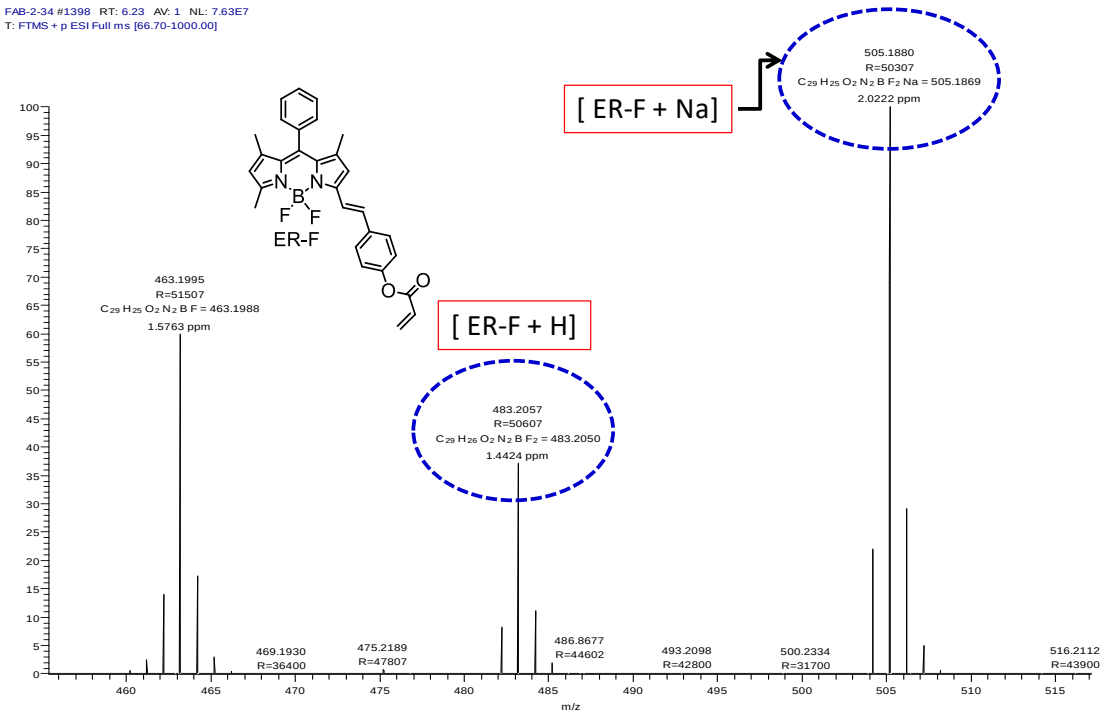

Figure 6. HR-Ms spectra of **ER-F** recorded in MeOH.

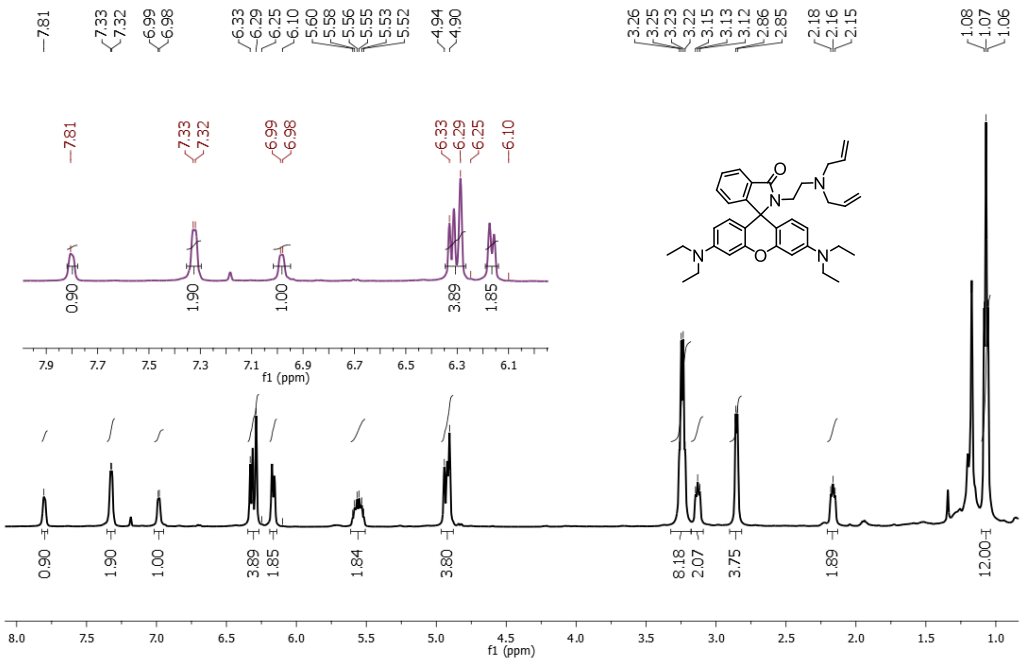

Figure 7. ^{1}H NMR spectra recorded in $CDCl_3$.

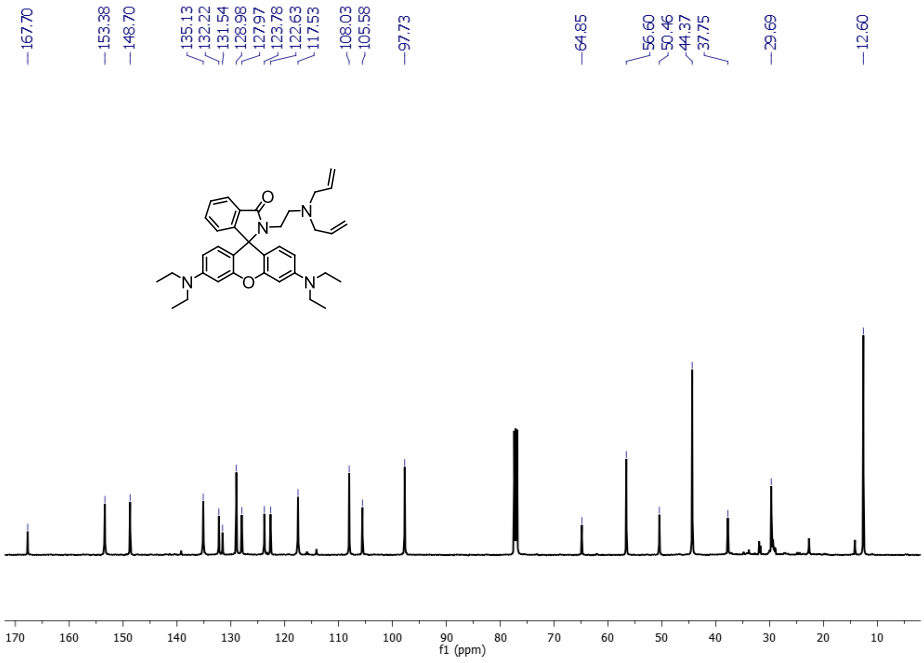

Figure 8. ^{13}C NMR spectra recorded in $CDCl_3$

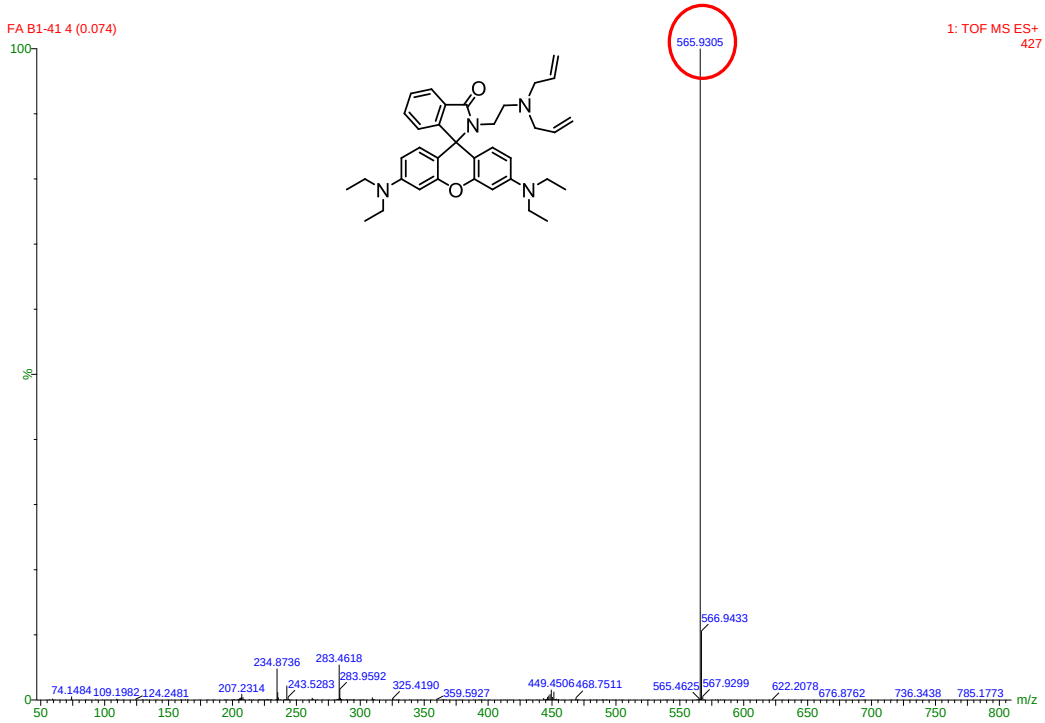

Figure 9. ESI-Ms spectra recorded in MeOH.

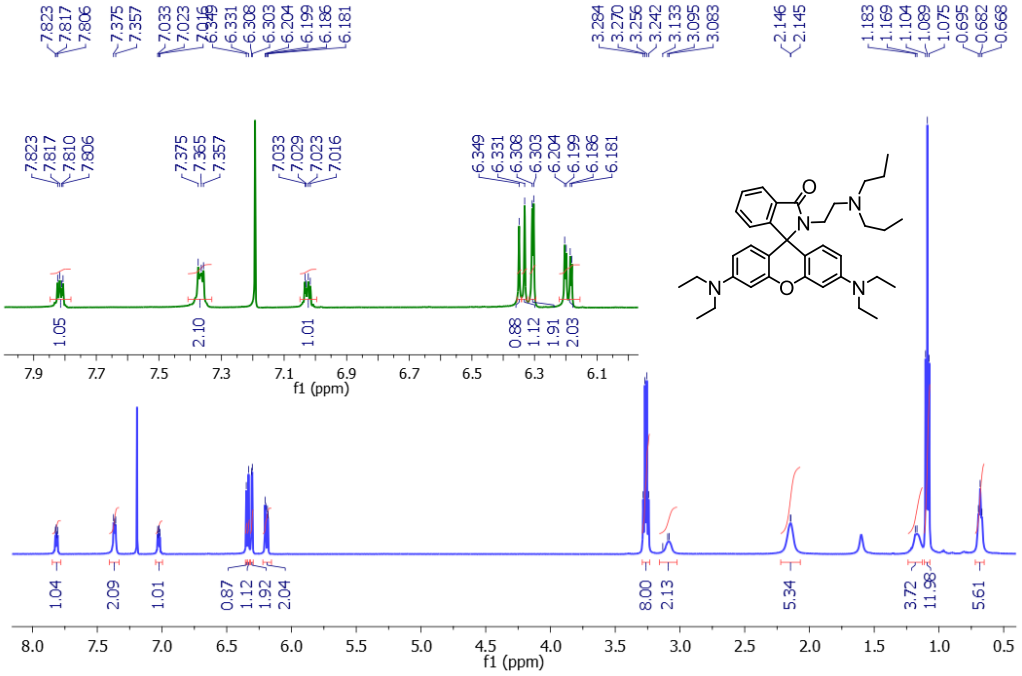

Figure 10. ^{1}H NMR spectra recorded in $CDCl_3$.

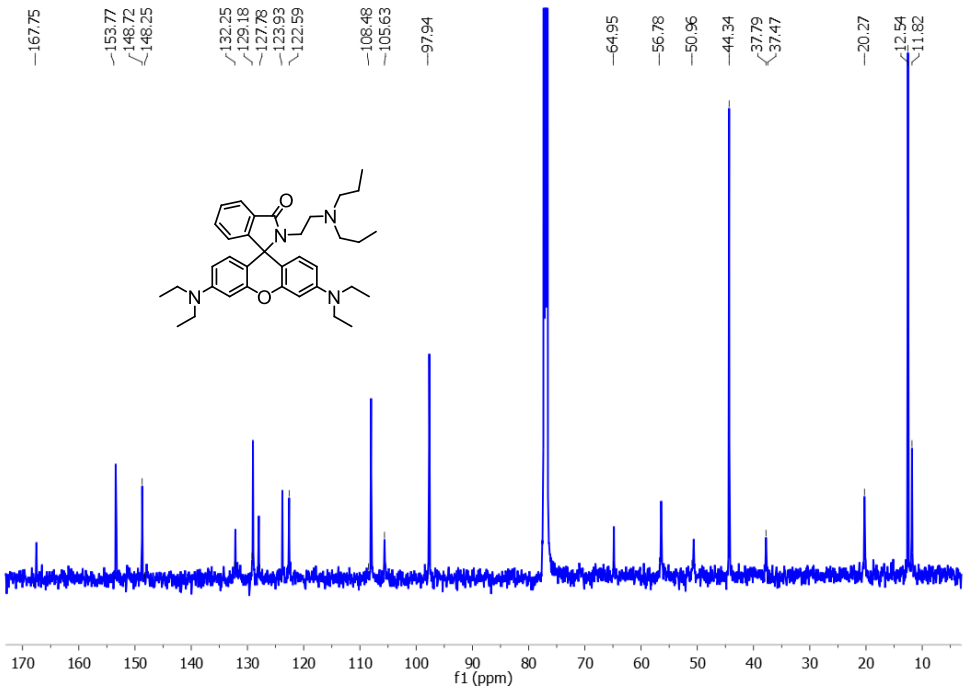

Figure 11. ^{13}C NMR spectra recorded in CD_3CN.

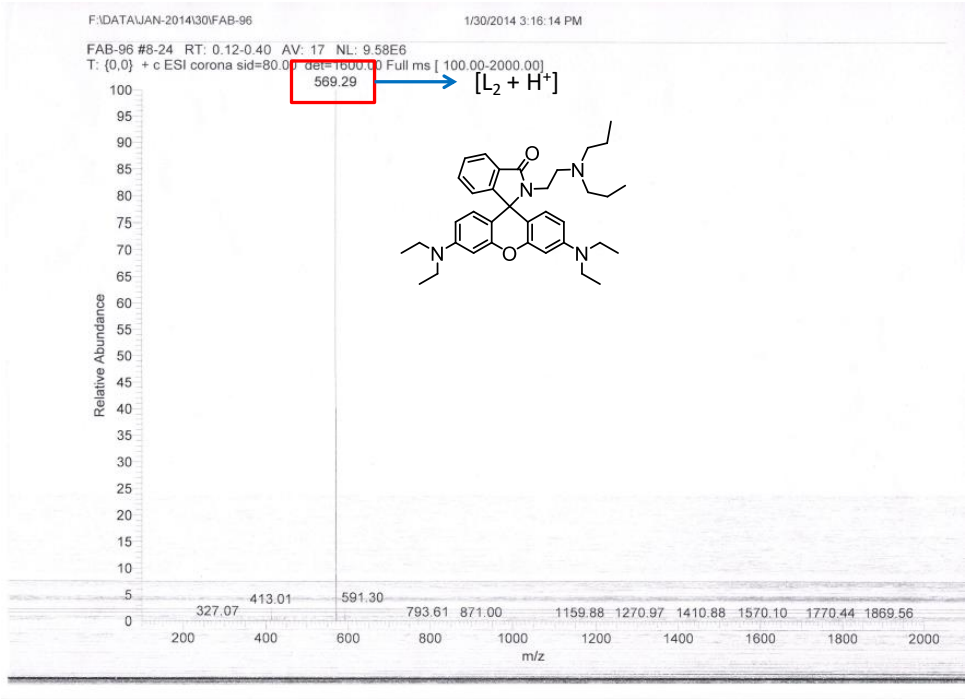

Figure 12. ESI-Ms spectra recorded in MeOH.

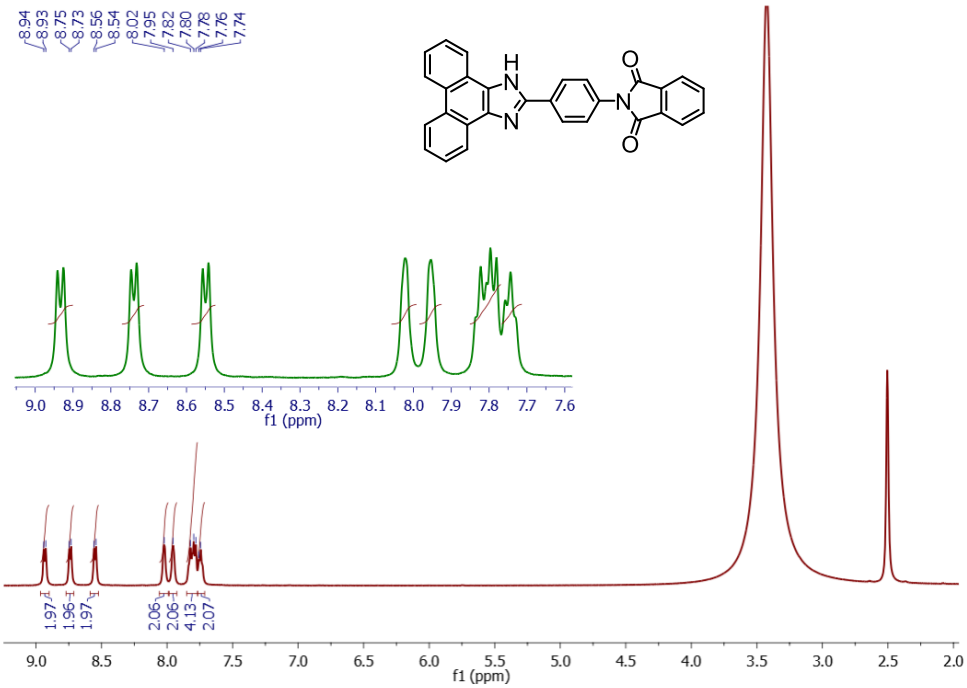

Figure 13. ^{1}H NMR spectra recorded in DMSO-d_6.

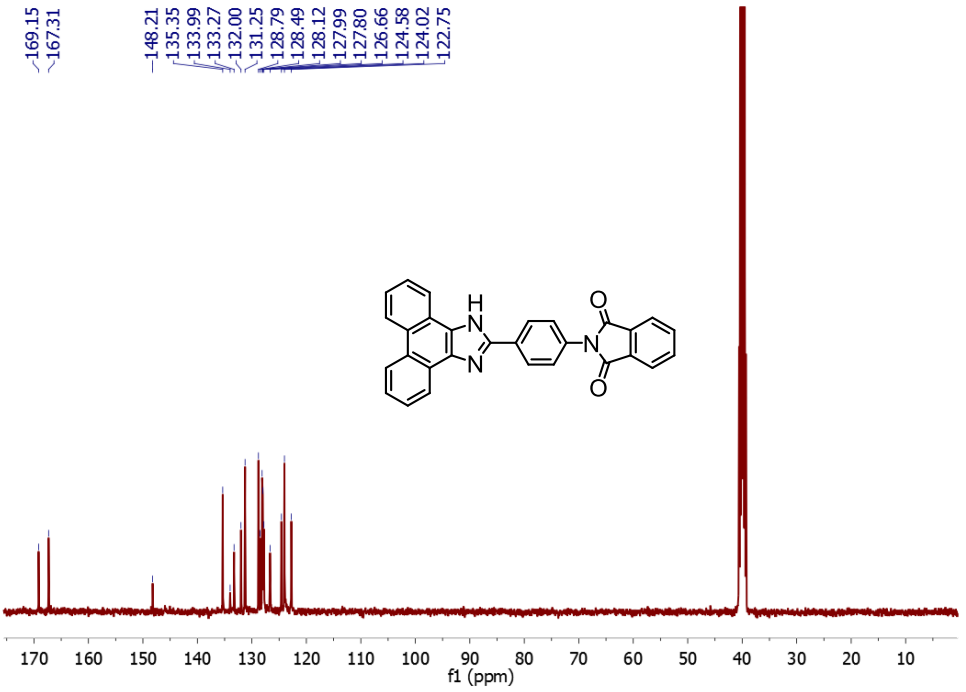

Figure 14. ^{13}C NMR spectra recorded in DMSO-d_6.

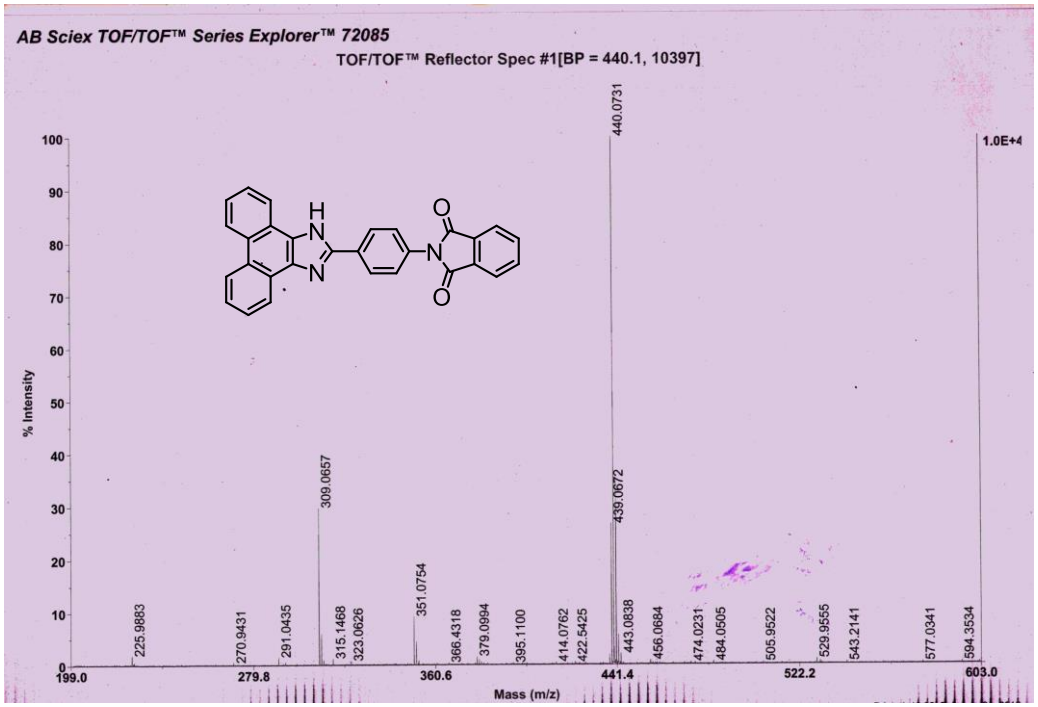

Figure 15. Maldi-Ms spectra using Dithranol (1,8-dihydroxy-9,10-dihydroanthracen-9-one) as the inert matrix using instrument AB SCIEX MALDI TOF/TOFTM 5800.

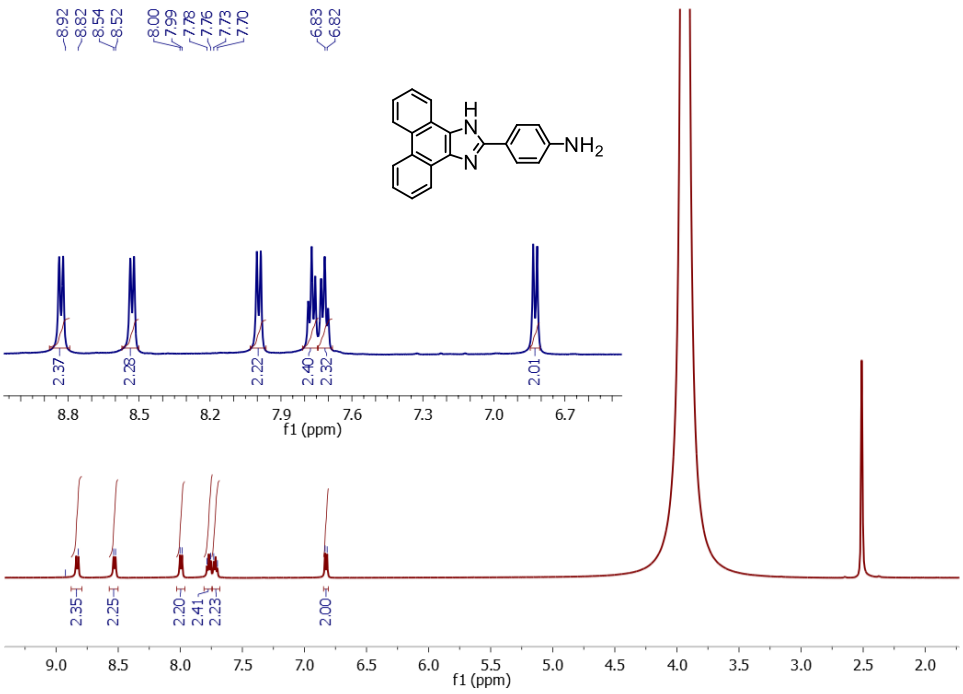

Figure 16. ^{1}H NMR spectra recorded in DMSO-d_6.

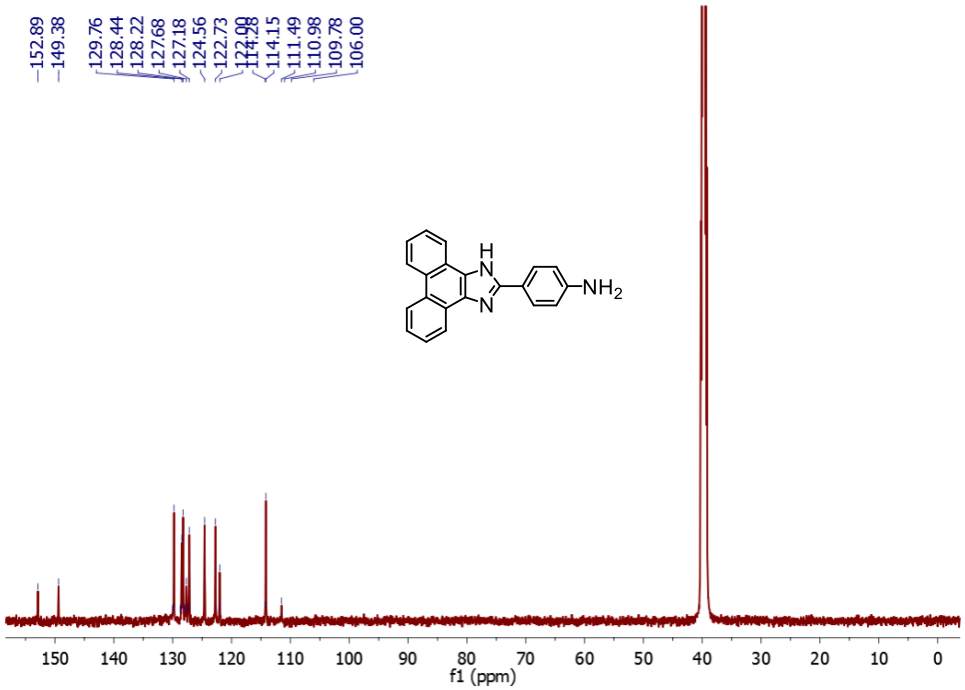

Figure 17. ^{13}C NMR spectra recorded in DMSO-d_6.

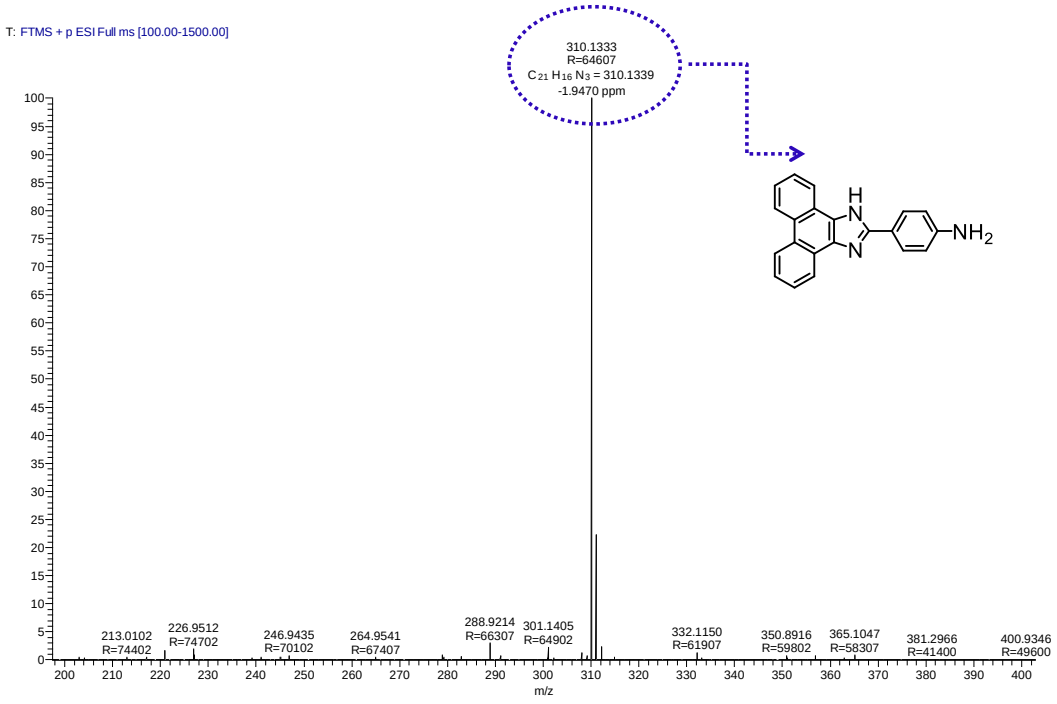

Figure 18. HRMS spectra recorded in Methanol.

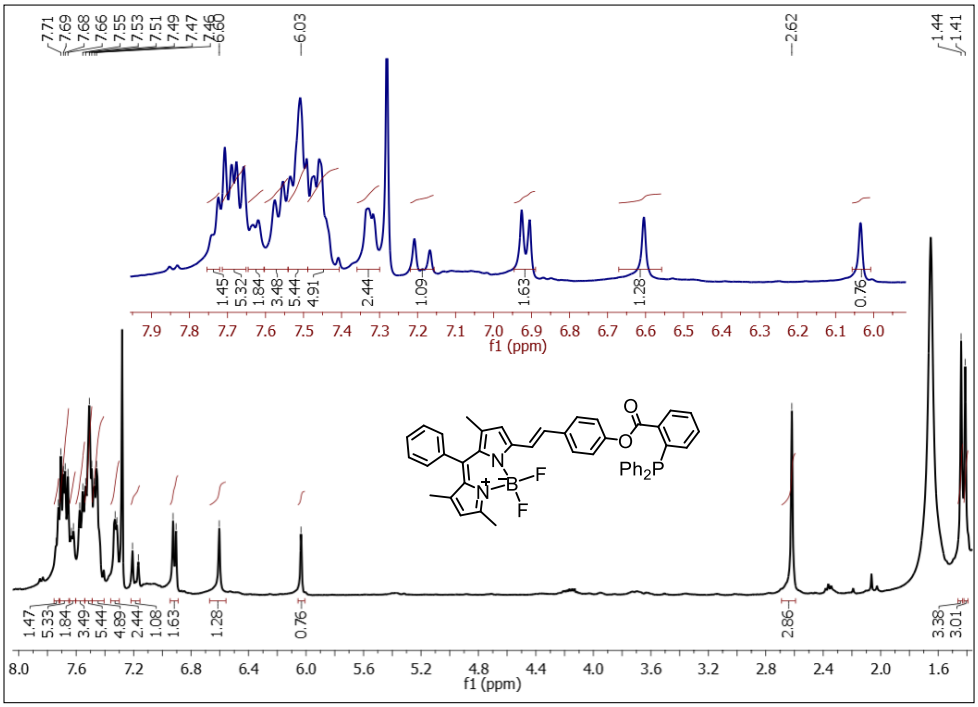

Figure 19. ^{1}H NMR spectra recorded in $CDCl_3$.

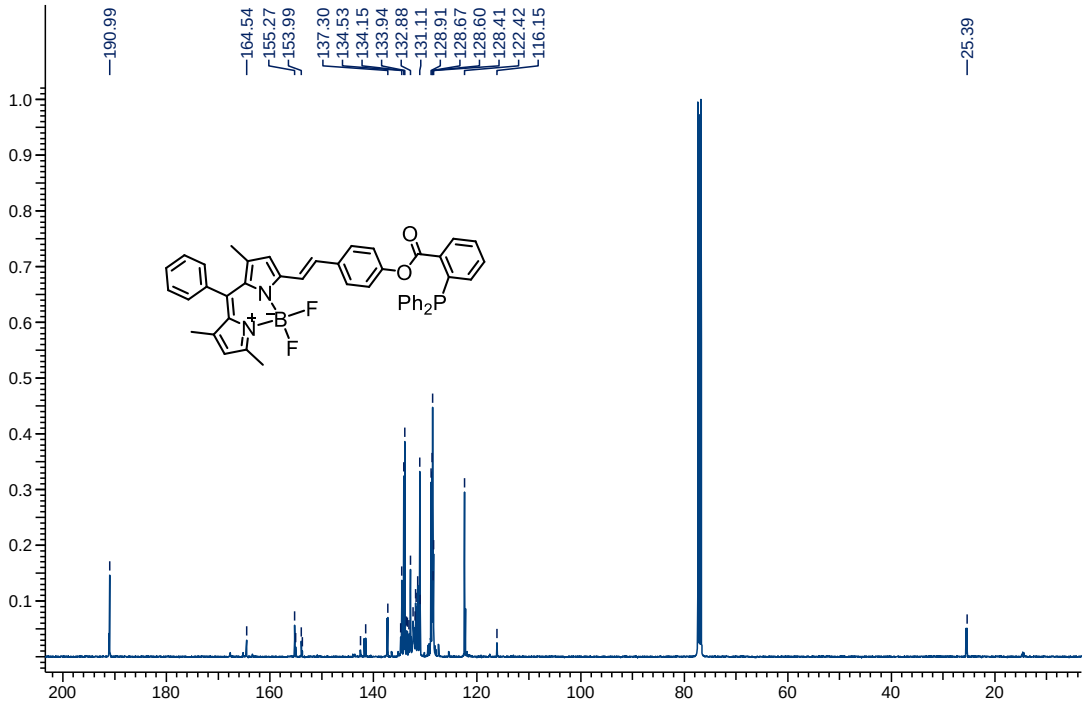

Figure 20. ^{1}H NMR spectra recorded in $CDCl_3$.

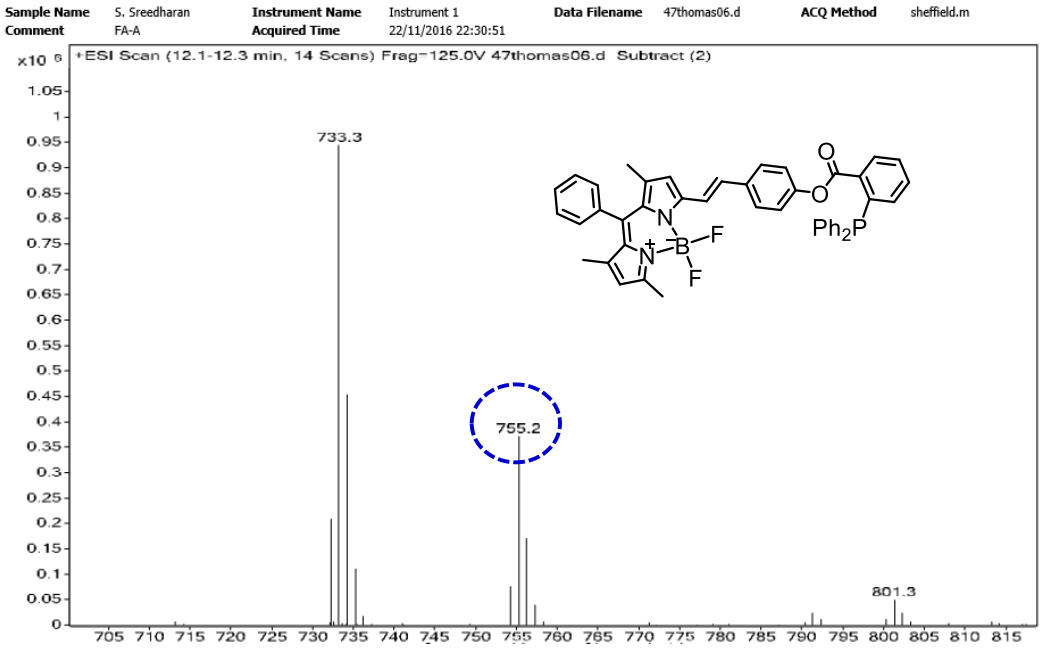

Figure 21. ESI-MS spectra recorded in Acetonitrile.

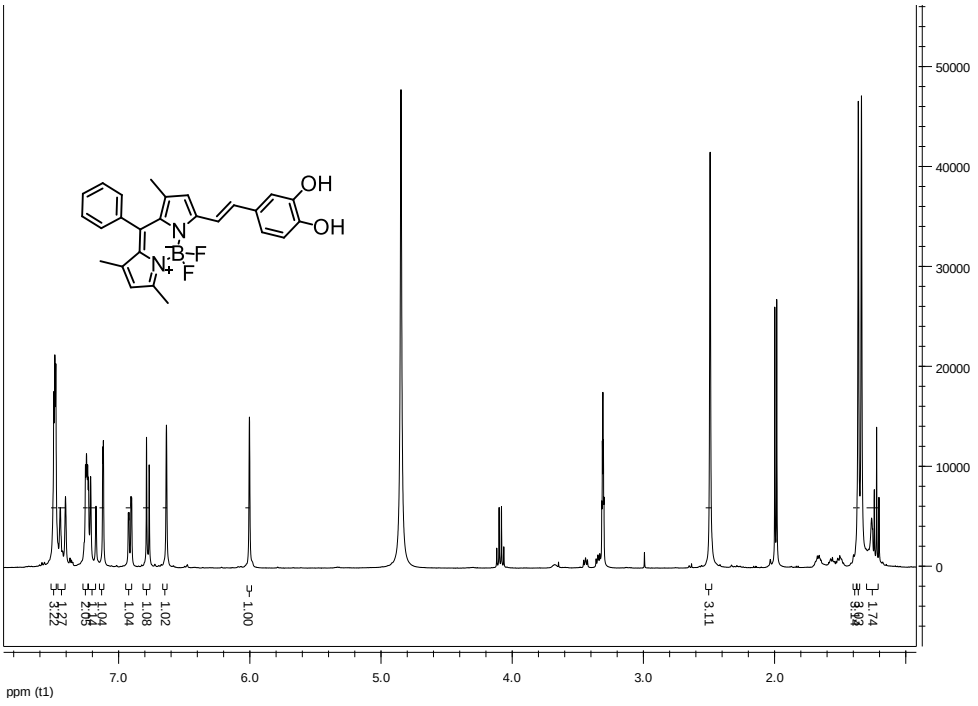

Figure 22. ^{1}H NMR spectra recorded in $CDCl_3$.

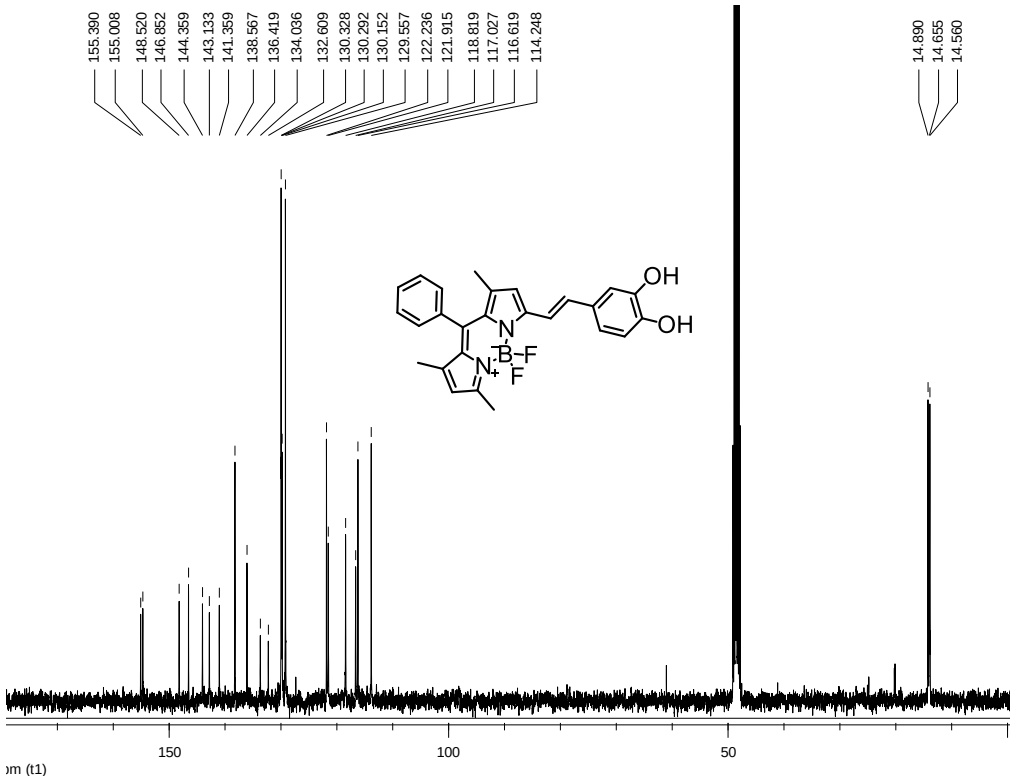

Figure 23. ^{13}C NMR spectra recorded in $CDCl_3$

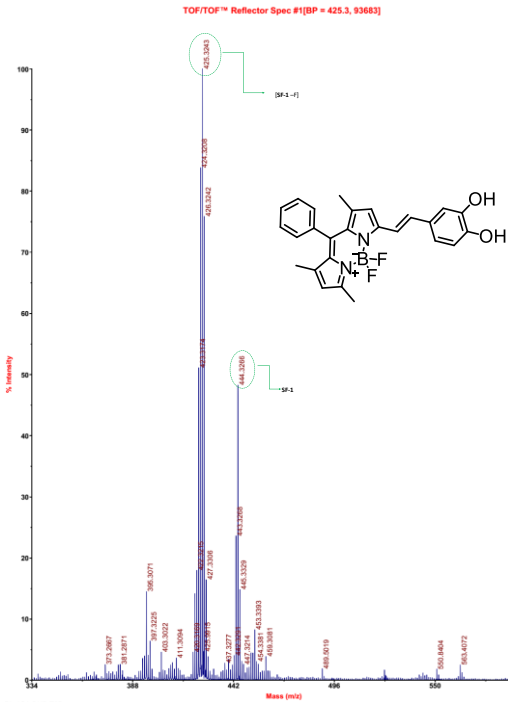

Figure 24. Maldi-Ms spectra using Dithranol (1,8-dihydroxy-9,10-dihydroanthracen-9-one) as the inert matrix using instrument AB SCIEX MALDI TOF/TOFTM 5800.

Computational details

M06-2X optimized Cartesian co-ordinate of compound 3.6B(i) and 3.6C(i) (C, N, H, O were treated with 6-31G* basis set and Cr was treated with LANL2DZ basis set in water solvent).

Compound 3.6B(i)

E = -738.09653745 a.u.

C	2.31647000	-0.14118400	0.78768600
N	1.19067300	-0.81496300	0.59759400
C	0.78723400	-2.16558200	0.26704300
H	1.07153500	-2.86964200	1.05399000
H	1.24348700	-2.49741900	-0.67242000
C	-0.73681500	-2.07078600	0.17750500
H	-1.17371800	-2.93418800	-0.33539900
H	-1.13862400	-2.01266300	1.18977700
N	-1.14227700	-0.81284900	-0.52615800
C	-0.71987000	-0.81876500	-1.96378200
C	-2.61800700	-0.57030500	-0.41345800
H	-1.46485900	-0.26556200	-2.53954300
H	-3.13033000	-1.36489500	-0.97114200
H	-2.81437000	0.38439800	-0.90837500
C	-3.08904300	-0.51445100	1.01241000
C	-3.32169400	0.63512300	1.64341600
H	-3.26406300	-1.45875700	1.52202900
H	-3.18681700	1.59362200	1.14773600
H	-3.66695500	0.65640900	2.67190200
H	-0.66965800	-1.84189900	-2.34497300
C	0.61632600	-0.10859900	-2.05014300
C	0.70682500	1.24002200	-2.13525200
H	1.52793400	-0.70079900	-2.02916000
H	1.67324500	1.73545700	-2.14986800
H	-0.17881900	1.85734600	-2.27877100
C	3.65881600	-0.73481300	1.01461400
H	4.25836900	-0.05715100	1.62325900
H	3.57709100	-1.71345200	1.48982000
H	4.14497000	-0.85625000	0.04005700
O	2.11341300	1.12384000	0.71120400
Cr	0.15786400	0.72953200	0.21253600
O	-0.33472100	2.76402600	0.24855600
H	0.36902800	3.43504400	0.27220000
H	-1.13594300	3.18942500	-0.10034200

Compound 3.6C(i)

E = -738.10440936 a.u.

C	2.13741400	-0.38250600	0.33268200
N	1.29329500	0.39937600	1.02127000
C	1.29827800	1.85239900	0.83737200
H	2.32235800	2.23896100	0.85168400
H	0.75027900	2.31742200	1.65884700
C	0.63998300	2.09243700	-0.51647100
H	0.38167700	3.14116700	-0.69329500
H	1.30737800	1.75986300	-1.31748000
N	-0.58826800	1.24892000	-0.57240300
C	-1.68919300	1.78275600	0.30445500
C	-1.02099900	0.94011300	-1.97759500
H	-2.61995000	1.79025400	-0.26335600
H	-0.72651500	1.76146500	-2.63616500
H	-2.10816100	0.85114900	-1.99051600
C	-0.39905900	-0.37958800	-2.36627400
C	-1.05978900	-1.53995900	-2.25766200
H	-2.10968700	-1.57166000	-1.96720500
H	-0.57648600	-2.48553600	-2.48399400
H	-1.45768300	2.80862200	0.59900000
C	-1.81691800	0.87671200	1.51226400
C	-2.62743600	-0.19765900	1.53992500
H	-1.21645300	1.11146200	2.39079400
H	-2.68351200	-0.82481900	2.42478700
H	-3.27843700	-0.44569300	0.70255100
C	3.57651200	-0.10533000	0.08776700
H	3.68050100	0.40678100	-0.87573200
H	3.99957600	0.51990400	0.87462000
H	4.10781800	-1.05640800	0.02700000
O	1.54921900	-1.40635300	-0.14632600
Cr	-0.26465400	-0.64692100	0.33126400
O	-0.60259100	-2.55372900	0.97513500
H	0.15654600	-3.14862200	0.82699900
H	-0.95986900	-2.76485300	1.85638000
H	0.64135200	-0.37704500	-2.68658700

List of Publications

1. **Firoj Ali**, Anila H. A., Nandaraj Taye, Devraj G. Mogare, Samit Chattopadhyay and Amitava Das, ***Chem. Commun***., 2016*, 52,* 6166—6169.

2. **Firoj Ali**, Anila H. A., Nandaraj Taye, Rajesh G. Gonnade, Samit Chattopadhyay and Amitava Das, ***Chem. Commu***, 2015*, 51,* 16932-16935.

3. **Firoj Ali**, Sukdeb Saha, Arunava Maity, Nandaraj Taye, Mrinal Kanti Si, E. Suresh, Bishwajit Ganguly, Samit Chattopadhyay and Amitava Das, ***J. Phys. Chem. B****,* 2015, 119, 13018−13026.
4. Vadde Ramu, **Firoj Ali**, Nandaraj Taye, Bikash Garai, Aftab Alam, Samit Chattopadhyay and Amitava Das, ***J. Mater. Chem. B*****,** 2015*, 3,* 7177-7185***.***
5. Upendar Reddy G., **Firoj Ali**, Nandaraj Taye, Samit Chattopadhyay and Amitava Das, ***Chem. Commun.,*** *2015*, 51, 3649-3652**.**

6. Arunava Maity, **Firoj Ali**, Hridesh Agarwalla, Bihag Anothumakkool and Amitava Das, ***Chem. Commun.,*** *2015*, 51, 2130-2133**.**

7. Anila H. A., Upendar Reddy G, **Firoj Ali**, Nandaraj Taye, Samit Chattopadhyay and Amitava Das, ***Chem. Commun.,*** *2015*, 51, 15592-15595**.**

8. Upendar Reddy G, Anila H. A., **Firoj Ali**, Nandaraj Taye, Samit Chattopadhyay and Amitava Das, ***Org. Lett.,*** *2015, 17,* 5532-5535**.**
9. Anila H A, **Firoj Ali**, Shilpi Kushwaha, Nandaraj Taye, Samit Chattopadhyay, and Amitava Das, ***Anal. Chem***., 2016, *88*, 12161 −12168**.**

10. **Firoj Ali**, Sreejesh Sreedharan, Anila H. A, Carl Smythe, Amitava Das and Jim A. Thomas. (**Communicated**)

11. **Firoj Ali**, Sunil Aute, Sreejesh Sreedharan, Anila H. A, Carl Smythe, Amitava Das and Jim A. Thomas. Manuscript to be communicated.

Book Chapter:

Book: Comprehensive Supramolecular Chemistry II: Chapter: 12617; 2016 Elsevier Inc.; Title: Specific Receptors and Imaging Reagents for Certain Heavy Metal Toxins Anila HA and **Firoj Ali** and Amitava Das, **2016** (***Just Accepted*...**)

List of Patents

1. New reagent for specific detection of Cr(III) in pure aqueous medium. *Application No:* **PCT/IN2013/000646**, *Publication No*: **2015052731A1**.

2. New reagent for specific detection of Cysteine in physiological condition as well as by using modified silica coated test strip. *Provisional Application No*: **1061/DEL/2015**, Provisional filing date: 16/4/2015.

3. Selective determination of Free Cysteine. *Provisional Application No*: **2354/DEL/2015**, Provisional filing date: 31/07/2015.

4. New reagent as scavenger of Hydrazine in drug induced cytotoxicity and in vitro enzymatic assay. *Provisional Application No*: **2332/DEL/2015**, Provisional filing date: 30/7/2015.

5. An ER-Specific reagent for monitoring HNO in biological objects. *Provisional Application No*: **201611041925**, Provisional filing date: 12/8/2016.

6. A new reagent for specific detection of HOCl in physiological condition. *Provisional Application No*: **20171106120**, Provisional filing date: 08/05/2017.

1. Presented poster at International Conference on Structural and Inorganic Chemistry hosted by CSIR- National Chemical Laboratory, IISER Pune, and SP Pune University on December 4-5, 2014, in India.

2. Presented poster at 18th CRSI-National Symposium in chemistry held from February,
2016 at IISER Mohali, Punjab, India.

3. Attended 17th CRSI-National Symposium in chemistry held from February 6-8, 2015 at CSIR-National Chemical Laboratory, Pune, India

4. Poster presentation in “National Science day for 2015” in CSIR-NCL, Pune, India. February 25-28, 2015.

5. Poster presentation in “National Science day for 2016” in CSIR-NCL, Pune, India. February 25-28, 2016.

ChemComm

COMMUNICATION

View Article Online
View Journal | View Issue

Cite this: *Chem. Commun.*, 2016, 52, 6166

Received 28th February 2016,
Accepted 29th March 2016

DOI: 10.1039/c6cc01787h

www.rsc.org/chemcomm

Specific receptor for hydrazine: mapping the *in situ* release of hydrazine in live cells and in an *in vitro* enzymatic assay†

Firoj Ali,[a] Anila H. A.,[a] Nandaraj Taye,[b] Devraj G. Mogare,[b] Samit Chattopadhyay‡*[b] and Amitava Das§*[a]

We report a new chemodosimetric reagent capable of detecting hydrazine in the presence of several other competing amine derivatives and ionic analytes of biological relevance. This reagent has been utilized for real time monitoring of *in situ* N_2H_4 release during the metabolism of a crucial tuberculosis drug, isoniazid, in live HepG2 cells. The fluorescence response of the reagent based on its specific reaction with N_2H_4 is used for developing an *in vitro* assay for aminoacylase-1.

Despite being branded as a potent carcinogen, hydrazine is widely used as a reagent in industry.[1] Further reports have confirmed that hydrazine induces hepatotoxicity, neurotoxicity and mutagenicity.[2] It is also known to cause lipid peroxidation and ROS formation, to elevate oxidative stress and leads eventually to nonspecific damage to proteins and DNA.[3,4] Owing to such adverse influences on human physiology and the environment, the United States Environmental Protection Agency (EPA) has classified hydrazine as a human carcinogen with a low threshold limit value (TLV) of 10 ppb.[5] Typically, in clinical diagnosis, hydrazine estimation is performed using capillary gas chromatography using an electron capture detector.[5b] Hydrazine has also been found to be a metabolite of an important drug, isoniazid, which has featured in the World Health Organization's (WHO's) list of essential medicines that constitute the bare minimum for a basic health system, and it is used as a first-line agent in the prevention and treatment of both latent and active tuberculosis.[5c] Hydrazine, produced *in situ*, adds to high hepatotoxicity in human physiology and adds to the severe health concern.[6,7] Accordingly, a number of hydrazine specific molecular probes have been synthesized and utilized for its detection in aqueous media and biological samples.[8] However, an example of a reagent that could be used for detection of the intracellular release of hydrazine through a biochemical transformation as well as for its efficient scavenging has eluded us to date. Such a reagent could be used for reducing the cytotoxicity induced by isoniazid. Thus, it would have serious implications for clinical diagnosis and for developing a more effective drug formulation. Considering the scope for such a reagent, we report herein a turn on luminescent molecular probe ($\mathbf{L_2}$) for the detection of hydrazine in aqueous buffer medium at physiological pH. This reagent is specific towards N_2H_4 in the presence of other possible interfering analytes, including other amines and hydrazine derivatives. We discuss the possibility of using this reagent for the detection of intracellular release of hydrazine by isoniazid through an enzymatic process caused by intracellular enzymes in live HepG2 cells. Importantly, an MTT assay reveals that the rapid and near quantitative reaction of N_2H_4 with this chemodosimetric probe is effective in lowering the cytotoxic influence of isoniazid on the live HepG2 cells. To the best of our knowledge, such an example is not available in the contemporary literature.¶

Probe $\mathbf{L_2}$ was synthesized following the methodology outlined in Scheme 1. This and the intermediate reagent ($\mathbf{L_1}$) were adequately characterized using various analytical and spectroscopic techniques (ESI).†

Reagent $\mathbf{L_2}$ showed limited solubility in a pure aqueous medium. However, in the presence of 0.4 mM (micellar concentration) of

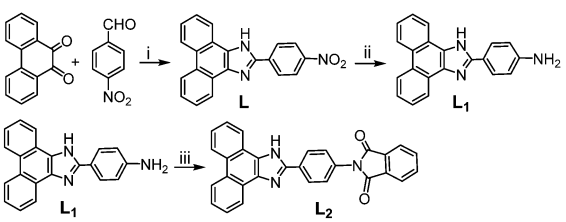

i : CH_3COONH_4 / CH_3COOH / Δ, 2h; ii : Fe/ HCl/ THF-Water mixture, 6 h;
iii : Phthalic anhydride / CH_3COOH / Δ, 24h.

Scheme 1 Synthetic route for $\mathbf{L_1}$ and $\mathbf{L_2}$.

[a] *Organic Chemistry Division, CSIR-National Chemical Laboratory, Pune-411008, India*
[b] *Chromatin and Disease Biology Lab, National Centre for Cell Science, Pune 411007, India*

† Electronic supplementary information (ESI) available. See DOI: 10.1039/c6cc01787h

‡ Present address: CSIR-Indian Institute of Chemical Biology, Kolkata: 700032, India. E-mail: samit samit@iicb.res.in.
§ Present address: CSIR-Central Salt & Marine Chemicals Research Institute, Bhavnagar 364002, Gujarat, India. E-mail: a.das@csmcri.org; Fax: +91 278 2567562.

ChemComm

COMMUNICATION

View Article Online
View Journal | View Issue

Cite this: *Chem. Commun.*, 2015, **51**, 16932

Received 4th September 2015,
Accepted 24th September 2015

DOI: 10.1039/c5cc07450a

www.rsc.org/chemcomm

A fluorescent probe for specific detection of cysteine in the lipid dense region of cells†

Firoj Ali,[a] Anila H. A.,[a] Nandaraj Taye,[b] Rajesh G. Gonnade,[c] Samit Chattopadhyay*[b] and Amitava Das*[a]

A new cysteine (Cys) specific chemodosimetric reagent (ER-F) is used in imaging of endogenous Cys localized in the lipid dense region of the live Hct116 cells and the release of Cys within HepG2 cells from a drug following a biochemical transformation. A silica surface, modified with ER-F, could be used for quantitative estimation of Cys present in aqueous solution (pH 7.2) and in a human blood plasma (HBP).

For eukaryotic cells, Endoplasmic Reticulum (ER)—a lipid dense region, plays a central role in biosynthesis of lipids and proteins.[1] Oxidized glutathione (GSH) and Cys are believed to participate in disulfide interchange reactions for an ER-resident as well as newly made proteins.[2] It has been argued that the homeostasis of the redox state in the ER depends on the flux of small disulfides, secreted together with their reduced counterparts, primarily GSH and Cys, which are being released during the process of protein disulfide bond formation.[2] Cys is the important precursor for the synthesis of GSH, which plays crucial roles in maintaining a cellular antioxidant immune system.[3] Apart from these, Cys is also involved in various biological activities like cellular detoxification and metabolism.[4,5] A nuance in Cys concentration in cells or in HBP affects crucial biological processes. For example diseases like haematopoiesis, leucocyte loss, hair depigmentation caused by a decreased Cys level,[5,6] while its elevated level is responsible for neurotoxicity, cardiovascular and Alzheimer's diseases.[7] Thus, any reagent that allows specific detection and quantification of Cys in biological fluids as well as imaging of endogenous Cys in live cells is of immense importance, as this has a direct relevance for diagnostic applications. Such a reagent is even more significant if it is capable of detecting subtle changes in Cys distribution in ER, as this would help in probing protein modification in the ER through a conversion of Cys to formylglycine.[8] Among various analytical techniques, high-performance liquid chromatography (HPLC) with post column derivatisation and a spectrophotometric assay using 5,5′-dithiobis(2-nitrobenzoic acid) (DTNB; Ellman's Reagent) are most common for estimation of Cys in bio-fluids or in protein residues.[9] Use of HPLC technique involves skilled manpower, expensive instrumentation and a time consuming analysis process, while Ellman's reagent is sensitive to O_2/OH^- and produces strongly absorbing 4-nitrothiophenolate upon reaction with various amino acids (AAs) and protein residues having sulfhydryl groups. Thus, this reagent fails to delineate between Cys from Hcy/GSH and the Cys/Hcy/GSH residue with the free –SH functionality present in a protein. Furthermore, none of these two procedures is appropriate for imaging applications. Some recent reports on chemodosimetric reagents with α,β-unsaturation reveal that such receptors fail to distinguish between Cys and the Cys residue in protein molecules having free sulfhydryl (–SH) groups.[10] Receptors that work on the cleavage of –S–S– or –alkoxy bonds, induced by –SH groups, fail to distinguish between Cys and Hcy/GSH.[11] Considering these limitations, a receptor that is specific for Cys and capable of showing instant fluorescence ON response is highly desirable. However such an example remained elusive until recently, when Peng *et al.* reported a fluorescent probe for specific detection of Cys.[12] Also Strongin *et al.* and Yoon *et al.* developed an acrylate based reagent for Cys detection.[13]

Herein, we have described a new molecular probe **ER-F** that is specific towards Cys and capable of detecting Cys localized in the lipid dense region in live Hct116 cells as well as in bio-fluids like HBP samples. Moreover, this reagent could be used for imaging the release of Cys during metabolism of the drug *N*-acetyl cysteine in live HepG2 cells and for developing a test strip based technique for quantitative estimation of Cys in HBP.

[a] *Organic Chemistry Division, CSIR-National Chemical Laboratory, Pune-411008, India. E-mail: a.das@ncl.res.in; Tel: +91 2025902385*
[b] *Chromatin and Disease Biology Lab, National Centre for Cell Science, Pune 411007, India. E-mail: samit@nccs.res.in*
[c] *Center for Materials Characterization, CSIR-National Chemical Laboratory, Pune-411008, India*

† Electronic supplementary information (ESI) available: Invention disclosure no.: 2015-INV-0021. Details of synthesis, X-ray crystal data for **ER-F**, photophysical studies, and imaging studies. CCDC 1420800. For ESI and crystallographic data in CIF or other electronic format see DOI: 10.1039/c5cc07450a

THE JOURNAL OF PHYSICAL CHEMISTRY B

Article

pubs.acs.org/JPCB

Specific Reagent for Cr(III): Imaging Cellular Uptake of Cr(III) in Hct116 Cells and Theoretical Rationalization

Firoj Ali,[†] Sukdeb Saha,[‡] Arunava Maity,[†] Nandaraj Taye,[§] Mrinal Kanti Si,[‡] E. Suresh,[‡] Bishwajit Ganguly,*[,‡] Samit Chattopadhyay,*[,§] and Amitava Das*[,†]

[†]Organic Chemistry Division, CSIR-National Chemical Laboratory, Pune, Maharashtra 411008, India

[‡]Analytical Science and Centralized Instrument Facility, CSIR-Central Salt & Marine Chemicals Research Institute, Bhavnagar, Gujarat 364002, India

[§]Chromatin and Disease Biology Lab, National Centre for Cell Science, Pune 411007, India

Supporting Information

ABSTRACT: A new rhodamine-based reagent ($\mathbf{L_1}$), trapped inside the micellar structure of biologically benign Triton-X 100, could be used for specific recognition of Cr(III) in aqueous buffer medium having physiological pH. This visible light excitable reagent on selective binding to Cr(III) resulted in a strong fluorescence *turn-on* response with a maximum at ~583 nm and tail of that luminescence band extended until 650 nm, an optical response that is desired for avoiding the cellular autofluorescence. Interference studies confirm that other metal ions do not interfere with the detection process of Cr(III) in aqueous buffer medium having pH 7.2. To examine the nature of binding of Cr(III) to $\mathbf{L_1}$, various spectroscopic studies are performed with the model reagent $\mathbf{L_2}$, which tend to support Cr(III)-η^2-olefin π-interactions involving two olefin bonds in molecular probe $\mathbf{L_1}$. Computational studies are also performed with another model reagent $\mathbf{L_M}$ to examine the possibility of such Cr(III)-η^2-olefin π-interactions. Presumably, polar functional groups of the model reagent $\mathbf{L_M}$ upon coordination to the Cr(III) center effectively reduce the formal charge on the metal ion and this is further substantiated by results of the theoretical studies. This assembly is found to be cell membrane permeable and shows insignificant toxicity toward live colon cancer cells (Hct116). Confocal laser scanning microscopic studies further revealed that the reagent $\mathbf{L_1}$ could be used as an imaging reagent for detection of cellular uptake of Cr(III) in pure aqueous buffer medium by Hct116 cells. Examples of a specific reagent for paramagnetic Cr(III) with luminescence *ON* response are scanty in the contemporary literature. This ligand design helped us in achieving the turn on response by utilizing the conversion from spirolactam to an acyclic xanthene form on coordination to Cr(III).

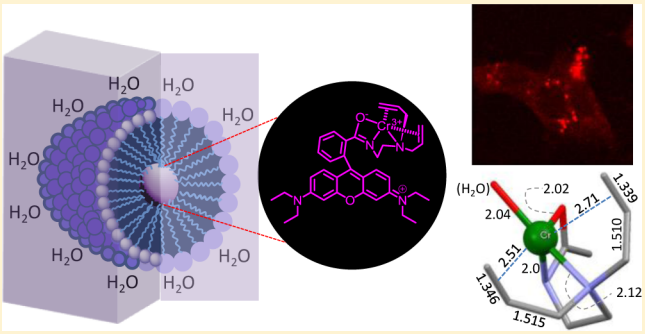

INTRODUCTION

Apart from its natural source, chromium is also added to the soil through anthropogenic and various industrial activities.[1,2] The most common form of chromium that exists in soil is Cr(III). Cr(III) is an important analyte for biological processes at the cellular level.[3] Cr(VI) is known to be reduced by intracellular reducing agents to Cr(III), which binds DNA through guanine N_7 and the adjacent phosphate backbone.[4] Studies also reveal that Cr(VI) to Cr(III) reduction takes place in certain wetland plants.[5] It is argued that this Cr(VI) to Cr(III) reduction initially happens in the fine lateral roots, while the Cr(III) subsequently translocates to leaf tissues and gets localized there presumably in the form of oxalate salt. Cr(III) is believed to be less toxic than Cr(VI) for mammalians, and for certain biological processes, Cr(III) is used as a nutrient. Cr(III) containing glucose tolerance factor is believed to be an important cofactor of insulin and catalyzes the glucose metabolism to enhance the peripheral actions of insulin. Cr(III) is also available in many common food stuffs, vegetables, and animal fats.[6,7] Deficiency of Cr(III) may cause several chronic diseases such as diabetes, cardiovascular, and nervous system disorders.[8] Though Cr(III) is known to be nontoxic, high doses may have adverse influences on human physiology.[9] Several researchers have expressed their reservations about the usefulness of Cr(III) as a long-term nutritional supplement for its possible genotoxic effects, and the general notion is that all forms of chromium, including Cr(III), are to be considered as human carcinogens.[10−12] This is especially true, as the risk to benefit ratio for usages of Cr(III) has not yet been adequately characterized.[6,7] The solubility of Cr(III) compounds is generally less in aqueous medium, and this accounts for its lower mobility and bioaccumulation.[13] Thus, there is a pressing

Received: August 4, 2015
Revised: September 21, 2015
Published: September 21, 2015

DOI: 10.1021/acs.jpcb.5b07565
J. Phys. Chem. B 2015, 119, 13018−13026

Title: Specific Reagent for Cr(III): Imaging Cellular Uptake of Cr(III) in Hct116 Cells and Theoretical Rationalization

Author: Firoj Ali, Sukdeb Saha, Arunava Maity, et al

Publication: The Journal of Physical Chemistry B

Publisher: American Chemical Society

Date: Oct 1, 2015

PERMISSION/LICENSE IS GRANTED FOR YOUR ORDER AT NO CHARGE

This type of permission/license, instead of the standard Terms & Conditions, is sent to you because no fee is being charged for your order. Please note the following:

- Permission is granted for your request in both print and electronic formats, and translations.
- If figures and/or tables were requested, they may be adapted or used in part.
- Please print this page for your records and send a copy of it to your publisher/graduate school.
- Appropriate credit for the requested material should be given as follows: "Reprinted (adapted) with permission from (COMPLETE REFERENCE CITATION). Copyright (YEAR) American Chemical Society." Insert appropriate information in place of the capitalized words.
- One-time permission is granted only for the use specified in your request. No additional uses are granted (such as derivative works or other editions). For any other uses, please submit a new request.

Title: A Cysteine-Specific Fluorescent Switch for Monitoring Oxidative Stress and Quantification of Aminoacylase-1 in Blood Serum

Author: Anila H A, Firoj Ali, Shilpi Kushwaha, et al

Publication: Analytical Chemistry

Publisher: American Chemical Society

Date: Dec 1, 2016

PERMISSION/LICENSE IS GRANTED FOR YOUR ORDER AT NO CHARGE

This type of permission/license, instead of the standard Terms & Conditions, is sent to you because no fee is being charged for your order. Please note the following:

- Permission is granted for your request in both print and electronic formats, and translations.
- If figures and/or tables were requested, they may be adapted or used in part.
- Please print this page for your records and send a copy of it to your publisher/graduate school.
- Appropriate credit for the requested material should be given as follows: "Reprinted (adapted) with permission from (COMPLETE REFERENCE CITATION). Copyright (YEAR) American Chemical Society." Insert appropriate information in place of the capitalized words.
- One-time permission is granted only for the use specified in your request. No additional uses are granted (such as derivative works or other editions). For any other uses, please submit a new request.

If credit is given to another source for the material you requested, permission must be obtained from that source.

BACK CLOSE WINDOW

Chapter: 10 Fluorescent Probes for HNO Detection
Book: The Chemistry and Biology of Nitroxyl (HNO)
Author: M. Ren,B. Dong,W. Lin
Publisher: Elsevier
Date: 2017

Permission Request Submitted

Your request is now under review.
You will be notified of the decision via email.
Please print this request for your records.

Printable details.

Order Number	501281561
Order Date	Jun 21, 2017
Licensed Content Publisher	Elsevier
Licensed Content Publication	Elsevier Books
Licensed Content Title	The Chemistry and Biology of Nitroxyl (HNO)
Licensed Content Author	M. Ren,B. Dong,W. Lin
Licensed Content Date	2017
Licensed Content Volume	n/a
Licensed Content Issue	n/a
Licensed Content Pages	18
Type of Use	reuse in a thesis/dissertation
Portion	figures/tables/illustrations
Number of figures/tables/illustrations	1
Format	both print and electronic
Are you the author of this Elsevier chapter?	No
Will you be translating?	No
Order reference number	
Original figure numbers	Figure 10.1
Title of your thesis/dissertation	Design & Synthesis of photo-reactive Receptors for the recognition of analytes having biological Significance
Expected completion date	Jul 2017
Estimated size (number of pages)	160
Elsevier VAT number	GB 494 6272 12
Requestor Location	Mr. Firoj Ali Organic Chemistry Division CSIR National Chemical Laboratory, Pune Pune-411008 Pune, Maharashtra 411008 India Attn: Mr. Firoj Ali
Total	Not Available

ORDER MORE CLOSE WINDOW

Chapter: 11 Phosphine-Based HNO Detection
Book: The Chemistry and Biology of Nitroxyl (HNO)
Author: Z. Miao,S. Bruce King
Publisher: Elsevier
Date: 2017

Permission Request Submitted

Your request is now under review.
You will be notified of the decision via email.
Please print this request for your records.

Printable details.

Order Number	501281560
Order Date	Jun 21, 2017
Licensed Content Publisher	Elsevier
Licensed Content Publication	Elsevier Books
Licensed Content Title	The Chemistry and Biology of Nitroxyl (HNO)
Licensed Content Author	Z. Miao,S. Bruce King
Licensed Content Date	2017
Licensed Content Volume	n/a
Licensed Content Issue	n/a
Licensed Content Pages	14
Type of Use	reuse in a thesis/dissertation
Portion	figures/tables/illustrations
Number of figures/tables/illustrations	1
Format	both print and electronic
Are you the author of this Elsevier chapter?	No
Will you be translating?	No
Order reference number	
Original figure numbers	Figure 10.5
Title of your thesis/dissertation	Design & Synthesis of photo-reactive Receptors for the recognition of analytes having biological Significance
Expected completion date	Jul 2017
Estimated size (number of pages)	160
Elsevier VAT number	GB 494 6272 12
Requestor Location	Mr. Firoj Ali Organic Chemistry Division CSIR National Chemical Laboratory, Pune Pune-411008 Pune, Maharashtra 411008 India Attn: Mr. Firoj Ali
Total	Not Available

ORDER MORE CLOSE WINDOW

Title: A highly selective ratiometric near-infrared fluorescent cyanine sensor for cysteine with remarkable shift and its application in bioimaging

Author: Zhiqian Guo,SeongWon Nam,Sungsu Park,Juyoung Yoon

Publication: Chemical Science

Publisher: Royal Society of Chemistry

Date: Jun 13, 2012

Order Completed

Thank you for your order.

This Agreement between Mr. Firoj Ali ("You") and Royal Society of Chemistry ("Royal Society of Chemistry") consists of your license details and the terms and conditions provided by Royal Society of Chemistry and Copyright Clearance Center.

Your confirmation email will contain your order number for future reference.

Printable details.

License Number	4133490485803
License date	Jun 21, 2017
Licensed Content Publisher	Royal Society of Chemistry
Licensed Content Publication	Chemical Science
Licensed Content Title	A highly selective ratiometric near-infrared fluorescent cyanine sensor for cysteine with remarkable shift and its application in bioimaging
Licensed Content Author	Zhiqian Guo,SeongWon Nam,Sungsu Park,Juyoung Yoon
Licensed Content Date	Jun 13, 2012
Licensed Content Volume	3
Licensed Content Issue	9
Type of Use	Thesis/Dissertation
Requestor type	non-commercial (non-profit)
Portion	figures/tables/images
Number of figures/tables/images	1
Distribution quantity	1
Format	print and electronic
Will you be translating?	no
Order reference number	
Title of the thesis/dissertation	Design & Synthesis of photo-reactive Receptors for the recognition of analytes having biological Significance
Expected completion date	Jul 2017
Estimated size	160
Requestor Location	Mr. Firoj Ali Organic Chemistry Division CSIR National Chemical Laboratory, Pune Pune-411008 Pune, Maharashtra 411008 India Attn: Mr. Firoj Ali
Billing Type	Invoice
Billing address	Mr. Firoj Ali Organic Chemistry Division CSIR National Chemical Laboratory, Pune Pune-411008

Pune, India 411008
Attn: Mr. Firoj Ali

Total 0.00 USD

ORDER MORE CLOSE WINDOW

Title: Fluorescein-Based Chromogenic and Ratiometric Fluorescence Probe for Highly Selective Detection of Cysteine and Its Application in Bioimaging

Author: Zhen-Hai Fu, Xiao Han, Yongliang Shao, et al

Publication: Analytical Chemistry

Publisher: American Chemical Society

Date: Feb 1, 2017

PERMISSION/LICENSE IS GRANTED FOR YOUR ORDER AT NO CHARGE

This type of permission/license, instead of the standard Terms & Conditions, is sent to you because no fee is being charged for your order. Please note the following:

- Permission is granted for your request in both print and electronic formats, and translations.
- If figures and/or tables were requested, they may be adapted or used in part.
- Please print this page for your records and send a copy of it to your publisher/graduate school.
- Appropriate credit for the requested material should be given as follows: "Reprinted (adapted) with permission from (COMPLETE REFERENCE CITATION). Copyright (YEAR) American Chemical Society." Insert appropriate information in place of the capitalized words.
- One-time permission is granted only for the use specified in your request. No additional uses are granted (such as derivative works or other editions). For any other uses, please submit a new request.

If credit is given to another source for the material you requested, permission must be obtained from that source.

Title: A sensitive and selective red fluorescent probe for imaging of cysteine in living cells and animals

Author: Xuezhen Song,Baoli Dong,Xiuqi Kong,Chao Wang,Nan Zhang,Weiying Lin

Publication: Analytical Methods

Publisher: Royal Society of Chemistry

Date: Feb 27, 2017

Order Completed

Thank you for your order.

This Agreement between Mr. Firoj Ali ("You") and Royal Society of Chemistry ("Royal Society of Chemistry") consists of your license details and the terms and conditions provided by Royal Society of Chemistry and Copyright Clearance Center.

Your confirmation email will contain your order number for future reference.

Printable details.

License Number	4133491105547
License date	Jun 21, 2017
Licensed Content Publisher	Royal Society of Chemistry
Licensed Content Publication	Analytical Methods
Licensed Content Title	A sensitive and selective red fluorescent probe for imaging of cysteine in living cells and animals
Licensed Content Author	Xuezhen Song,Baoli Dong,Xiuqi Kong,Chao Wang,Nan Zhang,Weiying Lin
Licensed Content Date	Feb 27, 2017
Licensed Content Volume	9
Licensed Content Issue	12
Type of Use	Thesis/Dissertation
Requestor type	non-commercial (non-profit)
Portion	figures/tables/images
Number of figures/tables/images	1
Distribution quantity	4
Format	print and electronic
Will you be translating?	no
Order reference number	
Title of the thesis/dissertation	Design & Synthesis of photo-reactive Receptors for the recognition of analytes having biological Significance
Expected completion date	Jul 2017
Estimated size	160
Requestor Location	Mr. Firoj Ali Organic Chemistry Division CSIR National Chemical Laboratory, Pune Pune-411008 Pune, Maharashtra 411008 India Attn: Mr. Firoj Ali
Billing Type	Invoice
Billing address	Mr. Firoj Ali Organic Chemistry Division CSIR National Chemical Laboratory, Pune Pune-411008 Pune, India 411008 Attn: Mr. Firoj Ali

Total	0.00 USD

ORDER MORE CLOSE WINDOW

Title:	Cysteine-Mediated Intracellular Building of Luciferin to Enhance Probe Retention and Fluorescence Turn-On
Author:	Mengmeng Zheng,Haixiao Huang,Mi Zhou,Yuqi Wang,Yan Zhang,Deju Ye,Hong-Yuan Chen
Publication:	Chemistry - A European Journal
Publisher:	John Wiley and Sons
Date:	Jun 11, 2015

Order Completed

Thank you for your order.

This Agreement between Mr. Firoj Ali ("You") and John Wiley and Sons ("John Wiley and Sons") consists of your license details and the terms and conditions provided by John Wiley and Sons and Copyright Clearance Center.

Your confirmation email will contain your order number for future reference.

Printable details.

License Number	4133500102456
License date	Jun 21, 2017
Licensed Content Publisher	John Wiley and Sons
Licensed Content Publication	Chemistry - A European Journal
Licensed Content Title	Cysteine-Mediated Intracellular Building of Luciferin to Enhance Probe Retention and Fluorescence Turn-On
Licensed Content Author	Mengmeng Zheng,Haixiao Huang,Mi Zhou,Yuqi Wang,Yan Zhang,Deju Ye,Hong-Yuan Chen
Licensed Content Date	Jun 11, 2015
Licensed Content Pages	7
Type of use	Dissertation/Thesis
Requestor type	University/Academic
Format	Print and electronic
Portion	Figure/table
Number of figures/tables	2
Original Wiley figure/table number(s)	Figure 5 & Figure 7
Will you be translating?	No
Title of your thesis / dissertation	Design & Synthesis of photo-reactive Receptors for the recognition of analytes having biological Significance
Expected completion date	Jul 2017
Expected size (number of pages)	160
Requestor Location	Mr. Firoj Ali Organic Chemistry Division CSIR National Chemical Laboratory, Pune Pune-411008 Pune, Maharashtra 411008 India Attn: Mr. Firoj Ali
Publisher Tax ID	EU826007151
Billing Type	Invoice
Billing address	Mr. Firoj Ali Organic Chemistry Division CSIR National Chemical Laboratory, Pune Pune-411008

Pune, India 411008
Attn: Mr. Firoj Ali

Total 0.00 USD

Would you like to purchase the full text of this article? If so, please continue on to the content ordering system located here: Purchase PDF

If you click on the buttons below or close this window, you will not be able to return to the content ordering system.

ORDER MORE CLOSE WINDOW

Title: Mitochondria-Targeting Chromogenic and Fluorescence Turn-On Probe for the Selective Detection of Cysteine by Caged Oxazolidinoindocyanine

Author: Chae Yeong Kim, Hyo Jin Kang, Sang J. Chung, et al

Publication: Analytical Chemistry

Publisher: American Chemical Society

Date: Jul 1, 2016

PERMISSION/LICENSE IS GRANTED FOR YOUR ORDER AT NO CHARGE

This type of permission/license, instead of the standard Terms & Conditions, is sent to you because no fee is being charged for your order. Please note the following:

- Permission is granted for your request in both print and electronic formats, and translations.
- If figures and/or tables were requested, they may be adapted or used in part.
- Please print this page for your records and send a copy of it to your publisher/graduate school.
- Appropriate credit for the requested material should be given as follows: "Reprinted (adapted) with permission from (COMPLETE REFERENCE CITATION). Copyright (YEAR) American Chemical Society." Insert appropriate information in place of the capitalized words.
- One-time permission is granted only for the use specified in your request. No additional uses are granted (such as derivative works or other editions). For any other uses, please submit a new request.

If credit is given to another source for the material you requested, permission must be obtained from that source.

BACK CLOSE WINDOW

Title: Rapid and Ratiometric Fluorescent Detection of Cysteine with High Selectivity and Sensitivity by a Simple and Readily Available Probe

Author: Yao Liu, Dehuan Yu, Shuangshuang Ding, et al

Publication: Applied Materials

Publisher: American Chemical Society

Date: Oct 1, 2014

PERMISSION/LICENSE IS GRANTED FOR YOUR ORDER AT NO CHARGE

This type of permission/license, instead of the standard Terms & Conditions, is sent to you because no fee is being charged for your order. Please note the following:

- Permission is granted for your request in both print and electronic formats, and translations.
- If figures and/or tables were requested, they may be adapted or used in part.
- Please print this page for your records and send a copy of it to your publisher/graduate school.
- Appropriate credit for the requested material should be given as follows: "Reprinted (adapted) with permission from (COMPLETE REFERENCE CITATION). Copyright (YEAR) American Chemical Society." Insert appropriate information in place of the capitalized words.
- One-time permission is granted only for the use specified in your request. No additional uses are granted (such as derivative works or other editions). For any other uses, please submit a new request.

If credit is given to another source for the material you requested, permission must be obtained from that source.

Title: Mitochondria-Targeted Near-Infrared Fluorescent Off–On Probe for Selective Detection of Cysteine in Living Cells and in Vivo

Author: Chunmiao Han, Huiran Yang, Min Chen, et al

Publication: Applied Materials

Publisher: American Chemical Society

Date: Dec 1, 2015

PERMISSION/LICENSE IS GRANTED FOR YOUR ORDER AT NO CHARGE

This type of permission/license, instead of the standard Terms & Conditions, is sent to you because no fee is being charged for your order. Please note the following:

- Permission is granted for your request in both print and electronic formats, and translations.
- If figures and/or tables were requested, they may be adapted or used in part.
- Please print this page for your records and send a copy of it to your publisher/graduate school.
- Appropriate credit for the requested material should be given as follows: "Reprinted (adapted) with permission from (COMPLETE REFERENCE CITATION). Copyright (YEAR) American Chemical Society." Insert appropriate information in place of the capitalized words.
- One-time permission is granted only for the use specified in your request. No additional uses are granted (such as derivative works or other editions). For any other uses, please submit a new request.

If credit is given to another source for the material you requested, permission must be obtained from that source.

Title: Near-Infrared and Naked-Eye Fluorescence Probe for Direct and Highly Selective Detection of Cysteine and Its Application in Living Cells

Author: Jianjian Zhang, Jianxi Wang, Jiting Liu, et al

Publication: Analytical Chemistry

Publisher: American Chemical Society

Date: May 1, 2015

PERMISSION/LICENSE IS GRANTED FOR YOUR ORDER AT NO CHARGE

This type of permission/license, instead of the standard Terms & Conditions, is sent to you because no fee is being charged for your order. Please note the following:

- Permission is granted for your request in both print and electronic formats, and translations.
- If figures and/or tables were requested, they may be adapted or used in part.
- Please print this page for your records and send a copy of it to your publisher/graduate school.
- Appropriate credit for the requested material should be given as follows: "Reprinted (adapted) with permission from (COMPLETE REFERENCE CITATION). Copyright (YEAR) American Chemical Society." Insert appropriate information in place of the capitalized words.
- One-time permission is granted only for the use specified in your request. No additional uses are granted (such as derivative works or other editions). For any other uses, please submit a new request.

If credit is given to another source for the material you requested, permission must be obtained from that source.

BACK CLOSE WINDOW

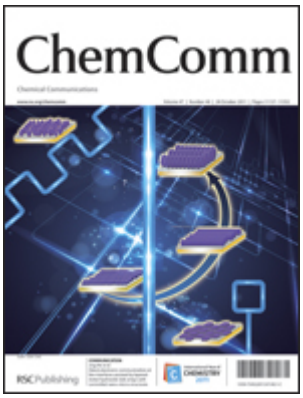

Title: Highly selective two-photon imaging of cysteine in cancerous cells and tissues

Author: Yun Hak Lee,Wen Xiu Ren,Jiyou Han,Kyoung Sunwoo,Ja-Yun Lim,Jong-Hoon Kim,Jong Seung Kim

Publication: Chemical Communications (Cambridge)

Publisher: Royal Society of Chemistry

Date: Jul 31, 2015

Order Completed

Thank you for your order.

This Agreement between Mr. Firoj Ali ("You") and Royal Society of Chemistry ("Royal Society of Chemistry") consists of your license details and the terms and conditions provided by Royal Society of Chemistry and Copyright Clearance Center.

Your confirmation email will contain your order number for future reference.

Printable details.

License Number	4133501339027
License date	Jun 21, 2017
Licensed Content Publisher	Royal Society of Chemistry
Licensed Content Publication	Chemical Communications (Cambridge)
Licensed Content Title	Highly selective two-photon imaging of cysteine in cancerous cells and tissues
Licensed Content Author	Yun Hak Lee,Wen Xiu Ren,Jiyou Han,Kyoung Sunwoo,Ja-Yun Lim,Jong-Hoon Kim,Jong Seung Kim
Licensed Content Date	Jul 31, 2015
Licensed Content Volume	51
Licensed Content Issue	76
Type of Use	Thesis/Dissertation
Requestor type	non-commercial (non-profit)
Portion	figures/tables/images
Number of figures/tables/images	2
Distribution quantity	4
Format	print and electronic
Will you be translating?	no
Order reference number	
Title of the thesis/dissertation	Design & Synthesis of photo-reactive Receptors for the recognition of analytes having biological Significance
Expected completion date	Jul 2017
Estimated size	160
Requestor Location	Mr. Firoj Ali Organic Chemistry Division CSIR National Chemical Laboratory, Pune Pune-411008 Pune, Maharashtra 411008 India Attn: Mr. Firoj Ali
Billing Type	Invoice
Billing address	Mr. Firoj Ali Organic Chemistry Division CSIR National Chemical Laboratory, Pune Pune-411008

Pune, India 411008
Attn: Mr. Firoj Ali

Total 0.00 USD

ORDER MORE CLOSE WINDOW

Title: Highly Selective Two-Photon Fluorescent Probe for Ratiometric Sensing and Imaging Cysteine in Mitochondria

Author: Weifen Niu, Lei Guo, Yinhui Li, et al

Publication: Analytical Chemistry

Publisher: American Chemical Society

Date: Feb 1, 2016

PERMISSION/LICENSE IS GRANTED FOR YOUR ORDER AT NO CHARGE

This type of permission/license, instead of the standard Terms & Conditions, is sent to you because no fee is being charged for your order. Please note the following:

- Permission is granted for your request in both print and electronic formats, and translations.
- If figures and/or tables were requested, they may be adapted or used in part.
- Please print this page for your records and send a copy of it to your publisher/graduate school.
- Appropriate credit for the requested material should be given as follows: "Reprinted (adapted) with permission from (COMPLETE REFERENCE CITATION). Copyright (YEAR) American Chemical Society." Insert appropriate information in place of the capitalized words.
- One-time permission is granted only for the use specified in your request. No additional uses are granted (such as derivative works or other editions). For any other uses, please submit a new request.

If credit is given to another source for the material you requested, permission must be obtained from that source.

Title: Two-Photon Near Infrared Fluorescent Turn-On Probe Toward Cysteine and Its Imaging Applications

Author: Junfeng Wang, Bin Li, Weiyu Zhao, et al

Publication: ACS Sensors

Publisher: American Chemical Society

Date: Jul 1, 2016

PERMISSION/LICENSE IS GRANTED FOR YOUR ORDER AT NO CHARGE

This type of permission/license, instead of the standard Terms & Conditions, is sent to you because no fee is being charged for your order. Please note the following:

- Permission is granted for your request in both print and electronic formats, and translations.
- If figures and/or tables were requested, they may be adapted or used in part.
- Please print this page for your records and send a copy of it to your publisher/graduate school.
- Appropriate credit for the requested material should be given as follows: "Reprinted (adapted) with permission from (COMPLETE REFERENCE CITATION). Copyright (YEAR) American Chemical Society." Insert appropriate information in place of the capitalized words.
- One-time permission is granted only for the use specified in your request. No additional uses are granted (such as derivative works or other editions). For any other uses, please submit a new request.

If credit is given to another source for the material you requested, permission must be obtained from that source.

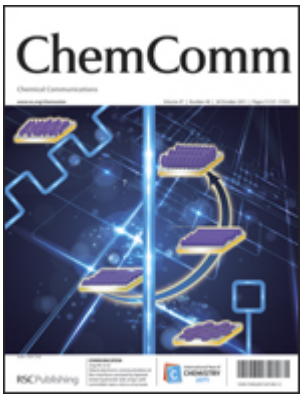

Title: A fluorescent chemodosimeter specific for cysteine: effective discrimination of cysteine from homocysteine

Author: Honglin Li,Jiangli Fan,Jingyun Wang,Maozhong Tian,Jianjun Du,Shiguo Sun,Pingping Sun,Xiaojun Peng

Publication: Chemical Communications (Cambridge)

Publisher: Royal Society of Chemistry

Date: Aug 20, 2009

Order Completed

Thank you for your order.

This Agreement between Mr. Firoj Ali ("You") and Royal Society of Chemistry ("Royal Society of Chemistry") consists of your license details and the terms and conditions provided by Royal Society of Chemistry and Copyright Clearance Center.

Your confirmation email will contain your order number for future reference.

Printable details.

License Number	4133510308749
License date	Jun 21, 2017
Licensed Content Publisher	Royal Society of Chemistry
Licensed Content Publication	Chemical Communications (Cambridge)
Licensed Content Title	A fluorescent chemodosimeter specific for cysteine: effective discrimination of cysteine from homocysteine
Licensed Content Author	Honglin Li,Jiangli Fan,Jingyun Wang,Maozhong Tian,Jianjun Du,Shiguo Sun,Pingping Sun,Xiaojun Peng
Licensed Content Date	Aug 20, 2009
Licensed Content Issue	39
Type of Use	Thesis/Dissertation
Requestor type	non-commercial (non-profit)
Portion	figures/tables/images
Number of figures/tables/images	1
Distribution quantity	4
Format	print and electronic
Will you be translating?	no
Order reference number	
Title of the thesis/dissertation	Design & Synthesis of photo-reactive Receptors for the recognition of analytes having biological Significance
Expected completion date	Jul 2017
Estimated size	160
Requestor Location	Mr. Firoj Ali Organic Chemistry Division CSIR National Chemical Laboratory, Pune Pune-411008 Pune, Maharashtra 411008 India Attn: Mr. Firoj Ali
Billing Type	Invoice
Billing address	Mr. Firoj Ali Organic Chemistry Division CSIR National Chemical Laboratory, Pune Pune-411008

Pune, India 411008
Attn: Mr. Firoj Ali

Total 0.00 USD

ORDER MORE CLOSE WINDOW

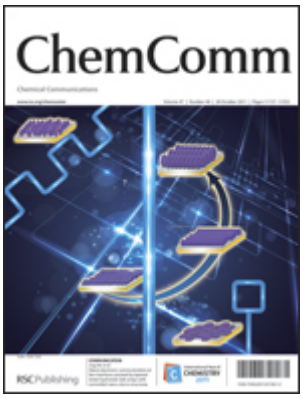

Title: A ratiometric fluorescent probe for specific detection of cysteine over homocysteine and glutathione based on the drastic distinction in the kinetic profiles

Author: Lin Yuan,Weiying Lin,Yueting Yang

Publication: Chemical Communications (Cambridge)

Publisher: Royal Society of Chemistry

Date: Apr 18, 2011

Order Completed

Thank you for your order.

This Agreement between Mr. Firoj Ali ("You") and Royal Society of Chemistry ("Royal Society of Chemistry") consists of your license details and the terms and conditions provided by Royal Society of Chemistry and Copyright Clearance Center.

Your confirmation email will contain your order number for future reference.

Printable details.

License Number	4133510512605
License date	Jun 21, 2017
Licensed Content Publisher	Royal Society of Chemistry
Licensed Content Publication	Chemical Communications (Cambridge)
Licensed Content Title	A ratiometric fluorescent probe for specific detection of cysteine over homocysteine and glutathione based on the drastic distinction in the kinetic profiles
Licensed Content Author	Lin Yuan,Weiying Lin,Yueting Yang
Licensed Content Date	Apr 18, 2011
Licensed Content Volume	47
Licensed Content Issue	22
Type of Use	Thesis/Dissertation
Requestor type	non-commercial (non-profit)
Portion	figures/tables/images
Number of figures/tables/images	2
Distribution quantity	4
Format	print and electronic
Will you be translating?	no
Order reference number	
Title of the thesis/dissertation	Design & Synthesis of photo-reactive Receptors for the recognition of analytes having biological Significance
Expected completion date	Jul 2017
Estimated size	160
Requestor Location	Mr. Firoj Ali Organic Chemistry Division CSIR National Chemical Laboratory, Pune Pune-411008 Pune, Maharashtra 411008 India Attn: Mr. Firoj Ali
Billing Type	Invoice
Billing address	Mr. Firoj Ali Organic Chemistry Division CSIR National Chemical Laboratory, Pune Pune-411008

Pune, India 411008
Attn: Mr. Firoj Ali

Total 0.00 USD

ORDER MORE CLOSE WINDOW

Title:	A cysteine-selective fluorescent probe for the cellular detection of cysteine
Author:	Hyo Sung Jung,Ji Hye Han,Tuhin Pradhan,Sooyeon Kim,Seok Won Lee,Jonathan L. Sessler,Tae Woo Kim,Chulhun Kang,Jong Seung Kim
Publication:	Biomaterials
Publisher:	Elsevier
Date:	January 2012

Order Completed

Thank you for your order.

This Agreement between Mr. Firoj Ali ("You") and Elsevier ("Elsevier") consists of your license details and the terms and conditions provided by Elsevier and Copyright Clearance Center.

Your confirmation email will contain your order number for future reference.

Printable details.

License Number	4133510705125
License date	Jun 21, 2017
Licensed Content Publisher	Elsevier
Licensed Content Publication	Biomaterials
Licensed Content Title	A cysteine-selective fluorescent probe for the cellular detection of cysteine
Licensed Content Author	Hyo Sung Jung,Ji Hye Han,Tuhin Pradhan,Sooyeon Kim,Seok Won Lee,Jonathan L. Sessler,Tae Woo Kim,Chulhun Kang,Jong Seung Kim
Licensed Content Date	Jan 1, 2012
Licensed Content Volume	33
Licensed Content Issue	3
Licensed Content Pages	9
Type of Use	reuse in a thesis/dissertation
Portion	figures/tables/illustrations
Number of figures/tables/illustrations	1
Format	both print and electronic
Are you the author of this Elsevier article?	No
Will you be translating?	No
Order reference number	
Original figure numbers	
Title of your thesis/dissertation	Design & Synthesis of photo-reactive Receptors for the recognition of analytes having biological Significance
Expected completion date	Jul 2017
Estimated size (number of pages)	160
Elsevier VAT number	GB 494 6272 12
Requestor Location	Mr. Firoj Ali Organic Chemistry Division CSIR National Chemical Laboratory, Pune Pune-411008 Pune, Maharashtra 411008 India Attn: Mr. Firoj Ali
Total	0.00 USD

ORDER MORE CLOSE WINDOW

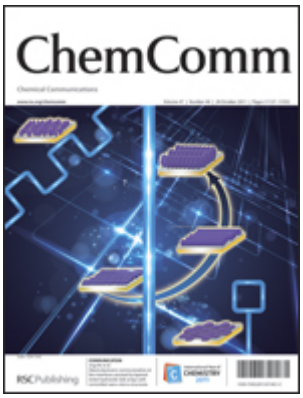

Title: A reagent for specific recognition of cysteine in aqueous buffer and in natural milk: imaging studies, enzymatic reaction and analysis of whey protein

Author: Anila H. A.,Upendar Reddy G.,Firoj Ali,Nandaraj Taye,Samit Chattopadhyay,Amitava Das

Publication: Chemical Communications (Cambridge)

Publisher: Royal Society of Chemistry

Date: Aug 26, 2015

Title: Multisignal Chemosensor for Cr3+ and Its Application in Bioimaging

Author: Kewei Huang, Hong Yang, Zhiguo Zhou, et al

Publication: Organic Letters

Publisher: American Chemical Society

Date: Jun 1, 2008

PERMISSION/LICENSE IS GRANTED FOR YOUR ORDER AT NO CHARGE

This type of permission/license, instead of the standard Terms & Conditions, is sent to you because no fee is being charged for your order. Please note the following:

- Permission is granted for your request in both print and electronic formats, and translations.
- If figures and/or tables were requested, they may be adapted or used in part.
- Please print this page for your records and send a copy of it to your publisher/graduate school.
- Appropriate credit for the requested material should be given as follows: "Reprinted (adapted) with permission from (COMPLETE REFERENCE CITATION). Copyright (YEAR) American Chemical Society." Insert appropriate information in place of the capitalized words.
- One-time permission is granted only for the use specified in your request. No additional uses are granted (such as derivative works or other editions). For any other uses, please submit a new request.

If credit is given to another source for the material you requested, permission must be obtained from that source.

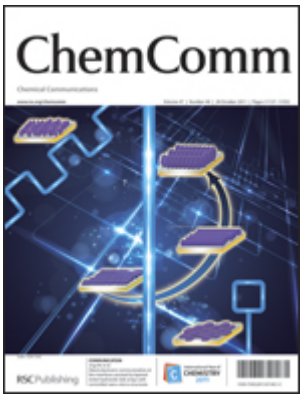

Title: FRET-based sensor for imaging chromium(iii) in living cells

Author: Zhiguo Zhou,Mengxiao Yu,Hong Yang,Kewei Huang,Fuyou Li,Tao Yi,Chunhui Huang

Publication: Chemical Communications (Cambridge)

Publisher: Royal Society of Chemistry

Date: May 23, 2008

Order Completed

Thank you for your order.

This Agreement between Mr. Firoj Ali ("You") and Royal Society of Chemistry ("Royal Society of Chemistry") consists of your license details and the terms and conditions provided by Royal Society of Chemistry and Copyright Clearance Center.

Your confirmation email will contain your order number for future reference.

Printable details.

License Number	4133551397570
License date	Jun 21, 2017
Licensed Content Publisher	Royal Society of Chemistry
Licensed Content Publication	Chemical Communications (Cambridge)
Licensed Content Title	FRET-based sensor for imaging chromium(iii) in living cells
Licensed Content Author	Zhiguo Zhou,Mengxiao Yu,Hong Yang,Kewei Huang,Fuyou Li,Tao Yi,Chunhui Huang
Licensed Content Date	May 23, 2008
Licensed Content Issue	29
Type of Use	Thesis/Dissertation
Requestor type	non-commercial (non-profit)
Portion	figures/tables/images
Number of figures/tables/images	1
Distribution quantity	4
Format	print and electronic
Will you be translating?	no
Order reference number	
Title of the thesis/dissertation	Design & Synthesis of photo-reactive Receptors for the recognition of analytes having biological Significance
Expected completion date	Jul 2017
Estimated size	160
Requestor Location	Mr. Firoj Ali Organic Chemistry Division CSIR National Chemical Laboratory, Pune Pune-411008 Pune, Maharashtra 411008 India Attn: Mr. Firoj Ali
Billing Type	Invoice
Billing address	Mr. Firoj Ali Organic Chemistry Division CSIR National Chemical Laboratory, Pune Pune-411008 Pune, India 411008 Attn: Mr. Firoj Ali
Total	0.00 USD

Title: Unique Tri-Output Optical Probe for Specific and Ultrasensitive Detection of Hydrazine

Author: Lei Cui, Chunfei Ji, Zhixing Peng, et al

Publication: Analytical Chemistry

Publisher: American Chemical Society

Date: May 1, 2014

PERMISSION/LICENSE IS GRANTED FOR YOUR ORDER AT NO CHARGE

This type of permission/license, instead of the standard Terms & Conditions, is sent to you because no fee is being charged for your order. Please note the following:

- Permission is granted for your request in both print and electronic formats, and translations.
- If figures and/or tables were requested, they may be adapted or used in part.
- Please print this page for your records and send a copy of it to your publisher/graduate school.
- Appropriate credit for the requested material should be given as follows: "Reprinted (adapted) with permission from (COMPLETE REFERENCE CITATION). Copyright (YEAR) American Chemical Society." Insert appropriate information in place of the capitalized words.
- One-time permission is granted only for the use specified in your request. No additional uses are granted (such as derivative works or other editions). For any other uses, please submit a new request.

If credit is given to another source for the material you requested, permission must be obtained from that source.

Title: Naked-Eye and Near-Infrared Fluorescence Probe for Hydrazine and Its Applications in In Vitro and In Vivo Bioimaging

Author: Jianjian Zhang, Lulu Ning, Jiting Liu, et al

Publication: Analytical Chemistry

Publisher: American Chemical Society

Date: Sep 1, 2015

PERMISSION/LICENSE IS GRANTED FOR YOUR ORDER AT NO CHARGE

This type of permission/license, instead of the standard Terms & Conditions, is sent to you because no fee is being charged for your order. Please note the following:

- Permission is granted for your request in both print and electronic formats, and translations.
- If figures and/or tables were requested, they may be adapted or used in part.
- Please print this page for your records and send a copy of it to your publisher/graduate school.
- Appropriate credit for the requested material should be given as follows: "Reprinted (adapted) with permission from (COMPLETE REFERENCE CITATION). Copyright (YEAR) American Chemical Society." Insert appropriate information in place of the capitalized words.
- One-time permission is granted only for the use specified in your request. No additional uses are granted (such as derivative works or other editions). For any other uses, please submit a new request.

If credit is given to another source for the material you requested, permission must be obtained from that source.

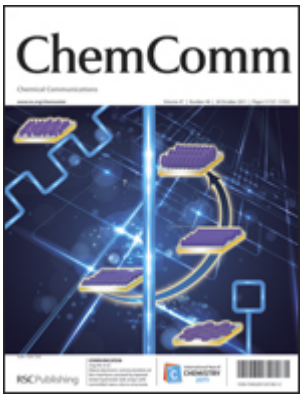

Title: An ICT-based ratiometric probe for hydrazine and its application in live cells

Author: Jiangli Fan,Wen Sun,Mingming Hu,Jianfang Cao,Guanghui Cheng,Huijuan Dong,Kedong Song,Yingchao Liu,Shiguo Sun,Xiaojun Peng

Publication: Chemical Communications (Cambridge)

Publisher: Royal Society of Chemistry

Date: Jun 21, 2012

Order Completed

Thank you for your order.

This Agreement between Mr. Firoj Ali ("You") and Royal Society of Chemistry ("Royal Society of Chemistry") consists of your license details and the terms and conditions provided by Royal Society of Chemistry and Copyright Clearance Center.

Your confirmation email will contain your order number for future reference.

Printable details.

License Number	4133560673208
License date	Jun 21, 2017
Licensed Content Publisher	Royal Society of Chemistry
Licensed Content Publication	Chemical Communications (Cambridge)
Licensed Content Title	An ICT-based ratiometric probe for hydrazine and its application in live cells
Licensed Content Author	Jiangli Fan,Wen Sun,Mingming Hu,Jianfang Cao,Guanghui Cheng,Huijuan Dong,Kedong Song,Yingchao Liu,Shiguo Sun,Xiaojun Peng
Licensed Content Date	Jun 21, 2012
Licensed Content Volume	48
Licensed Content Issue	65
Type of Use	Thesis/Dissertation
Requestor type	non-commercial (non-profit)
Portion	figures/tables/images
Number of figures/tables/images	1
Distribution quantity	4
Format	print and electronic
Will you be translating?	no
Order reference number	
Title of the thesis/dissertation	Design & Synthesis of photo-reactive Receptors for the recognition of analytes having biological Significance
Expected completion date	Jul 2017
Estimated size	160
Requestor Location	Mr. Firoj Ali Organic Chemistry Division CSIR National Chemical Laboratory, Pune Pune-411008 Pune, Maharashtra 411008 India Attn: Mr. Firoj Ali
Billing Type	Invoice
Billing address	Mr. Firoj Ali Organic Chemistry Division CSIR National Chemical Laboratory, Pune

Pune-411008
Pune, India 411008
Attn: Mr. Firoj Ali

Total 0.00 USD

ORDER MORE CLOSE WINDOW

Title: Detection of Nitric Oxide and Nitroxyl with Benzoresorufin-Based Fluorescent Sensors

Author: Ulf-Peter Apfel, Daniela Buccella, Justin J. Wilson, et al

Publication: Inorganic Chemistry

Publisher: American Chemical Society

Date: Mar 1, 2013

PERMISSION/LICENSE IS GRANTED FOR YOUR ORDER AT NO CHARGE

This type of permission/license, instead of the standard Terms & Conditions, is sent to you because no fee is being charged for your order. Please note the following:

- Permission is granted for your request in both print and electronic formats, and translations.
- If figures and/or tables were requested, they may be adapted or used in part.
- Please print this page for your records and send a copy of it to your publisher/graduate school.
- Appropriate credit for the requested material should be given as follows: "Reprinted (adapted) with permission from (COMPLETE REFERENCE CITATION). Copyright (YEAR) American Chemical Society." Insert appropriate information in place of the capitalized words.
- One-time permission is granted only for the use specified in your request. No additional uses are granted (such as derivative works or other editions). For any other uses, please submit a new request.

If credit is given to another source for the material you requested, permission must be obtained from that source.

Title: A Reductant-Resistant and Metal-Free Fluorescent Probe for Nitroxyl Applicable to Living Cells

Author: Kodai Kawai, Naoya Ieda, Kazuyuki Aizawa, et al

Publication: Journal of the American Chemical Society

Publisher: American Chemical Society

Date: Aug 1, 2013

PERMISSION/LICENSE IS GRANTED FOR YOUR ORDER AT NO CHARGE

This type of permission/license, instead of the standard Terms & Conditions, is sent to you because no fee is being charged for your order. Please note the following:

- Permission is granted for your request in both print and electronic formats, and translations.
- If figures and/or tables were requested, they may be adapted or used in part.
- Please print this page for your records and send a copy of it to your publisher/graduate school.
- Appropriate credit for the requested material should be given as follows: "Reprinted (adapted) with permission from (COMPLETE REFERENCE CITATION). Copyright (YEAR) American Chemical Society." Insert appropriate information in place of the capitalized words.
- One-time permission is granted only for the use specified in your request. No additional uses are granted (such as derivative works or other editions). For any other uses, please submit a new request.

If credit is given to another source for the material you requested, permission must be obtained from that source.

Title:	Development of green to near-infrared turn-on fluorescent probes for the multicolour imaging of nitroxyl in living systems
Author:	Baoli Dong,Kaibo Zheng,Yonghe Tang,Weiying Lin
Publication:	Journal of Materials Chemistry B
Publisher:	Royal Society of Chemistry
Date:	Dec 24, 2015

Order Completed

Thank you for your order.

This Agreement between Mr. Firoj Ali ("You") and Royal Society of Chemistry ("Royal Society of Chemistry") consists of your license details and the terms and conditions provided by Royal Society of Chemistry and Copyright Clearance Center.

Your confirmation email will contain your order number for future reference.

Printable details.

License Number	4133580542540
License date	Jun 21, 2017
Licensed Content Publisher	Royal Society of Chemistry
Licensed Content Publication	Journal of Materials Chemistry B
Licensed Content Title	Development of green to near-infrared turn-on fluorescent probes for the multicolour imaging of nitroxyl in living systems
Licensed Content Author	Baoli Dong,Kaibo Zheng,Yonghe Tang,Weiying Lin
Licensed Content Date	Dec 24, 2015
Licensed Content Volume	4
Licensed Content Issue	7
Type of Use	Thesis/Dissertation
Requestor type	non-commercial (non-profit)
Portion	figures/tables/images
Number of figures/tables/images	3
Distribution quantity	4
Format	print and electronic
Will you be translating?	no
Order reference number	
Title of the thesis/dissertation	Design & Synthesis of photo-reactive Receptors for the recognition of analytes having biological Significance
Expected completion date	Jul 2017
Estimated size	160
Requestor Location	Mr. Firoj Ali Organic Chemistry Division CSIR National Chemical Laboratory, Pune Pune-411008 Pune, Maharashtra 411008 India Attn: Mr. Firoj Ali
Billing Type	Invoice
Billing address	Mr. Firoj Ali Organic Chemistry Division CSIR National Chemical Laboratory, Pune Pune-411008 Pune, India 411008 Attn: Mr. Firoj Ali

Total	0.00 USD

ORDER MORE CLOSE WINDOW